Investigating the importance of methane for future climate change: wetland methane emissions, the permafrost carbon feedback, and methane mitigation

by

Claude-Michel Nzotungicimpaye

M.Sc. (Environmental & Geographical Science), University of Cape Town, 2014

B.Sc. (Applied Mathematics), National University of Rwanda, 2009

Thesis Submitted in Partial Fulfillment of the

Requirements for the Degree of

Doctor of Philosophy

in the

Department of Geography

Faculty of Environment

SIMON FRASER UNIVERSITY

Spring 2021

Declaration of Committee

Name:	**Claude-Michel Nzotungicimpaye**
Degree:	**Doctor of Philosophy (Geography)**
Thesis title:	**Investigating the importance of methane for future climate change: wetland methane emissions, the permafrost carbon feedback, and methane mitigation**
Committee:	**Chair: Eugene McCann** Professor, Geography
	Kirsten Zickfeld Supervisor Professor, Geography
	Lance F. W. Lesack Committee Member Professor, Geography and Biological Sciences
	Joe R. Melton Committee Member Research Scientist Climate Research Division Environment and Climate Change Canada
	Andrew H. MacDougall Committee Member Assistant Professor Climate and Environment St. Francis Xavier University
	W. Jesse Hahm Examiner Assistant Professor, Geography
	Victor A. Brovkin External Examiner Head of Climate-Biogeosphere Interactions Group Land in the Earth System Department Max Planck Institute for Meteorology, Germany

Abstract

Methane (CH_4) is a major greenhouse gas (GHG), second only to carbon dioxide (CO_2) in the contribution to historical climate forcing. Yet, the level of understanding of how CH_4 will influence the future climate remains low because CH_4 processes are generally not represented in Earth system models used for future climate projections. The objective of this thesis is to investigate the importance of CH_4 for future climate change with a focus on CH_4 mitigation as well as wetland CH_4 emissions from thawing permafrost soils, and their respective impact on global warming. The thesis includes a description of a new model for wetland CH_4 emissions implemented in an Earth system model of intermediate complexity (EMIC) and applications of the EMIC (including a simplified representation of the CH_4 cycle) to: (i) investigate the importance of CH_4 mitigation to comply with stringent global warming limits, and (ii) project the additional warming due to wetland CH_4 emissions from previously frozen carbon following gradual permafrost thaw over the next three centuries. Salient results of this thesis are: (i) immediate cuts in anthropogenic CH_4 emissions, alongside CO_2 mitigation, are needed to increase the likelihood of limiting global warming to 2°C above pre-industrial levels; (ii) the warming due to wetland CH_4 emissions from thawing permafrost soils is projected to be small (<0.05°C) throughout the 21st century independent of the future anthropogenic emission scenario, (iii) the warming due to such permafrost CH_4 emissions has the potential to increase substantially beyond the 21st century, reaching 0.09 (0.01-0.24) °C in the year 2300 under a scenario of high anthropogenic emissions. Overall, by incorporating a simplified representation of the CH_4 cycle in Earth system model simulations, this thesis suggests that (i) delaying CH_4 mitigation to after the year 2040 will constitute a challenge for limiting global warming to 2°C even if anthropogenic CO_2 emissions were reduced aggressively, (ii) reducing anthropogenic GHG emissions will allow to limit the warming due to wetland CH_4 emissions from thawing permafrost soils to well below 0.1°C over the next three centuries.

Keywords: Methane; Wetland methane emissions; Methane mitigation; Permafrost carbon feedback.

To my dear wife Larissa for her love, patience, and encouragement.

To our unborn child.

Acknowledgements

I would like to take this opportunity to extent my gratitude to my senior supervisor, Dr. Kirsten Zickfeld, for her valuable time, guidance, and support throughout my doctoral studies. I am deeply thankful for the immense opportunity I got to learn to be(come) a scientist under her mentorship. I also owe thanks to my supervisory committee: Dr. Lance F. W. Lesack for his consistency to help me improve my understanding of wetland methane processes; Dr. Joe R. Melton for his fundamental inputs during the model development phase as well as regular updates on methane research; Dr. Andrew H. MacDougall for his willingness to share his model code and to answer my numerous questions throughout the model implementation phase. Everyone on my doctoral committee provided constructive feedbacks and thoughtful suggestions that allowed me to refine my ideas. I am also grateful to Dr. Michael Eby for hosting me at the University of Victoria and providing hands-on guidance on the model implementation. His instructions on how to run the UVic ESCM on a PC were a breakthrough during the model implementation phase. I also thank Dr. Victor A. Brovkin and Dr. W. Jesse Hahm for taking the time to read my thesis and sitting on my examining committee, as well as Dr. Eugene McCann for serving as my thesis defence chair.

I benefited a lot from interacting with fellow members of the climate research lab at Simon Fraser University. Special acknowledgements to Rachel Chimuka who assisted in post-processing of observational data, Nesha Wright and Jesse Kemp who contributed to the pre-processing of model forcing data, as well as Alex J. MacIsaac who willingly shared his model code based on which I built my atmospheric methane work.

I am very grateful to Iris and Isaac, Danella and Armel, Margaret and Douw for their kind hospitality in the weeks that preceded the beginning of this doctoral journey. Thanks to Larissa who accepted to follow me on this journey and has always been there.

This research was funded by a National Science Engineering and Research Council of Canada (NSERC) Discovery Grant awarded to Dr. Kirsten Zickfeld. A substantial part of this work would not have been possible without an access to supercomputing facilities from WestGrid - Compute Canada.

All the glory to the Almighty God for everything!

Table of Contents

List of Tables

List of Figures

Chapter 1. Introduction

The industrial revolution of the 18th century marked the beginning of intensive use of fossil fuels by humans, which resulted in economic growth followed by a sustained increase in greenhouse gas (GHG) emissions from anthropogenic sources and a gradual rise of the average global surface temperature (IPCC, 2014). The increase in global mean surface air temperature of about 1.1°C above pre-industrial (1850-1900) levels has induced severe impacts on both natural and human systems in many regions of the Earth (WMO, 2019). Climate-related impacts are expected to increase and worsen in a future without an effective action to mitigate anthropogenic emissions (IPCC, 2014).

As part of international efforts to combat climate change, the 2015 Paris Agreement by parties to the United Nations Framework Convention on Climate Change (UNFCCC) aims at "holding the increase in the global average temperature to well below 2°C above pre-industrial levels and pursuing efforts to limit the temperature increase to 1.5°C above pre-industrial levels, recognizing that this would significantly reduce the risks and impacts of climate change" (UNFCCC, 2015). Holding global warming to the limits set by the Paris Agreement requires achieving net zero carbon dioxide (CO_2) emissions and substantial reductions in non-CO_2 emissions from anthropogenic sources by the year 2050 (IPCC, 2018).

Methane (CH_4) is the second most important contributor to total radiative forcing after CO_2 (Myhre et al., 2013). While CO_2 stays in the atmosphere for centuries, CH_4 has a residence time of only about a decade in the atmosphere (Ciais et al., 2013). Yet, the global warming potential of CH_4 is 28-34 over 100 years: that is, each molecule of CH_4 added to the atmosphere is 28-34 times more effective at absorbing heat than a molecule of CO_2 over a period of 100 years (Myhre et al., 2013). The global CH_4 cycle involves several sources (e.g. fossil fuels, landfills, rice paddies, natural wetlands and freshwater systems) and sinks (e.g. chemical reactions in the atmosphere and microbial uptake at the soil surface) (Saunois et al., 2020). Ongoing climate change has the potential to increase CH_4 emissions from natural wetlands and permafrost environments, which could trigger positive feedbacks between climate change and these CH_4 emissions (Dean et al., 2018; O'Connor et al., 2010). CH_4 is an integral part of the permafrost carbon feedback (Schuur et al., 2015), which is a positive (i.e. amplifying)

Earth system feedback involving wetland CH_4 emissions resulting from microbial decomposition of previously frozen carbon under anaerobic decomposition (see Section 1.1.2). Moreover, CH_4 is a major component of so-called short-lived climate pollutants (SLCPs) targeted by international policies for mitigating climate change (Harmsen et al., 2019b; Ramanathan and Xu, 2010; Weaver, 2011) and achieving the temperature goals of the Paris Agreement (IPCC, 2018; Rogelj et al., 2018). However, fully coupled Earth system models (ESMs) used for future climate projections do not generally incorporate wetland CH_4 emissions and the global CH_4 cycle. There is a growing need to (i) represent wetland CH_4 processes and the global CH_4 cycle in fully coupled ESMs, (ii) assess the relevance of CH_4 as part of the permafrost carbon feedback to climate change, and (iii) investigate the importance of CH_4 mitigation in the context of complying with the warming limits set by the Paris Agreement.

1.1. Background

1.1.1. Wetland CH_4 emissions

Wetlands are vegetated land areas that are inundated with water on a permanent, seasonal, or recurrent basis (Wheeler, 1999). Natural wetlands can be found in all climate zones across the globe (Bridgham et al., 2013; Turetsky et al., 2014). Wetlands are the dominant natural source of CH_4, accounting for approximately a third of total (i.e. anthropogenic and natural) global CH_4 emissions (Kirschke et al., 2013; Saunois et al., 2020). The release of CH_4 from a wetland site is regulated by two main processes: (i) the production of CH_4 following decomposition of organic matter by specialized microbes (methanogens) under anaerobic conditions, and (ii) the oxidation of CH_4 by specialized microbes (methanotrophs) primarily occurring in aerobic soil layers (Segers, 1998). Wetland CH_4 emissions can vary by several orders of magnitude within and between sites depending on many factors such as the dominant vegetation type, water table fluctuations, soil composition, and predominant climate conditions (Bridgham et al., 2013; Cooper et al., 2017; Levy et al., 2012; Turetsky et al., 2014). The high heterogeneity of site-scale wetland CH_4 emissions imply that regional and global wetland CH_4 emissions are difficult to predict (Bridgham et al., 2013; Melton et al., 2013; Saunois et al., 2020).

Wetland CH_4 emissions are commonly linked to climate change. On the one hand, wetland CH_4 emissions are sensitive to changes in climate conditions (e.g. temperature and precipitation shifts) which influence both the production and oxidation of CH_4 in wetlands (Bridgham et al., 2013). On the other hand, wetland CH_4 emissions can affect the global climate through changes in atmospheric CH_4 levels and radiative forcing (O'Connor et al., 2010). While analyses of ice cores suggest that wetland CH_4 emissions were an important contributor to climate changes during past glacial-interglacial transitions (Loulergue et al., 2008; Rhodes et al., 2017), it remains difficult to predict how wetland CH_4 emissions and climate will interact in the future because wetland CH_4 processes are not commonly represented in fully coupled Earth system models (ESMs) (Xu et al., 2016).

1.1.2. The permafrost carbon feedback

Permafrost is ground (soil, rock, ice) that remains at or below 0°C for two or more consecutive years (Woo, 2012). Permafrost prevails in the boreal and Arctic regions where soils and sediments store 1100-1500 Pg (10^{15} g) of carbon (Pg C) (Hugelius et al., 2014), which is roughly twice the amount of carbon held in the pre-industrial atmosphere (Ciais et al., 2013; MacDougall and Knutti, 2016; Schuur et al., 2015). In their top 3 m alone, these northern terrains store 885-1185 Pg C including a substantial fraction of perennially frozen carbon (i.e. permafrost carbon) (Hugelius et al., 2014). Permafrost carbon has been inert for centuries due to the predominant cold conditions (Hugelius et al., 2014; Schuur et al., 2015). However, permafrost is warming at a global scale with highest warming rates observed across the northern circumpolar region (Biskaborn et al., 2019).

There have been concerns that the ongoing and projected warming across the northern circumpolar region could amplify global warming through a positive feedback involving permafrost carbon emissions (Schaefer et al., 2014). Thawing permafrost exposes previously frozen carbon (i.e. soil carbon previously frozen for at least two consecutive years) to accelerated microbial decomposition resulting in so-called permafrost CO_2 and CH_4 emissions into the atmosphere (Schuur et al., 2015; Zimov et al., 2006). Such permafrost carbon emissions would accelerate climate warming, which would lead to substantial permafrost degradation, more permafrost carbon release to the atmosphere, and thus an amplifying feedback loop (Figure 1.1). This positive Earth

system feedback is commonly referred to as the permafrost carbon feedback (Schuur et al., 2015). While permafrost CO_2 emissions mainly occur following microbial decomposition under oxic conditions, permafrost CH_4 emissions result from microbial decomposition in anaerobic environments such as wetlands (Schuur et al., 2008).

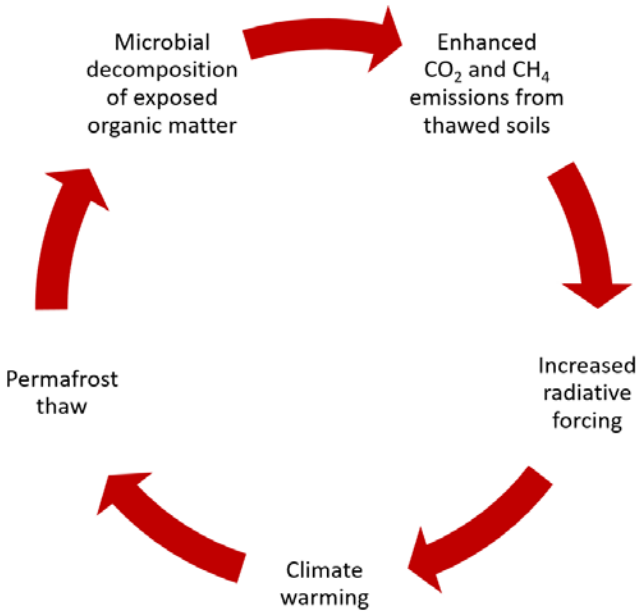

Figure 1.1. Illustration of the permafrost carbon feedback loop, a positive (i.e. amplifying) Earth system feedback.

In the past 10-12 years, considerable progress has been made in research related to the permafrost carbon feedback. For instance, the distribution of permafrost has been estimated with a focus on the northern hemisphere (Gruber, 2012; Zhang et al., 2008) and stocks of soil organic carbon in permafrost environments have been estimated (Hugelius et al., 2014; Tarnocai et al., 2009). The decay of organic matter from thawing permafrost soils has been investigated through incubation experiments in laboratories (Knoblauch et al., 2018; Treat et al., 2015; Walz et al., 2017) and field measurements (Corbett et al., 2015; Helbig et al., 2017; Neumann et al., 2019; Olefeldt et al., 2017). Advancements have also been made in the understanding of processes regulating CO_2 and CH_4 emissions from soils in the northern permafrost region (Cooper et al., 2017; Kwon et al., 2019; McCalley et al., 2014; Schädel et al., 2016; Song et al., 2012; Walter Anthony et al., 2016; Walter et al., 2006; Zona et al., 2016). However, large uncertainties remain with regard to many aspects of the permafrost carbon feedback such as the distribution and quality of soil carbon across the northern permafrost region (Hugelius et al., 2014), the ecological response to permafrost thaw (Schuur and Mack,

2018), microbial processes regulating permafrost carbon emissions (Kwon et al., 2019; Schuur et al., 2015; Treat et al., 2015), the impact of abrupt thaw processes on soil carbon decomposition (Schuur et al., 2008; Turetsky et al., 2020), the relative roles of ancient versus modern soil carbon in CO_2 and CH_4 emissions from wet environments underlain by permafrost (Bogard et al., 2019; Cooper et al., 2017; Elder et al., 2018; Turetsky et al., 2020), and the partition of permafrost carbon emissions between CO_2 and CH_4 (Schuur et al., 2013, 2015).

Numerical models of different complexities have been applied to investigate the permafrost carbon feedback. Simple 1-D and 2-D models representing the northern high-latitude regions have been developed and applied to project permafrost carbon emissions and their climate impact (Schneider von Deimling et al., 2012, 2015). In addition, many complex land surface models have been developed or upgraded to represent permafrost freeze-thaw processes, vegetation dynamics, and terrestrial carbon fluxes (McGuire et al., 2016, 2017). While some uncoupled terrestrial components of Earth System Models (ESMs) have been used to simulate carbon emissions from thawing permafrost soils (Chadburn et al., 2017; Comyn-Platt et al., 2018; Kleinen and Brovkin, 2018; Koven et al., 2015b) as well as the potential for northern vegetation growth and expansion to offset some of the CO_2 emissions (McGuire et al., 2017), at present only Earth system models of intermediate complexity (EMICs) simulate the permafrost carbon feedback loop but with CO_2 emissions alone (Crichton et al., 2016; MacDougall et al., 2012). The lack of permafrost CH_4 emissions in climate projections might result in an underestimation of the strength of the permafrost carbon feedback, and hence future global warming levels (Dean et al., 2018; Schuur et al., 2013, 2015).

1.1.3. CH_4 mitigation

Limiting global mean temperature rise to 1.5 or 2°C above pre-industrial levels will require reaching net zero CO_2 emissions and deep reductions in non-CO_2 emissions from anthropogenic sources over the next three decades (IPCC, 2018). However, current strategies adopted by different countries to reduce GHG emissions (i.e. nationally determined contributions or NDCs) mostly focus on CO_2 mitigation and generally do not explicitly target non-CO_2 GHGs such as CH_4 (Harmsen et al., 2019a). Meanwhile, atmospheric CH_4 concentration ([CH_4]) has been increasing rapidly and

tracking future scenarios of unmitigated emissions since the last few years (Nisbet et al., 2019; Saunois et al., 2016b).

Atmospheric [CH_4] has increased from about 700 parts per billion (ppb) in the year 1750 to more than 1850 ppb today (Ciais et al., 2013; Nisbet et al., 2019). Such a rise in [CH_4] is unprecedented over the past 800,000 years (O'Connor et al., 2010) and is primarily driven by increased emissions from anthropogenic sources of CH_4 such as fossil fuels (e.g. coal, oil, natural gas), biomass burning, agriculture and waste (Saunois et al., 2020). Over the past few decades, anthropogenic sources of CH_4 accounted for more than 60% of the global CH_4 emissions (Kirschke et al., 2013; Saunois et al., 2020). After decades of sustained growth, [CH_4] stabilized between the 1999-2006 period and its growth resumed since the year 2007 (Dlugokencky et al., 2011; Nisbet et al., 2019). The exact causes driving the evolution of [CH_4] in recent years are not fully understood and still being debated (Saunois et al., 2020; Schaefer, 2019).

Reducing CH_4 emissions from anthropogenic sources is often proposed to be one way to tackle climate change in the near-term, in parallel with efforts to achieve net zero CO_2 emissions and decarbonize the world economy (Ramanathan and Xu, 2010; Shoemaker et al., 2013; Weaver, 2011). Targeting CH_4 for the mitigation of climate change is motivated with the dominance of anthropogenic sources in current global CH_4 emissions, the strong global warming potential of CH_4 as well as its short residence time in the atmosphere (Crill and Thornton, 2017; Kirschke et al., 2013; Ramanathan and Xu, 2010). Given that [CH_4] has been growing fast over the last decade (Nisbet et al., 2019; Saunois et al., 2016b), there is a compelling need to investigate the importance of CH_4 mitigation as part of international efforts to achieve the temperature limits set by the Paris Agreement and minimize the future impacts of climate change.

1.2. Research objectives

The main objective of this thesis is to investigate the importance of CH_4 for future climate change. Specific objectives are:

1. To assess the relevance of CH_4 as part of the permafrost carbon feedback through literature review.

2. To implement a model for wetland CH_4 emissions in an Earth system model of intermediate complexity and evaluate its performance.

3. To examine the importance of CH_4 mitigation as part of strategies to comply with stringent global warming limits based on Earth system model simulations.

4. To quantify the warming to expect in response to CH_4 emissions from thawing permafrost soils over the next three centuries based on Earth system model simulations.

1.3. Model choice and rationale

To investigate the importance of CH_4 in future climate projections, I use the University of Victoria Earth System Climate Model (UVic ESCM) into which I implemented a model for wetland CH_4 emissions and a simplified representation of the global CH_4 cycle. The UVic ESCM is an Earth system model of intermediate complexity (EMIC) suitable for multi-centennial climate simulations and studies of feedbacks between various components of the Earth system (Weaver et al., 2001). As an EMIC, the UVic ESCM has an adequate level of detail for representing Earth system processes while being computationally efficient for running long-term climate simulations and a broad range of sensitivity experiments unlike more comprehensive ESMs (Eby et al., 2009, 2013).

Since its development in the 1990s, the UVic ESCM has undergone a series of upgrades in order to allow simulations of several physical processes as well as the carbon cycle (Eby et al., 2009; Mengis et al., 2020). In the 2010s, the EMIC was upgraded to represent permafrost dynamics (Avis et al., 2011), carbon accumulation and related CO_2 emissions (MacDougall et al., 2012; MacDougall and Knutti, 2016). When compared to other models, the UVic ESCM performs well in simulating the areal extent of the northern circumpolar permafrost and regional carbon cycling over the past few decades (McGuire et al., 2016).

However, the UVic ESCM lacks a representation of wetland CH_4 processes and the global CH_4 cycle. A major objective of this research is to implement a numerical scheme for wetland CH_4 emissions in the UVic ESCM. In the past few years, there has been a growing need for representing the effects of depth-dependent controls on soil

biogeochemistry (e.g. the quality of soil carbon and the spread of microbial communities) in terrestrial ecosystem models (Koven et al., 2013, 2017). This need is particularly relevant for the simulation of soil carbon decomposition in permafrost regions (Ahrens and Reichstein, 2017; Koven et al., 2015b; McGuire et al., 2017). By conducting a survey of models for wetland CH_4 emissions published before the year 2017, I found that existing wetland CH_4 models compatible with the complexity of the UVic ESCM are limited to the soil surface (i.e. surface inundation) or to only a few centimeters in the soil with regard to the parameterization of microbial CH_4 production in wetlands (Cao et al., 1996; Christensen et al., 1996; Eliseev et al., 2008; Gedney et al., 2004; Hodson et al., 2011; Hopcroft et al., 2011; Tagesson et al., 2013; Wania et al., 2013; Xu et al., 2016). Therefore, I developed a new wetland CH_4 model for implementation in the UVic ESCM and potentially more comprehensive ESMs. To represent the global CH_4 cycle in the EMIC, I applied a simple formulation for the decay of CH_4 in the atmosphere given simulated wetland CH_4 emissions and prescribed CH_4 emissions from non-wetland sources. A detailed description of the UVic ESCM is provided in Chapters 3-5.

1.4. Thesis structure

The remainder of this thesis is structured as follows:

- Chapter 2 reviews the literature on the potential contribution from CH_4 to the permafrost carbon feedback with a focus on peer-reviewed articles published between 2011 and 2016. This chapter was published in Current Climate Change Reports in early 2017.

- Chapter 3 describes a new model for wetland CH_4 emissions (WETMETH) developed for implementation in the UVic ESCM. This chapter includes an evaluation of WETMETH against recent estimates of wetland CH_4 emissions.

- Chapter 4 describes a simplified representation of the global CH_4 cycle in the UVic ESCM and includes an evaluation of the global CH_4 budget simulated by the UVic ESCM. This chapter provides an application of this newly developed version of the UVic ESCM to investigate the importance of CH_4 mitigation in the context of complying with global warming limits set by the Paris Agreement.

- Chapter 5 seeks to quantify permafrost CH_4 emissions and their climate impact over the next three centuries based on global climate projections with the UVic ESCM. This chapter focuses on quantifying wetland CH_4 emissions associated with the decomposition of previously frozen carbon and their impact on changes in global mean surface air temperature.

- Chapter 6 summarizes the thesis conclusions with an emphasis on key results and their significance as well as novel contributions to research. This chapter also presents recommendations for future research.

Chapter 2. The relevance of methane in the permafrost carbon feedback: A literature review

A version of this chapter was published in Current Climate Change Reports as a literature review focusing on research published between 2011 and 2016.

Citation details: Nzotungicimpaye, C-M., and Zickfeld K.: The contribution from methane to the permafrost carbon feedback, Current Climate Change Reports, 87, 228-238, 2017.

Contribution statement: I conducted the literature review and was the main author of the paper. Dr. Kirsten Zickfeld provided feedback on the structure and content of the paper.

Abstract

We assess the level of importance of methane (CH_4) in the permafrost carbon feedback by reviewing recent scientific publications. Studies that consider permafrost degradation in wetlands suggest that CH_4 could have a share of ~20% in the warming caused by total permafrost carbon release by the year 2100. When CH_4 emissions from thermokarst lakes are considered, the contribution from permafrost CH_4 to surface warming increases to between 30% and 50%. Based on the reviewed literature, we report that gradual degradation of the near-surface permafrost under scenarios of unmitigated emissions could result in an additional warming of ~0.3 (0.08-0.50) °C by the year 2100, out of which up to 0.1°C would be from wetland CH_4 emissions. However, these values can be underestimates as the degradation of ice-rich permafrost and subsequent CH_4 emissions from thermokarst lakes are not accounted for in the calculations.

2.1. Introduction

The unequivocal warming presently observed over the boreal and Arctic regions is projected to worsen throughout this century (Kirtman et al., 2013). This regional warming will likely result in substantial thawing and degradation of the perennially frozen ground (permafrost), with potential impacts on the regional hydrology (Woo, 2012), modification of landscapes (Kokelj and Jorgenson, 2013), and damage of infrastructures (de Grandpré et al., 2012). As soils and sediments of the northern circumpolar permafrost region store 1100-1500 Pg (10^{15} g) of carbon (Pg C) (Hugelius et al., 2014), permafrost thawing is also expected to have global impacts through the potential release of a significant amount of carbon that could be enough to influence the global climate (Schaefer et al., 2014).

The fate of thawed carbon depends on whether it undergoes microbial decomposition in aerobic or anaerobic soils, or dissolves in rivers (Christensen et al., 2015). When the microbial decomposition occurs under aerobic conditions, most of the thawed carbon enters the global carbon cycle as carbon dioxide (CO_2). Otherwise, when thawed carbon is decomposed by microbes in anaerobic environments such as wetlands and lakes, a fraction of it is released as CH_4 (Schuur et al., 2015). Once in the atmosphere, CO_2 and CH_4 from thawed soils contribute to increase radiative forcing, and subsequently to amplify climate warming which would lead to additional permafrost CO_2 and CH_4 emissions, thus creating a feedback loop linking surface temperature and permafrost carbon emissions. This positive feedback is generally referred to as the permafrost carbon feedback (Schaefer et al., 2014; Schuur et al., 2015).

The permafrost carbon feedback has not been considered in climate projections for the latest assessment report by the Intergovernmental Panel on Climate Change (IPCC) because permafrost dynamics and carbon content are not represented in most Earth system models (Arora et al., 2013; Ciais et al., 2013). So far, only simple models for the northern high-latitudes incorporate the complete loop for the permafrost carbon feedback with both CO_2 and CH_4 emissions (Schneider von Deimling et al., 2012, 2015). Moreover, an Earth system model of intermediate complexity represents the complete feedback loop but with permafrost CO_2 emissions alone (MacDougall et al., 2012).

In comparison to CO_2, however, CH_4 is the more powerful greenhouse gas on a per molecule basis. Each molecule of CH_4 in the atmosphere has 28 to 34 times the global warming potential of a molecule of CO_2 over a period of 100 years, and more over shorter timescales (Myhre et al., 2013). Furthermore, atmospheric CH_4 has an indirect effect on climate as its oxidation generally results in the formation of ozone (O_3), water vapor (H_2O) and CO_2 which all contribute to the greenhouse effect (Isaksen et al., 2011). Therefore, there is justifiable concern for ignoring the feedback between climate warming and CH_4 emissions from thawed soils.

To assess the level of importance of CH_4 in the permafrost carbon feedback, we review the available scientific literature on anaerobic environments in the northern permafrost region, estimates of regional CH_4 emissions as well as projected warming due to carbon release from thawed soils. Our review is guided by the following questions: (i) How prevalent are anaerobic environments in the northern circumpolar permafrost region? (ii) How much of the produced CH_4 escapes to the atmosphere? (iii) What is the share of CH_4 in the permafrost carbon feedback on global mean surface air temperature?

We base our review mostly on peer-reviewed research articles published between 2011 and 2016 with the consideration of earlier studies on the distribution of wetlands in the northern high-latitudes (Matthews and Fung, 1987), substantial CH_4 release through bubbling in the Arctic (Walter et al., 2006), mechanisms of permafrost degradation (O'Connor et al., 2010; Schuur et al., 2008), vulnerability of soil carbon in the northern high-latitudes under climate change (McGuire et al., 2009), and potential destabilization of CH_4 trapped in hydrates below subsea permafrost on the continental shelves of the Arctic Ocean (O'Connor et al., 2010; Shakhova et al., 2010). To allow comparison between different studies projecting permafrost carbon emissions and their impact on global climate, we focus on results based on scenarios of unmitigated emissions with 2100 as the time horizon.

2.2. Anaerobic environments in the northern permafrost region

2.2.1. Wetlands

Natural wetlands are prevalent in the northern high-latitudes mostly because permafrost prevents vertical drainage (Woo, 2012). However, the area occupied by these wetlands is poorly constrained despite extensive research in the past three decades. The earliest study on the distribution of global wetlands suggests that these anaerobic environments cover 5.3 x 10^6 km^2 of the global terrestrial area, and that ~50% of this area is occupied by wetlands located north of 50°N (Matthews and Fung, 1987). This study was based on three independent digital sources for vegetation, soil properties and fractional inundation. More recent estimates of global wetland area based on regional wetland inventories, updated datasets, satellite observations and numerical models vary between 5.7 and 10.5 x 10^6 km^2, with larger estimates often associated with seasonal inundated areas (Bridgham et al., 2013; Saunois et al., 2016a). Despite this wide range of estimated global wetland area, there is a consensus among studies on the location of the largest wetland area in the northern high-latitudes. Most importantly, wetlands are shown to be widespread in the permafrost zones of Alaska, Canada and Russia (Woo, 2012), suggesting that CH_4 emissions can occur in many locations as permafrost thaws.

2.2.2. Thermokarst lakes

Apart from wetlands, lakes are other anaerobic environments commonly found in the northern high-latitudes. These water bodies cover ~3% of the northern permafrost region, compared to ~9% for northern wetlands (Burke et al., 2012). Of particular importance with respect to the permafrost carbon feedback are shallow lakes that develop following degradation of ice-rich permafrost. In the following paragraphs, we describe processes related to the formation of these lakes and subsequent CH_4 emissions.

Permafrost thaw can result in ground subsidence and thermokarst development in locations where the ground incorporates ice wedges or where permafrost is underlain by massive ground ice (Kokelj and Jorgenson, 2013; Schuur et al., 2008; Woo, 2012). Thermokarst refers to the uneven (karst-like) topography that is developed as thawing

occurs in ice-rich permafrost (Woo, 2012) or following melting of excessive ground ice such as those found in Alaska and northern Siberia (Kokelj and Jorgenson, 2013; Walter et al., 2006). Thermokarst landscape is characterized by depressions that are due to ground subsidence, and this terrain configuration is commonly observed throughout most permafrost regions of the globe (Kokelj and Jorgenson, 2013). In the northern permafrost region, current thermokarst landscapes and lands susceptible to future thermokarst development cover ~3.6 x 10^6 km^2 with 75% of this area in zones with characteristics of wetlands and lakes (Olefeldt et al., 2016).

When thermokarst development occurs near waterlogged environments, flooding of the depressions formed by ground subsidence creates so-called thermokarst lakes (Schuur et al., 2008; Woo, 2012). Mobilization of water from melting ground ice can contribute to the formation of these shallow lakes or to raise their water table (O'Connor et al., 2010). Ground subsidence and rapid increase of anaerobic environments in the northern high-latitudes can also be driven by changes in vegetation cover. A recent study has shown how, within five years, change in vegetation cover can induce thermokarst development with subsequent snowpack increase and water accumulation in the created depressions (Nauta et al., 2015). At present, there is increasing manifestation of frozen peatlands transforming into collapsed wetlands due to high rates and magnitudes of thermokarst development (Kokelj and Jorgenson, 2013).

In the context of permafrost CH_4, the occurrence of thermokarst lakes is generally associated with labile carbon eroding into anaerobic sediments and subsequent high rates of CH_4 emissions (Walter et al., 2006). Particularly, the formation of thermokarst lakes could transform CH_4 sinks into CH_4 sources (Nauta et al., 2015). Therefore, the decomposition of thawed carbon into CH_4 occurs, not only in existing wetlands, but also in newly formed thermokarst lakes.

Thermokarst lakes are found in various locations of Alaska, northern Canada, Scandinavia and northern Siberia (Walter Anthony et al., 2016). Potential hotspots of thermokarst CH_4 emissions in a warming climate are currently refrozen thermokarst deposits as well as yedoma deposits which are ice-rich and organic-rich silt deposits presently identified in Alaska, Yukon, and northern Siberia (Strauss et al., 2013).

2.3. An overview of CH_4 production and oxidation in anaerobic environments

2.3.1. CH_4 production

The production of CH_4 in soils occurs through decomposition of organic matter by specialized anaerobic microbes (methanogens) found in wetlands and other inland water areas. The organic matter decomposed by methanogens originates from litter-fall, root exudates as well as dead plants and roots (Christensen et al., 2015). Another source of substrates used by methanogens is the lateral hydrological transport of soil carbon (Bastviken et al., 2011), in the form of dissolved and particulate organic carbon (Christensen et al., 2015). In the northern permafrost region, thawed carbon constitutes an additional source of organic matter to methanogens (Olefeldt et al., 2013; Treat et al., 2015).

Methanogens rely on the available organic matter to drive their metabolism. In the presence of alternate electron acceptors such as sulfate and nitrate, however, methanogens are outcompeted by other anaerobic microbes in accessing carbon substrates required for their lives (Schlesinger and Bernhardt, 2013). When sulfate, nitrate and other alternate acceptors are depleted but labile carbon is still available, a sequence of fermentation processes takes place and leads to CH_4 production through the respiration of methanogens (Bridgham et al., 2013; Christensen et al., 2015). This heterotrophic respiration accelerates with increasing soil temperatures (Bridgham et al., 2013; Treat et al., 2015).

2.3.2. CH_4 oxidation

Like CH_4 production, the oxidation of CH_4 in anaerobic environments is a biological process regulated by specialized microbes (methanotrophs). Unlike methanogens, however, methanotrophs are adapted to aerobic conditions. These aerobic microbes are found in the more aerated water columns near the surface (Bridgham et al., 2013; Schlesinger and Bernhardt, 2013). Methanotrophs consume CH_4 that is being transported from the zones of production at depth to the overlying water columns and atmosphere. In general, these microbes consume CH_4 and produce CO_2 as a by-product of their heterotrophic respiration (Bridgham et al., 2013; Christensen et al., 2015).

In analogy to CH_4 production, increasing soil temperature enhances the activity of methanotrophs and results in higher rates of CH_4 oxidation. However, the temperature response for CH_4 oxidation has been shown to be lower than that for CH_4 production (Bridgham et al., 2013; Lofton et al., 2014), suggesting that CH_4 oxidation can decrease while CH_4 production is increasing in a warming climate. Other environmental controls such as soil acidity (pH) and nutrient availability contribute to the regulation of both CH_4 production and oxidation in anaerobic environments (Bridgham et al., 2013; Christensen et al., 2015; Schädel et al., 2016).

2.3.3. Link between the oxidation and release of CH_4

The rate of CH_4 oxidation highly depends on whether CH_4 is released via molecular diffusion, ebullition (gas bubbling) or through a transport mediated by plants that are equipped with conduit tissues (aerenchyma), referred to as vascular plants (Christensen et al., 2015). The position of the water table plays a crucial role in this process because a lowering of the water level favors methanotrophs (O'Connor et al., 2010). Diffusion of CH_4 is the most typical transport pathway, whereby molecules of CH_4 from the zones of production slowly ascend to the overlying water columns. When the water table is below the soil surface, methanotrophs may oxidize all of the diffusing CH_4 before it reaches the atmosphere (Bridgham et al., 2013). In the presence of vascular plants, a lower proportion of the produced CH_4 is oxidized because these plants transport the gas through their aerenchyma, allowing CH_4 to bypass the aerobic zones where methanotrophs are hosted (Christensen et al., 2015; Schlesinger and Bernhardt, 2013). However, the aerenchyma also serve as a conduit for oxygen (O_2) from the aerated water columns to the plant roots such that methanotrophs and subsequent CH_4 oxidation can also occur at depth (Bridgham et al., 2013).

CH_4 can also accumulate in anaerobic sediments and later ascend within the water column in the form of gas bubbles (ebullition). In this case, CH_4 escapes to the atmosphere with little opportunity for oxidation (Christensen et al., 2015). Particularly in thermokarst lakes, the majority of CH_4 emissions can occur by ebullition with the remainder being dominated by molecular diffusion (Walter et al., 2006), implying that CH_4 oxidation is relatively minimal in these shallow lakes. Consequently, the amount of CH_4 emitted from anaerobic permafrost sites can depend on whether decomposition occurs in a wetland or in a thermokarst lake. Because thermokarst lakes increased in

number and size during recent decades (Christensen et al., 2015; Walter et al., 2006), we would expect these lakes to be key contributors to CH_4 emissions and the permafrost carbon feedback.

2.4. Permafrost CH_4 emissions

2.4.1. The dominance of CO_2 over CH_4 emissions in anaerobic environments

The proportion of CH_4 that is produced or emitted from thawed carbon has been assessed with anaerobic laboratory incubations. Some of the most recent results suggest that CO_2 production dominates over CH_4 production even under anaerobic conditions (Schädel et al., 2016; Schuur et al., 2015; Treat et al., 2015). For instance, anaerobic incubations of samples collected from multiple sites across the northern permafrost region indicate that maximum CH_4 production rates can reach 0.05 g CH_4-C m^{-2} day^{-1}, compared to median anaerobic CO_2 production rates of 1.5 g CO_2-C m^{-2} day^{-1} (Treat et al., 2015). The highest CH_4 production is observed for incubations with herbaceous plants (Treat et al., 2015), indicating the role of vegetation in enhancing CH_4 production. Moreover, laboratory incubations suggest that permafrost CH_4 emissions are higher in organic soils than in mineral soils, but all in small proportion compared to anaerobic CO_2 emissions (Schuur et al., 2015). A recent meta-analysis of 25 incubation studies suggest that CH_4 emissions may rarely exceed 20% of total permafrost carbon emissions in few samples from tundra and peatland ecosystems (Schädel et al., 2016).

Field data has also been used to investigate the proportion of CH_4 in permafrost carbon emissions. An analysis of data collected with static chambers across the northern permafrost region supports the dominance of CO_2 in carbon emissions under anaerobic conditions (Olefeldt et al., 2013). The analyzed data is from 303 sites and collected only during the growing season because measurements of CH_4 emissions in the northern high-latitudes are sparse for colder seasons (Christensen et al., 2015; Olefeldt et al., 2013). The results from the collected chambers show that rates of CH_4 emissions are generally less than 20% of the CO_2 emissions depending on the site location, soil moisture and vegetation cover. Median rates of CH_4 emissions range between 0% and 5% of the CO_2 emissions, with the highest rates in warm and saturated wetlands and

littoral sites covered by sedges, which are highly productive vascular plants (Olefeldt et al., 2013).

Although deduced from a limited number of sites, the reported results from laboratory incubations and static chambers highlight the relatively small proportion of CH_4 in permafrost carbon emissions. The dominance of permafrost CO_2 emissions from anaerobic sites can be attributed to either metabolic pathways that produce CO_2 but not CH_4 (Schlesinger and Bernhardt, 2013) or to CO_2 production following CH_4 oxidation, or to a combination of the two.

2.4.2. Current permafrost CH_4 emissions

The concentration of CH_4 in the global atmosphere ($[CH_4]$) has increased from about 700 parts per billion (ppb) in the year 1750 to more than 1850 ppb at present due to changes in anthropogenic and natural emissions (Ciais et al., 2013; O'Connor et al., 2010). Trends of $[CH_4]$ stabilized between the 1999-2006 period, perhaps due to a combination of decreasing-to-stable fossil fuel emissions and increasing-to-stable microbial emissions, but then increased again after the year 2006 probably due to a combination of increased fossil fuel and wetland emissions (Kirschke et al., 2013). The contribution from permafrost CH_4 emissions to these trends is uncertain (Ciais et al., 2013; Kirschke et al., 2013).

Syntheses of global CH_4 fluxes report that permafrost emitted a maximum of 1 Tg (10^{12} g) of CH_4 per year (Tg CH_4 yr^{-1}) throughout the 1980-2012 period (Kirschke et al., 2013; Saunois et al., 2016a). However, this estimate does not include CH_4 emissions from wetlands and freshwater systems (lakes and rivers), which are separately reported in the CH_4 syntheses (Kirschke et al., 2013; Saunois et al., 2016a). For instance, wetlands in the boreal region of North America, Europe and Asia released ~23 (15-40) Tg CH_4 yr^{-1} during the 2000-2009 decade (Kirschke et al., 2013). Over the same period, research on Arctic CH_4 estimates that wetlands located north of 60°N emitted ~15.5 (11-28) Tg CH_4 yr^{-1} (Bruhwiler et al., 2015). Furthermore, it is estimated that, in the current climate, northern lakes and rivers emit ~8.3 (3.6-13.0) Tg CH_4 yr^{-1} and ~0.3 Tg CH_4 yr^{-1}, respectively (Bastviken et al., 2011; Wik et al., 2016). The proportion of these emissions associated with thawed carbon is not explicitly provided in the literature such that

present-day permafrost CH_4 emissions in wetlands, lakes and rivers are difficult to estimate.

For the case of thermokarst lakes, however, a recent study provides an estimate for CH_4 emissions associated with thawed soil carbon eroding in these lakes since the 1950s (Walter Anthony et al., 2016). This study suggests that margins of thermokarst lakes across the northern high-latitudes released 100-300 Tg CH_4 in the past 60 years, which is equivalent to 1.6-5.0 Tg CH_4 yr^{-1}. Interestingly, CH_4 emissions by ebullition are shown to be proportional to soil organic carbon eroded around thermokarst lakes as evidence of permafrost thaw fueling CH_4 production in these lakes (Walter Anthony et al., 2016). Total CH_4 emissions from thermokarst lakes are estimated to range from 1.9 to 6.3 Tg CH_4 yr^{-1} (Wik et al., 2016).

2.4.3. CH_4 emissions from hydrates

A large but poorly estimated amount of CH_4 is trapped in ocean sediments along continental shelves (Parmentier et al., 2015) and below deep terrestrial permafrost (Walter Anthony et al., 2012) in the form of gas hydrates. CH_4 hydrates are water or ice cages enveloping molecules of CH_4 (Ciais et al., 2013; Thornton and Crill, 2015). In the literature, there is no consensus on the global amount of CH_4 in marine hydrates, with estimates ranging from thousands to millions of Tg CH_4 (Ciais et al., 2013; Parmentier et al., 2015; Saunois et al., 2016a). The mass of CH_4 contained in terrestrial hydrates is in the range of hundred thousands of Tg CH_4 (Ciais et al., 2013). Marine CH_4 hydrates originated from various sources including volcanic gas, geologic seeps, deposition by rivers and microbial production in the water column (O'Connor et al., 2010; Parmentier et al., 2015; Shakhova et al., 2010), whereas most terrestrial CH_4 hydrates formed following thermal and microbial decomposition of organic compounds in sediments (Walter Anthony et al., 2012).

In general, gas hydrates are stable under specific conditions of high pressure and low temperature, and the sediment zone with ideal conditions for the stability of these hydrates is referred to as the gas hydrate stability zone (GHSZ) (O'Connor et al., 2010). Globally, the GHSZ occurs at ocean depths exceeding 300 m, but CH_4 hydrates below subsea permafrost along the Arctic coastline may be found at shallower depths of ~200 m (Parmentier et al., 2015). Ocean warming under climate change could

destabilize these hydrates and liberate CH_4 that would dissolve in the water column (O'Connor et al., 2010). Terrestrial hydrates are less vulnerable to destabilization than marine hydrates on the shelf of the Arctic Ocean (McGuire et al., 2009). The more stable conditions for CH_4 hydrates below terrestrial permafrost can be attributed to a relatively deeper GHSZ compared to shallow offshore regions (O'Connor et al., 2010). The major concern regarding climate feedbacks is whether and when ocean warming will lead to substantial degradation of the subsea permafrost and to an eventual release of liberated CH_4 to the atmosphere.

In the Arctic Ocean, the total amount of hydrates sequestered beneath subsea permafrost is estimated to be ~27000 Tg CH_4 (Ruppel, 2015). Several studies have been conducted to assess the risk associated with the destabilization of these hydrates, with a focus on the East Siberian Arctic Shelf (ESAS) (Dmitrenko et al., 2011; Overduin et al., 2015; Shakhova et al., 2010; Thornton and Crill, 2015). The particular interest in the ESAS is because it is the largest and shallowest continental shelf among the world oceans, and thus expected to be the most vulnerable with respect to subsea permafrost degradation and CH_4 release (Shakhova et al., 2010).

A number of field campaigns between the years 2005 and 2007 allowed detecting significant CH_4 fluxes from the marine seabed into the water column, high concentration of dissolved CH_4 reaching 5 micromolar (μM) and episodic increase of airborne CH_4 by more than 6 parts per million (ppm) (Shakhova et al., 2010). Based on these observations, it was suggested that the subsea permafrost is already degrading due to long-lasting warming of the ocean (Shakhova et al., 2010). However, this hypothesis of ongoing degradation of the subsea permafrost has been challenged by a combination of long-term summer observations and numerical thermal modelling with extreme warming scenarios (Dmitrenko et al., 2011). Thermal modelling simulated that only 1 m of subsea permafrost on the shelf of the eastern Arctic Ocean thawed between the 1985-2009 period, and suggested that ~70 m of the submerged permafrost will thaw after 1000 years (Dmitrenko et al., 2011). Consequently, destabilization of gas hydrates in the Arctic Ocean and a subsequent release of significant CH_4 to influence global climate seem unlikely in the current century, in agreement with the recent IPCC assessment report (Ciais et al., 2013) and the most recent comprehensive review on the permafrost carbon feedback (Schuur et al., 2015).

Furthermore, ocean biogeochemistry suggests that a large amount of dissolved CH_4 is consumed in the water column. Recent studies have shown that the abundance of sulfate in the ESAS result in a substantial removal of dissolved CH_4 (Overduin et al., 2015; Thornton and Crill, 2015). The current understanding is that this sulfate-driven oxidation of dissolved CH_4 can effectively prevent the release of large quantities of CH_4 to the atmosphere (Thornton and Crill, 2015). However, these results are all based on observations from the Laptev Sea of the ESAS and may not be valid elsewhere across the Arctic Ocean. According to the latest global CH_4 budget, marine hydrates worldwide emitted less than 5 Tg CH_4 yr^{-1} to the atmosphere between the 2003-2012 decade (Saunois et al., 2016a).

2.4.4. Projected permafrost CH_4 emissions

The magnitude of permafrost CH_4 emissions in the future under climate change is of particular interest, as these emissions would contribute to amplify global warming. In this section, we focus on permafrost CH_4 emissions projected by the year 2100 under scenarios of unmitigated emissions to allow easier comparison between the available studies. Figure 2.1 illustrates how the magnitude of future CH_4 emissions from natural sources across the northern permafrost region is projected to increase during the current century in comparison to present-day regional CH_4 emissions. Only future CH_4 emissions from wetlands, lakes and thermokarst lakes are documented in the literature. In the rest of this section, we discuss projected permafrost CH_4 emissions by the year 2100 in detail. Later in the text, we discuss results for mitigation scenarios and projections beyond the 21st century.

Numerical models are essential tools to assess the amount of permafrost CH_4 emissions in the future. A number of ecosystem and climate models of different complexity have been used to assess the magnitude of permafrost carbon emissions in a warming climate (Koven et al., 2015a; Schaefer et al., 2014; Schneider von Deimling et al., 2015). However, most models simulate permafrost CO_2 emissions but not CH_4 release. The few modelling studies with simulations of permafrost CH_4 emissions are listed in Table 2.1 and their results are discussed below.

Simulations by a terrestrial ecosystem model that has a representation of the permafrost carbon pool, frozen ground dynamics and wetland CH_4 biogeochemistry

suggest that CH_4 emissions in the northern high-latitudes will increase from 34 Tg CH_4 yr^{-1} at present-day to 41-70 Tg CH_4 yr^{-1} by the year 2100, mostly due to permafrost carbon loss (Koven et al., 2011). Another study projected permafrost CH_4 emissions to vary between 2 and 59 Tg CH_4 yr^{-1} by the year 2100 (Burke et al., 2012). Recent data-constrained projections of permafrost carbon emissions suggest a total increase of CH_4 emissions of 5.3-14 Tg CH_4 yr^{-1} between the years 2010 and 2100 (Koven et al., 2015a). However, the latter results are based on the assumption of fixed wetland extent. Moreover, none of the above studies include a representation of CH_4 emissions from thermokarst lakes or account for the complete feedback loop between permafrost carbon emissions and climate.

Thus far, only two studies estimate permafrost CH_4 emissions by accounting for the complete loop for the permafrost carbon feedback, although with 1-D and 2-D models for the northern high-latitudes (Schneider von Deimling et al., 2012, 2015). The first study suggests that permafrost CH_4 emissions could accumulate to 207-1336 Tg CH_4 by the year 2100 following gradual permafrost degradation and CH_4 emissions from wetlands (Schneider von Deimling et al., 2012). This study is based on simulations by a 1-D (latitude) module for the uppermost (3 m) permafrost coupled to a climate-carbon cycle model of reduced complexity. In the second study, a 2-D (latitude x depth) modeling approach is considered, with a parameterization of the areal extent of thermokarst lakes as a function of surface air temperature (Schneider von Deimling et al., 2015). The study indicates that permafrost CH_4 emissions could accumulate to 836-2614 Tg CH_4 by the year 2100 with a substantial contribution from thermokarst lakes. In terms of CH_4 fluxes, the simulations suggest that thermokarst lakes alone could emit 50 Tg CH_4 yr^{-1} in the middle of the 21st century when these lakes will reach their maximum areal extent (Schneider von Deimling et al., 2015). In the latest IPCC assessment report, a maximum of 5000 Tg CH_4 was estimated for permafrost CH_4 emissions by the year 2100 (Ciais et al., 2013).

Permafrost CH_4 emissions will occur along with CO_2, contributing to the total permafrost carbon emissions. By assuming a global warming potential of 33 for CH_4 (over 100 years), an assessment based on a survey with permafrost experts suggests that, if climate change follows the Representative Concentration Pathway (RCP) 8.5 scenario, the fraction of CH_4 in total permafrost carbon emissions will vary between 1.5% and 3.5% throughout the next two centuries, with a best estimate of 2.3% (Schuur et al.,

2013). This estimate has been adopted by more recent studies of the permafrost carbon feedback (Schaefer et al., 2014; Schuur et al., 2015). Studies based on simple models support a range of 1-4% for the fraction of CH_4 in total permafrost carbon release by and beyond the year 2100 (Schneider von Deimling et al., 2012, 2015).

2.5. The future warming to expect from permafrost CH_4 emissions

There are currently few published studies on the impact of permafrost CH_4 emissions on global mean surface air temperature. This is mostly due to the fact that most climate models still lack a representation of the permafrost carbon pool and CH_4 emissions from anaerobic environments (Arora et al., 2013; Ciais et al., 2013). Up to now, only four studies with CH_4 emissions estimate the total warming to expect from permafrost carbon emissions (Table 2.1). Among these studies, the two that represent the complete feedback loop with simple coupled climate-carbon cycle models estimate the weakest permafrost carbon feedback, perhaps due to relatively small cumulative CO_2 emissions from thawed soils compared to other studies (Table 2.1).

A meta-analysis of several modelling studies on future permafrost carbon emissions and their climate impact provides a constrained estimate of the strength of the permafrost carbon feedback by the end of the century (Schaefer et al., 2014). This meta-analysis constrains the warming associated with permafrost CO_2 emissions by the year 2100 to 0.06-0.40°C, with the best estimate of 0.23°C (Table 2.1). By assuming a fraction of 2.3% for CH_4 in total permafrost carbon emissions and a global warming potential of 33 for CH_4 (over 100 years), the strength of the permafrost carbon feedback by the year 2100 is increased to 0.29 (0.08-0.50) °C due to a contribution of 0.06 (0.01-0.11) °C from wetland CH_4 emissions (Schaefer et al., 2014). However, thermokarst CH_4 emissions are missing in these calculations.

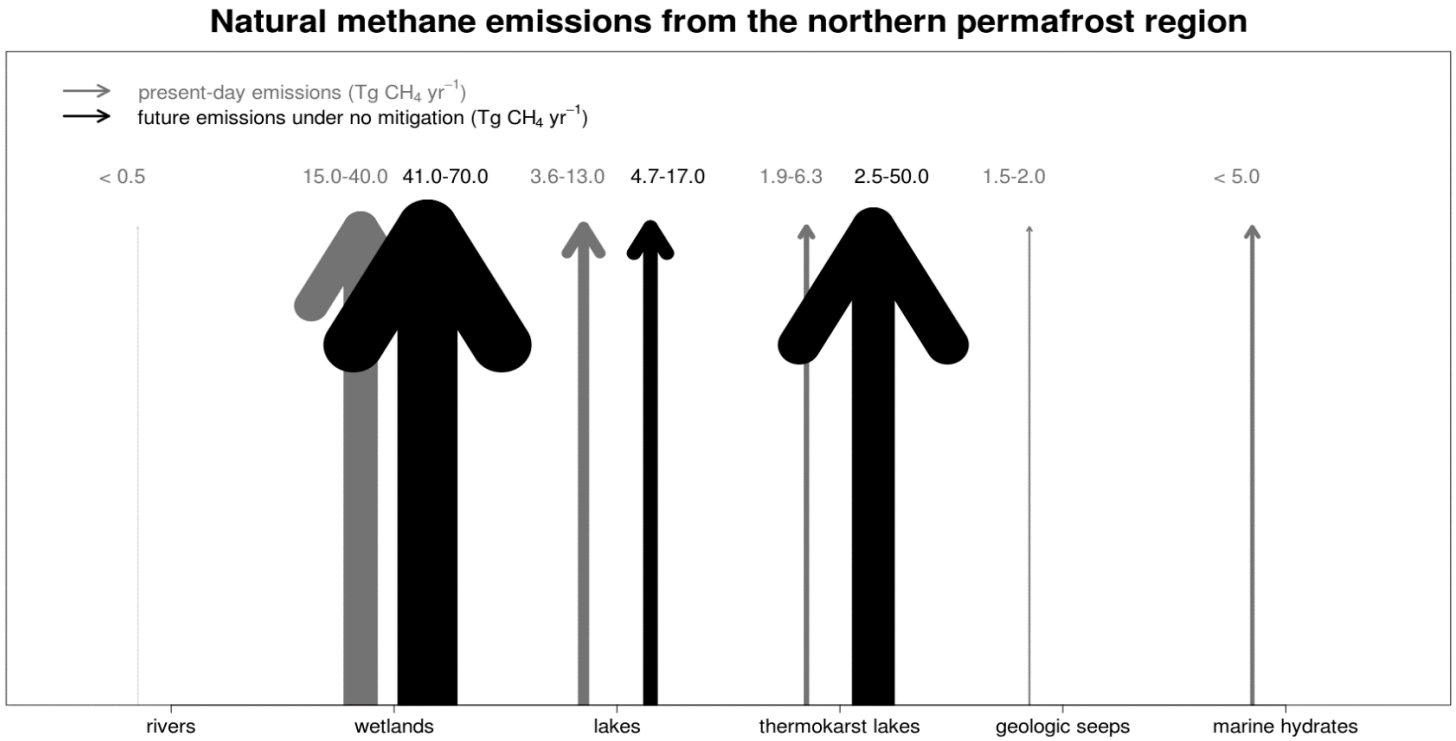

Figure 2.1. **Illustration of how annual rates of natural CH_4 emissions (Tg CH_4 yr^{-1}) from the northern permafrost region could change during the current century. Grey and black arrows indicate present-day and future CH_4 emissions, respectively. The width of each arrow is proportional to regional CH_4 emissions from sources documented in the literature. Sources of CH_4 considered here are rivers (present-day: (Bastviken et al., 2011)), wetlands (present-day: (Christensen et al., 2015; Kirschke et al., 2013); future: (Koven et al., 2011, 2015a)), lakes (present-day: (Bastviken et al., 2011; Wik et al., 2016); future: (Wik et al., 2016)), thermokarst lakes (present-day: (Walter Anthony et al., 2016; Wik et al., 2016); future: (Schneider von Deimling et al., 2015; Wik et al., 2016)), geologic seeps (present-day : (Walter Anthony et al., 2012)), and marine hydrates (present-day: (Saunois et al., 2016a)).**

Although CH_4 may not exceed 4% of total permafrost carbon emissions (Schaefer et al., 2014; Schneider von Deimling et al., 2015; Schuur et al., 2013), the contribution from CH_4 to the warming associated with the permafrost carbon feedback by the year 2100 is assessed to be 10-50% (Table 2.1). Constrained estimates suggest that CH_4 emitted following gradual thaw in wetlands will contribute to 20.6% of the warming by the end of the century (Schaefer et al., 2014). However, expert assessment, review and modelling studies that explicitly or implicitly consider additional CH_4 emissions from thermokarst lakes suggest that the contribution from CH_4 to climate warming by the year 2100 could be higher, ranging between 30% and 50% (Table 2.1). It follows that projections of the permafrost carbon feedback based on CO_2 emissions alone are missing a substantial fraction of the warming to be expected by the year 2100.

2.6. Policy implications of the permafrost carbon feedback

In the natural world, permafrost CH_4 and CO_2 emissions occur concomitantly and their impact on the global climate should not be separated. For this reason, we discuss policy implications associated with both CH_4 and CO_2 emissions from thawed carbon in this section.

2.6.1. Avoiding the warming associated with permafrost carbon release

The projected permafrost degradation and change in carbon storage under climate change are regarded as irreversible on the scale of human lifetime (Schaefer et al., 2011; Schuur et al., 2015). But, will it be possible for humans to have a control on the release of CO_2 and CH_4 from thawed soils and the associated warming?

Experts assess that two-thirds of the projected carbon release from thawed soils could be avoided if mitigation of climate change in line with the RCP 2.6 scenario is effectively achieved (Schuur et al., 2013). However, even if anthropogenic emissions would cease immediately, the permafrost carbon feedback has been shown to be a self-sustained process, with the capacity of leading to continued accumulation of CO_2 in the atmosphere throughout the 21st and 22nd centuries, especially if the Earth system has a climate sensitivity larger than 3°C (MacDougall et al., 2012). The latter result highlights how the permafrost carbon feedback might offset efforts to mitigate climate change.

Therefore, for limiting the global mean temperature below a certain threshold, the permafrost carbon feedback needs to be considered in the carbon budget compatible with that threshold.

MacDougall and colleagues investigated the effect of the permafrost carbon feedback on remaining carbon budgets for the 2°C, 2.5°C and 3°C warming thresholds (MacDougall et al., 2015). Considering the 2°C threshold, for example, their results suggest that the permafrost carbon feedback could reduce allowable emissions by 85-150 Pg C depending on the future concentration pathway. As the carbon budget for 2°C was estimated at 770-800 Pg C (with the consideration of non-CO_2 greenhouse gases and aerosols) (MacDougall et al., 2015), we deduce that the permafrost carbon emissions could contribute to 10-19% of the allowable carbon emissions for this warming threshold. In the case of eventual exceedance of the 2°C threshold, the permafrost carbon feedback would require larger reductions (> 300 Pg C) of the carbon budget in order to return to 2°C by means of artificial CO_2 removal (MacDougall et al., 2015).

Based on the above information, we consider that aiming for the 2°C warming threshold without accounting for the permafrost carbon feedback could be futile. In addition, further studies should be conducted to assess the implications of the feedback on the carbon budget compatible with the 1.5°C warming threshold.

2.6.2. The permafrost carbon feedback beyond the 21st century

Throughout the 21st century and beyond, CH_4 emissions in the northern permafrost zones highly depend on the response of wetlands and lakes to climate change. For instance, wetlands could become drier or wetter (Lawrence et al., 2015), their areal extent could decline (Avis et al., 2011), and thermokarst lakes could drain in the discontinuous permafrost zone and expand in the continuous permafrost zone (Schuur et al., 2015). Numerical models suggest that CH_4 emissions from thermokarst lakes will peak in the middle of the 21st century, and decline throughout the 22nd and 23rd centuries following a reduced extent of these lakes through increased drainage (Schneider von Deimling et al., 2015). CH_4 emissions from wetlands could be more important after the 21st century, due to a relatively slower progression of permafrost thaw in wetlands than in thermokarst lakes (Schneider von Deimling et al., 2015). As discussed earlier, CH_4 from hydrates could also come into play beyond the 21st century.

Table 2.1. Projected cumulative permafrost CH_4 and CO_2 emissions and their impact on global mean surface air temperature by the year 2100.

	Cumulative permafrost carbon emissions		Impact on global climate expressed as change in global mean surface air temperature			Share of CH4 in the global climate impact
Study reference	CH_4 (Tg CH_4)	CO_2 (Pg C)	ΔT (CH_4) (° C)	ΔT (CO_2) (° C)	ΔT (Total) (° C)	Fraction of ΔT or RF (%)
Koven et al. (2011)	n. a.	62 (55-69)	n. a.	n. a.	n. a.	n. a.
Ciais et al. * (2013)	Max. 5000	Max. 250	n. a.	n. a.	n. a.	n. a.
Schneider von Deimling et al. (2012) [a]	533 (207-1336)	63 (33-114)	n. a.	n. a.	0.1 (0.04-0.23)	Up to 13
Koven et al. (2015) [a]	n. a.	57.4 (27.9-112.6)	n. a.	n. a.	n. a.	10-18
Schaefer et al. (2014) [b]	n. a.	120 (45-205)	0.06 (0.01-0.11)	0.23 (0.06-0.40)	0.29 (0.08-0.50)	20.6
Burke et al. (2012)	n. a.	50-270	n. a.	n. a.	0.08-0.36	25
Schneider von Deimling et al. (2015) *	1474 (836-2614)	87 (42-141)	n. a.	n. a.	0.09 (0.05-0.14)	Up to 40
Schuur et al. (2015) *	n. a.	37-174	n. a.	n. a.	n. a.	35-48
Schuur et al. (2013) *	n. a.	158 (120-196) [c]	n. a.	n. a.	n. a.	33-50

The reported numbers correspond to projections under scenarios of unmitigated emissions. ΔT and RF stand for temperature change and radiative forcing, respectively. The results are listed in order of increasing share of permafrost CH_4 in the impact on global climate. Studies that consider CH_4 emissions from both wetlands and thermokarst lakes are indicated by an asterisk (*). Otherwise, permafrost CH_4 emissions are from wetlands alone. Where available, best estimates are reported with ranges in brackets.

[a] The results in Schneider von Deimling et al. (2012) and Koven et al. (2015) are based on the assumption of fixed areal extent of wetlands.

[b] The study by Schaefer et al. (2014) is a meta-analysis of all studies on projected permafrost carbon emissions and their impact on global climate published before 2014.

[c] The reported cumulative permafrost CO_2 emissions for Schuur et al. (2013) are values based on results from the meta-analysis by Schaefer et al. (2014).

Experts assess that permafrost carbon emissions could double between the years 2100 and 2300 under scenarios of unmitigated emissions (Schuur et al., 2013). However, it has been suggested that the largest warming from permafrost carbon release after the year 2100 should not be expected from a scenario of unmitigated emissions but from low to medium mitigation scenarios (MacDougall et al., 2012; Schneider von Deimling et al., 2015). This counter-intuitive result is generally attributed to the decreasing radiative efficiency of CO_2 and CH_4 under high levels of these greenhouse gases in the atmosphere (MacDougall et al., 2012; Schneider von Deimling et al., 2015).

2.7. Research gaps and sources of uncertainties

None of the reviewed studies considers the complete feedback loop between climate warming and the release of both CO_2 and CH_4 from thawed carbon with an Earth system model. While some studies use terrestrial ecosystem models and simple climate models to estimate permafrost degradation and carbon emissions (Koven et al., 2011) or induced warming (Burke et al., 2012), some others are based on expert opinions (Schuur et al., 2013) or consider a coupled modelling approach for the northern high-latitudes (Schneider von Deimling et al., 2012, 2015). So far, projections of the permafrost carbon feedback with a consistent representation of the feedback loop in a 3-D Earth system model do not include permafrost CH_4 emissions (MacDougall et al., 2012). In addition, most studies that model CH_4 release from thawed soils focus on emissions from wetlands and ignore those from thermokarst lakes, which could be substantial in the future (Schneider von Deimling et al., 2015).

Uncertainties in projections of the permafrost carbon feedback can arise from several aspects including the biogeochemical processes regulating CH_4 emissions, the geographical distribution of soil carbon across the northern permafrost region and the variation of decomposition rates. A whole set of uncertainties is associated with processes of CH_4 production and oxidation as well as the outgassing pathways that determine CH_4 emissions in anaerobic environments (Christensen et al., 2015). In addition, the carbon content is not homogeneous throughout the northern permafrost region (Hugelius et al., 2014) and the initial carbon pool set in modelling studies has been shown to be the most important source of uncertainties for estimating the permafrost carbon feedback for a given future climate scenario (Burke et al., 2012).

Moreover, there are different types of frozen soils (Hugelius et al., 2014), each type being associated with a particular range of rates of permafrost degradation and carbon decomposition (Olefeldt et al., 2013; Schuur et al., 2015; Treat et al., 2015). Uncertainties in permafrost CH_4 emissions can also arise from the influence of small-scale changes in vegetation cover (Nauta et al., 2015) and the dynamics of microbial communities (Bridgham et al., 2013; McCalley et al., 2014).

Representing anaerobic environments with their geographical distribution in global models is challenging for both wetlands (Melton et al., 2013) and thermokarst lakes (Kokelj and Jorgenson, 2013). In particular, global models might not resolve well the transition from aerobic to anaerobic conditions associated with thermokarst development in various ice-rich permafrost locations, because ground subsidence generally occurs at localized scale (Kokelj and Jorgenson, 2013). In addition, because thawing may enhance soil drainage and therefore reducing CH_4 release in some locations, or permafrost degradation may result in ground subsidence and more prevalent anaerobic environments with higher CH_4 emissions in other locations, the complex interplay between permafrost dynamics and hydrology is an important factor for quantifying permafrost CH_4 emissions (O'Connor et al., 2010). Furthermore, acceleration of permafrost carbon losses associated with wildfires (Turetsky et al., 2011), river and coastal erosion (Schuur et al., 2008) might not be well resolved by global models. Sub-grid parameterizations of these processes in global models are required for constraining the magnitude of permafrost carbon emissions.

Atmospheric CH_4 is a chemically active gas whose oxidation generates other greenhouse gases and its impact on radiative forcing is also associated with potential uncertainties. Lastly, the strength of the permafrost carbon feedback will depend on the response of the human society to climate change which is highly unpredictable (Burke et al., 2012; MacDougall et al., 2012; Schneider von Deimling et al., 2015).

2.8. Conclusions

The positive feedback between climate warming and permafrost CH_4 emissions is expected following increasing surface temperatures across the northern high-latitudes. Although considerable progress in permafrost carbon research has been made in the

last decade, more research is needed to better quantify the contribution from CH_4 to the permafrost carbon feedback.

Our review emphasizes how CH_4 emissions from thermokarst lakes, generally unrepresented in climate models, could increase the share of CH_4 in the permafrost carbon feedback on global mean surface air temperature. Although CH_4 might not exceed 4% of total permafrost carbon emissions, available climate projections suggest that permafrost CH_4 emissions from wetlands could contribute to 20.6 % of the warming induced by permafrost carbon release by the year 2100, while CH_4 emissions from both wetlands and thermokarst lakes could contribute to 30-50% by the end of the century. Parameterization of processes regulating CH_4 emissions in thermokarst lakes is a required step towards better projections of the permafrost carbon feedback.

The permafrost carbon feedback has considerable policy implications. Research suggests that this feedback could claim up to 150 Pg C from the amount of carbon emissions required to keep the global warming below 2°C above pre-industrial levels (MacDougall et al., 2015). Further research on the implications of the permafrost carbon feedback on the 1.5°C warming threshold is needed for current climate policy.

Chapter 3. A new wetland methane model for implementation in Earth system models

A version of this chapter is under review with Geoscientific Model Development.

Citation details: Nzotungicimpaye, C-M., MacDougall, A. H., Melton, J. R., Treat, C. C., Eby, M., Lesack, L. F. W., and Zickfeld K.: WETMETH 1.0: A new wetland methane model for implementation in Earth system models, Geoscientific Model Development, https://doi.org/10.5194/gmd-2020-176, in review, 2020.

Contribution statement: I developed the wetland CH4 model and implemented it in the UVic ESCM. I performed the model calibration, carried out the model simulations, evaluated the model performance, and drafted the manuscript. Dr. Andrew H. MacDougall implemented TOPMODEL for wetland identification in the UVic ESCM. Dr. Joe R. Melton and Dr. Kirsten Zickfeld contributed to the model development. Dr. Lance F.W. Lesack contributed to illustrated soil profiles. Dr. Andrew H. MacDougall and Dr. Michael Eby provided guidance during the model implementation in the UVic ESCM. Dr. Claire C. Treat contributed to the model calibration. All authors provided critical feedback on the manuscript.

Abstract

Wetlands are the single largest natural source of methane (CH_4), a powerful greenhouse gas affecting the global climate. In turn, wetland CH_4 emissions are sensitive to changes in climate conditions such as temperature and precipitation shifts. However, biogeochemical processes regulating wetland CH_4 emissions are not routinely included in fully coupled Earth system models that simulate feedbacks between the physical climate, the carbon cycle, and other biogeochemical cycles. This chapter introduces a process-based wetland CH_4 model (WETMETH) developed for implementation in Earth system models and currently embedded in an Earth system model of intermediate complexity. Here we: (i) describe the wetland CH_4 model; (ii) evaluate the model performance against available datasets and estimates from the literature; (iii) analyze the model sensitivity to perturbations of poorly constrained parameters. Historical simulations show that WETMETH is capable of reproducing mean annual emissions consistent with present-day estimates across spatial scales. For the 2008-2017 decade the model simulates global mean wetland emissions of 158.6 Tg CH_4 yr^{-1}, of which 33.1 Tg CH_4 yr^{-1} are from wetlands north of 45°N. WETMETH is highly sensitive to parameters for the microbial oxidation of CH_4, which is the least constrained process in the literature.

3.1. Introduction

Wetlands are vegetated locations that are inundated with water on a permanent, seasonal or recurrent basis (Wheeler, 1999). In the context of this study, wetlands are defined following the latest global CH_4 budget report (Saunois et al., 2020): natural ecosystems with inundated or water-saturated soils where anoxic conditions lead to the production of CH_4. Wetlands across the globe are the single largest natural source of atmospheric CH_4, accounting for approximately a third of total global emissions (Bridgham et al., 2013; Saunois et al., 2016a). Estimates of global wetland CH_4 emissions over the past few decades vary between 140 and 210 Tg CH_4 yr^{-1} (Kirschke et al., 2013). Although there exist different types of wetlands such as bogs, fens, swamps, marshes and floodplains (Aselmann and Crutzen, 1989; Saunois et al., 2016a), the release of CH_4 from any wetland results from the balance between two biogeochemical processes (Segers, 1998): the production of CH_4 by anaerobic microbes (namely methanogens) and the oxidation of CH_4 primarily by aerobic microbes (namely methanotrophs).

Both CH_4 production and oxidation in wetlands are sensitive to changes in climate conditions. For instance, soil warming accelerates the microbial activity with a higher response for methanogenic than methanotrophic activity (Bridgham et al., 2013; Dunfield et al., 1993; Segers, 1998). At the landscape or larger scale, increased wet conditions tend to enhance methanogenic activity to the detriment of methanotrophic activity (Duval and Radu, 2018; Helbig et al., 2017; Kim, 2015). In turn, wetland CH_4 emissions can affect the global climate through changes in atmospheric CH_4 levels and associated radiative forcing (Dean et al., 2018; O'Connor et al., 2010). Analyses of ice cores suggest that CH_4 emissions from tropical and northern wetlands contributed significantly to climate changes during past glacial-interglacial transitions (Loulergue et al., 2008; Rhodes et al., 2017).

The interactions between climate conditions and wetland CH_4 emissions translate into a positive feedback loop that has the potential to amplify changes in global mean surface air temperature, which is a major concern for future climates (Dean et al., 2018; O'Connor et al., 2010). Research on feedbacks between the physical climate and biogeochemical cycles is generally conducted with 3-dimensional (3-D) fully coupled Earth system models (ESMs) (Arora et al., 2013). Over the past decade, these ESMs

have proven very useful to investigate and inform international climate policies such as the accounting of carbon emissions required to avoid the risk of dangerous climate change (Zickfeld et al., 2009) and achieve the goals of the Paris Agreement (Tokarska and Gillett, 2018). Yet, biogeochemical processes regulating CH_4 emissions in wetlands are not commonly included in fully coupled ESM simulations.

In the past, several process-based models have been developed for investigating the response of wetland CH_4 emissions to climate variability and climate change (Hodson et al., 2011; Hopcroft et al., 2011; Pandey et al., 2017; Paudel et al., 2016; Shindell et al., 2004; Zhang et al., 2018; Zhu et al., 2015). These wetland CH_4 models are generally embedded in terrestrial or land surface models and forced with observational datasets or reanalysis products (Melton et al., 2013; Wania et al., 2013; Xu et al., 2016). A second application for wetland CH_4 models has been to quantify the climate response to wetland CH_4 emissions (Gedney et al., 2004, 2019; Zhang et al., 2017b). In this case, results from wetland CH_4 models are used in climate-carbon cycle model emulators to assess their impact on radiative forcing (Gedney et al., 2019; Zhang et al., 2017b). These modelling studies have contributed to advance research on the possible evolution of wetland CH_4 emissions in the 21st century (Koven et al., 2011; Shindell et al., 2004), the magnitude of their impact on the global climate (Gedney et al., 2019; Zhang et al., 2017b), and their implications for international climate policy (Comyn-Platt et al., 2018). However, their quasi-coupling methods do not reflect the complete feedback loop between climate conditions and wetland CH_4 emissions as expected in the natural world. So far, only 1-D and 2-D models of the northern high-latitude regions have been applied for simulating the feedback between climate conditions (temperature changes) and wetland CH_4 emissions in a fully coupled mode (Schneider von Deimling et al., 2012, 2015).

The implementation of process-based wetland CH_4 models in fully coupled ESMs is needed in order to advance research on wetland CH_4-climate feedbacks in the context of global climate projections (Dean et al., 2018). In particular, this addition to Earth system modelling should be beneficial to ongoing research on the permafrost carbon feedback (Nzotungicimpaye and Zickfeld, 2017; Schuur et al., 2015) and the remaining carbon budget for achieving the goals of the Paris Agreement (Rogelj et al., 2019).

This chapter introduces a wetland CH_4 model developed for implementation in ESMs and currently embedded in an Earth system model of intermediate complexity (EMIC). Our study aims at developing a computationally efficient process-based model for simulating large-scale wetland CH_4 emissions constrained with sparse observations. Section 3.2 gives an overview of processes regulating CH_4 emissions in wetlands. Section 3.3 provides the model description and an outline of performed model simulations. Section 3.4 describes the model calibration and choice of parameter values. Section 3.5 presents the model performance evaluation. Section 3.6 describes the model sensitivity to poorly constrained parameters. Sections 3.7 and 3.8 are for discussions and conclusions, respectively.

3.2. Overview of processes regulating CH_4 emissions in wetlands

3.2.1. Microbial production of CH_4

Wetlands host several communities of microbes adapted to the predominant anoxic conditions of these environments (Bridgham et al., 2013). Some of these microbes are methanogens, which decompose organic matter for their metabolism and produce CH_4 as a by-product of their respiration (McCalley et al., 2014; Segers, 1998). The organic matter decomposed by methanogens in wetlands originates from litter-fall, root exudates, dead plants and dissolved organic carbon (Bridgham et al., 2013; Conrad, 2009; Girkin et al., 2018; Mitsch and Mander, 2018). In the northern permafrost region, carbon from thawed soils constitutes an additional source of organic matter to methanogens (Kwon et al., 2019; Olefeldt et al., 2013).

There are three pathways through which methanogens produce CH_4 from soil organic matter (Le Mer and Roger, 2001; Segers, 1998; Whalen, 2005). The first pathway is operated by methanogens that rely on acetate for their metabolism, resulting in the production of both CH_4 and carbon dioxide (CO_2) (Bridgham et al., 2013; Whalen, 2005). The second pathway is operated by methanogens that produce CH_4 through CO_2 reduction in the presence of hydrogen (Bridgham et al., 2013). The third pathway is operated by methanogens that use methylated substrates (e.g. methanol, methylamines, and dimethysulfide) for their metabolism (Zalman et al., 2018).

Rates of CH_4 production in wetlands are generally highest in upper anoxic layers due to several factors such as the quality of organic matter and the spread of active microbial populations. For instance, in comparison to soil layers at depth where organic matter can be recalcitrant to microbial decomposition, the organic matter in near-surface soil layers is more labile due to fresh inputs from litter-fall and vegetation mortality (Treat et al., 2015; Walz et al., 2017; Wild et al., 2016). Furthermore, observations at various sites show that methanogenic activity decreases as depth increases (Bridgham et al., 2013; Cadillo-Quiroz et al., 2006).

Increasing soil temperatures stimulate the dynamics and growth of methanogenic communities in wetlands, resulting in an increase of CH_4 production rates (Bridgham et al., 2013; Segers, 1998). However, several studies indicate that there is an optimal temperature for methanogenic activity between 25°C and 30°C (Dean et al., 2018; Dunfield et al., 1993). Other factors promoting the occurrence of CH_4 production in wetlands include the persistence of anoxic conditions as well as soil pH varying between acidic and neutral (Dunfield et al., 1993; Segers, 1998).

3.2.2. Microbial oxidation of CH_4

In wetlands, methanotrophs (CH_4-oxidizing microbes) populate oxic portions of the soil column (Bridgham et al., 2013; Conrad, 2009; Whalen, 2005). Such oxic portions are primarily soil layers close to the surface which are in contact with the atmosphere, commonly near and above the water table (Bridgham et al., 2013; Le Mer and Roger, 2001; Segers, 1998). In the presence of vascular plants, other oxic portions of the soil column can be found near the roots due to the downward transport of oxygen (O_2) through plant aerenchyma (Kwon et al., 2019; Whalen, 2005). All these oxic portions of the soil column constitute the so-called oxic zone, which is predominantly made of soil layers near and above the water table (Bridgham et al., 2013; Conrad, 2009; Segers, 1998). Methanotrophs consume CH_4 that ascends from the zones of production at depth to the overlying oxic zone for their metabolism, and primarily produce CO_2 as part of their respiration (Bridgham et al., 2013; Segers, 1998).

While O_2 has been considered for years to be the only electron acceptor involved in the microbial oxidation of CH_4, there is a growing evidence of the occurrence of CH_4 oxidation under anoxic conditions operated by anaerobic microbes that rely on alternate

electron acceptors such as nitrate and sulfate (Dean et al., 2018). However, although anaerobic CH_4 oxidation in marine environments has been well established for decades (Hoehler et al., 1994; Reeburgh, 1976), this process remains poorly investigated in wetlands despite its potential importance for the CH_4 cycle (Gauthier et al., 2015; Smemo and Yavitt, 2011).

In analogy to CH_4 production, CH_4 oxidation is influenced by changes in soil temperatures (Bridgham et al., 2013; Segers, 1998). For instance, CH_4 oxidation rates increase during the summer because of intensified microbial activity but also the availability of substantial CH_4 in response to increased soil temperatures (Segers, 1998). However, the temperature response for CH_4 oxidation is generally lower than that for CH_4 production (Bridgham et al., 2013; Dean et al., 2018; Dunfield et al., 1993; Segers, 1998).

3.2.3. Mechanisms transporting CH_4 to the atmosphere

There exist various mechanisms transporting CH_4 produced in wetlands to the atmosphere. Three transport mechanisms are well documented in the literature and generally monitored in situ (Bridgham et al., 2013; Whalen, 2005): the diffusion of CH_4 whereby molecules of CH_4 slowly ascend the overlying water column, the ebullition of CH_4 whereby bubbles of CH_4 rapidly ascend towards the soil surface, as well as the transport of CH_4 through the aerenchyma of vascular plants. However, other transport mechanisms for CH_4 in wetlands have been revealed: the hydrodynamic transport of CH_4 in the form of upwelling caused by temperature gradients primarily at nighttime (Poindexter et al., 2016), and the transport of CH_4 through tree stems (Bridgham et al., 2013; Conrad, 2009; Pangala et al., 2017) whose driving processes are still not well understood (Barba et al., 2019).

Methane oxidation is highly dependent on the predominant transport mechanism for CH_4. The water table position plays a crucial role in affecting what fraction of the produced CH_4 reaches the atmosphere (Blodau, 2002; Moore and Roulet, 1993; Segers, 1998). When the water table is well below the surface, methanotrophs may oxidize all of the diffusing CH_4 before the gas reaches the atmosphere (Segers, 1998). In the presence of vascular plants, a lower fraction of the produced CH_4 is oxidized because these plants allow the gas to bypass the oxic zone where methanotrophs are hosted

(Blodau, 2002; Bridgham et al., 2013; Segers, 1998). In the case of ebullition, which often occurs episodically, CH_4 may escape to the atmosphere with reduced opportunities for oxidation (Bridgham et al., 2013; Whalen, 2005). How CH_4 oxidation relates to the transport of CH_4 through tree stems (Barba et al., 2019) or by hydrodynamic processes (Poindexter et al., 2016) is not well established.

3.2.4. A synopsis of wetland CH_4 dynamics

Figure 3.1 illustrates vertical profiles of soil organic content, CH_4 concentration, and CH_4 oxidation rates in a soil column with and without inundation at the surface based on principles outlined in the literature (Blodau et al., 2004; Whiticar and Faber, 1985). In general, the water table position determines the maximum depth at which O_2 is available in the soil column (i.e. the oxic-anoxic interface). When the surface is flooded and the water is stagnant (Figure 3.1a), O_2 diffuses slowly into the soil column and may only be present in a portion of the upper soil layer which is in contact with the atmosphere. Under such predominantly anoxic conditions, CH_4 production occurs throughout the soil column and the concentration of CH_4 mirrors soil organic content – eventually with a small reduction near the surface due to CH_4 oxidation. A modest amount of ascending CH_4 may be oxidized throughout the soil column, but with highest oxidation rates near the surface where some O_2 may be available as an electron acceptor. The combination of high CH_4 production and only modest CH_4 oxidation in the soil column results in large CH_4 emissions into the atmosphere.

When the flooding recedes, O_2 becomes more prevalent in the upper soil column where CH_4 concentration decreases following a slow down or shut down of CH_4 production as aerobic microbes dominate the competition for organic matter (Figure 3.1b). CH_4 production persists below the oxic-anoxic interface where the concentration of CH_4 mirrors soil organic content owing to the predominant anoxic conditions. Ascending CH_4 becomes subject to substantial oxidation in the soil column with the highest oxidation rates above the oxic-anoxic interface where O_2 is abundant. The combination of decreased CH_4 production and substantial CH_4 oxidation in the soil column results in small or no CH_4 emissions into the atmosphere.

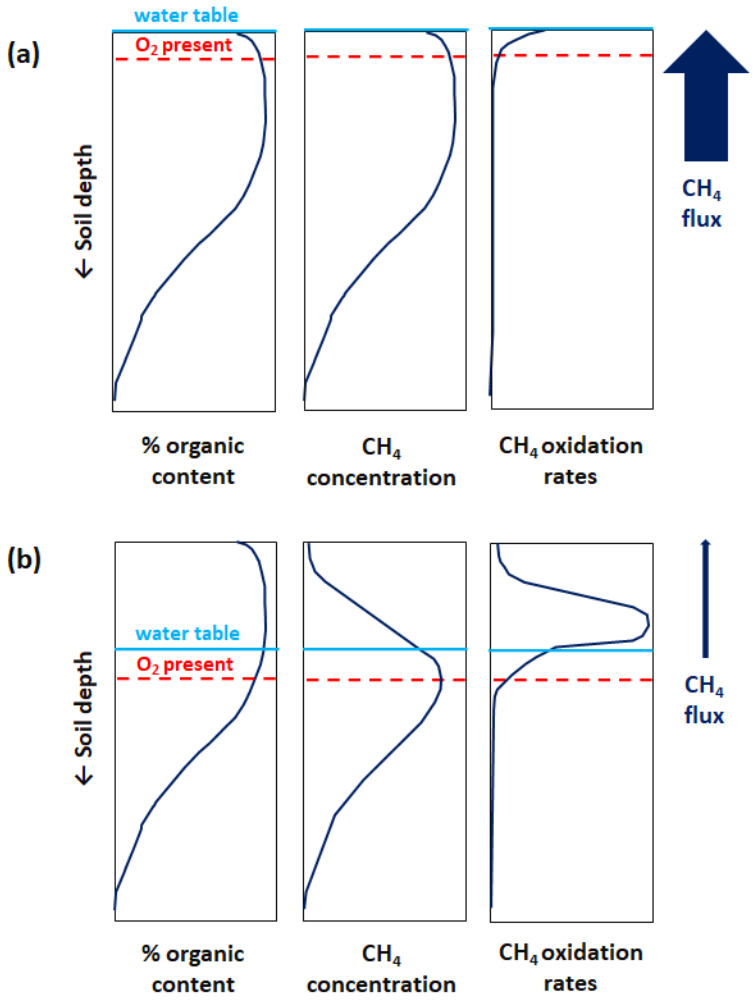

Figure 3.1. **Illustrated vertical profiles of soil organic content, CH_4 concentration and oxidation rates in a soil column with inundation at the surface (a) and without inundation at the surface (b). The vertical profiles are based on principles outlined in the literature (Blodau et al., 2004; Whiticar and Faber, 1985). For simplicity, the soil organic content is assumed to be identical in (a) and (b). In each case, the blue horizontal line illustrates the water table position and the dashed red horizontal line illustrates the oxic-anoxic interface or maximum depth at which O_2 is available in the soil column. The relative magnitude of CH_4 flux in the soil column is shown by the upward arrow to the right, also characterizing the relative magnitude of CH_4 emissions into the atmosphere.**

3.3. Model description and simulations

3.3.1. The new wetland CH_4 model: WETMETH

Microbial production and oxidation of CH_4 are parameterized in WETMETH using a multi-layer ground structure with information on the moisture distribution, the amount of organic matter (carbon content), and the average temperature in each soil layer. These soil variables are commonly simulated by ESMs. Figure 3.2 provides a schematic representation of WETMETH for a soil column with and without inundation at the surface. By configuration, it is considered that CH_4 emissions in WETMETH may occur not only from inundated locations, but also from non-inundated ecosystems with a relatively high level of soil moisture content (Saunois et al., 2016a, 2020).

For any land location, the rate of microbial CH_4 production in an underlying soil layer *i* (P_i in kg C m^{-3} s^{-1}) is parameterized as:

$$P_i = S(\theta_i)\, C_i\, r\, Q_{10}^{\frac{T_i - T_0}{10}}\, \exp\left(-\frac{z_i}{\tau_{prod}}\right), \qquad (3.1)$$

where $S(\theta_i)$ is the fraction of soil layer that is saturated with water, and C_i is the amount of soil carbon (in kg C m^{-3}) in the layer. The product of $S(\theta_i)$ and C_i represents the organic matter (in kg C m^{-3}) available for microbial decomposition under anoxic conditions. When the soil surface is not flooded (Figure 3.2b), dry soil layers ($S(\theta_i)$ = 0) are assumed to be predominantly oxic and not producing CH_4 (P_i = 0) mostly due to aerobic microbes dominating the competition for organic matter which results in the starvation of methanogens (Segers, 1998).

The global factor r is the specific CH_4 production rate (in kg kg^{-1} s^{-1}), which can be defined as the mass of CH_4-C that is produced per kilogram of available soil C per unit of time. A meta-analysis of incubated soil samples from various anaerobic landscapes indicates that r can vary between 0.3 to 27.2 µg of CH_4-C per g of soil C per day (equivalent to the range from 3.5 x 10^{-12} to 3.1 x 10^{-10} kg kg^{-1} s^{-1}) depending on the landscape type, relative water table position, and soil depth (Treat et al., 2015). Section 3.4.1 discusses the choice of the value for r as part of the model calibration.

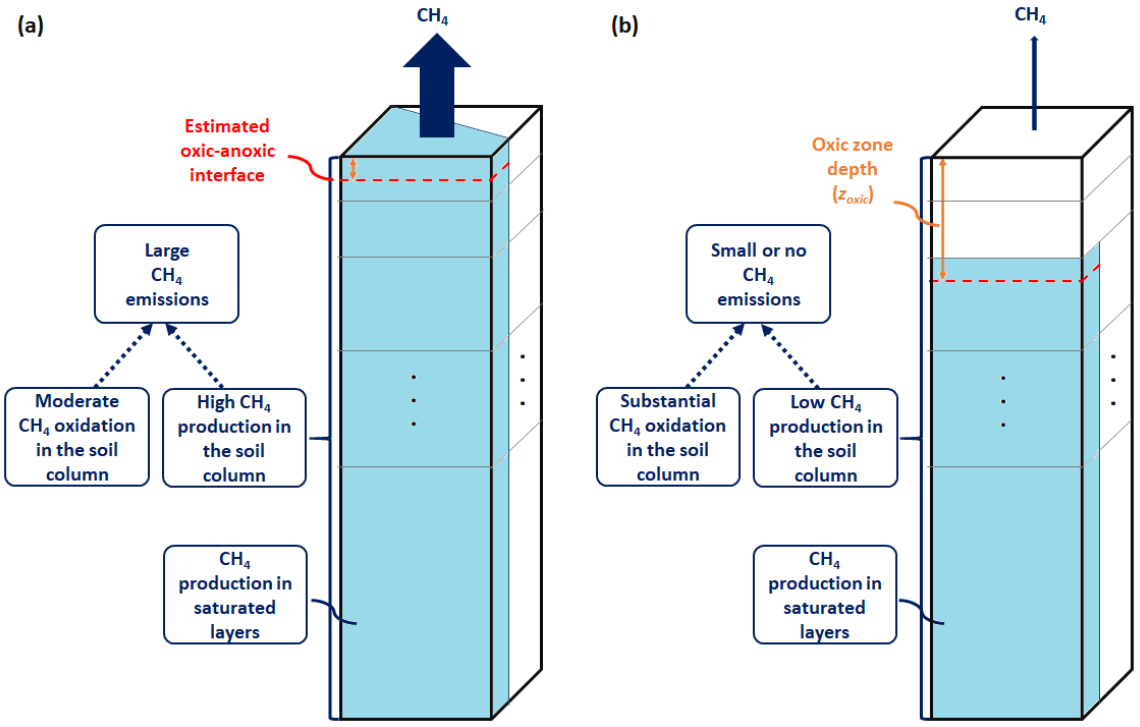

Figure 3.2. Illustration of the new wetland CH_4 model (WETMETH) and the dynamics of wetland CH_4 processes as represented in the model. This schematic representation depicts a soil column (model grid box) with inundation at the surface (a) and without inundation at the surface (b). The soil column is shown here with multiple layers of unequal thicknesses. The blue area at the surface of (a) represents the inundated surface area. The blue sections in the different soil layers of (a) and (b) represent water-saturated zones. For both (a) and (b), the dashed red horizontal line illustrates the oxic-anoxic interface and the orange vertical arrow shows the relative thickness of the oxic zone or oxic zone depth (z_{oxic}). Larger CH_4 emissions are expected to occur when the soil surface is flooded than when it is not due to relatively high CH_4 production and moderate CH_4 oxidation in the soil column.

The expression $Q_{10}^{\frac{T_i - T_0}{10}}$, which depends on the average layer temperature T_i (in Kelvin, K) and a baseline temperature T_0 (273.15 K), represents the temperature-dependency of CH_4 production expressed with a Q_{10} coefficient as commonly done to approximate the sensitivity of biological processes to a temperature change of 10 K (Hegarty, 1973). While some biological processes double in rate with a warming of 10 K, several studies report a higher temperature sensitivity for CH_4 production (i.e. Q_{10} > 2) although with large uncertainties (Lupascu et al., 2012; Sjögersten et al., 2018; Walz et al., 2017; Whalen, 2005). Nevertheless, a meta-analysis of temperature-response studies suggests an average Q_{10} of about 4.2 for CH_4 production in pure cultures of

methanogens (Hoehler and Alperin, 2014; Yvon-Durocher et al., 2014) in agreement with previous estimates (Blodau, 2002). In order to account for uncertainties with this coefficient and define the occurrence of an optimal temperature for CH_4 production (Blake et al., 2015; Dean et al., 2018; Dunfield et al., 1993), a temperature-dependent Q_{10} is considered in WETMETH. Its mathematical formulation is $Q_{10}(T_i) = 1.7 + 2.5 \tanh [0.1 (T_{ref} - T_i)]$, where $T_{ref} = 308.15$ K is a reference temperature (Table 3.1). This formulation is defined following an expression used for soil respiration in another study (Wu et al., 2016). Additional information on this formulation and its implications for the temperature-dependency of CH_4 production are provided in Appendix A. Furthermore, CH_4 production in WETMETH is assumed to shut down in frozen soil layers although research suggests that slow microbial activity can occur at temperatures below 273.15 K (Panikov and Dedysh, 2000; Rivkina et al., 2004).

The expression $\exp(-\frac{z_i}{\tau_{\mathrm{prod}}})$, which depends on the depth of the soil layer *i* relative to the surface (z_i in m, positive downwards), describes the declining effect of various environmental controls on CH_4 production with depth that are generally unresolved by ESMs. These environmental factors include the quality of organic matter and the spread of methanogens among other factors (Bridgham et al., 2013; Koven et al., 2015b; Treat et al., 2015; Walz et al., 2017; Wild et al., 2016). Here, τ_{prod} (in m) is a scaling parameter for CH_4 production. The choice of the value for τ_{prod} is discussed later as part of the model calibration (see Section 3.4.1).

Table 3.1. Model parameters for CH_4 production and oxidation in WETMETH.

Parameter	Description	Units	Chosen value
r	Specific CH_4 production rate	kg kg^{-1} s^{-1}	[a] 2.6 x 10^{-10}
Q_{10}	Temperature coefficient for CH_4 production	—	[b] 4.2
T_{ref}	Reference temperature for CH_4 production	K	[c] 308.15
τ_{prod}	Scaling parameter for CH_4 production	m	0.75
z_{oatz}	Thickness of the oxic-anoxic transition zone	m	0.05
τ_{oxid}	Scaling parameter for CH_4 oxidation	m	0.0146

[a] This value is equivalent to 22.8 µg CH_4-C produced per g of soil C per day; [b] A temperature-dependent Q_{10}, approximating 4.2 for a wide range of temperatures, is used instead (see Appendix A); [c] The reference temperature is used to define an optimal temperature for CH_4 production (see Appendix A).

The total amount of CH_4 produced in the soil column (P in kg C m^{-2} s^{-1}) is calculated as:

$$\mathrm{P} = \int_{i=1}^{i=k} \mathrm{P}_i \, d\mathrm{z}_i \ , \tag{3.2}$$

where P_i (in kg C m^{-3} s^{-1}) is the rate of CH_4 production in the soil layer *i* from Eq. (3.1), dz_i (in m) is the thickness of the soil layer *i*, and *k* represents the bottom-most soil layer. This amount of CH_4 (P) is then subject to oxidation in transit to emission into the atmosphere.

Microbial CH_4 oxidation is parameterized based on the amount of CH_4 produced in the soil column and the relative thickness of the oxic zone. Specifically, the total amount of CH_4 oxidized in the soil column (O_x in kg C m^{-2} s^{-1}) and net CH_4 emissions to the atmosphere (E in kg C m^{-2} s^{-1}) are calculated as:

$$\mathrm{O}_x = \mathrm{P}\,(1 - \exp(-\frac{z_{\mathrm{oxic}}}{\tau_{\mathrm{oxid}}})), \tag{3.3}$$

$$\mathrm{E} = \mathrm{P} - \mathrm{O}_x \ , \tag{3.4}$$

which is equivalent to the following expression:

$$\mathrm{E} = \mathrm{P}\ \exp(-\frac{z_{\mathrm{oxic}}}{\tau_{\mathrm{oxid}}}) \ , \tag{3.5}$$

where P (in kg C m^{-2} s^{-1}) is the total amount of CH_4 produced in the soil column as defined in Eq. (3.2), z_{oxic} (in m) is the relative depth (positive downwards) to the oxic-anoxic interface (Figure 3.2), and τ_{oxid} (in m) is a scaling parameter for CH_4 oxidation. As for τ_{prod}, the choice of the value for τ_{oxid} is discussed as part of the model calibration (see Section 3.4.2).

Regarding z_{oxic}, we assume that O_2 may be present in soil layers unsaturated with water as well as in a shallow oxic-anoxic transition zone within the upper-most soil layer saturated with water (Figure 3.2). In this first development of WETMETH, we consider a constant thickness (z_{oatz}) of 0.05 m for the oxic-anoxic transition zone, with its bottom defined as the oxic-anoxic interface (Frolking et al., 2002; Singleton et al., 2018). The penetration of O_2 into the soil and its dynamics with changing moisture conditions can be complex depending on site-specific factors such as the soil composition (Estop-Aragonés et al., 2012) and the presence of vascular plants (Brune et al., 2000). In addition, methanotrophs may be present at depth (> 0.05 m) below the water table probably following some adaptation to low O_2 conditions (Singleton et al.,

2018). Nevertheless, the approach applied here for z_{oxic} is reasonable for ESMs not resolving O_2 dynamics and microbial communities in the soil.

For Eq. (3.3), the expression $(1-\exp(-\frac{z_{\mathrm{oxic}}}{\tau_{\mathrm{oxid}}}))$ represents the fraction of P that gets oxidized in transit to emission into the atmosphere. Various studies report estimates of CH_4 oxidation as a fraction of produced CH_4 in the soil column (Blazewicz et al., 2012; Le Mer and Roger, 2001; Roslev and King, 1996; Segers, 1998; Singleton et al., 2018). From sample-to-sample and site-to-site, however, CH_4 oxidation exhibits a broad range of values ranging from less than 20% to more than 95% depending on the sampled soil depth ranges, whether or not potential CH_4 oxidation under anoxic conditions is considered, the monitored transport mechanisms for CH_4 among many other factors (Blazewicz et al., 2012; Couwenberg et al., 2010; Jauhiainen et al., 2005; Kwon et al., 2019; Le Mer and Roger, 2001; Moosavi and Crill, 1998; Roslev and King, 1996; Segers, 1998; Singleton et al., 2018; Whalen, 2005). Nevertheless, the largest fractions of oxidized CH_4 are generally associated with the deepest water tables or oxic-anoxic interfaces (Bridgham et al., 2013; Couwenberg et al., 2010; Jauhiainen et al., 2005; Roslev and King, 1996; Segers, 1998; Whalen, 2005).

The parameterization described in Eq. (3.3) is a simple approach for characterizing CH_4 oxidation in the soil column. Such a parameterization is practical when there is little knowledge on the soil chemistry (e.g. O_2 and alternate electron acceptors), the dynamics of methanotrophs and other environmental factors exerting a control on CH_4 oxidation (Blazewicz et al., 2012; Blodau, 2002; Dean et al., 2018; Kwon et al., 2019; Singleton et al., 2018; Smemo and Yavitt, 2011). Most importantly, this parameterization considers the net effect of all mechanisms transporting CH_4 from the anoxic soil layers where the gas is produced to the atmosphere. The oxidized CH_4 is assumed to produce CO_2 that becomes part of the soil respiration routinely simulated by ESMs.

3.3.2. The embedding Earth system model

WETMETH has been embedded in the University of Victoria Earth System Climate Model (UVic ESCM), an Earth system model of intermediate complexity (EMIC) (Weaver et al., 2001). A modified version of the EMIC based on UVic ESCM 2.9 (Eby et al., 2009) is used here. The UVic ESCM consists of a 3-D ocean general circulation model that is

coupled to a dynamic-thermodynamic sea ice model, a 2-D (vertically-integrated) energy-moisture balance model for the atmosphere, and a land surface model (Weaver et al., 2001). The land surface model is a modified version of the Met Office Surface Exchange Scheme (MOSES) with 14 ground layers of unequal thickness extending down to a depth of 250 m that can simulate permafrost processes such as freeze-thaw dynamics (Avis et al., 2011). The top eight ground layers (~10 m in total depth) are soil layers and contribute to the water cycle, whereas the bottom six ground layers are bedrock layers (Avis et al., 2011). In the hydraulically active layers, porosity and permeability are determined based on the relative abundance of prescribed sand, clay, and silt-sized particles. Water phase changes are determined over a range of soil temperatures to determine the fraction of frozen and unfrozen water in the ground (Avis et al., 2011). All components of the UVic ESCM have a horizontal grid resolution of 3.6° in longitude and 1.8° in latitude (Eby et al., 2009; Weaver et al., 2001).

Wetlands in the UVic ESCM are identified in grid cell areas based on soil moisture content and topography. Model grid cells in which wetlands can occur are those with unfrozen soil moisture contents greater than 65% of the saturated moisture content in the upper soil layer for at least one day in a year (Avis et al., 2011). Instead of using a fixed global threshold value for topography (Avis et al., 2011), the version of the UVic ESCM used in this study identifies wetland coverage at the sub-grid scale following a TOPMODEL approach for global models (Gedney and Cox, 2003). Appendix B describes a minor modification applied to this TOPMODEL approach. Section 3.5.1 presents an evaluation of wetlands simulated by the UVic ESCM.

The UVic ESCM includes a representation of the global carbon cycle. The terrestrial carbon cycle (CO_2 fluxes) is simulated using the Top-down Representation of Interactive Foliage and Flora including Dynamics (TRIFFID), a dynamic global vegetation model that is coupled to the land surface model (Avis et al., 2011; Meissner et al., 2003). TRIFFID defines the state of the terrestrial biosphere in terms of soil carbon as well as the structure and coverage of five plant functional types (PFTs): broadleaf trees, needleleaf trees, shrubs, C3 grasses and C4 grasses (Cox, 2001; Matthews et al., 2004; Meissner et al., 2003). Terrestrial carbon gain occurs through photosynthesis that is simulated as a function of atmospheric CO_2 concentration, shortwave radiation, air temperature, humidity, and soil moisture. Soil carbon gain occurs through litter-fall and vegetation mortality. The present-day permafrost carbon pool is simulated by the UVic

ESCM following a method that approximates the effect of long-term freeze-thaw cycles on the vertical distribution of carbon in permafrost-affected soils, a process referred to as cryoturbation (MacDougall and Knutti, 2016). Soil carbon can accumulate in the top six ground layers (~3.35 m in total depth). Terrestrial carbon loss occurs through autotrophic respiration by plants and heterotrophic respiration by soil microbes (Matthews et al., 2004; Meissner et al., 2003). By configuration, permafrost carbon can only be lost through microbial respiration and this heterotrophic respiration is assumed to shut down in frozen soil layers (MacDougall et al., 2012; MacDougall and Knutti, 2016).

The marine carbon cycle in the UVic ESCM is represented with organic and inorganic carbon cycle models (Eby et al., 2009). The organic carbon cycle is based on marine biology simulated with a nutrient-phytoplankton-zooplankton-detritus (NPZD) ecosystem model (Schmittner et al., 2008). The inorganic carbon cycle model simulates the air-sea exchange of CO_2 and ocean carbonate chemistry following the protocols of the Ocean Carbon-Cycle Model Intercomparison Project (OCMIP) (Orr, 1999; Weaver et al., 2001). Dissolved inorganic carbon is treated as a passive tracer that is subject to ocean circulation (Weaver et al., 2001). Carbonate dissolution in ocean sediments is simulated with a model of respiration in marine sediments (Archer, 1996; Eby et al., 2009).

3.3.3. Model simulations

For this research, three series of model simulations are performed with the UVic ESCM in its standard fully coupled mode and including WETMETH parameterizations. Firstly, the UVic ESCM is spun up for ~5000 years at year 1850 conditions to allow the model to reach an equilibrium climate state representing the pre-industrial period. Secondly, a transient run over the 1850-2019 period is performed in order to evaluate the model performance. This transient run is based on prescribed CO_2 concentration and other forcing data (such as solar radiation, sulfate aerosols and non-CO_2 greenhouse gases) from the fifth phase of the Coupled Model Intercomparison Project (CMIP5) (Taylor et al., 2012). The UVic ESCM is driven by historical data over the 1850-2005 period and by Representative Concentration Pathway (RCP) 8.5 data over the 2006-2019 period. Figure D1 illustrates how the simulated historical climate conditions compare to observations in terms of global mean surface air temperature. Thirdly, a set of transient runs from 2000 to 2009 is performed to analyze the model sensitivity to poorly

constrained parameters. This set of model simulations (sensitivity runs) is performed by perturbing values of poorly constrained parameters associated with wetland CH_4 processes.

3.4. Choice of model parameter values

Here, we describe the choice of three WETMETH parameters (r and τ_{prod} for CH_4 production; τ_{oxid} for CH_4 oxidation) as part of the model calibration. These model parameters are tuned to observations from northern high-latitude regions due to the scarcity of large-scale datasets from other regions. The model calibration against northern observations is based on the assumption that tuned parameter values will be valid across the globe, which is an important limitation as it will be discussed later. Nonetheless, this approach is deemed reasonable given the present state of data availability. Section 3.5.1 describes northern wetlands simulated by the UVic ESCM as part of the model validation.

3.4.1. CH_4 production parameters

Parameters for CH_4 production in WETMETH are calibrated against maximum CH_4 production rates measured in laboratory incubations of soil samples from several anaerobic environments across northern high-latitude regions (>50°N). These potential CH_4 production rates are obtained from a synthesis dataset, which includes information on other environmental variables such as the relative depth of the soil samples (Treat et al., 2015).

To allow a fair model-data comparison, measured CH_4 production rates with corresponding soil bulk density from the sites of origin are converted into units of kg C m^{-3} s^{-1} (see Appendix C). Furthermore, measurements from landscapes identified as uplands and lakes (in the dataset) are excluded from the dataset used in this model calibration. The remaining measurements are potential CH_4 production rates in soil samples from landscapes identified (in the dataset) as wetlands, floodplains, and lowlands across Alaska.

To set values for r and τ_{prod} from Eq. (3.1), the depth profile of simulated CH_4 production rates across Alaska for the year 2000 is tuned to that of the measurements.

By setting r to 22.8 µg CH_4-C produced per g of soil C per C day (equivalent to 2.6 x 10^{-10} kg kg^{-1} s^{-1}) and τ_{prod} to 0.75 m, we obtain a depth profile of simulated CH_4 production rates that compares fairly well to that of potential CH_4 production rates from the laboratory incubations (Figure 3.3). These default values for r and τ_{prod} are listed in Table 3.1. Section 3.6 presents a sensitivity analysis on these model parameters.

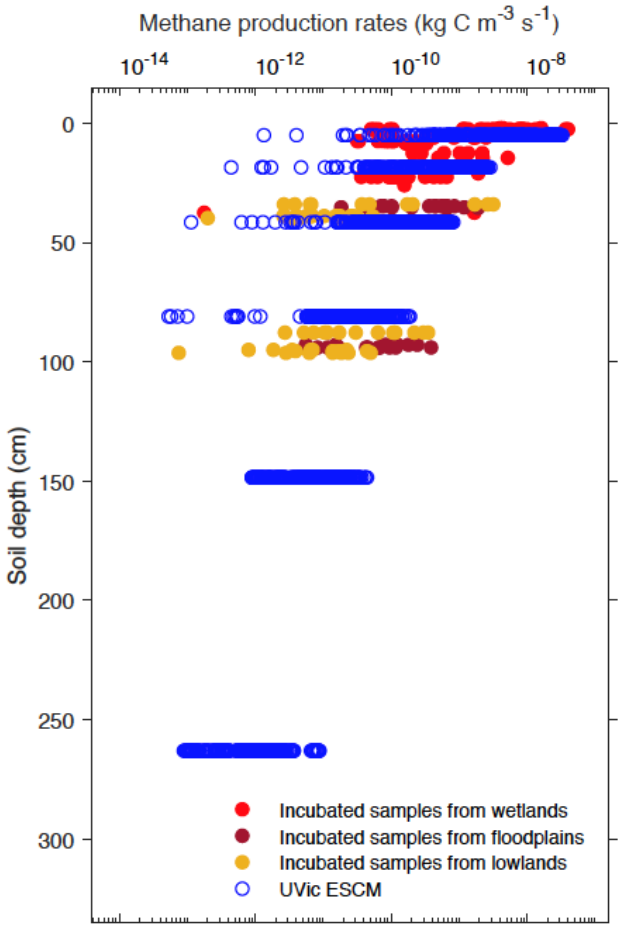

Figure 3.3. Vertical profiles of simulated and potential CH_4 production rates from wetlands across Alaska. Potential CH_4 production rates are measurements from laboratory incubations of soil samples collected from various anaerobic ecosystems (Treat et al., 2015). Both simulated and measured CH_4 production rates are shown here with a log-transformed axis (base-10 logarithmic scale).

3.4.2. CH_4 oxidation parameter

Unlike for CH_4 production, there are no published large-scale measurements of CH_4 oxidation rates that could be used in this research for the calibration of CH_4 oxidation.

For that reason, CH_4 oxidation in WETMETH is indirectly calibrated via CH_4 emissions. A synthesis dataset of seasonal and annual CH_4 emissions from various terrestrial sites across temperate, boreal and Arctic regions is used to this end (Treat et al., 2018). The model calibration focuses on annual CH_4 emissions from sites north of 50°N for which many data points are available in the dataset.

While most data points are from direct measurements of CH_4 emissions, some data points are associated with different modelling methods for estimating CH_4 emissions (Treat et al., 2018). To allow a fair model-data comparison, only data points associated with direct measurements of CH_4 emissions are included in the model calibration. Furthermore, measurements from lakes, uplands and alpine landscapes are excluded from this model calibration. In particular, the exclusion of data points from uplands and alpine landscapes sorts out measurements of terrestrial CH_4 uptake (negative CH_4 flux). The retained data points (n = 119) include measurements by chambers (85.7%), flux towers (13.4%) and a combination of flux towers and chambers (0.8%).

The model calibration in this section aims at choosing a value of τ_{oxid} from Eq. (3.5) such that the range (minimum - maximum) of annual CH_4 emissions across northern wetlands (>50°N) simulated by the UVic ESCM is comparable to that of annual CH_4 emissions from the data points (0.1-60.6 g CH_4 m^{-2} yr^{-1}). By setting τ_{oxid} to 0.0146 m, we constrain simulated CH_4 emissions from northern wetlands (specifically, grid-cell CH_4 emissions divided by the inundated fraction of the grid cell) over the 2000-2009 decade in the range of 0.04-65.6 g CH_4 m^{-2} yr^{-1}. This default value for τ_{oxid} is listed in Table 3.1. Section 3.6 presents a sensitivity analysis on this model parameter.

3.5. Evaluation of the model performance

3.5.1. Wetlands

Figure 3.4 shows the latitudinal distribution of wetland areas simulated by the UVic ESCM in comparison to two global datasets. The first dataset is Global Inundation Extent from Multi-Satellites (GIEMS), which is based on remotely sensed inundation areas (Papa et al., 2010; Prigent et al., 2001, 2007a, 2012). The second dataset is Surface Water Microwave Product Series-Global Lakes and Wetlands Database

(SWAMPS-GLWD), which is based on a combination of information from satellites and maps of inundated areas in order to reduce uncertainties associated with the distribution of global wetlands (Poulter et al., 2017). The comparison between the model and the datasets is done over 2000-2007, which is the overlap period for the datasets. Over this period the UVic ESCM simulates an annual maximal extent of ~12.6 million km^2 for global wetlands, whereas GIEMS and SWAMPS-GLWD estimate ~9.3 and ~10.6 million km^2, respectively.

The UVic ESCM agrees better with SWAMPS-GLWD in regions north of 40°N although with some underestimations around 55°N, and relatively well with GIEMS between 20-40°S (Figure 3.4). However, the model simulates too small wetland areas between 20-30°N when compared to both GIEMS and SWAMPS-GLWD. While our model could be underestimating wetland areas in this latitude zone, inundated areas estimated by GIEMS include rice paddies which prevail in tropical and sub-tropical regions (Prigent et al., 2007a, 2012). Rice paddies are likely not represented in SWAMPS-GLWD as there were efforts to only include natural wetlands during the development of this dataset (Poulter et al., 2017). In comparison to GIEMS and SWAMPS-GLWD, our model simulates small wetland areas in South-East Asia especially near Bangladesh (Figure 3.5 and Figure 3.6).

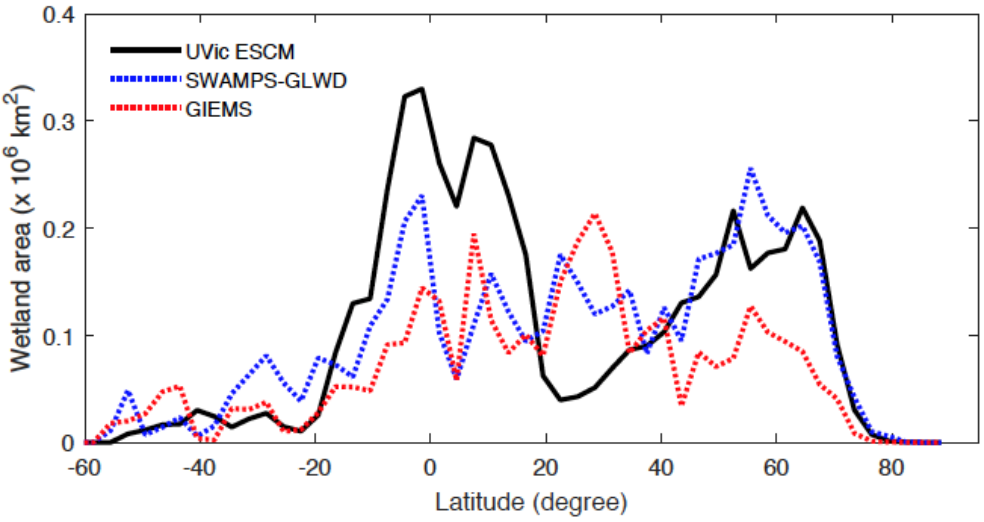

Figure 3.4. Latitudinal distribution of wetland areas simulated by the UVic ESCM over the 2000-2007 period in comparison to two global datasets: GIEMS and SWAMPS-GLWD. The comparison period corresponds to the overlap period for the two datasets. The wetland areas are summed across latitude bins of 3°.

Between 20°N and 20°S, the UVic ESCM simulates a bimodal distribution of the wetland extent that is consistent with the two datasets although the model simulates too large wetland areas (Figure 3.4). Unlike for GIEMS and SWAMPS-GLWD, wetlands simulated by the UVic ESCM are widespread in Amazonia, West and Central Africa (Figure 3.5 and Figure 3.6). Although the UVic ESCM could be overestimating the extent of wetlands in some of these equatorial regions, it is possible that GIEMS and SWAMPS-GLWD do not detect inundated areas in densely forested regions due to forest canopies. Recent studies suggest that tropical wetlands are commonly underestimated in large-scale datasets (Dargie et al., 2017; Gumbricht et al., 2016).

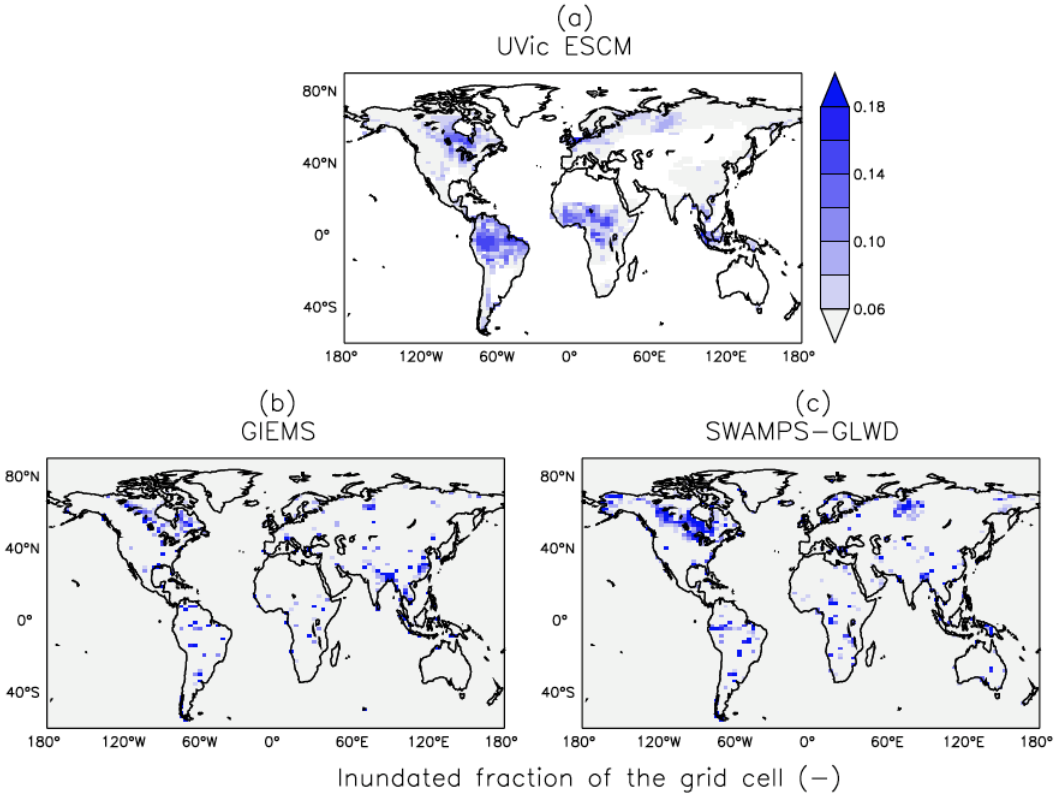

Figure 3.5. Average wetland extents (inundated fractions of grid cells) across the globe over the 2000-2007 period as simulated by the UVic ESCM (a) in comparison to two datasets: (b) GIEMS and (c) SWAMPS-GLWD. The datasets are regridded to 3.6° x 1.8° for a fair comparison with the UVic ESCM. The comparison period corresponds to the overlap period for the two datasets.

Conversely, it is possible that the UVic ESCM overestimates tropical wetland areas due to soil hydraulic properties unrepresented in the model. A potential cause for the overestimation of tropical wetlands in our model is the standard approach for

simulating global hydrology in land surface models based on the concentration of only sand, clay, and silt in the soil. A recent study suggests that the inclusion of ferralsols (weathered soils with micro-aggregated particles that are common in the humid tropics) in a global terrestrial model can help improve the simulation of tropical wetlands (Gedney et al., 2019).

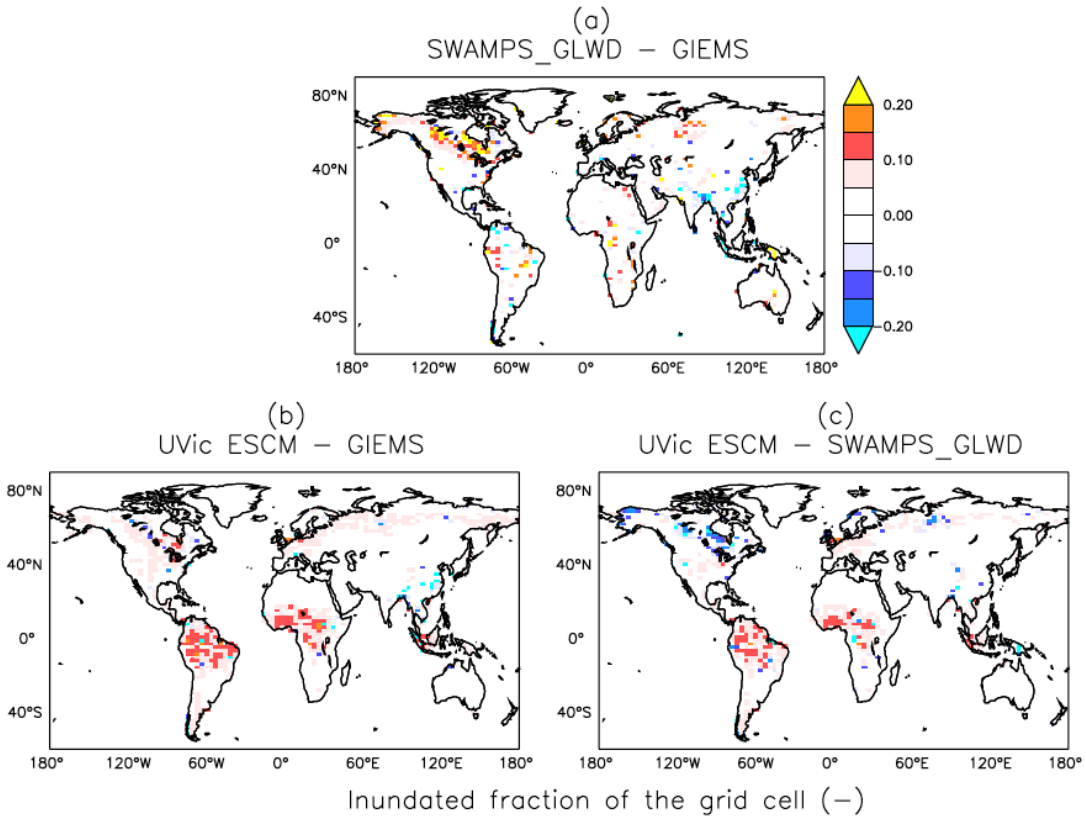

Figure 3.6. Differences in global wetland extents (inundated fractions of grid cells) between two datasets (GIEMS and SWAMPS-GLWD) and the UVic ESCM over the 2000-2007 period: (a) SWAMPS-GLWD – GIEMS, (b) UVic ESCM – GIEMS, and (c) UVic ESCM – SWAMPS-GLWD. The comparison period corresponds to the overlap period for the two datasets.

Outside of the tropics, the UVic ESCM does a better job at simulating the distribution of wetlands in sub-Arctic and Arctic regions (Figure 3.7). The model simulates the occurrence of wetlands (i.e. surface inundation) across the West Siberian Lowlands (WSL) in Russia, the Hudson Bay Lowlands (HBL) in Canada as well as over other parts of northern Canada in agreement with both SWAMPS-GLWD and GIEMS (Figure 3.7). However, some disagreements between the UVic ESCM and the two datasets can also be identified: (i) in comparison to GIEMS, the UVic ESCM simulates

more wetland area in the Hudson Bay Lowlands (HBL) as well as widespread wetlands in parts of northern Eurasia (Figure 3.7b and Figure D2b); (ii) in comparison to SWAMPS-GLWD, the model simulates less wetland area over the WSL and northern Canada including the HBL and more wetland area in parts of Europe (Figure 3.7c and Figure D2c).

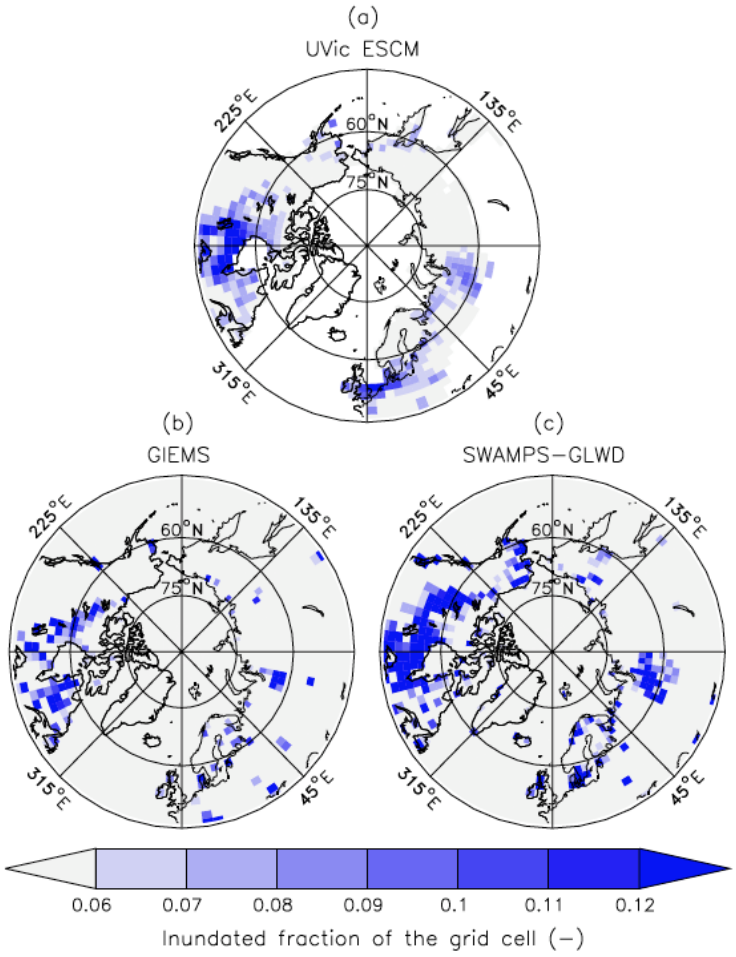

Figure 3.7. Average wetland extents (inundated fractions of grid cells) in the north of 45°N over the 2000-2007 period as simulated by the UVic ESCM (a) in comparison to two datasets: (b) GIEMS and (c) SWAMPS-GLWD. The datasets are regridded to 3.6° x 1.8° for a fair comparison with the UVic ESCM. The comparison period corresponds to the overlap period for the two datasets.

3.5.2. Wetland CH_4 emissions

Given the relative coarse grid resolution of the UVic ESCM, the model validation with respect to wetland CH_4 emissions focuses on large-scale emissions such as regional,

zonal, and global emissions. Moreover, this model validation focuses on northern high-latitude regions because observations and estimates of wetland CH_4 emissions from other regions (e.g. the tropics) are scarce. This focus is further justified by the fact that our model better simulates the distribution of wetlands in northern high-latitude regions than in the tropics (see Section 3.5.1). Indeed, the extent of wetlands is a major control for wetland CH_4 emissions simulated by process-based models and probably the primary contributor to related uncertainties (Melton et al., 2013; Saunois et al., 2020; Zhang et al., 2017a).

The UVic ESCM simulates total CH_4 emissions from northern wetlands that are in the range of recent estimates. Over the 2013-2014 period, the model simulates mean annual emissions of 33.2 Tg CH_4 yr^{-1} for wetlands north of 45°N (Table 3.2). These CH_4 emissions are consistent with estimates from recent upscaled flux measurements (UFMs) over the same period based on a random forest (RF) algorithm and three wetland maps (Peltola et al., 2019): 30.6 ± 9.2 Tg CH_4 yr^{-1} (RF-DYPTOP), 31.7 ± 9.4 Tg CH_4 yr^{-1} (RF-PEATMAP), and 37.6 ± 11.8 Tg CH_4 yr^{-1} (RF-GLWD) (Table 3.2). Table E2 (see Appendix E) shows that the UVic ESCM has no preferential agreement with one of the three UFMs.

Figure 3.8 shows the spatial distribution of simulated CH_4 emissions in comparison to the three UFMs. When compared to each other, the three UFMs exhibit substantial differences primarily attributed to the distinct wetland distributions (Peltola et al., 2019). Considering the general pattern and magnitude of wetland CH_4 emissions, the UVic ESCM agrees with either two or all three UFMs over key source regions such as the Hudson Bay Lowlands (HBL), the West Siberian Lowlands (WSL), western Europe and south-central Canada (Figure 3.8). The UVic ESCM simulates less CH_4 emissions over parts of northeastern Canada and Fennoscandia in comparison to the UFMs (Figure 3.8). However, the three UFMs do not necessarily agree on both the distribution and magnitude of wetland CH_4 emissions in these regions. Furthermore, the UVic ESCM does not simulate wetland CH_4 emissions in southern Eurasia (40-135°E; 45-60°N) while the three UFMs suggest that CH_4 can be emitted from sporadic wetlands in this region (Figure 3.8). Overall, the mismatch between the UFMs and our model in terms of northern CH_4 emissions can be primarily attributed to differences in the areal extent of wetlands, but also to the spatial distribution of soil carbon simulated by the UVic ESCM (MacDougall and Knutti, 2016).

In terms of mean annual emissions from key source regions, the UVic ESCM simulates 2.9 Tg CH_4 yr^{-1} for the Hudson Bay Lowlands (HBL) over the 2013-2014 period (Table 3.2). Although these emissions are lower than estimates by the three UFMs (3.1-6.5 Tg CH_4 yr^{-1}) (Peltola et al., 2019), estimates by inverse models (2.0-3.4 Tg CH_4 yr^{-1}) over this region are comparable to our model results (Miller et al., 2014; Pickett-Heaps et al., 2011; Thompson et al., 2017). Furthermore, the UVic ESCM simulates total wetland emissions of 4.1 Tg CH_4 yr^{-1} for the West Siberian Lowlands (WSL) over the 2013-2014 period (Table 3.2). Regional estimates based on the three UFMs are higher (4.9-8.5 Tg CH_4 yr^{-1}) than our model results over the same period (Peltola et al., 2019), whereas previous observation-based estimates for the WSL suggest regional wetland emissions (3.9 ± 1.3 Tg CH_4 yr^{-1}) that are similar to our model results (Glagolev et al., 2011). Estimates by inverse models over the WSL are relatively high but comparable to our model estimates (Table 3.2): 6.1 ± 1.2 Tg CH_4 yr^{-1} (Bohn et al., 2015) and 6.9 ± 3.6 Tg CH_4 yr^{-1} (Thompson et al., 2017).

The UVic ESCM is also evaluated with respect to wetland CH_4 emissions over the 2000-2009 and 2008-2017 decades, which both are reference periods for the latest global CH_4 budget report (Saunois et al., 2020). For wetlands north of 40°N, the UVic ESCM simulates emissions of 37.7 Tg CH_4 yr^{-1} over the 2000-2009 decade and 38.5 Tg CH_4 yr^{-1} over the 2008-2017 decade. These wetland CH_4 emissions are consistent with recent estimates (37.4 ± 7.2 Tg CH_4 yr^{-1}) from data-constrained model ensembles over the same region (Treat et al., 2018). For wetlands north of 45°N, the model simulates total CH_4 emissions that are in the range of estimates for the 2013-2014 period discussed earlier (32.4 Tg CH_4 yr^{-1} over 2000-2009 and 33.1 Tg CH_4 yr^{-1} over 2008-2017). For Pan-Arctic wetlands (>60°N), the UVic ESCM simulates emissions of 17.4 Tg CH_4 yr^{-1} over the 2000-2009 decade and a similar amount over the 2008-2017 decade (Table 3.2). These wetland CH_4 emissions correspond to the upper limit of bottom-up estimates (2-18 Tg CH_4 yr^{-1}) from the latest global CH_4 budget report (Saunois et al., 2020).

Table 3.2. Mean annual wetland CH_4 emissions simulated by the UVic ESCM in comparison to estimated emissions from the literature. All emissions are reported in Tg CH_4 yr^{-1} and uncertainty ranges are provided for estimates from the literature. Three periods are used to allow a fair comparison between the UVic ESCM and estimates from the literature where possible: 2008-2017 as in the latest global CH_4 budget report (Saunois et al., 2020), 2013-2014 as for recent upscaled flux measurements across the northern high-latitudes (Peltola et al., 2019), and 1993-2004 as for the WETCHIMP model ensemble (Melton et al., 2013). Principal methods used in the different references for estimates are reported in the last column: Top-down (TD) methods including inverse models (IM), and bottom-up (BU) methods including upscaled measurements (UM) as well as process-based models (PM).

	Geographical delimitation	UVic ESCM period	UVic ESCM emissions	Estimated emissions	Reference for estimates	Method in reference
Hudson Bay Lowlands	50 – 60°N; 75 – 96°W	2013-2014	2.9	2.3 ± 0.3	Pickett-Heaps et al., 2011	BU
				2.4 ± 0.3	Miller et al., 2014	IM
				2.7 - 3.4	Thompson et al., 2017	IM
West Siberian Lowlands	50 – 75°N; 60 – 95 °E	2013-2014	4.1	3.9 ± 1.3	Glagolev et al., 2011	UM
				6.1 ± 1.2	Bohn et al., 2015 [a]	IM
				6.9 ± 3.6	Thompson et al., 2017	IM
Pan-Arctic Wetlands	60°N – 90°N	2008-2017	17.3	7 – 16	Saunois et al., 2020	TD
				2 – 18	Saunois et al., 2020	BU
Northern Wetlands	40°N – 90°N	2008-2017	38.5	37.4 ± 7.2	Treat et al., 2018	BU
	45°N – 90°N	2013-2014	33.2	30.6 ± 9.2	Peltola et al., 2019	UM
				31.7 ± 9.4	Peltola et al., 2019	UM
				37.6 ± 11.8	Peltola et al., 2019	UM
Tropical Wetlands	30°S – 30°N	1993-2004	105.5	126 ± 31	Melton et al., 2013 [a]	PM
				90 ± 77	Sjögersten et al. 2014	UM
Global Wetlands	90°S – 90°N	2008-2017	158.6	155 – 200	Saunois et al., 2020	TD
				102 – 182	Saunois et al., 2020	BU

[a] These reported estimates are model ensemble means. For the West Siberian Lowlands, the range between the inverse models is 3.1–9.8 Tg CH_4 yr^{-1} (Bohn et al., 2015). For tropical wetlands, the range between the process-based models is 85–184 Tg CH_4 yr^{-1} (Melton et al., 2013).

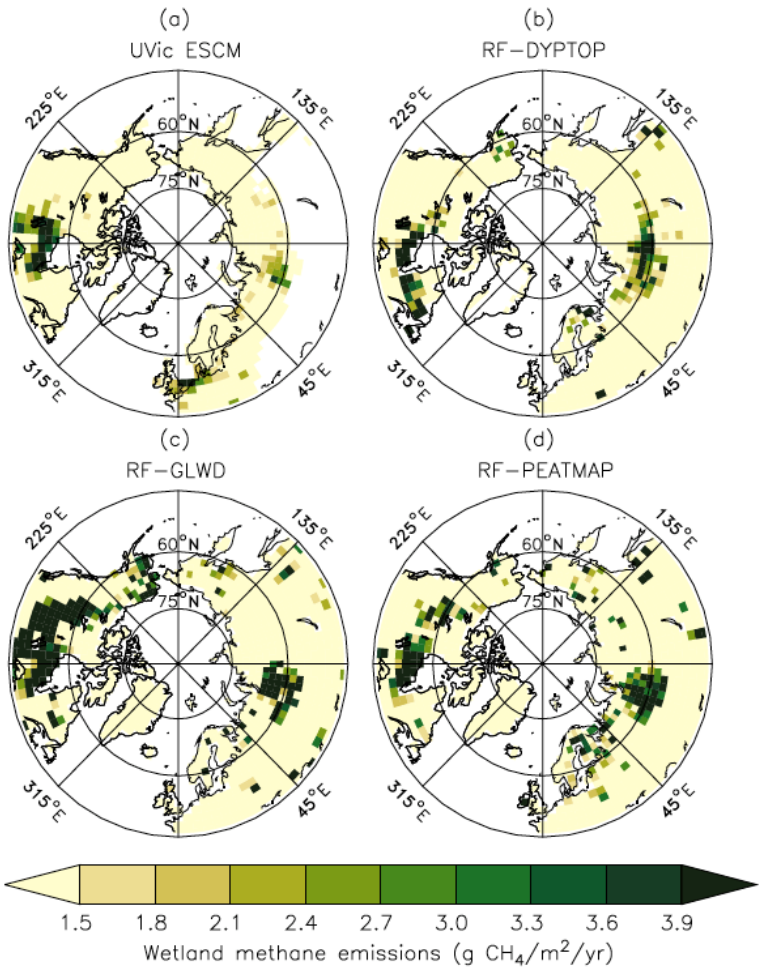

Figure 3.8. Average CH_4 emissions from wetlands north of 45°N over the 2013-2014 period as simulated by the UVic ESCM (a) in comparison to three datasets (upscaled flux measurements): (b) RF-DYPTOP, (c) RF-GLWD and (d) RF-PEATMAP. The datasets are regridded to 3.6° x 1.8° for a fair comparison with the UVic ESCM. The comparison period corresponds to the overlap period for the three datasets.

Figure 3.9 shows seasonal cycles of CH_4 emissions from wetlands north of 45°N over the 2013-2014 period as simulated by the UVic ESCM and estimated from the three UFMs (Peltola et al., 2019). The pattern and magnitude of simulated seasonal emissions compare well to that of the UFMs. For both the model and UFMs, minimal emissions vary between 0.2-0.6 Tg CH_4 $month^{-1}$ and occur in December while peak emissions are well below 10 Tg CH_4 $month^{-1}$ and occur in July (Figure 3.9). However, simulated peak emissions (~8.5 Tg CH_4 $month^{-1}$) are relatively higher than peak emissions for the UFMs (range of best estimates: 5.6-7.5 Tg CH_4 $month^{-1}$). Moreover, in comparison to the three UFMs, the UVic ESCM simulates lower CH_4 emissions between December and May but higher CH_4 emissions between July and September (Figure 3.9).

The UVic ESCM simulates the occurrence of wetland CH_4 emissions during the non-growing season. For wetlands north of 45°N, our model simulates total emissions of 2.1 Tg CH_4 yr^{-1} between November and March. The UFMs predict total emissions of 4.6-10.2 Tg CH_4 yr^{-1} during these cold months (Peltola et al., 2019). For wetlands north of 60°N, the UVic ESCM simulates emissions of 1.2 Tg CH_4 yr^{-1} from October through May in agreement with recent estimates (1.6 ± 0.1 Tg CH_4 yr^{-1}) from data-constrained model ensembles for these months (Treat et al., 2018). Based on our calculations, the three UFMs predict about 3.5-4.5 Tg CH_4 yr^{-1} emitted from wetlands north of 60°N between October and May. Overall, this analysis shows that WETMETH is capable of simulating non-negligible CH_4 emissions from northern wetlands during cold months as emphasized by recent studies (Treat et al., 2018; Zona et al., 2016).

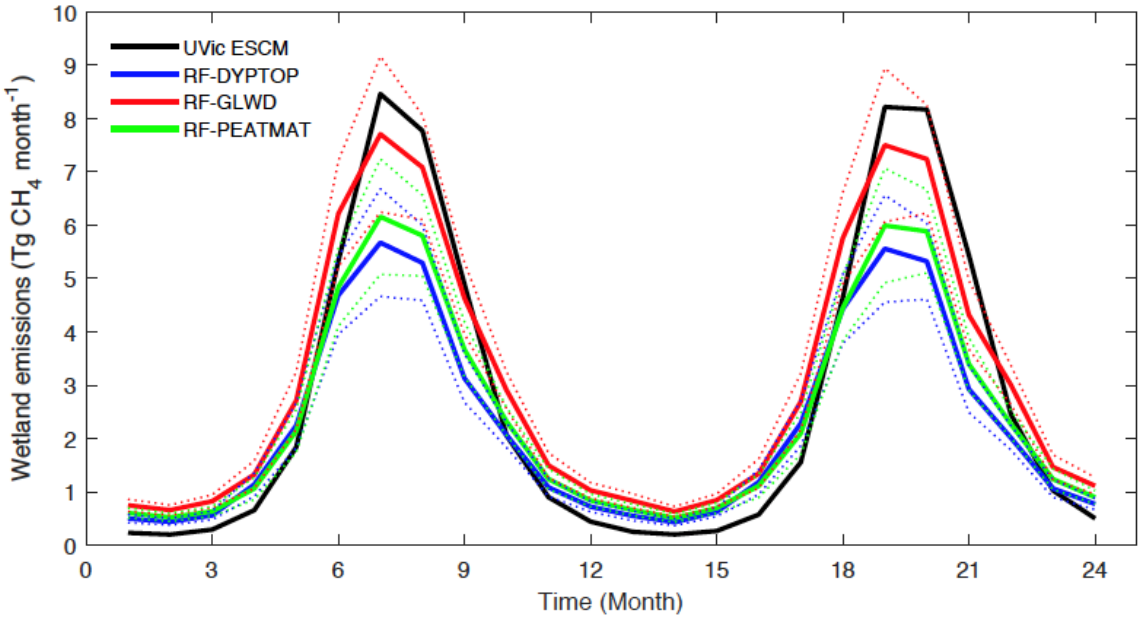

Figure 3.9. Seasonal variations of CH_4 emissions from wetlands north of 45°N over the 2013-2014 period as simulated by the UVic ESCM in comparison to three upscaled flux measurements (RF-DYPTOP, RF-GLWD and RF-PEATMAP). The dashed lines show the uncertainty range for the upscaled flux measurements.

At the global scale, the UVic ESCM simulates total global wetland CH_4 emissions of 155.1 and 158.6 Tg CH_4 yr^{-1} over the 2000-2009 and 2008-2017 decades, respectively. According to the latest global CH_4 budget report, these wetland emissions are in the mid-range of bottom-up estimates (102-179 and 102-182 Tg CH_4 yr^{-1}) but close to the lower limit of top-down estimates (153-196 and 155-200 Tg CH_4 yr^{-1}) over

the two decades (Saunois et al., 2020). Previous bottom-up estimates are significantly high (Melton et al., 2013; Saunois et al., 2016a) primarily due to possible double counting of emissions from wetlands and other inland water areas (Saunois et al., 2020; Thornton et al., 2016) in addition to uncertainties associated with the areal extent of wetlands and model parameterizations (Melton et al., 2013). Table 3.2 summarizes the comparison between the model results and estimates from the latest global CH_4 budget report for the 2008-2017 decade.

Figure 3.10 shows the spatial distribution of simulated wetland CH_4 emissions over the 2001-2004 period in comparison to three process-based model ensembles: GCP-CH4 (Poulter et al., 2017), WetCHARTs (Bloom et al., 2017), and WETCHIMP (Melton et al., 2013). The UVic ESCM simulates few CH_4-emitting areas over South-East Asia in comparison to the three model ensembles. The potential underestimation of wetland CH_4 emissions in that region is associated with the relatively few wetland areas simulated by the UVic ESCM (see Section 3.5.1). In tropical Africa, our model simulates too many CH_4-emitting locations in comparison to the model ensembles (Figure 3.10), which is also associated with the distribution of simulated wetlands (see Section 3.5.1). Nevertheless, the UVic ESCM simulates the occurrence of wetland CH_4 emissions in key source regions such as the Amazon and Congo River basins, South Sudan (Sudd swamps), and Indonesian islands (Figure 3.10). For the Amazon and Congo River basins, however, the UVic ESCM simulates lower wetland CH_4 emissions than predicted by the model ensembles (Figure 3.10). This can be due to either the consideration of an optimal temperature for CH_4 production (around 27°C) in our model unlike many other process-based models, or the fact that model parameters in this study are tuned to northern estimates.

Figure 3.11a shows the latitudinal distribution of simulated wetland CH_4 emissions in comparison to the model ensembles. Interestingly, although GCP-CH4 and WetCHARTs are based on the same wetland dataset (SWAMPS-GLWD) (Bloom et al., 2017; Poulter et al., 2017), their zonal wetland CH_4 emissions are very different especially near the Equator and across northern high-latitude regions (Figure 3.11a). Using the three model ensembles as reference, the UVic ESCM simulates significantly lower wetland CH_4 emissions around the Equator (Figure 3.11a), despite that the model simulates too large equatorial wetland areas (Figure 3.4). In fact, wetland emission intensities (emissions per unit of wetland area) by the UVic ESCM are lower than those

by the model ensembles between 10°S and 10°N (Figure 3.11b) due to relatively large wetland areas but small CH_4 emissions in equatorial regions (Figure 3.4 versus Figure 3.11a). As previously discussed, the relatively small CH_4 emissions simulated by the UVic ESCM in equatorial regions can be associated with either the optimal temperature for CH_4 production considered in WETMETH but not in most other process-based models, or the fact that model parameters in this study are tuned to northern estimates.

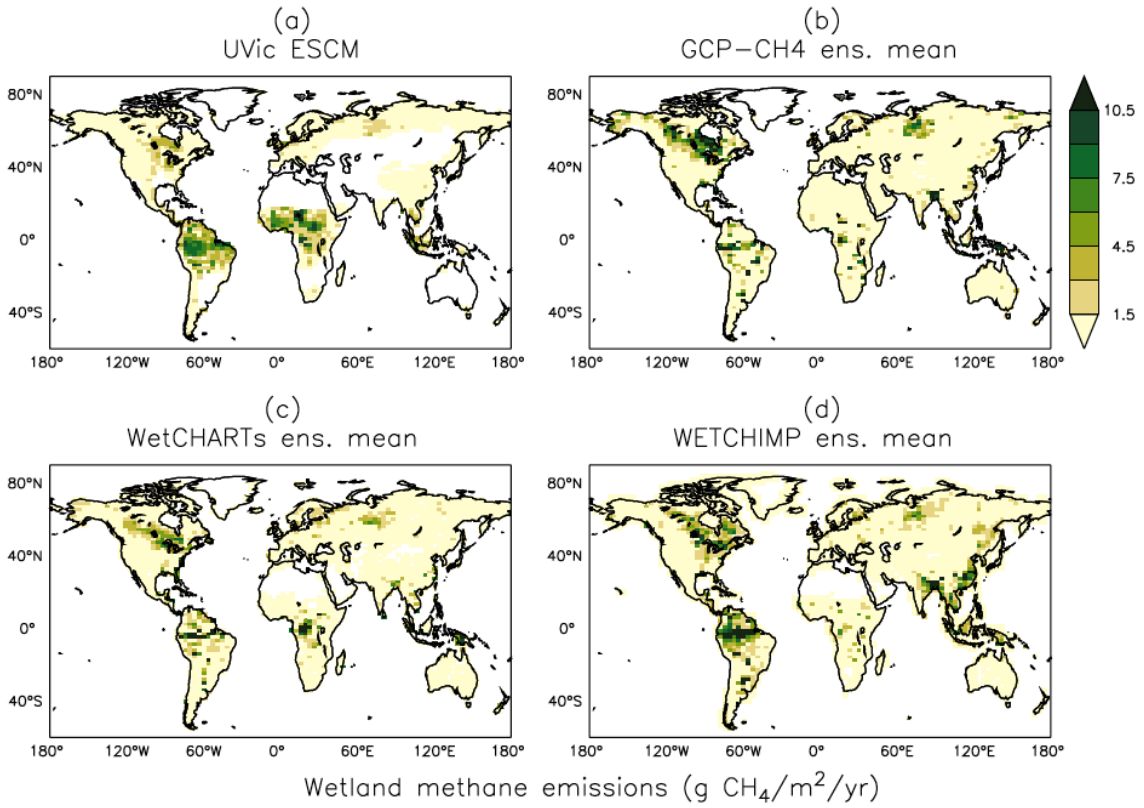

Figure 3.10. Average methane emissions from global wetlands over the 2001-2004 period as simulated by the UVic ESCM (a) in comparison to three process-based model ensembles: (b) GCP-CH4, (c) WetCHARTs, and (d) WETCHIMP. The model ensembles are regridded to 3.6° x 1.8° for a fair comparison with the UVic ESCM. The comparison period corresponds to the overlap period for the three model ensembles.

Furthermore, the UVic ESCM simulates more wetland CH_4 emissions between 10-20°N than the three model ensembles (Figure 3.11a) and this can be attributed to the widespread wetlands in West and Central Africa simulated by our model (Figure 3.5 and Figure 3.6). In addition, the UVic ESCM simulates significantly less wetland CH_4 emissions between 20-35°N in comparison to the WETCHIMP ensemble (Figure 3.11a) and this can be attributed to the relatively small wetland areas simulated by the UVic

ESCM in South-East Asia where some models include agricultural wetlands such as rice paddies. Moreover, wetland emission intensities by the UVic ESCM feature low variability with latitude unlike the three model ensembles (Figure 3.11b). Such a relative lack of variability can be attributed to two factors: (i) both wetland areas and CH_4 emissions simulated by the UVic ESCM feature relatively low variability with latitude compared to the datasets and model ensembles (Figure 3.4 and Figure 3.11a); and (ii) as previously discussed, our model likely simulates too large wetland areas but too small CH_4 emissions around the Equator implying a lack of variability across tropical latitudes.

Despite the various discrepancies between the UVic ESCM and both model ensembles regarding the distribution of wetland CH_4 emissions in the tropics, our model simulates mean annual CH_4 emissions from tropical wetlands that are in the range of estimates from the literature (Table 3.2). For the 1993-2004 period, the UVic ESCM simulates tropical wetland CH_4 emissions of 105.5 Tg CH_4 yr^{-1} whereas the WETCHIMP ensemble predicts 126 ± 31 Tg CH_4 yr^{-1} (Melton et al., 2013). Another study suggests a lower mean value (90 ± 77 Tg CH_4 yr^{-1}) for wetland CH_4 emissions in the tropics although with large uncertainties (Sjögersten et al., 2014). Indeed, several studies indicate that wetland CH_4 emissions in the tropics are highly uncertain due to limited ground-based measurements and poorly delimitated wetland extent (Dargie et al., 2017; Gumbricht et al., 2016; Hu et al., 2018; Pangala et al., 2017; Saunois et al., 2020).

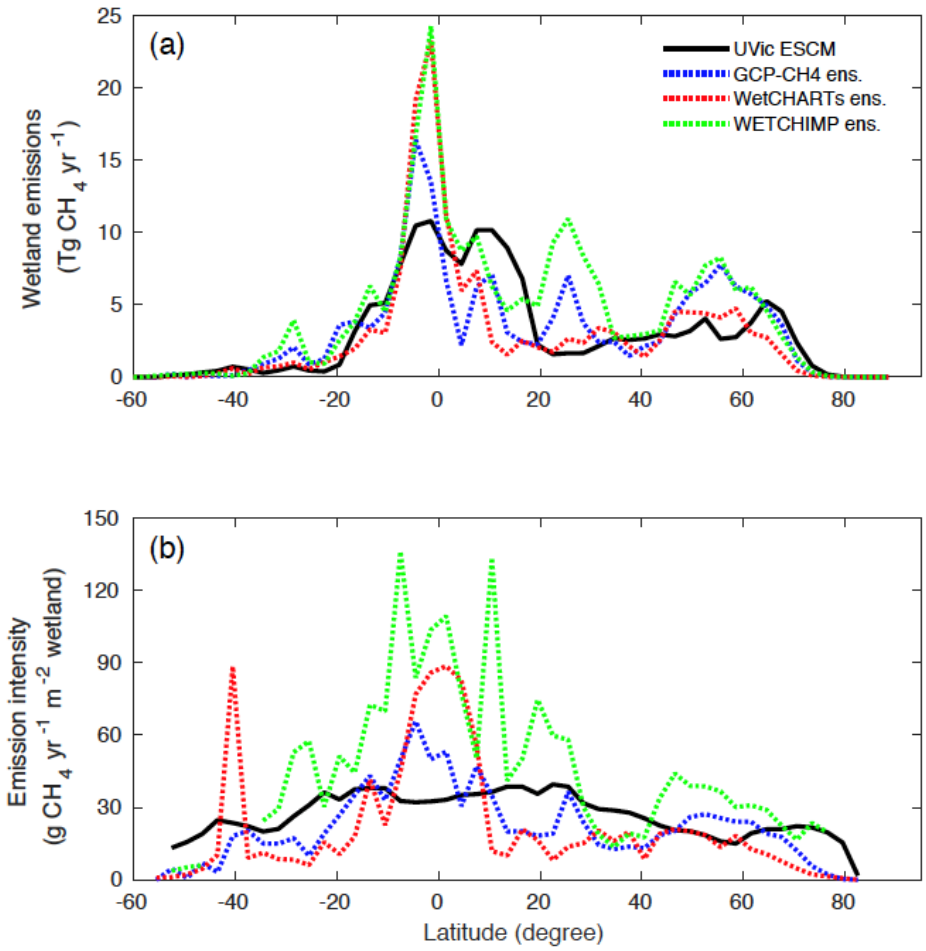

Figure 3.11. **(a) Latitudinal distribution of wetland methane emissions simulated by the UVic ESCM over the 2001-2004 period in comparison to three process-based model ensembles: GCP-CH4, WetCHARTs and WETCHIMP. The comparison period corresponds to the overlap period for the three model ensembles. (b) Latitudinal emission intensity (methane emissions per unit of wetland area) simulated by the UVic ESCM over the 2001-2004 period in comparison to the three process-based model ensembles. GCP-CH4 and WetCHARTs both use SWAMPS-GLWD as prescribed wetlands. The wetland methane emissions and emission intensities are summed across latitude bins of 3°.**

3.6. Model sensitivity to poorly constrained parameters

We performed a set of 30 model runs with perturbed parameter values (sensitivity runs) over the 2000-2009 decade in order to analyze the model sensitivity to poorly constrained parameters (T_{ref}, r, τ_{prod}, z_{oatz}, and τ_{oxid}). For each parameter, we increased or decreased the default value by 10, 20, and 30% while holding constant

values for other parameters (fixed to default values). We then compared results from the sensitivity runs to the model simulation with all parameter values set to default values (control run). This comparison focuses on the total simulated global (90°S-90°N), northern (45-90°N), and tropical (30°S-30°N) wetland CH_4 emissions over the 2000-2009 decade.

Our results show that the model sensitivity varies with the different parameters and across regions (Figure 3.12). Among the five poorly constrained parameters, the UVic ESCM is most sensitive to perturbations of the two parameters for CH_4 oxidation (z_{oatz} and τ_{oxid}) at both the global and regional scale. For z_{oatz}, a decrease (increase) of the default parameter value by 10-30% results in an augmentation (reduction) of default wetland CH_4 emissions by 41-179% (29-64%) at both the global and regional scale (Figure 3.12j-l). For τ_{oxid}, a decrease (increase) of the default parameter value by 10-30% implies a reduction (augmentation) of default wetland CH_4 emissions by 32-77% (37-120%) at both the global and regional scale (Figure 3.12m-o).

The UVic ESCM is also very sensitive to perturbations of T_{ref}, but this sensitivity is more pronounced for tropical regions than northern regions (Figure 3.12a-c). For northern regions, a decrease (increase) of T_{ref} by 10-30% results in a reduction (augmentation) of default wetland CH_4 emissions by 5-21% (3-5%). For tropical regions, however, a decrease (increase) of T_{ref} by 10-30% results in a reduction (augmentation) of default wetland CH_4 emissions by 34-82% (33-75%). Globally, a decrease (increase) of T_{ref} by 10-30% results in a reduction (augmentation) of default wetland CH_4 emissions by 26-66% (24-55%). The model sensitivity to perturbations of r is linear across all regions (Figure 3.12d-f). Lastly, the model is least sensitive to perturbation of τ_{prod} across the globe (Figure 3.12g-i).

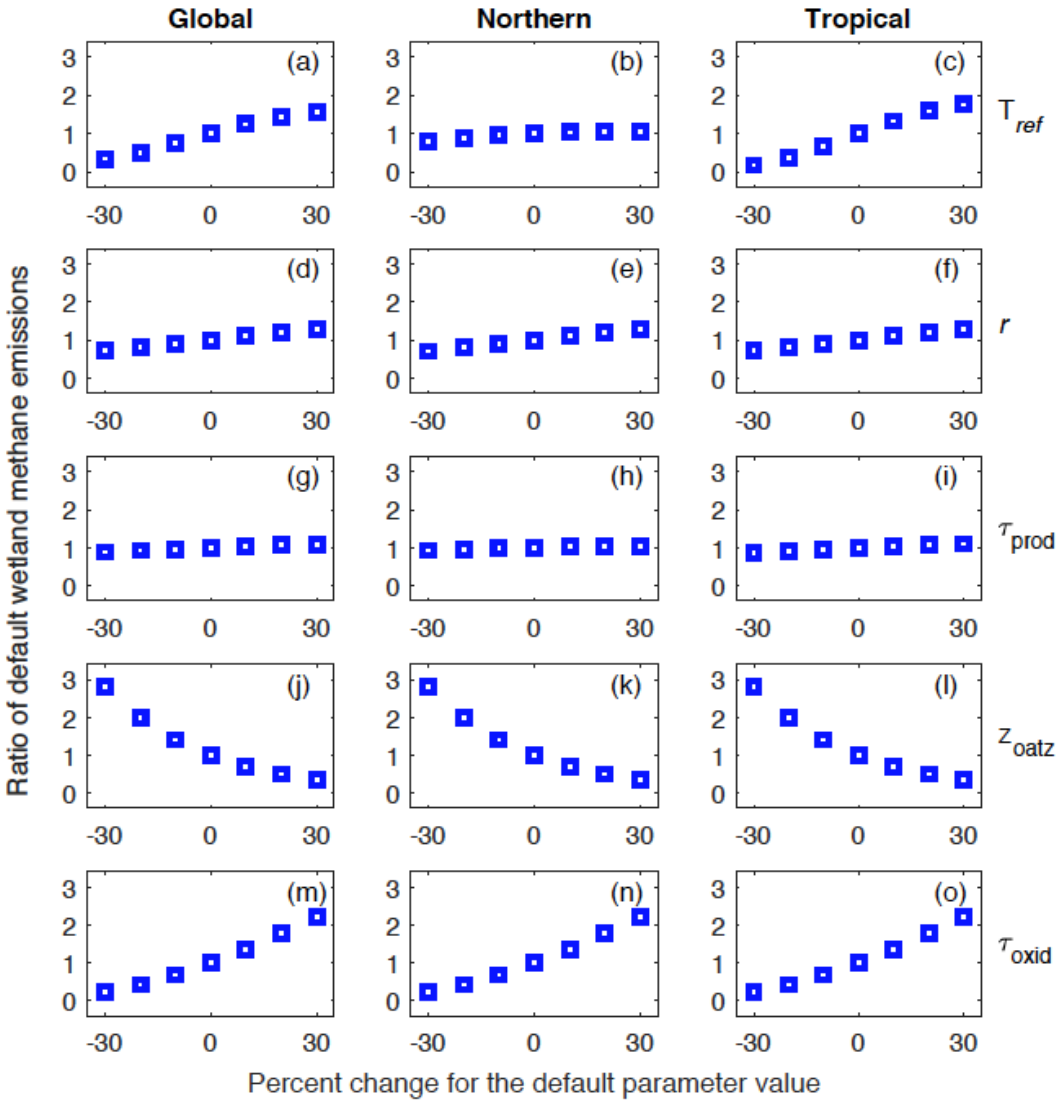

Figure 3.12. Analysis of the model sensitivity to perturbations of poorly constrained parameters: T_{ref}, r, τ_{prod}, z_{oatz}, and τ_{oxid}. For each parameter, the default value is increased or decreased by 10, 20, and 30% while values of other parameters are held constant (to default values). The model sensitivity is analyzed with respect to global (90°S-90°N), northern (45-90°N), and tropical (30°S-30°N) wetland methane emissions. Vertical axes show the ratio of the resulting emissions to the default emissions.

3.7. Discussions

3.7.1. WETMETH in the spectrum of wetland CH_4 models

A recent study reviewed 40 models of CH_4 emissions in terrestrial ecosystems (predominantly rice paddies and natural wetlands) and classified them into three

categories based on their level of complexity: relatively simple models, relatively mechanistic models, and mechanistic models (Xu et al., 2016). Relatively simple models are those that simulate net CH_4 emissions based on soil carbon or other environmental factors without explicit representations for the different CH_4 production and oxidation pathways as well as mechanisms transporting CH_4 to the atmosphere. Relatively mechanistic models are those that account for at least one transport mechanism for CH_4 release in addition to representing CH_4 production and oxidation with simple functions. Mechanistic models are more comprehensive and explicitly simulate different pathways for both CH_4 production and oxidation, more than two mechanisms for CH_4 release, as well as their environmental controls. Based on this classification, WETMETH is a relatively simple model in the sense that it does not distinguish pathways for CH_4 production and oxidation as well as the various mechanisms transporting CH_4 to the atmosphere.

Although some wetland CH_4 models are claimed to be embedded in ESMs (Xu et al., 2016), none of these models are currently run in fully coupled models with feedbacks between climate conditions and the global carbon cycle. Most of these models are rather implemented in dynamic vegetation models or uncoupled land surface components of climate models (Arora et al., 2018; Eliseev et al., 2008; Hodson et al., 2011; Riley et al., 2011; Ringeval et al., 2011; Wania et al., 2009). Nonetheless, relatively simple models present the ideal level of complexity for the current generation of ESMs. More complex models generally imply detailed soil chemistry for O_2 and alternate electron acceptors (Riley et al., 2011; Wania et al., 2010), different carbon substrates and their effects on CH_4 production (Grant, 1998; Lovley and Klug, 1986), an explicit representation of the dynamics of different microbial communities (Grant, 1998; Xu et al., 2015), which all require comprehensive soil chemistry or model parameters that are currently not common in ESMs (Xu et al., 2016). Process parameterizations in mechanistic models generally imply too many degrees of freedom, making it difficult to constrain model parameters against sparse observations. Furthermore, mechanistic models may be too demanding computationally for fully coupled ESM runs without a proportional benefit for large-scale simulations of wetland CH_4 emissions.

The particularity of WETMETH among relatively simple models is that the model accounts for an optimum temperature for CH_4 production, a depth-dependent representation for CH_4 production allowing a calibration of parameters against potential

CH_4 production rates from laboratory incubations, dynamic CH_4 oxidation based on the vertical distribution of soil moisture, and the potential for CH_4 emissions in non-inundated ecosystems with relatively high level of soil moisture content. In conclusion, WETMETH is simple enough to be compatible with ESMs and yet complex enough to simulate in an implicit way biogeochemical processes regulating wetland CH_4 emissions.

3.7.2. Limitations for WETMETH

The new wetland CH_4 model is associated with several limitations, which are linked to either its level of complexity or the scarcity of large-scale datasets for model calibration:

1. The present state of global wetland modelling assumes generic wetlands without distinguishing their different types (Melton et al., 2013; Poulter et al., 2017). Like many other large-scale models of the current generation, WETMETH would not be appropriate for investigating the contribution from particular wetland types to regional or global CH_4 emissions (Aselmann and Crutzen, 1989).

2. Since WETMETH is not based on a comprehensive soil biochemistry module and does not include the different pathways for CH_4 production and oxidation, the model is not suited for investigating the role of specific biological and chemical controls on wetland CH_4 emissions (Bridgham et al., 2013; Kwon et al., 2019).

3. WETMETH does not simulate the contribution from wetland-specific vegetation species to CH_4 emissions, although some of these species can either lead to high emissions (e.g. sedges are vascular plants that can transport CH_4 through their aerenchyma) or low emissions (e.g. mosses are non-vascular plants that have been shown to develop a symbiotic relationship with methanotrophs) (Bridgham et al., 2013; Chen and Murrell, 2010).

4. Ebullition and aerenchyma of vascular plants allow CH_4 produced in wetlands to escape to the atmosphere with little opportunity for oxidation (Segers, 1998; Whalen, 2005). Moreover, stems of woody trees are important conduits for CH_4 emissions in Amazonia, a major source region in the world (Pangala et al., 2017). By considering the net effect of all mechanisms transporting

CH_4 to the atmosphere, WETMETH presents a limitation for investigating the relative contribution of transport mechanisms to CH_4 emissions across regions and at the global scale.

5. Methane produced in northern wetlands can be stored underneath frozen soil during the winter and be released abruptly upon spring thaw (Mastepanov et al., 2013; Song et al., 2012). WETMETH does not currently feature such a storage of CH_4 in the soil column, which is probably more relevant for small-scale (site) and short-term (daily) than large-scale (regional) and long-term (seasonal) emissions (Figure 3.9).

6. As presented in this study, poorly constrained WETMETH parameters are tuned to estimates from northern high-latitude regions because large-scale datasets from other regions are scarce (see Section 3.4). A strong limitation comes with the assumption that the chosen parameter values are representative for CH_4 production and oxidation across the globe. However, the applied model calibration remains a reasonable approach given the scarcity of observations for wetland CH_4 production, oxidation, and emissions at the global scale.

Despite these limitations and the model simplicity, WETMETH is skillful when it comes to the simulation of mean seasonal, annual, and decadal wetland CH_4 emissions at the regional, hemispheric, and global scale (see Section 3.5.2). The implementation of WETMETH in a fully coupled ESM should advance research on the interactions between climate change and wetland CH_4 emissions in the context of global climate projections.

3.8. Conclusions

We developed a process-based wetland CH_4 model (WETMETH) for implementation in ESMs. WETMETH is currently embedded in the UVic ESCM, a fully coupled EMIC. WETMETH is a computationally efficient model, applicable globally and, of appropriate complexity with respect to the current state of wetland CH_4 modelling. Unconstrained model parameters are tuned to potential CH_4 production rates from incubated soil samples and CH_4 emissions from northern wetlands due to the scarcity of large-scale datasets from other regions. Nevertheless, WETMETH reproduces well estimates of

mean annual CH_4 emissions over the past few decades at the regional, hemispheric, and global scale.

Despite the importance of tropical wetlands in the global CH_4 budget (Kirschke et al., 2013; Saunois et al., 2016a) and climate change (O'Connor et al., 2010; Zhang et al., 2017b), their areal extent and associated CH_4 emissions remain highly uncertain in both the literature and modelling work (including this study) due to a combination of limited ground-based measurements and process understanding (Pangala et al., 2017; Saunois et al., 2020; Sjögersten et al., 2014), as well as a low accuracy from remotely-sensed products especially over dense rainforests of Indonesia, Amazonia, and the Congo River basin where new peatlands continue to be discovered to date (Dargie et al., 2017). Large-scale wetland mapping is a field of ongoing research (Tootchi et al., 2019) and further model development should focus on the improvement of wetland simulations in the tropics. In parallel, a compilation of tropical wetland CH_4 measurements from various sources into synthesis datasets would be beneficial for constraining wetland CH_4 processes in large-scale models.

The inclusion of wetland CH_4 processes in a fully coupled ESM allows to advance the research on the feedback between climate change and wetland CH_4 emissions. The implementation of WETMETH in the UVic ESCM constitutes an ideal tool for investigating interactions between climate conditions and wetland CH_4 emissions from decadal to longer timescales. Of particular importance is the permafrost carbon feedback to climate change, in which CH_4 emissions from northern wetlands are expected to play an important role (Nzotungicimpaye and Zickfeld, 2017).

Chapter 4. The importance of methane mitigation to comply with the 2°C warming limit

Abstract

Methane (CH_4) mitigation is often proposed to be one way to tackle climate change in the short-term with co-benefits for air quality and human health. However, atmospheric CH_4 concentration ([CH_4]) is growing rapidly since the last decade and currently tracking projected [CH_4] under unmitigated emission scenarios. Here we use an Earth system model of intermediate complexity (EMIC) to investigate the importance of immediate versus delayed CH_4 mitigation as part of international efforts to limit global warming to 2°C above pre-industrial levels. The CH_4 cycle in the EMIC is represented with a process-based model for wetland CH_4 emissions, static CH_4 emissions from non-wetland natural sources, and a one box-model for atmospheric CH_4 whereby CH_4 decay depends on a constant lifetime of 9.3 years. The EMIC is driven with prescribed CH_4 emissions from anthropogenic sources among other forcing data. We explore scenarios with different initiation of CH_4 mitigation over the next three decades, all reaching the same amount of anthropogenic CH_4 emissions in the year 2100 as in a reference low emission scenario (SSP1-2.6). To explore the possibility of limiting global warming to 2°C, we assume that non-CH_4 forcings (greenhouse gas emissions, aerosols, and land-use changes) evolve according to SSP1-2.6 throughout the future. Our results suggest that CH_4 mitigation initiated between the years 2020 and 2030 under SSP1-2.6 could allow to keep global warming to well below 2°C relative to 1850-1900 levels, whereas delaying CH_4 mitigation to the years 2040 or 2050 under SSP1-2.6 could overshoot the 2°C warming target for at least two decades in the 21st century. Our results imply that immediate cuts in anthropogenic CH_4 emissions, alongside CO_2 mitigation, are needed to increase the likelihood of limiting global mean temperature rise to 2°C above pre-industrial levels.

4.1. Introduction

A key outcome of the 2015 Paris Agreement by the Conference of the Parties (COP) to the United Nations Framework Convention on Climate Change (UNFCCC) is the international commitment to hold the increase in the global average temperature to well below 2°C above pre-industrial levels and pursue efforts to limit the temperature increase to 1.5°C above pre-industrial levels (UNFCCC, 2015). Limiting global warming to 1.5 or 2°C above pre-industrial levels will require reaching net zero carbon dioxide (CO_2) emissions and deep reductions in non-CO_2 emissions by the year 2050 (IPCC, 2018). However, current strategies adopted by different countries to reduce anthropogenic emissions (i.e. nationally determined contributions or NDCs) generally do not explicitly target non-CO_2 emissions such as CH_4 (Harmsen et al., 2019a).

Atmospheric CH_4 is a trace gas of relevance to air quality and climate change. The gas contributes to the formation of ground-level ozone (O_3), an air pollutant, through a series of chemical reactions in the presence of nitrogen oxides (NO_x) and sunlight (Isaksen et al., 2011; O'Connor et al., 2010). Atmospheric CH_4 is also a powerful greenhouse gas (GHG). A molecule of CH_4 added in the atmosphere is 28-34 times more effective at absorbing infrared radiation than an additional molecule of carbon dioxide (CO_2) over a period of 100 years (Myhre et al., 2013). [CH_4] has increased from about 700 parts per billion (ppb) in the year 1750 to more than 1850 ppb today (Ciais et al., 2013). The rising [CH_4] is a major contributor to the increase in total radiative forcing, second only to CO_2 (Myhre et al., 2013).

The atmospheric CH_4 burden is regulated by many sources and sinks. Emissions of CH_4 into the atmosphere originate from a variety of anthropogenic and natural sources. Anthropogenic sources of CH_4 include fossil fuels, landfills, rice cultivation and domesticated ruminants, whereas natural sources of CH_4 include wetlands, lakes, geological seeps, wildfires, wild ruminants and termites (Saunois et al., 2020). In the past few decades, more than 60% of the global CH_4 emissions were from anthropogenic sources mostly related to fossil fuel exploitation, livestock production, agriculture and waste (Kirschke et al., 2013; Saunois et al., 2020). Sinks of CH_4 are entirely natural processes mostly occurring in the atmosphere. The main removal of CH_4 occurs in the troposphere through its reaction with the hydroxyl (OH) radical (Isaksen et al., 2011; Saunois et al., 2016b). In the stratosphere, CH_4 is removed through its reaction with

chlorine and oxygen radicals (Isaksen et al., 2011; Kirschke et al., 2013). CH_4 is also destroyed in the marine boundary layer through its reaction with chlorine radicals (Kirschke et al., 2013). Another sink of atmospheric CH_4 is the uptake by soils (Kirschke et al., 2013; Saunois et al., 2020).

There exist large uncertainties in the global CH_4 budget and its evolution in the future. Although the various sources and sinks of atmospheric CH_4 are well documented, their quantification and apportionment remain challenging (Saunois et al., 2020). Perhaps the most intriguing aspect of the CH_4 budget in the current era is the evolution of atmospheric CH_4 since the year 1999 characterized by approximately constant [CH_4] between the 1999-2006 period followed by a renewed increase of at least 5 ppb yr^{-1} from the year 2007 to present (Nisbet et al., 2019; Schaefer, 2019). The stabilization of [CH_4] between the years 1999 and 2006 has been attributed to a combination of decreasing-to-stable fossil fuel emissions and increasing-to-stable biogenic emissions such as ruminants, rice cultivation, wetlands and other inland waters (Kirschke et al., 2013). It is also possible that changes in CH_4 sinks (namely the oxidation of CH_4 by tropospheric OH) contributed to the brief plateau in global CH_4 levels in the late 1990s and early 2000s (Prather and Holmes, 2017). The causes driving the sustained [CH_4] increase after 2007 are still under debate after more than a decade (Prather and Holmes, 2017; Schaefer, 2019), with recent studies suggesting contributions from both sources and sinks of CH_4 (Jackson et al., 2020; Nisbet et al., 2019; Schaefer, 2019). Limitations in the understanding of the current CH_4 budget translate into uncertainties in the future evolution of the global CH_4 cycle.

The reduction of anthropogenic CH_4 emissions, alongside CO_2 mitigation, is often proposed to be an essential action for tackling climate change in the current century with co-benefits for air quality and human health (Anenberg et al., 2012; Ramanathan and Xu, 2010; Rao et al., 2016; Shindell et al., 2012; Shoemaker et al., 2013; Weaver, 2011; West et al., 2006). This proposal is justified by three main reasons: (i) the dominance of anthropogenic sources in current global CH_4 emissions, (ii) the strong global warming potential of CH_4, and (iii) its residence time in the atmosphere of only about a decade (Crill and Thornton, 2017; Kirschke et al., 2013; Ramanathan and Xu, 2010). Simulations by integrated assessment models (IAMs) and climate models of reduced complexity suggest that limiting global warming to 2°C will require a rapid decarbonization of the global economy as well as deep reductions in CH_4 and other non-CO_2 emissions

(Gernaat et al., 2015; Harmsen et al., 2019b; Rogelj et al., 2018). However, observed [CH_4] is tracking future scenarios of unmitigated emissions (Nisbet et al., 2019; Saunois et al., 2016b). There are concerns that sustained [CH_4] growth at current rates in the next few decades could constitute a challenge for meeting the temperature goals in the Paris Agreement, even under aggressive CO_2 mitigation (Nisbet et al., 2019).

Earth system models (ESMs) are fully coupled climate models that are appropriate for projecting future climate conditions and changes in biogeochemical cycles by considering different mitigation pathways and accounting for many Earth system feedbacks. In general, fully coupled climate models use prescribed [CH_4] scenarios to investigate the climate impacts of CH_4 mitigation because these models lack a representation of the global CH_4 cycle (Jones et al., 2018). Here we use a version of the University of Victoria Earth System Climate Model (UVic ESCM) into which we implemented a simplified representation of the CH_4 cycle (see Sections 4.2.2 and 4.2.3). The main question guiding this research is: What is the importance of immediate versus delayed CH_4 mitigation to comply with the global warming limits set by the Paris Agreement? The focus is on global reductions of anthropogenic CH_4 emissions without distinguishing which source sectors or regions would be cutting emissions down. The remainder of this chapter is structured as follows: Section 4.2 describes the methods used in this study. Section 4.3 presents the study results, and Section 4.4 provides the discussion and conclusions.

4.2. Methods

4.2.1. Description of the UVic ESCM

The UVic ESCM is an Earth system model of intermediate complexity (EMIC) with a horizontal grid resolution of 3.6° in longitude and 1.8° in latitude (Weaver et al., 2001). The UVic ESCM consists of a simplified atmosphere model coupled to a comprehensive ocean model, a sea ice model, and a land surface model (Weaver et al., 2001). In this study, we use a version of the EMIC based on UVic ESCM 2.10 (Mengis et al., 2020) into which we incorporated a simplified representation of the global CH_4 cycle (see Sections 4.2.2 and 4.2.3).

The atmosphere in the UVic ESCM is represented with a 2-D (vertically-integrated) energy-moisture balance model, which uses wind fields prescribed from observation-based data and accounts for dynamical feedbacks (e.g. water vapour and planetary longwave feedbacks). The ocean model is a 3-D ocean general circulation model, with 19 vertical layers of unequal thicknesses that range from 50 m near the surface to 500 m in the deep ocean (Weaver et al., 2001). The sea ice model incorporates representations of sea-ice dynamics (subject to atmospheric wind stress and ocean currents) as well as sea-ice thermodynamics and thickness distribution (Weaver et al., 2001). The marine carbon cycle is represented with organic and inorganic carbon cycle models. The organic carbon cycle is represented with an ocean biogeochemistry model that simulates phytoplankton and zooplankton dynamics (Keller et al., 2012). The inorganic carbon cycle model simulates the air-sea exchange of CO_2 and ocean carbonate chemistry following the protocols of the Ocean Carbon-cycle Model Intercomparison Project (Orr, 1999; Weaver et al., 2001). Dissolved inorganic carbon is treated as a passive tracer that is subject to ocean circulation (Weaver et al., 2001). Carbonate dissolution in ocean sediments is simulated with a model of respiration in marine sediments (Archer, 1996; Eby et al., 2009).

The land in the UVic ESCM 2.10 is represented with 14 ground layers of unequal thicknesses with a total thickness of 250 m (Avis et al., 2011; Mengis et al., 2020). The top eight ground layers (~10 m in total depth) are soil layers, whereas the bottom six ground layers are bedrock layers with thermal characteristics of granitic rock (Avis et al., 2011). The energy balance is determined for each ground layer and permafrost is identified whenever one ground layer is frozen for two or more consecutive years (Avis et al., 2011). Water phase changes in the soil layers are determined over a range of soil temperatures to determine the fraction of frozen and unfrozen water in the ground (Avis et al., 2011). Porosity and permeability are determined based on the relative abundance of prescribed sand, clay, and silt-sized particles. Moisture undergoes free drainage in these soil layers and subsurface runoff occurs when the water reaches the bedrock (Avis et al., 2011). Wetlands are simulated to occur in grid cells whose upper ground layer contains soil moisture exceeding 65% of saturation for at least one day in a year (Avis et al., 2011). Sub-grid scale wetlands are identified, in the model version used in this study, following a TOPMODEL approach for global models (Gedney and Cox, 2003). Terrestrial CO_2 fluxes are simulated using the Top-down Representation of Interactive Foliage and

Flora including Dynamics (TRIFFID), a dynamic global vegetation model that is coupled to the land model (Avis et al., 2011; Meissner et al., 2003). TRIFFID defines the state of the terrestrial biosphere in terms of soil carbon as well as the structure and coverage of five plant functional types: broadleaf trees, needleleaf trees, C3 grasses, C4 grasses, and shrubs (Cox, 2001; Matthews et al., 2004; Meissner et al., 2003). Terrestrial carbon gain occurs through photosynthesis and soil carbon gain occurs through litter-fall and vegetation mortality. Soil carbon can accumulate in the top six layers (~3.35 m in total depth). The buildup of carbon in permafrost-affected locations is simulated following a diffusion method that approximates cryoturbation, a process driven by long-term freeze-thaw cycles (MacDougall and Knutti, 2016). Terrestrial carbon loss occurs through autotrophic respiration by plants and heterotrophic respiration by soil microbes (Matthews et al., 2004; Meissner et al., 2003). Permafrost carbon can only be lost through microbial respiration, which only occurs in unfrozen soil layers (MacDougall et al., 2012; MacDougall and Knutti, 2016).

4.2.2. Wetland CH_4 emissions

Wetland CH_4 emissions are simulated in the UVic ESCM following a recent model development (Nzotungicimpaye et al., 2020). Chapter 3 provides a detailed description of the wetland CH_4 model (WETMETH) implemented in the UVic ESCM. For the sake of brevity, we provide a short description of the model here. Wetland CH_4 emissions in the UVic ESCM are calculated as the balance between microbial production and oxidation of CH_4 in the soil column. CH_4 production is calculated in each soil layer as a function of moisture content, carbon content, temperature, and the relative depth from the soil surface. In this approach, soil moisture (i.e. water saturation) represents potential anoxic conditions. Soil carbon represents organic matter that may be accessed by methanogens. Soil temperature allows to estimate potential changes in methanogenic activity, whereas the relative depth from the soil surface allows to represent the net effect of depth-dependent controls on CH_4 production that are unresolved by the UVic ESCM (e.g. the quality of organic matter and the distribution of methanogens in the soil). CH_4 production is assumed to not take place in dry soil layers (i.e soil layers unsaturated with water) as well as in frozen soil layers. CH_4 oxidation is calculated for the entire soil column as a fraction of the amount of CH_4 produced in the soil column. The oxidized CH_4 fraction is determined based on an estimated oxic zone depth, which represents the

prevalence of methanotrophs in the soil. This fraction increases as the oxic zone deepens.

4.2.3. Atmospheric CH_4 and associated radiative forcing

A simple one-box model is used to simulate the evolution of the atmospheric CH_4 burden (B) with time as the balance between total CH_4 emissions (E) and total CH_4 sinks (S):

$$\frac{\mathrm{dB}}{\mathrm{dt}} = (\mathrm{E} - \mathrm{S}), \quad (4.1)$$

where $\mathrm{E} = \mathrm{E}_a + \mathrm{E}_w + \mathrm{E}_n$ represents the sum of prescribed anthropogenic CH_4 emissions (E_a) (see Section 4.2.4), simulated wetland CH_4 emissions (E_w), as well as natural CH_4 emissions from non-wetland sources (E_n) such as termites, wild ruminants, wildfires, lakes, rivers, geologic seeps, and marine hydrates. Given that the UVic ESCM does not incorporate these non-wetland natural sources and in the absence of dataset for CH_4 emissions from these sources, we assume that non-wetland natural CH_4 emissions would remain constant in time at 45 Tg C yr^{-1}. This value is in the range of estimated total CH_4 emissions from non-wetland natural sources over the last four decades (Kirschke et al., 2013; Saunois et al., 2020) as well as pre-industrial periods (Houweling et al., 2000 and references therein). Sinks of atmospheric CH_4 are aggregated into a single term (S) calculated as $\mathrm{S} = \mathrm{B}\,(1 - \exp(-\frac{1}{\tau_{\mathrm{CH4}}}))$, where τ_{CH4} is the atmospheric CH_4 lifetime assumed to be 9.3 years (Saunois et al., 2020). Similar estimates for the atmospheric CH_4 lifetime have been reported for the pre-industrial era (9.5 ± 1.3 years) and present-day (9.1 ± 0.9 years) (Prather et al., 2012). At each time step, [CH_4] is determined based on the atmospheric CH_4 burden (B) by using a factor equivalent to ~2.8 Tg CH_4/ppb. Radiative forcing associated with changes in [CH_4] is calculated using the formulation of (Etminan et al., 2016) and is accounted separately from the aggregated forcing of other non-CO_2 GHGs that is prescribed to the UVic ESCM in its standard configuration (Mengis et al., 2020).

4.2.4. Prescribed anthropogenic CH_4 emissions

We prescribe global CH_4 emissions from anthropogenic sources over the historical period (1850-2014) and the future period (2015-2300) to the UVic ESCM. These emissions are from climate forcing datasets used in the Coupled Model Intercomparison

Project Phase 6 (CMIP6) in preparation for the Sixth Assessment Report (AR6) by the Intergovernmental Panel on Climate Change (IPCC) (Eyring et al., 2016). Future anthropogenic emissions are based on Shared Socioeconomic Pathways (SSPs), a set of alternative futures (scenarios) of societal development designed for CMIP6 (Gidden et al., 2019) and their extension beyond the 21st century (Meinshausen et al., 2019). In this study, we use two SSPs and their extension to the year 2300 for anthropogenic CH_4 emissions (Meinshausen et al., 2019; Nicholls et al., 2020): (i) SSP1-2.6, a scenario featuring an early CH_4 mitigation (prior to 2020), (ii) and SSP3-7.0, a scenario without CH_4 mitigation throughout the 21st century (Figure 4.1).

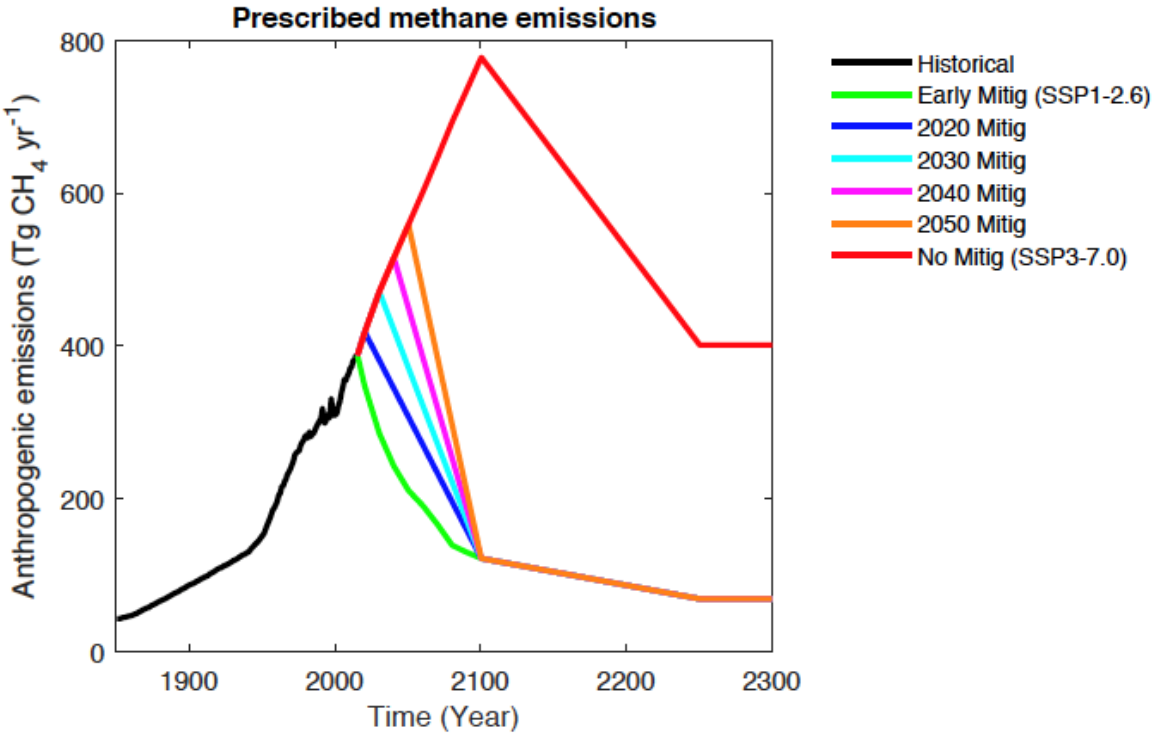

Figure 4.1. Anthropogenic CH_4 emissions prescribed to the UVic ESCM in this study. Emissions in the early mitigation scenario ("Early Mitig") correspond to SSP1-2.6, whereas emissions without mitigation ("No Mitig") correspond to SSP3-7.0. Immediate and delayed mitigation scenarios follow the SSP3-7.0 CH_4 emission trajectory to the specified point in time and decline linearly to reach the same amount of CH_4 emissions as SSP1-2.6 in 2100, and evolve according to the SSP1-2.6 extension beyond the 21st century.

We design four additional scenarios of anthropogenic CH_4 emissions by assuming different initiation of CH_4 mitigation over the next few decades. These scenarios follow the SSP3-7.0 trajectory up to a specified year (i.e. 2020, 2030, 2040,

and 2050) and decline linearly to reach the same amount of CH_4 emissions as SSP1-2.6 in the year 2100, and then evolve according to the SSP1-2.6 extension beyond the 21st century (Figure 4.1). All the considered mitigation scenarios assume deep reductions in anthropogenic CH_4 emissions. For instance, anthropogenic CH_4 emissions in the year 2100 correspond to a ~69% reduction of the peak emissions for the early mitigation scenario (SSP1-2.6), ~71% for the mitigation scenario starting in the year 2020, ~74% for the mitigation scenario starting in the year 2030, ~76% for the mitigation scenario starting in the year 2040, and ~78% for the mitigation scenario starting in the year 2050 (Table 4.1). These idealized scenarios allow to compare the effect of immediate versus delayed CH_4 mitigation on the global climate at the end of the 21st century and beyond.

4.2.5. Non-CH_4 radiative forcing agents

Apart from anthropogenic CH_4 emissions, we use CMIP6 data for natural forcing agents (volcanic and solar) as well as non-CH_4 anthropogenic GHGs and aerosols to drive the UVic ESCM over the 1850-2300 period. Natural forcing datasets consist of volcanic radiative forcing anomalies spanning the historical period based on (Schmidt et al., 2018) and solar constant data prescribed to the year 2300 (Matthes et al., 2017). To explore the possibility of achieving the warming limits set by the Paris Agreement, we assume that non-CH_4 GHGs as well as aerosols from anthropogenic sources evolve according to SSP1-2.6, which is a scenario representing a combination of mitigation strategies to achieve sustainable development in the future and eventually comply with the 2°C warming limit by the year 2100 (O'Neill et al., 2016). While such a future possibility (i.e. all anthropogenic GHGs and aerosols following SSP1-2.6 except for CH_4) sounds unrealistic, our experiment enables to investigate recent concerns about the sustained [CH_4] growth and the associated challenge for limiting global warming to 2°C above pre-industrial levels even under aggressive CO_2 mitigation (Nisbet et al., 2019). Therefore, we prescribe CO_2 emissions from fossil fuels as defined in the SSP1-2.6 scenario and their long-term extension (Meinshausen et al., 2019; Nicholls et al., 2020). The SSP1-2.6 scenario features strong reductions in CO_2 emissions as well as negative CO_2 emissions (i.e. artificial removal of atmospheric CO_2) in the second half of the 21st century (Gidden et al., 2019). Furthermore, we prescribe gridded land-use change (LUC) data according to SSP1-2.6 (Lawrence et al., 2016) and the UVic ESCM internally calculates corresponding LUC CO_2 emissions. The radiative forcing of CO_2 is calculated

within the UVic ESCM following the formulation of (Etminan et al., 2016). Radiative forcing values of other non-CH_4 GHGs are calculated externally using concentration data and their extension (Meinshausen et al., 2019), which are then summed up into an aggregated forcing that is prescribed to the UVic ESCM. For anthropogenic sulfate aerosols, we prescribe SSP1-2.6 gridded aerosol optical depth (AOD) data to the UVic ESCM (Fiedler et al., 2019; Stevens et al., 2017) and the model uses this data to internally calculate the associated radiative forcing. While forcing data for CO_2 and other non-CH_4 GHGs extend to the year 2300 (Meinshausen et al., 2019), forcing data for LUC and sulfate aerosols are prescribed to the year 2100 and their radiative forcing are held fixed at their year 2100 values in our climate simulations.

4.3. Results

4.3.1. Validation of the simulated CH_4 cycle

We validate the atmospheric [CH_4] simulated by the UVic ESCM against reconstructed as well as observed [CH_4] over the historical period (1850-2014). Our model reproduces the trend and magnitude of atmospheric [CH_4] for the decades prior to the 1980s reasonably well (Figure 4.2). The simulated [CH_4] for the 1850-1980 period is within a 10-30 ppb range of historical [CH_4] reconstructions (Etheridge et al., 1998; Meinshausen et al., 2017; Rhodes et al., 2013). For the 1980-2014 period, however, the trend in simulated [CH_4] does not feature the observed slowdown prior to the year 2007 and renewed rise afterwards (Figure 4.2). This trend mismatch can be associated with uncertainties in (i) CH_4 sources especially simulated wetland CH_4 emissions but also prescribed anthropogenic CH_4 emissions as well as natural CH_4 emissions from non-wetland sources, (ii) or simulated CH_4 sinks that are represented with a simple one-box model and a constant lifetime for atmospheric CH_4. It is difficult to pinpoint the exact reasons behind this mismatch given that causes driving the observed [CH_4] trends over the past few decades are also poorly understood (Ganesan et al., 2019; Schaefer, 2019). Nevertheless, the magnitude of simulated [CH_4] between the years 1980 and 2014 is within a 60-110 ppb range of observed [CH_4] with the highest [CH_4] difference occurring towards the end of the historical period (Figure 4.2).

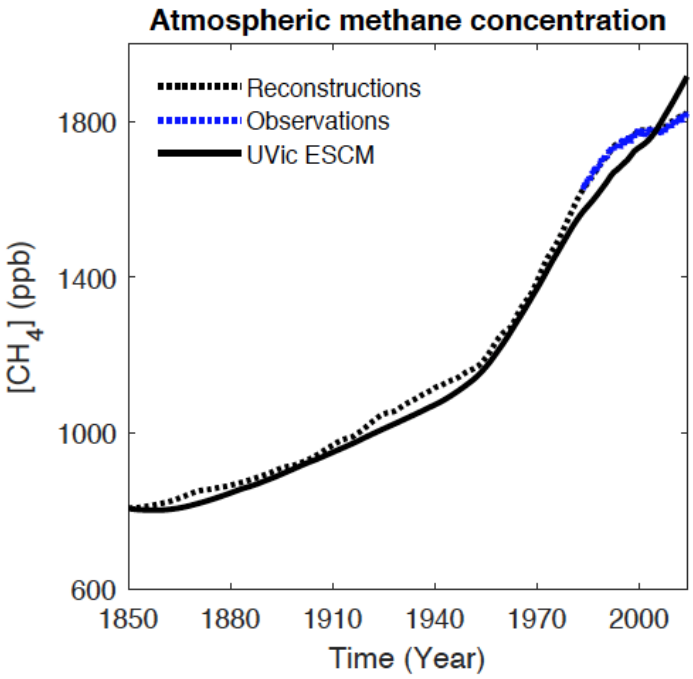

Figure 4.2. Simulated [CH_4] over the historical period (1850-2014) in comparison to reconstructed as well as observed [CH_4]. Reconstructions of [CH_4] are based on ice cores and firn (perennial snow) layers from polar regions (Etheridge et al., 1998; Rhodes et al., 2013), whereas observations of [CH_4] are from the NOAA Global Monitoring Laboratory (Dlugokencky, 2020).

We further validate the global CH_4 cycle simulated by the UVic ESCM over the past few decades (1980s, 1990s, 2000s) against syntheses from recent global CH_4 budget reports and other published estimates. Despite significant uncertainties in both the model inputs and parameters, our model reproduces relatively well the global CH_4 budget over the three decades (Table 4.2). Total CH_4 sources are 490, 515 and 549 Tg CH_4 yr^{-1} in 1980s, 1990s, and 2000s, respectively. At the exception of the 1980s, these values are in the range of either top-down (TD) or bottom-up (BU) estimates from the global CH_4 budget reports (Table 4.2). For the 1980s, total CH_4 sources are smaller than both TD and BU estimates from the global CH_4 budget reports. This underestimation of total CH_4 sources could be attributed to low total CH_4 emissions from anthropogenic sources prescribed to our model (see Table 4.2). For instance, research suggests that there has been a general underestimation of CH_4 emissions from the extraction, distribution, and use of fossil fuels (i.e. coal, oil, and natural gas) in recent decades (Hmiel et al., 2020; Schwietzke et al., 2016). However, we cannot rule out a potential underestimation of natural CH_4 emissions in this study. Depending on the decade,

wetland CH_4 emissions simulated by our model are in the range of either TD or BU estimates from the global CH_4 budget reports. As indicated in the model description, natural CH_4 emissions (excluding wetlands) prescribed to our model are consistently between TD and BU estimates from the global CH_4 budget reports throughout the three decades (Table 4.2). Simulated total CH_4 sinks are generally within the range of both TD and BU estimates, except for 1990s – a decade during which the simulated global CH_4 sinks are smaller than estimated in the global CH_4 budget reports (Table 4.2). Our model simulates an average atmospheric CH_4 burden of 4490, 4790, and 5056 Tg CH_4 for the 1980s, 1990s and 2000s, respectively – consistent with estimates from the Fifth Assessment Report (AR5) by the IPCC (Ciais et al., 2013).

Overall, our simple representation of the global CH_4 cycle displays a relatively good performance over most of the historical period since the year 1850 despite the complex level of uncertainties in the global CH_4 budget. The lowest performance by the model is with respect to the recent [CH_4] trends whose causes are still not well understood (Ganesan et al., 2019; Schaefer, 2019).

4.3.2. Effects of CH_4 mitigation on [CH_4] and surface air temperature

Our model simulations suggest that CH_4 mitigation initiated between the years 2020 and 2030 will result in 90-135 ppb more atmospheric [CH_4] in the year 2100 than for an early CH_4 mitigation represented by the SSP1-2.6 trajectory (Figure 4.3a). Delaying CH_4 mitigation to between the years 2040 and 2050 implies 185-260 ppb more atmospheric [CH_4] in the year 2100 than for an early CH_4 mitigation represented by the SSP1-2.6 trajectory. Eventually, [CH_4] for the different CH_4 mitigation scenarios would converge within the first half of the 22nd century (Figure 4.3a). Inaction on CH_4 mitigation in the 21st century (i.e. SSP3-7.0 trajectory) could result in ~2094 ppb more atmospheric [CH_4] in the year 2100 than if CH_4 mitigation evolves according to SSP1-2.6.

Our model simulations further suggest that different initiations of CH_4 mitigation over the next three decades under SSP1-2.6 will result in distinct surface air temperatures by the end of the century and beyond (Figure 4.3b). CH_4 mitigation initiated between the years 2020 and 2030 could result in 0.08-0.12°C more warming in the year 2100 than if CH_4 mitigation evolves according to SSP1-2.6. Delaying CH_4 mitigation to between the years 2040 and 2050 could result in 0.17-0.22°C more

warming in the year 2100 than for an early CH_4 mitigation represented by the SSP1-2.6 trajectory. Although [CH_4] for the different CH_4 mitigation scenarios are simulated to converge in the first half of the 22nd century (Figure 4.3a), our model suggests that differences in surface air temperature between the different mitigation scenarios will persist for more than two centuries (Figure 4.3b). The lack of CH_4 mitigation in the 21st century (i.e. SSP3-7.0 trajectory) could result in ~0.62°C more warming in the year 2100 than if CH_4 mitigation evolves according to SSP1-2.6. We note that CO_2 feedbacks amplify the surface air temperature response in late versus early CH_4 mitigation scenarios, as illustrated by the [CO_2] plots in Figure 4.3c.

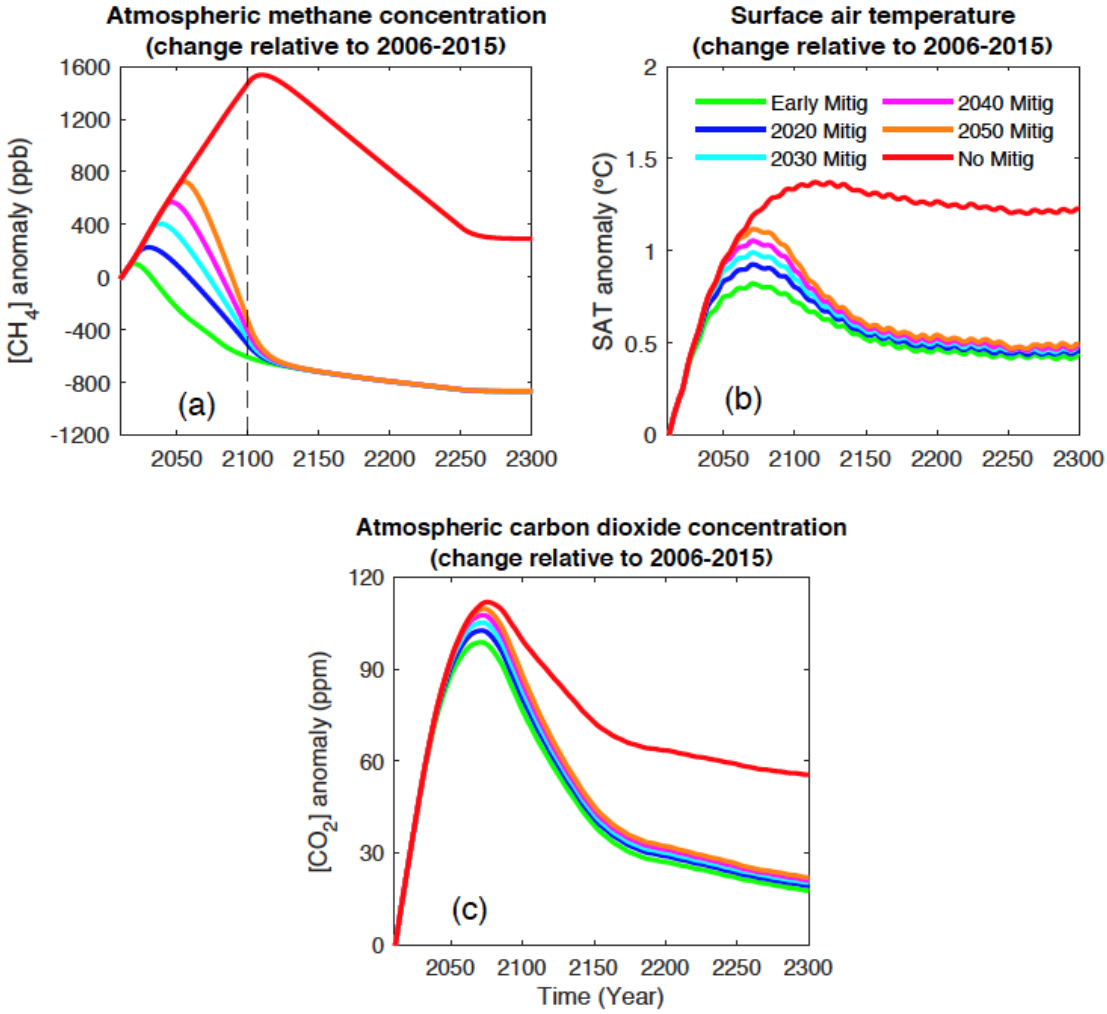

Figure 4.3. Projected changes in (a) atmospheric CH_4 concentration, (b) surface air temperature (SAT), and (c) atmospheric CO_2 concentration relative to 2006-2015 for different initiation of CH_4 mitigation under the assumption that non-CH_4 forcing agents evolve according to SSP1-2.6. The variability in the SAT curves is associated with the solar cycle.

To understand the reasons behind the differences in [CH_4] between the considered scenarios of CH_4 mitigation, we analyze the balance between total CH_4 sources (Figure 4.4a) and CH_4 sinks (Figure 4.4b) at the year 2100 when all mitigated anthropogenic CH_4 emissions converge to the SSP1-2.6 level (Figure 4.1). For the scenarios of CH_4 mitigation initiated between the years 2020 and 2050, our model suggests that total CH_4 sources will be relatively the same in the year 2100 (Figure 4.4a). This result is justified by the fact that: (i) simulated global wetland CH_4 emissions are relatively independent of the initiation of CH_4 mitigation, with very small differences (<0.5 Tg CH_4 yr^{-1}) between the considered mitigation scenarios in the year 2100 (Figure 4.4c); (ii) CH_4 emissions from non-wetland natural sources are assumed to be of the same magnitude (and constant) in this study (see Section 4.2.3).

According to our model simulations, differences in the initiation of CH_4 mitigation over the next few decades will be strongly reflected in CH_4 sinks at the year 2100 (Figure 4.4b). In our simple model, the decay of atmospheric CH_4 is parameterized as a function of the atmospheric CH_4 burden and a constant lifetime for atmospheric CH_4 (see Section 4.2.3). A delayed mitigation results in a higher atmospheric CH_4 burden than for an early mitigation throughout the 21st century (Figure 4.4d), which implies a lag in the decline of CH_4 sinks for the delayed mitigation in comparison to the early mitigation (Figure 4.4c). Our model suggests that total CH_4 sinks in the year 2100 will be 26-39 Tg CH_4 yr^{-1} higher for CH_4 mitigation initiated between the years 2020 and 2030 than for an early CH_4 mitigation represented by the SSP1-2.6 trajectory. Furthermore, total CH_4 sinks in the year 2100 will be 54-76 Tg CH_4 yr^{-1} higher for CH_4 mitigation delayed to between the years 2040 and 2050 than if CH_4 mitigation evolves according to SSP1-2.6 (Figure 4.4b).

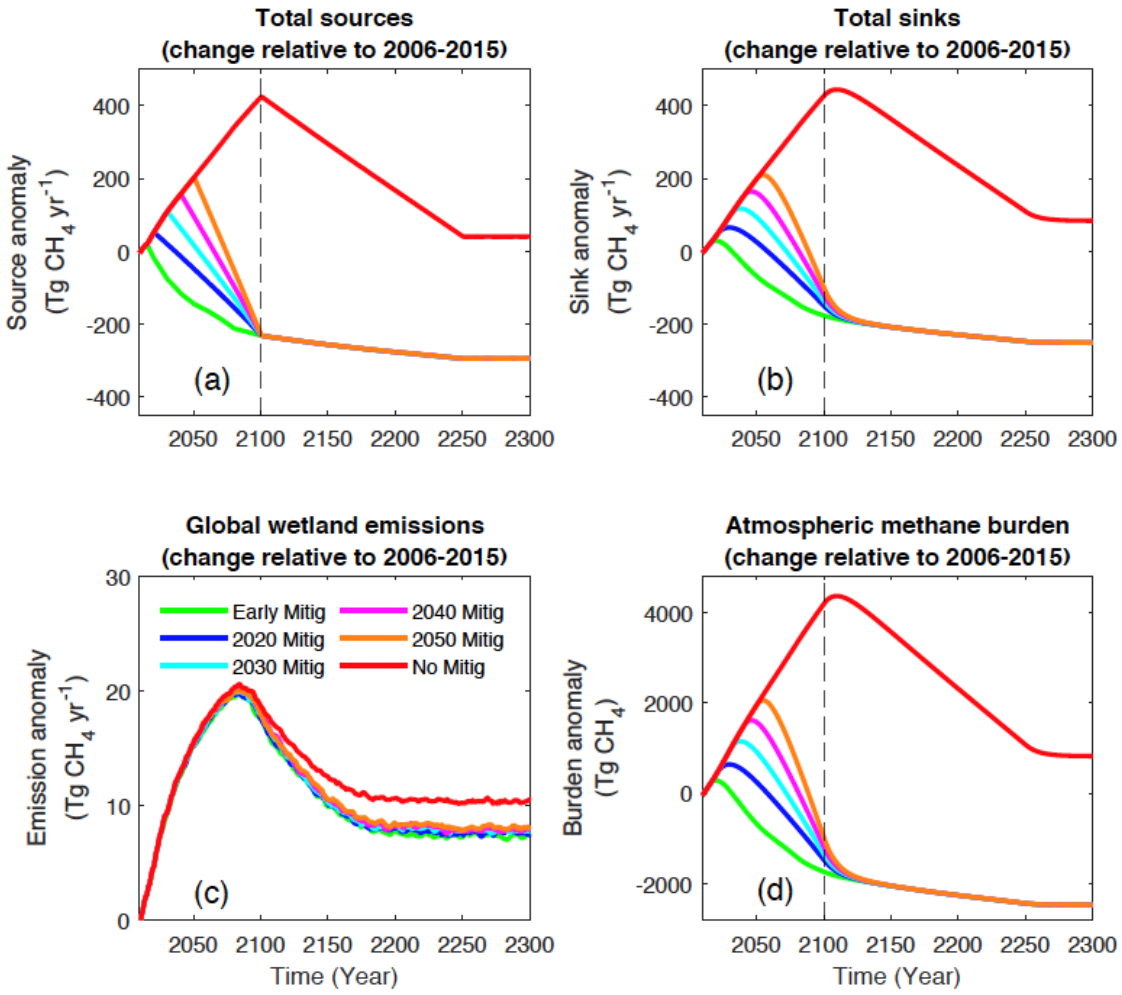

Figure 4.4. **Projected changes in (a) total CH_4 sources, (b) total CH_4 sinks, (c) global wetland CH_4 emissions, and (d) atmospheric CH_4 burden relative to 2006-2015 for different initiation of CH_4 mitigation under the assumption that non-CH_4 forcing agents evolve according to SSP1-2.6.**

4.3.3. Effects of CH_4 mitigation on stringent warming limits

Determining the historical warming level is a critical aspect for assessing the implications of future climate projections on global warming limits set by the Paris Agreement (Rogelj et al., 2019; Tokarska et al., 2019). A recent special report by the IPCC uses an estimate of 0.97°C for the global warming level in the 2006-2015 decade relative to the 1850-1900 period (IPCC, 2018), whereas our model suggests a slightly high value (1.10°C) for the global warming level in the same decade relative to the same baseline period. Hence, we adopt the IPCC estimate for the historical warming level to investigate global

warming levels associated with different scenarios of CH_4 mitigation in the 21st century under SSP1-2.6 (Figure 4.5).

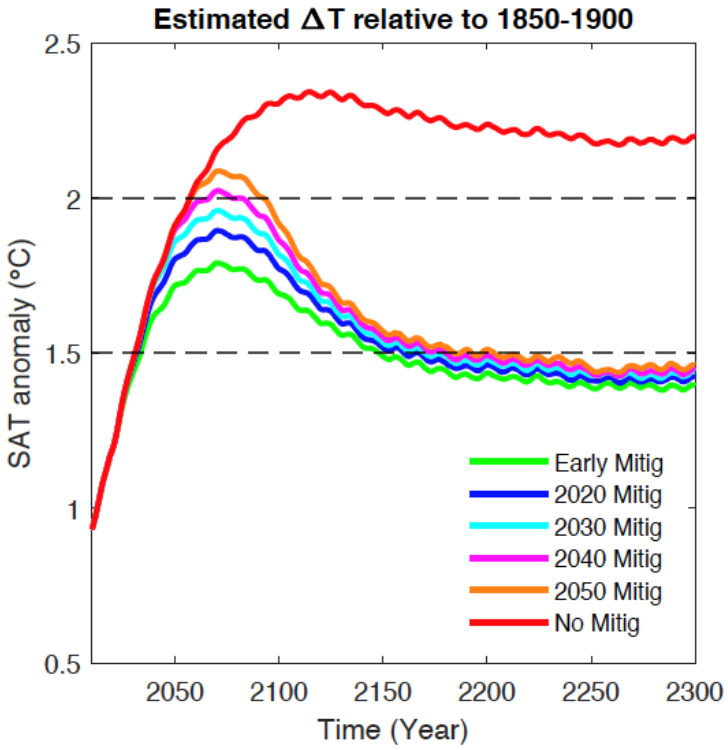

Figure 4.5. Projected changes in global mean surface air temperature (ΔT) relative to 1850-1900 for different initiation of CH_4 mitigation under the assumption that non-CH_4 forcing agents evolve according to SSP1-2.6. The variability in the SAT curves is associated with the solar cycle.

Our results suggest that none of the CH_4 mitigation scenarios (including the SSP1-2.6 trajectory or "Early Mitig") considered in this study will allow to limit global warming to below 1.5°C above 1850-1900 levels in the 21st century (Figure 4.5). By design, the SSP1-2.6 scenario represents mitigation strategies to limit global warming to 2°C by the year 2100 but not necessarily 1.5°C (O'Neill et al., 2016) implying that efforts to mitigate CH_4 under this scenario will not achieve much with regard to the 1.5°C warming limit during the current century (Figure 4.5). Our results suggest that, under SSP1-2.6, the 1.5°C warming limit will be breached in the early 2030s and the level of global warming will stay above the 1.5°C warming limit throughout the 21st century (Figure 4.5).

Our model simulations further suggest that global warming relative to 1850-1900 could be limited to below 2°C throughout the 21st century if non-CH_4 forcings evolve according to SSP1-2.6 and CH_4 mitigation is initiated by the year 2030 (Figure 4.5). Moreover, our results suggest that the 2°C warming limit could be breached for two decades if CH_4 mitigation is delayed to the year 2040 under SSP1-2.6. If non-CH_4 forcings evolve according to SSP1-2.6 and CH_4 mitigation is delayed to the year 2050, the 2°C warming target could be overshot for three to four decades in the remainder of the 21st century (Figure 4.5). In the long run, all mitigation scenarios considered in this study (i.e. CH_4 mitigation initiated between the years 2020 and 2050) under SSP1-2.6 could allow to limit global warming to 1.5°C from the second half of the 22nd century onwards (Figure 4.5). However, aggressive efforts to reduce CO_2 and other non-CH_4 forcings according to SSP1-2.6 without CH_4 mitigation in the 21st century could still increase global warming to above 2°C relative to 1850-1900 throughout the second half of the 21st century and beyond (Figure 4.5).

4.4. Discussion and conclusions

Our study applies the UVic ESCM, an Earth system model of intermediate complexity (EMIC), into which we implemented a simplified representation of the global CH_4 cycle as a first step to prognostically simulate the evolution of atmospheric CH_4 in the EMIC. The global CH_4 cycle in the UVic ESCM version used here consists of simulated CH_4 emissions from wetlands, static and aggregated CH_4 emissions non-wetland natural sources (termites, lakes, wildfires, wild ruminants, etc.), as well as simulated atmospheric CH_4 decay based on a simple one-box model with a constant lifetime. The EMIC is forced with prescribed anthropogenic CH_4 emissions among other forcing data. Although this approach for global CH_4 modelling is relatively simple, it allows to reproduce the evolution of atmospheric [CH_4] reasonably well in comparison to reconstructions over most of the past 170 years (see Figure 4.2). However, our model does not capture the slowdown and renewed growth in atmospheric [CH_4] observed in the 1990s and 2000s whose causes are still under debate (Prather and Holmes, 2017; Schaefer, 2019). Our simple modelling approach also allows to perform CH_4 mitigation experiments through intrinsic reductions in anthropogenic CH_4 emissions, instead of using prescribed atmospheric [CH_4] reductions (Jones et al., 2018).

There are concerns about the sustained growth in atmospheric [CH_4] since the year 2007 and the potential challenge of continued increase in CH_4 emissions over the next decades with regard to meeting the temperature goals in the Paris Agreement even if anthropogenic CO_2 emissions were reduced aggressively (Ganesan et al., 2019; Nisbet et al., 2019). Our study investigates the importance of immediate versus delayed CH_4 mitigation to comply with the global warming limits set by the Paris Agreement under the assumption that all non-CH_4 forcings (including anthropogenic CO_2 emissions) would evolve according to SSP1-2.6. Our results suggest that delaying CH_4 mitigation to between the years 2040 and 2050 under SSP1-2.6 could result in an overshoot of the 2°C warming limit for two to four decades in the remainder of the 21st century. In contrast, initiating stringent CH_4 mitigation by the year 2030 under SSP1-2.6 could allow to limit global warming to below 2°C above pre-industrial levels (Figure 4.5). Our results agree with simulations by integrated assessment models (IAMs) and climate models of reduced complexity, which are the tools commonly used to investigate CH_4 mitigation and its climate impacts. The major agreement between our results and those by IAMs is the need for deep reductions in CH_4 emissions, alongside stringent CO_2 mitigation by mid century, to limit global warming to below 2°C above pre-industrial levels (Gernaat et al., 2015; Harmsen et al., 2019b; Rogelj et al., 2018). The particularities of our results are: (i) the importance of immediate rather than delayed CH_4 mitigation to comply with the 2°C warming limit, (ii) the potential role of CO_2 feedbacks in the amplification of the surface air temperature response for delayed versus immediate CH_4 mitigation.

Our study further suggests that none of the CH_4 mitigation scenarios considered in this study would allow to limit global warming to 1.5°C in the 21st century. According to a previous study, limiting global warming to 1.5°C by the year 2100 would require reducing [CH_4] at four times the rate assumed in the Representative Concentration Pathway (RCP) 2.6 – a future scenario comparable to SSP1-2.6 (Jones et al., 2018). Such a scenario would imply an initial overshoot of the 1.5°C warming target for a couple of decades in the 21st century (Jones et al., 2018). Furthermore, this [CH_4] scenario would involve negative CH_4 emissions throughout the second half of the 21st century although required technologies are not yet developed (Jones et al., 2018). Nonetheless, our study suggests that CH_4 mitigation over the next three decades under SSP1-2.6 will increase the likelihood to limit global warming to 1.5°C in the long run (from the second

half of the 22nd century onwards) after an overshoot in the first half of the 21st century (Figure 4.5).

Overall, although there exist large uncertainties in the global CH_4 budget (Saunois et al., 2020), our results imply that cuts in anthropogenic CH_4 emissions should not be delayed to increase the likelihood of limiting global warming to 2°C above pre-industrial levels. Many anthropogenic sources of CH_4 could be reduced cost-efficiently (Harmsen et al., 2019b; Höglund-Isaksson, 2012) and previous studies suggest that the priority for deep emission cuts should be in the energy, industry and transport sectors without neglecting the high potential from the waste and agricultural sectors (Gernaat et al., 2015; Harmsen et al., 2019b; Jackson et al., 2020; Rogelj et al., 2018; Saunois et al., 2016b). Multilateral partnerships already exist to support large-scale CH_4 mitigation (e.g. the Climate and Clean Air Coalition: https://www.ccacoalition.org/, and the Global Methane Initiative: https://www.globalmethane.org/).

Limitations of this study include a whole set of uncertainties in the areal extent and dynamics of wetlands (including the impact of land-use change upon wetlands) as well as biogeochemical processes regulating wetland CH_4 emissions (Abdalla et al., 2016; Bridgham et al., 2013). Most of these limitations are discussed in detail in Chapter 3 (e.g. Section 3.7.2). Major limitations specific to this study are associated with the following assumptions: (i) a constant lifetime for atmospheric CH_4, (ii) static CH_4 emissions from non-wetland natural sources, (iii) an effective mitigation of CO_2 and other non-CH_4 climate forcers according to SSP1-2.6, except for CH_4. Regarding the first limitation, we chose to use a lifetime for atmospheric CH_4 fixed at 9.3 years as part of initial steps to simulating the evolution of atmospheric [CH_4] prognostically with the UVic ESCM. However, there exist variations (from fractions of a year to few years) in the atmospheric CH_4 lifetime mostly due to a positive chemical feedback involving the oxidation of CH_4 by the OH radical (Naik et al., 2013; Prather et al., 2012). This positive feedback is such that declining [CH_4] enhances the abundance of OH in the atmosphere, which results in more oxidation of CH_4, further lowering of [CH_4], and shortening of the atmospheric CH_4 lifetime. As such, declining [CH_4] in response to CH_4 mitigation would imply a decrease in the atmospheric CH_4 lifetime, a further reduction in [CH_4], and eventually a cooling of the Earth. However, the same feedback mechanism is such that increasing [CH_4] in response to the absence of CH_4 mitigation would increase the atmospheric CH_4 lifetime, a further rise in [CH_4], and imply a high level of global

warming. Therefore, one consequence of this assumption (of a constant CH_4 lifetime) is the potential underestimation of the peak [CH_4] in delayed mitigation scenarios. The assumption of a constant lifetime for atmospheric CH_4 in this study can be seen as a simple but more or less conservative approach for investigating the climate impact of CH_4 mitigation after decades of sustained [CH_4] growth. Furthermore, the atmospheric CH_4 lifetime used in our model simulations is consistent with estimates reported for the pre-industrial era (9.5 ± 1.3 years) and present-day (9.1 ± 0.9 years) (Prather et al., 2012). Regarding the second limitation, CH_4 emissions from non-wetland sources (e.g. termites, lakes, wildfires, geologic seeps, marine hydrates) in our model simulations are held fixed at 45 Tg C yr^{-1} (i.e. 60 Tg CH_4 yr^{-1}) mostly because the UVic ESCM does not incorporate these natural sources of CH_4. The amount of non-wetland natural CH_4 emissions used in our model simulations is within the range of estimates over the pre-industrial periods (Houweling et al., 2000 and references therein) as well as the last four decades (Kirschke et al., 2013; Saunois et al., 2020). We acknowledge that it is difficult to predict the evolution of non-wetland natural CH_4 sources in the future, especially for wildfires, lakes and other climate-sensitive sources (Dean et al., 2018; Saunois et al., 2020). The third limitation is related to the assumption that all anthropogenic GHGs and aerosols would evolve according SSP1-2.6, while anthropogenic CH_4 emissions continue to increase over the next three decades. Although this assumption may be unrealistic, it enables to investigate recent concerns raised about sustained [CH_4] growth in the next few decades and the associated challenge for achieving the 2°C warming limit despite stringent CO_2 mitigation by mid century (Ganesan et al., 2019; Nisbet et al., 2019).

In summary, our study suggests that aggressive reductions of anthropogenic CO_2 emissions without CH_4 mitigation over the next few years could push the Earth system beyond the 2°C warming limit above pre-industrial levels. Considering that (i) current NDCs are mostly focused on reducing CO_2 emissions (Harmsen et al., 2019a) and (ii) the sustained rise in [CH_4] since the year 2007 is tracking future scenarios of unmitigated emissions (Nisbet et al., 2019; Saunois et al., 2016b), we highlight the importance of immediate cuts in anthropogenic CH_4 emissions globally, along with CO_2 mitigation, in order to increase the likelihood of keeping global warming below 2°C above pre-industrial levels.

Table 4.1. Description of anthropogenic CH_4 emission scenarios used in this study.

Name	Description	Comments
Early Mitigation	SSP1-2.6 throughout the 21st century	Peak emissions reduced by ~69% in 2100
2020 Mitigation	SSP3-7.0 up to 2020, then linear decline to SSP1-2.6 value in 2100	Peak emissions reduced by ~71% in 2100
2030 Mitigation	SSP3-7.0 up to 2030, then linear decline to SSP1-2.6 value in 2100	Peak emissions reduced by ~74% in 2100
2040 Mitigation	SSP3-7.0 up to 2040, then linear decline to SSP1-2.6 value in 2100	Peak emissions reduced by ~76% in 2100
2050 Mitigation	SSP3-7.0 up to 2050, then linear decline to SSP1-2.6 value in 2100	Peak emissions reduced by ~78% in 2100
No Mitigation	SSP3-7.0 throughout the 21st century	No emission reductions in the 21st century

Table 4.2. The global CH_4 budget by the UVic ESCM for the 1980-1989, 1990-1999, and 2000-2009 decades in comparison to recent top-down (TD) and bottom-up (BU) estimates. All units are in Tg CH_4 yr^{-1}.

	UVic ESCM			Kirschke et al. (2013)		Kirschke et al. (2013)		Saunois et al. (2020)	
	1980s	1990s	2000s	1980s		1990s		2000s	
	Model inputs or results			TD	BU	TD	BU	TD	BU
Anthropogenic emissions	289	311	340	348 (305-383)	308 (292-323)	372 (290-453)	313 (281-347)	331 (310-346)	334 (325-357)
Wetland emissions	141	144	149	167 (115-231)	225 (183-266)	150 (144-160)	206 (169-265)	180 (153-196)	147 (102-179)
Other natural emissions	60	60	60	36 (35-36)	130 (61-200)	32 (23-37)	130 (61-200)	37 (21-50)	222 (143-306)
Total sources	490	515	549	551 (500-592)	663 (536-789)	554 (529-596)	649 (511-812)	545 (522-559)	703 (570-842)
Total sinks	458	488	515	511 (460-559)	539 (420-718)	542 (518-579)	596 (530-668)	540 (486-556)	625 (500-798)

Chapter 5. Multi-centennial projections of wetland methane emissions from gradual permafrost thaw and their climate impact

Abstract

Methane (CH_4) emissions from thawing permafrost soils remain under-represented in Earth system models used for future climate projections, implying a potential underestimation of future global warming. Here we use an Earth system model of intermediate complexity to project wetland CH_4 emissions from previously frozen carbon stored within the top ~3m of depth following gradual permafrost thaw (hereafter, permafrost CH_4 emissions) and their climate impact by the years 2100 and 2300. We account for uncertainties in wetland CH_4 biogeochemistry through model parameter perturbations, and our model simulations feature possibilities of high (low) production jointly with low (high) oxidation of CH_4 in wetlands underlain by permafrost. Moreover, through model experiments designed to isolate the climate effect of permafrost CH_4 emissions, our model projections represent an extreme situation whereby previously frozen carbon decays only into CH_4. According to our model, permafrost CH_4 emissions in the year 2100 will range from 3 (0-6) Tg C yr^{-1} (1 Tg C ~ 1.3 Tg CH_4) under the low anthropogenic emission scenario (SSP1-2.6) to 20 (1-51) Tg C yr^{-1} under the high anthropogenic emission scenario (SSP5-8.5). The warming due to these CH_4 emissions is projected to be small, ranging from ~0.0 (0.0-0.01) °C under SSP1-2.6 to 0.02 (0.0-0.04) °C under SSP5-8.5. Beyond the 21st century, our model suggests that permafrost CH_4 emissions will increase substantially in the 22nd and 23rd centuries under SSP5-8.5, reaching 58 (3-158) Tg C yr^{-1} in the year 2300. The warming due to these CH_4 emissions is projected to be 0.09 (0.01-0.24) °C by the year 2300. Under SSP1-2.6 and intermediate anthropogenic emission scenarios (SSP2-4.5 and SSP4-6.0), however, permafrost CH_4 emissions are projected to remain below 40 Tg C yr^{-1} and induce a modest warming (<0.08°C) throughout the 22nd and 23rd centuries. We conclude that reducing anthropogenic emissions could prevent potentially large permafrost CH_4 emissions and their climate impact over many centuries.

5.1. Introduction

Permafrost soils across the boreal and Arctic regions store vast amounts of organic carbon preserved from microbial decomposition for millennia owing to predominant cold temperatures (Hugelius et al., 2014). However, permafrost is thawing in many terrestrial locations of these northern regions as a consequence of climate warming (Biskaborn et al., 2019) and northern permafrost thaw is expected to increase in the future if anthropogenic emissions of greenhouse gases continue to rise (Kirtman et al., 2013; Schuur et al., 2015). Permafrost thaw in the future could result in increased wetland CH_4 emissions following anaerobic decomposition of previously frozen carbon, which could amplify global warming (Dean et al., 2018; Schuur et al., 2015). The scientific understanding is that previously frozen carbon in wetlands could be a new source of organic matter for methanogens (CH_4-producing microbes), which would enhance CH_4 production and lead to permafrost CH_4 emissions under the assumption that methanotrophs (CH_4-oxidizing microbes) will not consume all of the produced CH_4 (Kwon et al., 2019; Olefeldt et al., 2017; Schuur et al., 2015).

While wetland CH_4 emissions from thawing permafrost soils are already occurring in many locations, several studies suggest that such emissions will not induce a strong feedback to climate change throughout the 21st century. Measurements at two peatland sites in northern Canada show that CH_4 emissions from anaerobic decomposition of previously frozen carbon represent a small component (<2 g CH_4 m^{-2} yr^{-1}) of local total CH_4 emissions (>20 g CH_4 m^{-2} yr^{-1}) (Cooper et al., 2017). By upscaling model projections for wetlands in Russia, one study estimates a global temperature change of 0.012°C due to wetland CH_4 emissions from Russian permafrost regions by mid 21st century (Anisimov, 2007). Based on predictions constrained by field measurements, satellite observations and reanalysis data, a more recent study suggests an upper limit of 0.02°C for the future warming induced by wetland CH_4 emissions from Siberian permafrost regions by mid century (Anisimov and Zimov, 2020). Another study suggests that the warming induced by CH_4 emissions from previously frozen carbon in response to gradual permafrost thaw across the boreal and Arctic regions will not exceed 0.1°C by the year 2100 even when considering a potential increase in surface inundation (Gao et al., 2013). A meta-analysis of permafrost carbon modelling studies gives a similar result (0.01-0.11°C) for the warming due to CH_4 emissions from gradual

permafrost thaw by the year 2100 under various scenarios of high anthropogenic emissions (Schaefer et al., 2014). For comparison, multi-model projections suggest that permafrost CO_2 emissions will induce a warming of 0.06-0.40°C by the year 2100 under scenarios of high anthropogenic emissions (Schaefer et al., 2014).

The permafrost CH_4 feedback remains under-represented in Earth system models (ESMs) contributing to international climate assessment reports (Ciais et al., 2013) as well as research on feedbacks between climate change and biogeochemical processes (Arora et al., 2013, 2020). Here we use the University of Victoria Earth System Model (UVic ESCM) version 2.10 (Mengis et al., 2020), into which we implemented processes regulating wetland CH_4 emissions and their climate impact. Our study focuses on CH_4 emissions resulting from the decomposition of previously frozen carbon in wetlands following gradual permafrost thaw. The aim of this study is to project the potential evolution of wetland CH_4 emissions from thawing permafrost soils and quantify their climate impact on multi-centennial scales. In our analysis, we account for three major uncertainties in wetland CH_4 biogeochemistry (see Section 5.2.4). The remainder of this chapter is organized as follows: Section 5.2 describes the study methods, Section 5.3 presents the study results, and Section 5.4 provides the discussion and conclusions.

5.2. Methods

5.2.1. Description of the UVic ESCM

We use a modified version of the UVic ESCM, into which we implemented a simple model for wetland CH_4 emissions (see Chapter 3) and a one-box model for atmospheric CH_4 (see Chapter 4). The UVic ESCM is an Earth system model of intermediate complexity (EMIC) with a horizontal grid resolution of 3.6° in longitude and 1.8° in latitude (Weaver et al., 2001). The EMIC consists of a comprehensive ocean general circulation model with 19 vertical layers, coupled to a dynamic-thermodynamic sea ice model, a 2-D (vertically-integrated) energy-moisture balance model for the atmosphere, and a land surface model (Weaver et al., 2001). This study is based on modifications to version 2.10 of the UVic ESCM (Mengis et al., 2020).

The land in version 2.10 of the UVic ESCM is represented with 14 ground layers of unequal thicknesses with a total thickness of 250 m (Avis et al., 2011; Mengis et al., 2020). The top eight ground layers (~10 m in total depth) are soil layers, whereas the bottom six ground layers are bedrock layers with thermal characteristics of granitic rock (Avis et al., 2011). The energy balance is determined for each ground layer and grid cells containing permafrost are identified whenever one ground layer is frozen for at least two consecutive years (Avis et al., 2011). Permafrost thaw in the UVic ESCM occurs mainly in the form of active layer deepening but also talik expansion at the grid scale. Water phase changes in the soil layers are determined over a range of soil temperatures to determine the fraction of frozen and unfrozen water in the ground (Avis et al., 2011). Porosity and permeability are determined based on the relative abundance of prescribed sand, clay, and silt-sized particles. Moisture undergoes free drainage in these soil layers and subsurface runoff occurs when the water reaches the bedrock (Avis et al., 2011). In the model version used in this study, sub-grid scale wetlands are identified following a TOPMODEL approach for global models (Gedney and Cox, 2003).

The UVic ESCM includes a representation of the global carbon cycle. The marine carbon cycle is represented with organic and inorganic carbon cycle models embedded in the ocean general circulation model. The organic carbon cycle is simulated with an ocean biogeochemistry model describing phytoplankton and zooplankton dynamics (Keller et al., 2012). The inorganic carbon cycle model simulates the air-sea exchange of CO_2 and ocean carbonate chemistry following the protocols of the Ocean Carbon-cycle Model Intercomparison Project (Orr, 1999; Weaver et al., 2001), with updated numbers for the air-sea CO_2 exchange parameterization (Mengis et al., 2020; Wanninkhof, 2014). Dissolved inorganic carbon is treated as a passive tracer that is subject to ocean circulation (Weaver et al., 2001). Carbonate dissolution in ocean sediments is simulated with a model of respiration in marine sediments (Archer, 1996; Eby et al., 2009).

Terrestrial CO_2 fluxes are simulated using the Top-down Representation of Interactive Foliage and Flora including Dynamics (TRIFFID), a dynamic global vegetation model that is coupled to the land surface model (Avis et al., 2011; Meissner et al., 2003). TRIFFID defines the state of the terrestrial biosphere in terms of soil carbon as well as the structure and coverage of five plant functional types: broadleaf trees, needleleaf trees, shrubs, C3 grasses and C4 grasses (Cox, 2001; Matthews et al., 2004; Meissner et al., 2003). Terrestrial carbon gain occurs through photosynthesis that is

simulated as a function of atmospheric CO_2 concentration, shortwave radiation, air temperature, humidity, and soil moisture. Soil carbon gain occurs through litter-fall and vegetation mortality. Soil carbon can accumulate in the top six layers (~3.35 m in total depth). The buildup of carbon in permafrost-affected grid cells is simulated following a diffusion method that approximates cryoturbation, a process driven by long-term freeze-thaw cycles (MacDougall and Knutti, 2016). Terrestrial carbon loss occurs through autotrophic respiration by plants and heterotrophic respiration by soil microbes (Matthews et al., 2004; Meissner et al., 2003). Permafrost carbon can only be lost through microbial respiration, which only occurs in unfrozen (thawed) soil layers (MacDougall et al., 2012; MacDougall and Knutti, 2016). By design, following gradual thaw, previously frozen carbon (e.g. carbon frozen at pre-industrial time) in the UVic ESCM decays with its own decay rate relative to regular (non-permafrost) soil carbon (MacDougall and Knutti, 2016).

5.2.2. Wetland CH_4 emissions

Wetland CH_4 emissions are simulated in the UVic ESCM following a recent model development (Nzotungicimpaye et al., 2020). Chapter 3 provides a detailed description of the wetland CH_4 model (WETMETH) implemented in the UVic ESCM. Here, we give a brief description of the wetland CH_4 model and reproduce mathematical formulas from Chapter 3. The reader should note that some of the default model parameters in Section 3.3.1 are subject to perturbations in this study (see Section 5.2.4).

For any land grid cell, microbial CH_4 production is determined in an underlying soil layer *i* as:

$$P_i = S(\theta_i)\, C_i\, r\, Q_{10}^{\frac{T_i - T_0}{10}}\, \exp\left(-\frac{z_i}{\tau_{\text{prod}}}\right), \quad (5.1)$$

where $S(\theta_i)$ is the fraction of soil layer that is saturated with water, C_i is the amount of soil carbon (in kg C m^{-3}) in the layer, r (in kg kg^{-1} s^{-1}) is the specific CH_4 production rate, T_i is the average temperature (in Kelvin, K) for the layer, T_0 is a baseline temperature (T_0 = 273.15 K), and Q_{10} is a coefficient representing the temperature-sensitivity of CH_4 production in wetlands. CH_4 production is assumed to shut down in frozen soil layers. Furthermore, z_i (in m) is the depth of the layer relative to the soil surface (positive

downwards), and τ_{prod} (in m) is a scaling parameter. Dry soil layers ($S(\theta_i) = 0$) are assumed to be predominantly oxic and not producing CH_4 ($P_i = 0$).

The total amount of CH_4 produced in the soil column (P in kg C m^{-2} s^{-1}) is calculated as:

$$\mathrm{P} = \int_{i=1}^{i=k} \mathrm{P}_i \, dz_i \ , \tag{5.2}$$

where P_i (in kg C m^{-3} s^{-1}) is the rate of CH_4 production in the soil layer *i* from Eq. (5.1), dz_i (in m) is the thickness of the soil layer *i*, and *k* represents the bottom-most soil layer. This amount of CH_4 (P) is then subject to oxidation in transit to emission into the atmosphere.

Microbial CH_4 oxidation (O_x in kg C m^{-2} s^{-1}) is calculated for the entire soil column as:

$$\mathrm{O}_x = \mathrm{P}\,(1 - \exp(-\frac{z_{\mathrm{oxic}}}{\tau_{\mathrm{oxid}}})), \tag{5.3}$$

where P (in kg C m^{-2} s^{-1}) is the total amount of CH_4 produced in the soil column as defined in Eq. (5.2), z_{oxic} (in m) is the relative depth (positive downwards) to the oxic-anoxic interface, and τ_{oxid} (in m) is a scaling parameter for CH_4 oxidation. The function $(1 - \exp(-\frac{z_{\mathrm{oxic}}}{\tau_{\mathrm{oxid}}}))$ represents the fraction of produced CH_4 that gets oxidized in the soil column in transit to emission (i.e. fractional CH_4 oxidation).

Wetland CH_4 emissions (E_w in kg C m^{-2} s^{-1}) are calculated as the balance between microbial CH_4 production (P) and oxidation (O_x) in the soil column:

$$\mathrm{E}_w = \mathrm{P} - \mathrm{O}_x \ , \tag{5.4}$$

where P and O_x are given by Eq. (5.2) and Eq. (5.3), respectively.

5.2.3. Atmospheric CH_4 concentration

As in Chapter 4, we use a simple one-box model to simulate the evolution of the atmospheric CH_4 burden (B) with time as the balance between total CH_4 emissions (E) and total CH_4 sinks (S):

$$\frac{\mathrm{dB}}{\mathrm{dt}} = (\mathrm{E} - \mathrm{S}), \quad (5.5)$$

where E is the sum of simulated wetland CH_4 emissions, prescribed anthropogenic CH_4 emissions, and natural CH_4 emissions from non-wetland sources (e.g. termites, wild ruminants, wildfires, lakes, rivers, geologic seeps, and marine hydrates). We assume that CH_4 emissions from these non-wetland natural sources remain constant in time with a value of 45 Tg C yr^{-1}, which is in the range of estimates over the last few decades (Kirschke et al., 2013; Saunois et al., 2020). Sinks of atmospheric CH_4 are aggregated into a single term (S) calculated as $\mathrm{S} = \mathrm{B}\,(1 - \exp(-\frac{1}{\tau_{\mathrm{CH4}}}))$, where τ_{CH4} is the atmospheric CH_4 lifetime assumed to be 9.3 years (Saunois et al., 2020). At each time step, $[CH_4]$ is determined based on the atmospheric CH_4 burden (B) by using a factor equivalent to ~2.8 Tg CH_4/ppb.

5.2.4. Perturbations of model parameters

As mentioned in Section 5.2.1, permafrost carbon (i.e. previously frozen carbon) in the UVic ESCM decays with its own decay rate relative to non-permafrost soil carbon (MacDougall and Knutti, 2016; Mengis et al., 2020). This UVic ESCM feature has been used in a previous study to project CO_2 emissions from thawing permafrost soils (i.e. permafrost CO_2 emissions) through model parameter perturbations only applied to permafrost carbon decay (MacDougall and Knutti, 2016). In our study, we consider an analogous approach by: (i) perturbing model parameters associated with permafrost carbon decay into CH_4 and subsequent CH_4 emissions following gradual thaw in soil layers saturated with water, and (ii) using default model parameters for wetland CH_4 processes in locations without permafrost carbon (see Chapter 3).

We perturb three model parameters related to major uncertainties in CH_4 production and oxidation in wetlands underlain by permafrost: (i) the specific CH_4 production rate (i.e. the anaerobic decomposition rate for CH_4), (ii) the temperature-sensitivity of CH_4 production, and (iii) the proportion of CH_4 oxidized in transit to emission. Regarding CH_4 production, a synthesis of lab-incubated soil samples from northern environments suggests that the maximum rate of CH_4 production in wetland landscapes is 19.5 ± 2.2 µg CH_4-C g^{-1} soil C day^{-1} and slightly more (27.2 µg CH_4-C g^{-1} soil C day^{-1}) depending on the water table position and soil depth (Treat et al., 2015). A

meta-analysis of temperature-sensitivity studies across various ecosystems suggests that the activation energy for CH_4 production generally varies between 0.82 and 1.03 electron volt (eV) (Yvon-Durocher et al., 2014). This result translates into a range of 3.4-4.7 for the temperature coefficient (Q_{10}) of CH_4 production when assuming a temperature change from 0 to 10 °C. Regarding CH_4 oxidation, various studies report CH_4 oxidation as a fraction of produced CH_4 in the soil column, with estimates of fractional CH_4 oxidation ranging from less than 20% to more than 95% of produced CH_4 in wetlands (Le Mer and Roger, 2001; Moosavi and Crill, 1998; Popp et al., 2000; Roslev and King, 1996; Segers, 1998). Highest estimates of fractional CH_4 oxidation may be associated with the diffusion of CH_4 in the soil column especially when considering CH_4 production in very deep soils, whereas lowest estimates of fractional CH_4 oxidation may be associated with non-diffusive mechanisms transporting CH_4 towards the soil surface and atmosphere (e.g. ebullition and plant-mediated transfer of CH_4 to the atmosphere) (Bridgham et al., 2013; Whalen, 2005).

To investigate the possible evolution of wetland CH_4 emissions from thawing permafrost soils and their climate impact, we consider the following ranges for model parameter perturbations applied only to CH_4 production from previously frozen carbon and the associated CH_4 oxidation in wetlands following gradual permafrost thaw:

i. A range of 17.3-27.2 µg CH_4-C g^{-1} soil C day^{-1} for the mean maximum CH_4 production rate (i.e. 2.0-3.1 kg kg^{-1} s^{-1}).

ii. A range of 3.4-4.7 for the temperature coefficient (Q_{10}) of CH_4 production. To explore the upper bounds of wetland CH_4 emissions from thawing permafrost soils and their climate impact, we do not account for an optimal temperature for CH_4 production in our model perturbations (Dean et al., 2018; Dunfield et al., 1993; Metje and Frenzel, 2007).

iii. A range of 20-97% for the fraction of produced CH_4 that is oxidized in the soil column. We anticipate that the lower value for fractional CH_4 oxidation in wetlands assumed in this study (i.e. 20%) may result in large wetland CH_4 emissions, while the oxidation of CH_4 (in transit to emission) can be very efficient in some northern wetlands (Kettunen et al., 1999; Roulet et al., 1992).

Following the model parameter perturbations, we are able to generate an ensemble of model simulations featuring possibilities of high (low) production jointly with low (high) oxidation of CH_4 across the northern permafrost region that may imply very large (small) wetland CH_4 emissions from thawing permafrost soils. We consider that such extreme possibilities are useful to explore the limits (lower and upper bounds) of future wetland CH_4 emissions from thawing permafrost soils and their climate impact.

5.2.5. Model forcing and simulations

To perform climate simulations, we drive the UVic ESCM with natural and anthropogenic forcing data used in the Sixth Phase of Coupled Model Intercomparison Project (CMIP6) (Eyring et al., 2016). Our climate simulations span the 1850-2300 period, comprising a historical period (1850-2014) and a future period (2015-2300). Natural forcing datasets consist of volcanic radiative forcing anomalies prescribed over the historical period based on (Schmidt et al., 2018) and solar constant data prescribed to the year 2300 (Matthes et al., 2017). Regarding anthropogenic forcing data, we prescribe global CH_4 emissions spanning the historical and future periods (i.e. extended to the year 2300) (Meinshausen et al., 2019; Nicholls et al., 2020). For CO_2, we prescribe fossil fuel emissions extended to the year 2300 (Meinshausen et al., 2019; Nicholls et al., 2020). CO_2 emissions from land-use changes (LUC) are calculated by the UVic ESCM based on prescribed gridded LUC data to the year 2100 (Lawrence et al., 2016). For climate simulations beyond the 21st century, we assume that LUC values remain fixed at their 2100 configuration. Radiative forcing associated with changes in the atmospheric concentration of CH_4 and CO_2 is internally calculated by the UVic ESCM based on formulations of (Etminan et al., 2016). For other greenhouse gases, an aggregated radiative forcing is calculated externally based on concentration data extended to the year 2300 (Meinshausen et al., 2019) and prescribed as input to the UVic ESCM. Radiative forcing of anthropogenic sulfate aerosols is internally calculated by the UVic ESCM based on prescribed gridded aerosol optical depth data over the historical period to the year 2100 (Stevens et al., 2017). For climate projections beyond the 21st century, we assume that the aerosol optical depth data remain fixed at their year 2100 values.

Anthropogenic forcing data for the future period are based on the Shared Socioeconomic Pathways (SSPs), the set of emission scenarios used in CMIP6 in preparation for the Sixth Assessment Report (AR6) by the Intergovernmental Panel on

Climate Change (IPCC) (Riahi et al., 2017). By design, the SSPs span a wide range of assumptions on future societal changes with storylines combining projected population growth, economic development, technological advancement, potential shift towards renewable energy, stability of political institutions, and international cooperation (O'Neill et al., 2017; Riahi et al., 2017). In this study, we select four SSPs: SSP1-2.6, SSP2-4.5, SSP4-6.0, and SSP5-8.5. Like for the previous set of scenarios by the IPCC (i.e. Representative Concentration Pathways or RCPs), each SSP is named after the corresponding radiative forcing level in the year 2100 (e.g. 4.5 W m^{-2} for SSP2-4.5) (O'Neill et al., 2016). In the rest of this chapter, we refer to SSP5-8.5 as the high anthropogenic emission scenario, to SSP1-2.6 as the low anthropogenic emission scenario, and to both SSP2-4.5 and SSP4-6.0 as the intermediate anthropogenic emission scenarios.

5.2.6. Model experiments

Building on the UVic ESCM setting whereby permafrost carbon (i.e. previously frozen carbon) in the model decays with its own decay rate (MacDougall and Knutti, 2016; Mengis et al., 2020), we perform the following two experiments to quantify wetland CH_4 emissions from thawing permafrost soils and isolate their climate impact: (i) a baseline experiment in which, upon permafrost thaw, previously frozen carbon does not decay at all ("Baseline"); (ii) another experiment in which, upon permafrost thaw, previously frozen carbon decays only into CH_4 ("CH4-On") (Table 5.1). In these two experiments, all other processes simulated by the UVic ESCM (including soil respiration and wetland CH_4 emissions from non-permafrost locations) are represented as in the standard model configuration. Conceptually, the difference between the two experiments enables to quantify wetland CH_4 emissions from thawing permafrost soils and isolate their climate impact from that of other forcing agents (including non-permafrost CH_4 emissions). Hence, in the remainder of this study, we consider that the difference between the "CH4-On" and "Baseline" experiments characterizes the effect of the permafrost CH_4 feedback on the climate system. One particular implication from this experimental design is the potential overestimation of wetland CH_4 emissions from thawing permafrost soils, owing to the fact that previously frozen carbon (permafrost carbon substrates for microbial decomposition) may deplete more slowly relative to when both CO_2 and CH_4 are being produced from thawing permafrost soils. Therefore, our quantification of the permafrost

CH_4 feedback represents an extreme situation whereby previously frozen carbon substrates are abundantly available for CH_4 production.

Table 5.1. Description of the model experiments considered in this study. These experiments only pertains to permafrost carbon decay. Carbon decomposition in non-permafrost soil layers are defined as in the standard model configuration.

Key experiments	Description
Baseline	Upon permafrost thaw, previously frozen carbon does not decay at all
CH4-On	Upon permafrost thaw, previously frozen carbon decays only into CH_4
Additional experiment	Description
CO2-On	Upon permafrost thaw, previously frozen carbon decays only into CO_2

We perform an additional experiment focusing on the permafrost CO_2 feedback as one way to assess the potential significance of the climate impact due to wetland CH_4 emissions from thawing permafrost soils. The aim is to compare the warming induced by permafrost CH_4 emissions to that induced by permafrost CO_2 emissions. This additional experiment is such that, upon permafrost thaw, previously frozen carbon decays only into CO_2 ("CO2-On") (Table 5.1). Again, all other processes simulated by the UVic ESCM (including soil respiration and wetland CH_4 emissions from non-permafrost locations) are represented as in the standard model configuration. Conceptually, the difference between this additional experiment and the "Baseline" experiment characterizes the effect of the permafrost CO_2 feedback on the climate system.

5.2.7. Feedback gain

Building on previous studies on feedback analysis in climate research (Arora et al., 2013; Hansen et al., 1984), we define a feedback factor (f) such that:

$$\Delta \mathrm{F}_c = f\, \Delta \mathrm{F}_u \qquad (5.6)$$

where $f = 1/(1-g)$ characterizes the amplification (or dampening) of radiative forcing (ΔF) through a positive (or negative) feedback, $\Delta \mathrm{F}_c$ is radiative forcing for the climate system with the permafrost CH_4 feedback (i.e. "CH4-On" experiment), $\Delta \mathrm{F}_u$ is radiative forcing for the climate system without permafrost carbon emissions (i.e. "Baseline" experiment), and g represents the feedback gain associated with wetland CH_4 emissions from previously frozen carbon following gradual permafrost thaw.

The feedback gain (g) can be calculated as:

$$g = (\Delta F_c - \Delta F_u) / \Delta F_c \quad (5.7)$$

where $g > 0$ implies that $\Delta F_c > \Delta F_u$ and characterizes the amplification of ΔF_u through the feedback factor f.

5.3. Results

5.3.1. Permafrost extent, northern wetland extent, and remaining frozen carbon

Given our focus on the permafrost CH_4 feedback, results presented in this section are based on model simulations with the "CH4-On" experiment (see Section 5.2.6). In this experiment, the UVic ESCM simulates an areal permafrost extent of ~17.4 x 10^6 km^2 over the 2000-2009 decade, which is within the range of estimates (13 to 18 x 10^6 km^2) for exposed terrestrial permafrost area north of 60°S (i.e. excluding Antarctica) (Gruber, 2012). The simulated permafrost area is consistent with a more recent estimate (17.8 x 10^6 km^2) for the extent of global permafrost excluding exposed bedrock, glaciers, ice sheets, and water bodies (Hugelius et al., 2014). Our model suggests that permafrost thaw (mainly through active layer deepening) over the next few centuries will evolve differently depending on the future anthropogenic emission scenario (Figure 5.1a). Under the low anthropogenic emission scenario (SSP1-2.6), simulated permafrost thaw slows down in the 21st century with potential to recover slightly in the 22nd and 23rd centuries. By the year 2300, the permafrost areal extent is projected to be 12.4 x 10^6 km^2 (Figure 5.1a), corresponding to a 30% reduction relative to the pre-industrial (1850-1900) areal extent. In contrast, permafrost thaw continues throughout the 21st century and beyond under the intermediate and high anthropogenic emission scenarios. By the year 2300, the areal extent of permafrost is projected to be 7.6 x 10^6 km^2 under SSP2-4.5, 7.1 x 10^6 km^2 under SSP4-6.0, 6.1 x 10^6 km^2 under SSP5-8.5 (Figure 5.1a), corresponding to a 57-65% reduction relative to the areal extent of pre-industrial permafrost.

The UVic ESCM simulates an areal extent of ~5.1 x 10^6 km^2 for wetlands north of 45°N over the 2000-2009 decade, which is slightly high in comparison to estimates (4.7 x 10^6 km^2) from the SWAMPS-GLWD dataset (Poulter et al., 2017). The areal extent of

northern wetlands is projected to change throughout the current century and beyond depending on the future anthropogenic emission scenario (Figure 5.1b). Under the low anthropogenic emission scenario, the areal extent of northern wetlands is projected to increase slightly over the next few centuries. By the year 2300, simulated northern wetlands under SSP1-2.6 will extend to 5.3 x 10^6 km^2, corresponding to a 5% increase relative to the pre-industrial areal extent of northern wetlands (Figure 5.1b).

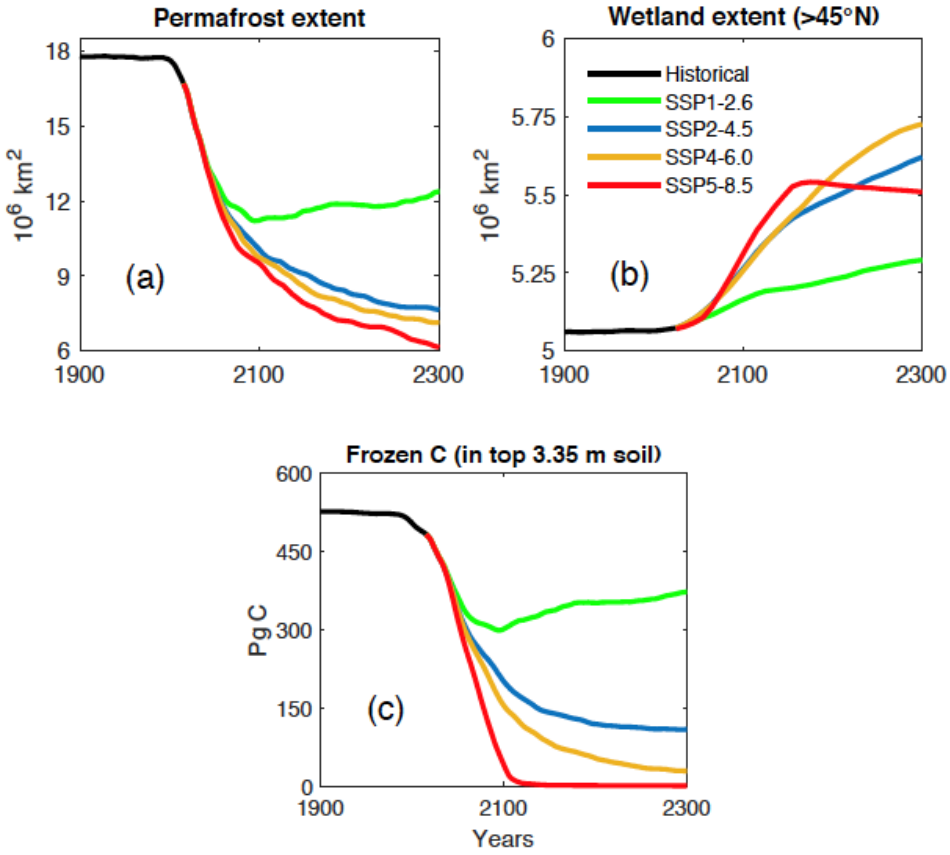

Figure 5.1. Projected changes in the areal extents of permafrost and northern wetlands (>45°N), as well as carbon that remains frozen in near-surface permafrost soils under different SSP scenarios based on the "CH4-On" experiment. In our model, carbon accumulates only in the top 3.35 m of soil, whereas areal permafrost extent accounts for the occurrence of perenially frozen ground down to a depth of 250 m.

In contrast, the areal extent of northern wetlands is projected to increase steadily under the intermediate anthropogenic emission scenarios but more substantially under SSP4-6.0 than under SSP2-4.5. Simulated northern wetlands are projected to extend to 5.6 x 10^6 km^2 under SSP2-4.5 and 5.7 x 10^6 km^2 under SSP4-6.0 by the year 2300 (Figure 5.1b), corresponding to an increase of 11% and 13% relative to the pre-industrial

areal extent, respectively. Under the high anthropogenic emission scenario, the areal extent of northern wetlands is projected to increase substantially in the 21st century and decline gradually in the 22nd and 23rd centuries (Figure 5.1b). A previous study with the UVic ESCM showed that the reduction in the areal extent of northern high-latitude wetlands is expected under a warmer climate in the future following permafrost thaw and subsequent drainage of near-surface moisture to deeper soil layers (Avis et al., 2011). By the year 2300, simulated northern wetlands under SSP5-8.5 are projected to extend to 5.5 x 10^6 km^2, corresponding to a 9% increase relative to pre-industrial areal extent.

The amount of frozen carbon stored in near-surface permafrost soils (i.e. carbon frozen for at least two consecutive years within 3.35 m of depth) simulated by the UVic ESCM in the 2000-2009 decade is ~496 Pg C, which is comparable to present-day estimates (476 Pg C) for carbon stored in the top 3 m of northern frozen soils characterized by cryoturbation (i.e. turbels) (Hugelius et al., 2014). Readers should note that our model does not represent soil carbon stored in yedoma and deltaic deposits. The amount of frozen soil carbon is projected to change as permafrost thaws or re-freezes depending on the future emission scenario (Figure 5.1c). Under the low anthropogenic emission scenario, the decrease in the amount of frozen carbon is projected to slow down in the 21st century and reverse after the year 2100 (Figure 5.1c). By the year 2300, about 370 Pg C will remain frozen under SSP1-2.6, corresponding to a 29% reduction relative to the pre-industrial of amount of simulated frozen carbon. In contrast, the amount of frozen carbon is projected to decrease significantly under the high anthropogenic emission scenario (Figure 5.1c). Only 0.1 Pg C will remain frozen (within 3.35 m of soil depth) by the year 2300 under SSP5-8.5, corresponding to roughly a 100% reduction relative to the pre-industrial amount of simulated carbon in permafrost soil layers. Such a near-complete depletion of frozen carbon is associated with substantial permafrost thaw within the upper 3.35 m of the soil where soil carbon can accumulate in our model, even though permafrost would remain present at greater depth (down to 250 m) (Figure 5.1a). Under the intermediate anthropogenic emission scenarios, the decrease in the amount of frozen carbon is projected to be relatively gradual although more pronounced under SSP4-6.0 than under SSP2-4.5. By the year 2300, the amount of frozen carbon is projected to be 29 Pg C under SSP4-6.0 and 109 Pg C under SSP2-4.5 (Figure 5.1c), corresponding to a 79 and 95% reduction relative to the pre-industrial amount of frozen carbon, respectively.

5.3.2. Release of CH_4 from thawing permafrost

As described in Section 5.2.6, we quantify permafrost CH_4 emissions based on the difference between model simulations in which previously frozen carbon only decays into CH_4 ("CH4-On" experiment) and model simulations in which the decay of previously frozen carbon is switched off ("Baseline" experiment). According to our model, wetland CH_4 emissions from thawing permafrost soils are projected to increase gradually throughout the 21st century although depending on the future anthropogenic emission scenarios (Figure 5.2a-d). By the year 2100, such permafrost CH_4 emissions are projected to be 3 (0-6) Tg C yr^{-1} under SSP1-2.6, 7 (0-18) Tg C yr^{-1} under SSP2-4.5, 10 (1-24) Tg C yr^{-1} under SSP4-6.0, and 20 (1-51) Tg C yr^{-1} under SSP5-8.5. Cumulative wetland CH_4 emissions from thawing permafrost soils by the year 2100 are projected to be 161 (17-429) Tg C under SSP1-2.6, 281 (30-764) Tg C under SSP2-4.5, 341 (36-928) Tg C under SSP4-6.0, and 550 (61-1537) Tg C under SSP5-8.5.

Beyond the year 2100, permafrost CH_4 emissions have the potential to increase substantially under the high anthropogenic emission scenario (Figure 5.2a-d). According to our model simulations, such a rise in wetland CH_4 emissions from thawing permafrost soils under SSP5-8.5 may be justified by two main factors when considered jointly: (i) the relatively large amount of previously frozen carbon that can be accessed by methanogens right after the year 2100 unlike for other anthropogenic emission scenarios (Figure 5.1c), which results in enhanced CH_4 production from newly thawed carbon under SSP5-8.5; (ii) the consideration of low fractional CH_4 oxidation (i.e. 20% of produced CH_4 being oxidized in transit to emission) in CH_4-producing locations underlain by permafrost, which implies high permafrost CH_4 emissions given increasing CH_4 production from previously frozen carbon throughout the next three centuries. By the year 2300, permafrost CH_4 emissions are projected to be 58 (3-158) Tg C yr^{-1} under SSP5-8.5. Under the low and intermediate emission anthropogenic scenarios, however, our model suggests that permafrost CH_4 emissions in the year 2300 will not exceed 40 Tg C yr^{-1}. These CH_4 emissions are projected to be 2 (0-4) Tg C yr^{-1} under SSP1-2.6, 9 (1-22) Tg C yr^{-1} under SSP2-4.5, 16 (1-40) Tg C yr^{-1} under SSP4-6.0. Cumulative wetland CH_4 emissions from thawing permafrost soils by the year 2300 are projected to be 491 (53-1305) Tg C under SSP1-2.6, 1943 (209-5361) Tg C under SSP2-4.5, 2897 (320-8117) Tg C under SSP4-6.0, and 9545 (1122-28889) Tg C under SSP5-8.5. We note that projected CH_4 emissions are potentially overestimated (especially under SSP5-

8.5) due to the fact that previously frozen carbon decays only into CH_4 as part of our model experiment design (see Section 5.2.6).

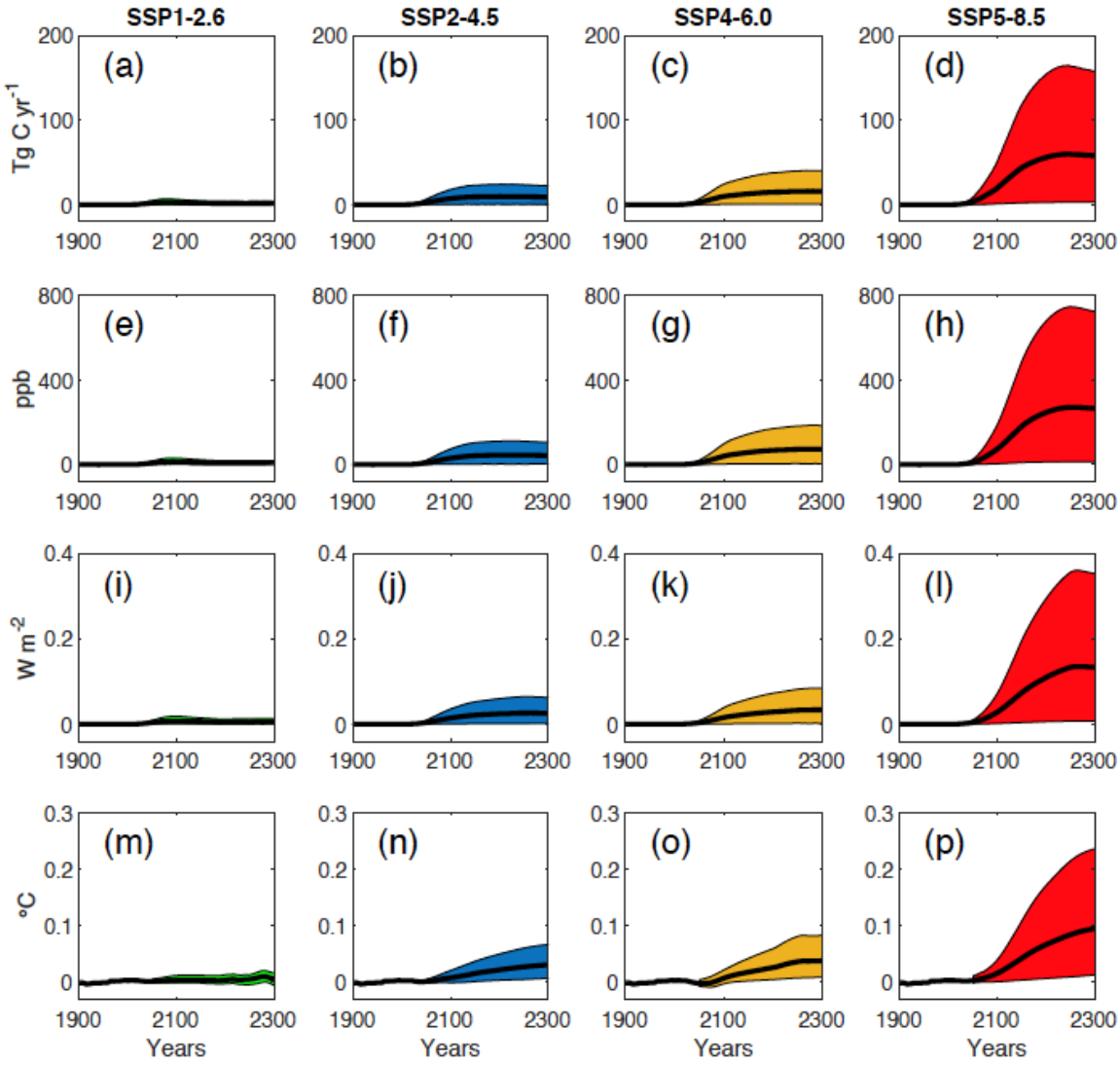

Figure 5.2. Projected wetland CH_4 emissions from thawing permafrost and their climate impact under different SSP scenarios: (a)-(d) permafrost CH_4 emissions, (e)-(h) changes in atmospheric [CH_4], (i)-(l) changes in radiative forcing, (m)-(p) changes in surface air temperature. The shaded areas show the delimitation by 5th and 95th percentiles, whereas the black solid line shows the mean.

5.3.3. Changes in atmospheric [CH_4] and radiative forcing

Rising permafrost CH_4 emissions in the future will result in increased atmospheric CH_4 concentration and radiative forcing (Figure 5.2e-l). By the year 2100, our model suggests

that [CH_4] will grow by 13 (1-30) ppb under SSP1-2.6, 30 (1-74) ppb under SSP2-4.5, 40 (2-98) ppb under SSP4-6.0, and 74 (4-188) ppb under SSP5-8.5 in response to wetland CH_4 emissions from thawing permafrost soils. Subsequent increase in radiative forcing in the year 2100 are projected to be 0.01 (0.0-0.02) W m^{-2} under SSP1-2.6, 0.02 (0.0-0.04) W m^{-2} under both SSP2-4.5 and SSP4-6.0, and 0.03 (0.0-0.07) W m^{-2} under SSP5-8.5. As for projected permafrost CH_4 emissions, both [CH_4] and radiative forcing have the potential to increase substantially beyond the year 2100 especially under the high anthropogenic emission scenario (Figure 5.2e-l). By the year 2300, changes in [CH_4] due to wetland CH_4 emissions from thawing permafrost soils are projected to be 266 (13-724) ppb under SSP5-8.5 with a corresponding change in radiative forcing of 0.13 (0.01-0.35) W m^{-2}. For other anthropogenic emission scenarios, changes in atmospheric [CH_4] in response to permafrost CH_4 emissions are projected to be 8 (1-18) ppb under SSP1-2.6, 43 (3-105) ppb under SSP2-4.5, and 74 (4-185) ppb under SSP4-6.0. Subsequent changes in radiative forcing are projected to remain below 0.08 W m^{-2} for the low and intermediate anthropogenic emission scenarios.

5.3.4. Warming induced by permafrost CH_4 emissions

According to our model, the warming induced by wetland CH_4 emissions from thawing permafrost soils throughout the 21st century is projected to be small independent of the future anthropogenic emission scenario (Figure 5.2m-p). By the year 2100, the warming due to such permafrost CH_4 emissions is projected to be ~0.0 (0.0-0.01) °C under SSP1-2.6, 0.01 (0.0-0.02) °C under SSP2-4.5, 0.01 (0.0-0.02) °C under SSP4-6.0, and 0.02 (0.0-0.04) °C under SSP5-8.5. Beyond the 21st century, however, the additional warming due to the permafrost CH_4 feedback has the potential to increase substantially under the high anthropogenic emission scenario (Figure 5.2p). By the year 2300, the warming induced by permafrost CH_4 emissions under SSP5-8.5 is projected to be 0.09 (0.01-0.24) °C. Under scenarios of low and intermediate anthropogenic emissions, however, the warming due to permafrost CH_4 emissions is projected to remain relatively small: ~0.0 (0.0-0.01) °C under SSP1-2.6, 0.03 (0.01-0.07) °C under SSP2-4.5, and 0.04 (0.01-0.08) °C under SSP4-6.0.

5.3.5. Feedback gains due to wetland CH_4 emissions from thawing permafrost soils

Results in Table 5.2 show that all calculated feedback gains are positive, translating into an amplification of radiative forcing through the permafrost CH_4 feedback associated with gradual thaw in wetlands. Most feedback gains are small (< 0.1), implying a relatively weak feedback factor throughout the next three centuries especially under the low and intermediate anthropogenic emission scenarios.

By the end of the current century, the feedback gain is very small independent of the anthropogenic emission scenarios (Table 5.2). The median feedback gain in the year 2100 varies between 0.006 and 0.008 for the low, intermediate, and high anthropogenic emission scenarios considered in this study. This result suggests that, by the year 2100, the amplification of radiative forcing due to wetland CH_4 emissions from thawing permafrost soils will be modest and largely independent of the future anthropogenic emission scenarios.

By the year 2200, the feedback gain is larger for SSP585 than for the low (SSP1-2.6) and intermediate (SSP2-4.5 and SSP4-6.0) emission scenarios. For the low and intermediate emission scenarios (SSP1-2.6, SSP2-4.5, SSP4-6.0), the feedback gain remains very small and independent of the future anthropogenic emission scenario (Table 5.2). By the year 2300, the feedback gain is largest for SSP585 than for the other emission scenarios. The lowest feedback gain is calculated for SSP1-2.6 (Table 5.2), which is characterized by substantial radiative forcing reduction throughout the 22nd and 23rd centuries due to sustained net zero CO_2 emissions as well as relatively low non-CO_2 emissions from anthropogenic sources starting from the second half of the 21st century.

Table 5.2. Calculated feedback gains with respect to radiative forcing due to CH_4 emissions following gradual permafrost thaw in wetlands by the years 2100, 2200 and 2300 under different future anthropogenic emission scenarios (SSP1-2.6, SSP2-4.5, SSP4-6.0 and SSP5-8.5). The numbers represent median feedback gains, with the 5th-95th confidence interval in brackets.

	2100	2200	2300
SSP1-2.6	0.008 (0.001 – 0.019)	0.012 (0.001 – 0.023)	0.011 (~0.00 – 0.032)
SSP2-4.5	0.007 (0.001 – 0.020)	0.014 (0.001 – 0.041)	0.022 (0.004 – 0.061)
SSP4-6.0	0.006 (0.001 – 0.018)	0.012 (0.002 – 0.036)	0.019 (0.003 – 0.054)
SSP5-8.5	0.007 (0.001 – 0.021)	0.023 (0.003 – 0.083)	0.037 (0.005 – 0.124)

5.3.6. Assessing the significance of the permafrost CH_4 feedback versus the permafrost CO_2 feedback

To assess the potential significance of the warming induced by wetland CH_4 emissions from thawing permafrost soils beyond the 21st century, we compare the results in Section 5.3.4 to temperature changes simulated by our model in response to CO_2 emissions from thawing permafrost soils in the year 2300. As for the permafrost CH_4 feedback, we quantify permafrost CO_2 emissions and their climate impact based on the difference between the "CO2-On" and "Baseline" experiments described in Section 5.2.6. Readers should note that CO_2 emissions from thawing permafrost soils and related temperature changes estimated here are based on climate projections with default model parameters (i.e. no uncertainty bounds for the projected permafrost CO_2 emissions and related temperature feedback). According to our model, cumulative CO_2 emissions from thawing permafrost soils in the year 2300 are projected to be 48 Pg C under SSP1-2.6, 105 Pg C under SSP2-4.5, 127 Pg C under SSP4-6.0, and 148 Pg C under SSP5-8.5. The warming associated with these permafrost CO_2 emissions is projected to be 0.08 °C under SSP1-2.6, 0.16 °C under SSP2-4.5, 0.18 °C under SSP4-6.0, and 0.08 °C under SSP5-8.5 (Figure 5.3). The projected warming due to long-term permafrost CO_2 emissions is lower for the high anthropogenic emission scenario (SSP5-8.5) than for the intermediate anthropogenic emissions scenarios (SSP2-4.5 and SSP4-6.0). This result is relatively well established (MacDougall et al., 2012; Schneider von Deimling et al., 2015): the radiative efficiency of CO_2 is expected to decrease under sustained anthropogenic emissions (e.g. SSP5-8.5), such that a given amount of additional CO_2 emissions from thawing permafrost soils would have a weaker climate impact under the high anthropogenic emission scenario than under intermediate anthropogenic emission scenarios. Overall, our results suggest that the warming due to wetland CH_4 emissions from thawing permafrost soils by the year 2300 will be consistently small (less than 20% for the mean values) in comparison to that associated with permafrost CO_2 emissions under scenarios of low and intermediate anthropogenic emissions. Under the high anthropogenic emission scenario, however, it is possible that the warming due to permafrost CH_4 emissions by the year 2300 will be comparable to that induced by permafrost CO_2 emissions.

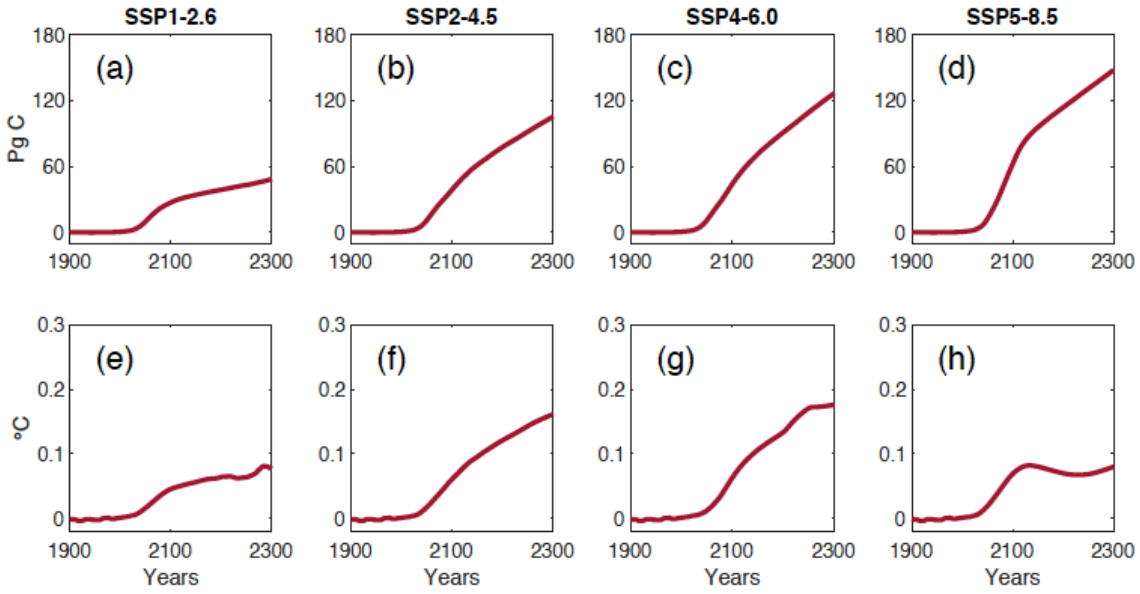

Figure 5.3. **Projected CO_2 emissions from thawing permafrost soils and the associated temperature feedback under different SSPs: (a)-(d) cumulative permafrost CO_2 emissions, (e)-(f) changes in surface air temperature. Note that these projections are based on default model parameters and hence do not feature uncertainty bounds.**

5.4. Discussion and conclusions

Our model suggests that the warming to expect in response to wetland CH_4 emissions from gradual permafrost thaw by the year 2100 will be small independent of the future anthropogenic emission scenario. The strongest temperature feedback is projected to be 0.02 (0.0-0.04) °C under the high anthropogenic emission scenario (SSP5-8.5), whereas the weakest temperature feedback is projected to be ~0.0 (0.0-0.01) °C under the low anthropogenic emission scenario (SSP1-2.6). Our results are consistent with previous estimates based on simple modelling approaches (Burke et al., 2012; Gao et al., 2013; Schneider von Deimling et al., 2012). In particular, our findings agree with previous studies that suggest an upper limit of 0.1°C for the warming associated with projected CH_4 emissions from gradual permafrost thaw by the end of the current century (Gao et al., 2013; Schaefer et al., 2014). Beyond the 21st century, however, the significance of CH_4 emissions from gradual permafrost thaw and their climate impact will strongly depend on the future anthropogenic emission scenario. Under scenarios of low and intermediate anthropogenic emissions, our model suggests that wetland CH_4 emissions from thawing permafrost soils will not exceed 40 Tg C yr^{-1} and the associated temperature feedback will remain below 0.1°C (max. 0.08°C) even under the assumption

of high rates of CH_4 production jointly with low (fractional) rates of CH_4 oxidation throughout the 22nd and 23rd centuries. In contrast, permafrost CH_4 emissions and their climate impact could increase substantially if anthropogenic emissions remain high in the future. Under the high anthropogenic emission scenario (SSP5-8.5), our model suggests that wetland CH_4 emissions from thawing permafrost soils will be 58 (3-158) Tg C yr^{-1} and induce a warming of 0.09 (0.01-0.24) °C by the year 2300. The upper bound of these projected CH_4 emissions is of similar magnitude as present-day global wetland CH_4 emissions (Saunois et al., 2020). As mentioned in Section 5.2.6, it is possible that these permafrost CH_4 emissions are overestimated due to the fact that previously frozen carbon decays only into CH_4 as part of our model experiment design. In addition, we note that these large CH_4 emissions are associated with the assumption of high production jointly with low oxidation of CH_4 in wetlands underlain by permafrost as part of our intention to explore the limits of the permafrost CH_4 feedback.

Several studies suggest that CO_2 will be the dominant component of the permafrost carbon feedback, with CH_4 only playing a secondary role (Olefeldt et al., 2013; Schädel et al., 2016; Schuur et al., 2013). Our results suggest that the warming due to wetland CH_4 emissions from thawing permafrost soils will be significantly smaller than that due to their CO_2 counterpart under the low and intermediate anthropogenic emission scenarios throughout the 21st century and beyond. Under the high anthropogenic emission scenario, however, CH_4 could become a significant contributor to the permafrost carbon feedback in the 22nd and 23rd century primarily owing to (i) sustained high CH_4 production and emissions from previously frozen carbon as well as the associated climate impact, and (ii) the expected decline in the radiative efficiency associated with increasing permafrost CO_2 emissions under high anthropogenic CO_2 emissions.

We indicate that estimates of the permafrost CO_2 feedback in this study are smaller than results from a pioneering study with the UVic ESCM (MacDougall et al., 2012), which sought to compare model simulations with and without the permafrost carbon pool. While our study only quantifies the warming due to CO_2 emissions from perennially frozen carbon upon thaw (i.e. carbon previously frozen for at least two consecutive years), the study by MacDougall et al. (2012) projects the warming due to CO_2 emissions from both seasonally frozen soil carbon in the active layer and perennially frozen carbon following permafrost thaw. Nevertheless, our projections for

permafrost CO_2 emissions are consistent with results from a more recent study using the UVic ESCM (MacDougall and Knutti, 2016), which focused on the microbial decomposition of previously frozen carbon and associated CO_2 release. According to MacDougall and Knutti (2016), cumulative CO_2 emissions from thawing permafrost soils will range from 32-175 Pg C under RCP2.6 to 159-587 Pg C under RCP8.5 in the year 2300.

While our study focuses on major uncertainties in wetland CH_4 biogeochemistry, there are poorly constrained physical factors that have the potential to influence the future evolution of wetland CH_4 emissions from thawing permafrost soils. For instance, the future evolution of Arctic amplification is ambiguous but it will affect rates of permafrost thaw and the subsequent mobilization of previously frozen carbon (Serreze and Barry, 2011). Changes in surface inundation and soil moisture content in response to permafrost thaw as well as shifts in precipitation, evaporation, and vegetation will influence future wetland extent and hence permafrost CH_4 emissions (Nauta et al., 2015; Walvoord and Kurylyk, 2016), but projections of these hydrological changes are poorly constrained for the northern permafrost region (Andresen et al., 2020; Walvoord and Kurylyk, 2016). Previous studies based on simple models accounted for key uncertainties in physical factors associated with permafrost CH_4 emissions and their results are consistent with our conclusions regarding the limited strength for the permafrost CH_4 feedback in the future especially under mitigated scenarios (Burke et al., 2012; Gao et al., 2013; Schneider von Deimling et al., 2012).

Our model only represents terrestrial permafrost whose response to climate warming (i.e. thaw) occurs gradually mainly through active layer deepening. However, permafrost thaw can occur abruptly in locations with ice wedges or excess ground ice creating so-called thermokarst landscapes (Kokelj and Jorgenson, 2013; Schuur and Mack, 2018). The formation of thermokarst lakes in response to abrupt thaw has the potential to enhance permafrost CH_4 emissions in the current century, especially under high anthropogenic emission scenarios (Schneider von Deimling et al., 2015; Turetsky et al., 2020; Walter Anthony et al., 2018). Thermokarst lakes may have very distinct CH_4 dynamics from wetlands, especially with regard to the prevalence of (i) erosion of previously frozen but potentially labile carbon into water-saturated soils and (ii) CH_4 release by ebullition in these lakes (Turetsky et al., 2020; Walter Anthony et al., 2016, 2018). Furthermore, soil carbon in our model only accumulates within the top 3.35 m of

depth although land permafrost stores substantial amounts of soil organic carbon at greater depth in yedoma regions of Alaska, Canada, and Siberia (Hugelius et al., 2014; Strauss et al., 2017) as well as deltaic deposits of major Arctic rivers (Hugelius et al., 2014). In particular, abrupt thaw and thermokarst lakes in yedoma regions have the potential to mobilize carbon stored in deep permafrost soils contributing to increase CH_4 emissions from gradual thaw (Schneider von Deimling et al., 2015; Walter Anthony et al., 2016, 2018). Under high anthropogenic emission scenarios, thermokarst lakes could be the dominant source of permafrost CH_4 emissions in the 21st century whereas wetlands would become the most important source beyond the 21st century (Schneider von Deimling et al., 2015). Non-thermokarst lakes across the boreal and Arctic regions are other potential sources of CH_4 from thawing permafrost soils (Dean et al., 2018; Wik et al., 2016), but their future CH_4 emissions are expected to be dominated by decaying young carbon (i.e. carbon fixed by recent photosynthesis) suggesting that these lakes will be a negligible contributor to the permafrost CH_4 feedback in comparison to thermokarst lakes (Elder et al., 2018). Our model does not resolve wildfires, river and coastal erosions, as well as lateral movement of soil carbon from upland environments, which have been associated with rapid permafrost carbon losses (Schuur et al., 2015; Turetsky et al., 2011; Vonk and Gustafsson, 2013). The contribution of these processes to permafrost CH_4 emissions is expected to be negligible in comparison to that of wetlands and thermokarst lakes (Dean et al., 2018; Ribeiro-Kumara et al., 2020; Schuur et al., 2015). In the long run, thawing of subsea permafrost and subsequent destabilization of CH_4 hydrates along the Arctic ocean could also contribute to enhance permafrost CH_4 emissions although the magnitude of these emissions and their climate impact remain highly uncertain (Ruppel and Kessler, 2017; Shakhova et al., 2019).

In summary, our modelling study investigates the possible evolution of wetland CH_4 emissions from gradual permafrost thaw and their climate impact over the next three centuries. We find that the warming to expect from such permafrost CH_4 emissions by the year 2100 will be small (<0.05°C) under different anthropogenic emission scenarios. This result agrees with previous studies that suggest an upper limit of 0.1°C for the warming due to CH_4 emissions from gradual permafrost thaw throughout the 21st century (Gao et al., 2013; Schaefer et al., 2014). Beyond the 21st century, the warming due to wetland CH_4 emissions from thawing permafrost soils are projected to increase substantially under the high anthropogenic emission scenario, with an estimate of 0.09

(0.01-0.24) °C by the year 2300. Under scenarios of low and intermediate anthropogenic emissions, however, the warming to expect from permafrost CH_4 emissions are projected to remain modest (<0.08°C) throughout the 22nd and 23rd centuries. Therefore, reducing anthropogenic emissions has the potential to limit the warming due to wetland CH_4 emissions from gradual permafrost thaw to well below 0.1°C over the next three centuries. To get a more complete picture of the permafrost CH_4 feedback, future work should account for two opposing factors in response to increasing warming across the northern high-latitude regions: the potential increase in permafrost CH_4 emissions associated with abrupt thaw (In't Zandt et al., 2020; Turetsky et al., 2020), and the potential increase in CH_4 uptake by soils (Oh et al., 2020).

Chapter 6. Conclusions

6.1. Summary of key results and their significance

This thesis seeks to contribute to the scientific understanding about the importance of CH_4 for future climate change by: (i) reviewing the literature on the CH_4 contribution to the permafrost carbon feedback (Chapter 2), (ii) developing a new wetland CH_4 model for implementation in Earth system models (Chapter 3), (iii) assessing the importance of CH_4 mitigation over the next few decades to comply with global warming limits set by the Paris Agreement based on Earth system model simulations (Chapter 4), and (iv) quantifying the possible evolution of wetland CH_4 emissions from thawing permafrost soils and their climate impact over the next few centuries based on Earth system model simulations (Chapter 5). Key results of this thesis and their significance are summarized in the following sections.

6.1.1. The relevance of CH_4 in the permafrost carbon feedback

Ongoing and projected permafrost thaw will contribute to amplify global warming through CO_2 and CH_4 emissions from microbial decomposition of previously frozen carbon (Koven et al., 2011; Schaefer et al., 2014). Chapter 2 provides a review of the literature on the importance of CH_4 as part of the permafrost carbon feedback. The literature review considers insights from a comprehensive review on the permafrost carbon feedback (Schuur et al., 2015), expert judgements (Schuur et al., 2013), meta-analyses (Schädel et al., 2016; Schaefer et al., 2014; Treat et al., 2015), uncoupled terrestrial ecosystem models (Burke et al., 2012; Koven et al., 2011, 2015a) as well as simple 1-D and 2-D models (Schneider von Deimling et al., 2012, 2015). According to the reviewed literature, wetlands and thermokarst lakes are expected to be the two major source contributors to the permafrost CH_4 feedback over the next three centuries (Nzotungicimpaye and Zickfeld, 2017; Schuur et al., 2015) – although permafrost CH_4 emissions from these sources and their future projections remain poorly constrained (Dean et al., 2018; In't Zandt et al., 2020). Under high anthropogenic emission scenarios, wetland CH_4 emissions from thawing permafrost soils could contribute to about 20% of the warming to expect from total permafrost carbon (CO_2 and CH_4)

emissions by the year 2100, which is projected to be 0.29 (0.08-0.50) °C (Schaefer et al., 2014). According to expert judgements and simple model projections, the CH_4 contribution to the permafrost carbon feedback by the end of the current century could increase to 30-50% when considering permafrost CH_4 emissions from both wetlands and thermokarst lakes under high anthropogenic emission scenarios (Schneider von Deimling et al., 2015; Schuur et al., 2013, 2015).

6.1.2. A new model for wetland CH_4 emissions

For this thesis, I developed a new wetland CH_4 model for implementation in Earth system models (WETMETH), which is currently embedded in the University of Victoria Earth System Climate Model (UVic ESCM) (see Chapter 3). WETMETH is a relatively simple model that simulates wetland CH_4 emissions as the balance between (i) CH_4 production that is mainly controlled by the vertical distribution of soil moisture, carbon, and temperature; and (ii) CH_4 oxidation that is controlled by the amount of produced CH_4 in the soil column and the vertical distribution of soil moisture. The calibration of WETMETH is based on small-scale observations from northern high-latitude regions, whereas its validation is done against regional to global estimates of wetland CH_4 emissions (see Chapter 3). Despite large uncertainties in wetland distribution and wetland CH_4 biogeochemistry, WETMETH is capable of reproducing mean annual wetland CH_4 emissions consistent with present-day estimates from the regional to the global scale (Chapter 3).

6.1.3. The importance of CH_4 mitigation to comply with the 2°C warming limit

Strategies adopted by different countries to reduce GHG emissions (i.e. nationally determined contributions or NDCs) mostly focus on CO_2 mitigation and generally do not explicitly target non-CO_2 GHGs such as CH_4 (Harmsen et al., 2019a). Meanwhile, atmospheric CH_4 levels have been growing rapidly over the last decade partly due to human activities (Nisbet et al., 2019; Saunois et al., 2016b). Sustained [CH_4] growth in the next decades could constitute a challenge for meeting temperature goals in the Paris Agreement, even under stringent CO_2 mitigation (Nisbet et al., 2019). Chapter 4 investigates the importance of immediate versus delayed CH_4 mitigation to comply with the global warming limits set by the Paris Agreement. This investigation is based on

climate simulations with a newly developed version of the UVic ESCM including a simplified representation of the global CH_4 cycle. The study assumes scenarios of immediate and delayed CH_4 mitigation over the next three decades with all other anthropogenic forcings (non-CH_4 GHG emissions, land-use changes, and aerosols) following a scenario consistent with limiting global warming to 2°C by the end of the current century (i.e. SSP1-2.6). According to our model simulations, initiating CH_4 mitigation by the year 2030 will allow to keep global warming below 2°C above 1850-1900 levels under SSP1-2.6, whereas delaying CH_4 mitigation to the year 2040 or 2050 will overshoot the 2°C warming limit for at least two decades in the remainder of the 21st century under SSP1-2.6. These results suggest that rapid reductions in anthropogenic CH_4 emissions are needed, along with CO_2 mitigation, to increase the likelihood of limiting global warming below 2°C above pre-industrial levels.

6.1.4. The strength of the permafrost CH_4 feedback

The permafrost carbon feedback is currently one of the least constrained biogeochemical feedbacks to climate change (Schuur et al., 2015). Chapter 5 focuses on quantifying the possible evolution of wetland CH_4 emissions from previously frozen carbon in response to gradual permafrost thaw as well as their climate impact over the next three centuries. This study is based on climate projections with the newly developed version of the UVic ESCM (i.e. UVic ESCM version 2.10 into which I implemented a representation of the global CH_4 cycle). Our results suggest that wetland CH_4 emissions from thawing permafrost soils by the year 2100 will range from 3 (0-6) Tg C yr^{-1} under a low anthropogenic emission scenario (SSP1-2.6) to 20 (1-51) Tg C yr^{-1} under a high anthropogenic emission scenario (SSP5-8.5). The warming to expect from such permafrost CH_4 emissions is projected to be small, ranging from ~0.0 (0.0-0.01) °C under SSP1-2.6 to 0.02 (0.0-0.04) °C under SSP5-8.5. These results are consistent with a previous study that considered changes in surface inundation (Gao et al., 2013) and findings from a meta-analysis of permafrost carbon modelling studies (Schaefer et al., 2014). Beyond the 21st century, wetland CH_4 emissions from thawing permafrost soils and their climate impact will strongly depend on the scenario of future anthropogenic emissions. Our model suggests that wetland CH_4 emissions from thawing permafrost soils will increase substantially under SSP5-8.5, primarily owing to a large amount of previously frozen carbon that will be accessible to methanogens from the early years of

the 22nd century. By the year 2300, wetland CH_4 emissions from thawing permafrost soils are projected to be 58 (3-158) Tg C yr^{-1} and induce a warming of 0.09 (0.01-0.24) °C under SSP5-8.5. The upper bound of these projected CH_4 emissions is of similar magnitude as present-day global wetland CH_4 emissions (Saunois et al., 2020). While the potential for large permafrost CH_4 emissions by the end of the 23rd century cannot be ruled out, it should be noted that these projected CH_4 emissions are: (i) associated with model runs assuming the possibility of high production of CH_4 jointly with low oxidation of CH_4 from previously frozen carbon in wetlands; (ii) potentially overestimated considering that, in our model projections, previously frozen carbon decays only into CH_4 as part of our model experiment design (see Section 5.2.6). Under the low (SSP1-2.6) and intermediate anthropogenic emission scenarios (SSP2-4.5 and SSP4-6.0), however, our model suggests that wetland CH_4 emissions from thawing permafrost soils will not exceed 40 Tg C yr^{-1} and the associated temperature feedback will remain well below 0.1°C even under the assumption of high rates of CH_4 production jointly with low rates of (fractional) CH_4 oxidation throughout the 22nd and 23rd centuries. Therefore, according to our study, reducing anthropogenic emissions in the 21st century could prevent large permafrost CH_4 emissions and their climate impact over the next three centuries.

6.2. Novel contributions

For this thesis, I developed a model for wetland CH_4 emissions and implemented it in the UVic ESCM (see Chapter 3) along with a simplified representation of the global CH_4 cycle (see Chapter 4). To the best of my knowledge, this thesis is the first research to apply an Earth system modelling framework to (i) investigating the importance of immediate rather than delayed CH_4 mitigation in the future to comply with temperature limits set by the Paris Agreement, and (ii) quantifying the potential evolution of wetland CH_4 emissions from thawing permafrost soils and their contribution to amplify global warming over the next three centuries. Representing the CH_4 cycle in Earth system models is essential for the prognostic simulation of atmospheric CH_4 concentration and its temporal evolution, which is a critical feature for investigating the climate response to changes in anthropogenic CH_4 emissions (e.g. in the context of CH_4 mitigation) and natural CH_4 emissions (e.g. wetland CH_4 emissions from thawing permafrost soils), as well as CH_4 sinks. Overall, Earth system model simulations analyzed in this thesis suggest that (i) the warming to expect from feedbacks between wetland CH_4 emissions

and future climate change will be relatively modest under scenarios of low anthropogenic emissions but potentially significant under scenarios of unmitigated emissions; (ii) delaying CH_4 mitigation increases the risk of breaching the 2°C warming limit.

6.3. Limitations

Major limitations for this research include the relative simplicity of the developed model for wetland CH_4 emissions, the lack of prognostic CH_4 emissions from non-wetland natural sources (e.g. termites, lakes, wildfires, wild ruminants, geologic seeps, marine hydrates) in our climate simulations, the assumption of a constant atmospheric CH_4 lifetime, and the non-representation of abrupt thaw in projections of the permafrost CH_4 feedback to climate change. These limitations and their implications for this research are discussed in detail in previous chapters (see Sections 3.7, 4.4, and 5.4). A brief discussion of these limitations is provided here:

1. The developed model for wetland CH_4 emissions (WETMETH) is relatively simple with respect to the wide array of physical, biological, and chemical controls on CH_4 production and oxidation in wetlands. Yet, this simple wetland CH_4 model is capable of reproducing mean annual wetland CH_4 emissions from the regional to the global scale based on soil moisture, carbon, and temperature simulated by the fully coupled UVic ESCM.

2. Non-wetland natural sources of CH_4 are not represented in the UVic ESCM. To the best of my knowledge, there is no dataset of CH_4 emissions from non-wetland natural sources for use in climate model simulations. To represent the global CH_4 cycle in the UVic ESCM, I assume that CH_4 emissions from these natural sources remain fixed at 45 Tg C yr^{-1} (i.e. ~60 Tg CH_4 yr^{-1}). This value is within the range of estimates for total CH_4 emissions from non-wetland natural sources over the last four decades (Kirschke et al., 2013; Saunois et al., 2020) as well as pre-industrial periods (Houweling et al., 2000 and references therein). While CH_4 emissions from wildfires as well as natural freshwater and marine systems have the potential to increase or decrease in a changing climate in the future (Dean et al., 2018), it is difficult to predict how the magnitude of total CH_4 emissions from non-wetland sources will change in the future under a given climate change scenario.

3. The consideration of a constant lifetime for atmospheric CH_4 is another assumption made in this thesis as part of initial steps to represent the global CH_4 cycle in the UVic ESCM. In the natural world, the atmospheric CH_4 lifetime may vary by a few months to a few years mostly due to changes in atmospheric chemistry associated with CH_4 sinks especially the abundance of the OH radical in the troposphere (Wuebbles and Hayhoe, 2002). In our model simulations, the atmospheric CH_4 lifetime is fixed at 9.3 years – which is an estimate from the latest global CH_4 budget report (Saunois et al., 2020). Similar estimates for the atmospheric CH_4 lifetime have been reported for the pre-industrial era (9.5 ± 1.3 years) and present-day (i.e. early 2010s) (9.1 ± 0.9 years) (Prather et al., 2012). However, I acknowledge that variations in the atmospheric CH_4 lifetime through changes in CH_4 sinks may be partially responsible for changes in the growth rates of atmospheric CH_4 over time (e.g. the slowdown observed in the 1990s through the 2000s as well as the renewed growth since the year 2007) (Kirschke et al., 2013; Prather and Holmes, 2017; Schaefer, 2019).

4. The UVic ESCM does not simulate abrupt permafrost thaw, which could contribute to rapid and substantial carbon (both CH_4 and CO_2) emissions from thawing permafrost soils (Turetsky et al., 2020; Walter Anthony et al., 2018). Simulations by a terrestrial ecosystem model suggests that abrupt permafrost thaw in the 21st century could accelerate the mobilization of ancient carbon previously stored in deep permafrost soils (up to 15 m of depth) and contribute to increase permafrost carbon emissions by more than 120% relative to gradual thaw alone (Walter Anthony et al., 2018). CH_4 emissions resulting from abrupt permafrost thaw occur primarily in thermokarst lakes but also in wetlands underlain by massive ground ice or affected by erosion (Turetsky et al., 2020; Walter Anthony et al., 2018). Thermokarst lakes are already hotspots of CH_4 emissions from ancient permafrost-derived carbon in response to abrupt thaw (Walter Anthony et al., 2016), and permafrost CH_4 emissions from these lakes are expected to be a key component of total carbon emissions from previously frozen carbon in the future (In't Zandt et al., 2020; Schneider von Deimling et al., 2015; Turetsky et al., 2020; Walter Anthony et al., 2018). According to expert judgements as well as simple and uncoupled model projections, permafrost CH_4 emissions resulting from both gradual and abrupt thaw could contribute a third to

a half of the climate forcing to expect from total permafrost carbon emissions in the 21st century and beyond (Schneider von Deimling et al., 2015; Schuur et al., 2013; Turetsky et al., 2020).

6.4. Future directions

6.4.1. Further studies

While this thesis focuses on investigating the strength of the permafrost CH_4 feedback to climate change, there is a need for more research on the significance of the positive feedback between future climate change and CH_4 emissions from global wetlands (Gedney et al., 2019). There is also a need for quantifying the impact of wetland CH_4 emissions on remaining carbon budgets to keep global warming below stringent limits (Rogelj et al., 2019). Furthermore, a quantification of the warming to expect from both CH_4 and CO_2 emissions in response to permafrost thaw remains a major research gap in climate science. I suggest that such a quantification be done by accounting for uncertainties in permafrost thaw and hydrology (Andresen et al., 2020; Schuur et al., 2015; Serreze and Barry, 2011; Walvoord and Kurylyk, 2016), as well as uncertainties in the decay of previously frozen carbon and subsequent carbon (both CO_2 and CH_4) emissions (Schädel et al., 2016; Treat et al., 2015).

6.4.2. Further model development

Further research should consider the following points about model development:

1. Our model simulations assume a constant lifetime of 9.3 years for atmospheric CH_4 (Saunois et al., 2020). However, research suggests that the atmospheric CH_4 lifetime may vary by a few months to years mostly due the changes in the abundance of the OH radical (Naik et al., 2013; Prather et al., 2012). Future research on the global CH_4 cycle with the UVic ESCM could explore the application of a dynamic CH_4 lifetime, which can be parameterized based on simple formulations (Arora et al., 2018; Christensen et al., 2019).

2. There is a need to revise how wetlands are identified in the UVic ESCM, especially for improving the distribution of tropical wetlands simulated by the

model. Wetlands in the UVic ESCM are currently simulated to occur in grid cells whose upper ground layer contains unfrozen soil moisture exceeding 65% of saturation for at least one day in a year (Avis et al., 2011) and contingent to a topography-based criterion determined with TOPMODEL (Gedney and Cox, 2003). One option for improving the wetland distribution in the UVic ESCM is to focus on the number of days for the moisture criterion, which could be increased to a few days to weeks. Another option, which may be combined with the revision of the moisture criterion, is to apply a recent topographic map to drive TOPMODEL in the UVic ESCM (Marthews et al., 2015). If none of the above options provides satisfactory results, two more options may be applied: (i) considering different parameter values for the tropics and extra-tropical regions, (ii) revising the soil properties in the UVic ESCM by including ferralsols, which are weathered soils with micro-aggregated particles that are common in the tropics (Gedney et al., 2019).

3. For future work on the permafrost CH_4 feedback with the UVic ESCM, there is a need for incorporating excess ground ice and their impacts in Earth system models. While the occurrence of thermokarst development in response to abrupt permafrost thaw remains under-represented in climate model simulations, there are ongoing efforts to incorporate excess ground ice and sub-grid scale thermokarst in terrestrial components of Earth system models (Aas et al., 2019; Ekici et al., 2019). These studies may serve to inform future model development in the UVic ESCM.

6.5. Final conclusion

The global climate is governed by many complex physical and biogeochemical processes as well as their interactions. Over the last few decades considerable progress has been made with regard to the inclusion of carbon cycle processes in Earth system models, enabling to enhance the scientific understanding of how CO_2 and climate will influence each other in the future through feedback mechanisms (Arora et al., 2013; Ciais et al., 2013; Cox et al., 2000; MacDougall et al., 2012; Zickfeld et al., 2013). Continuous efforts to incorporate or improve processes regulating biogeochemical cycles (e.g. CH_4 and nitrogen cycles) in Earth system models are needed to have a more complete representation of the global climate system and increase confidence in

future climate projections. This thesis contributes to such modelling efforts by incorporating a simplified representation of the CH_4 cycle in the UVic ESCM. Applications of this newly developed version of the UVic ESCM in this thesis provide policy-relevant results: (i) delaying CH_4 mitigation increases the risk of breaching the 2°C warming limit even under aggressive CO_2 mitigation by mid century; (ii) climate change mitigation in the 21st century could allow to limit the warming due to wetland CH_4 emissions from thawing permafrost soils to well below 0.1°C over the next three centuries. Although this thesis does not focus on quantifying the feedback between climate change and CH_4 emissions from global wetlands, I anticipate that the future warming to expect from wetland CH_4 emissions over the next three centuries will be: (i) small under low anthropogenic emission scenarios (e.g. mitigation scenarios), and (ii) potentially large under high anthropogenic emission scenarios (e.g. SSP5-8.5), but not strong enough to induce a runaway feedback in the climate system. However, the modelling approach applied in this thesis does not account for abrupt permafrost thaw in locations with massive ground ice as well as CH_4 emissions from thermokarst lakes, which have the potential to enhance the importance of climate-CH_4 feedbacks in the future (see Chapter 2). To provide a more complete assessment of the permafrost CH_4 feedback to climate change, there is need for representing abrupt permafrost thaw and subsequent CH_4 emissions from thermokarst lakes in Earth system model simulations.

References

Aas, K. S., Martin, L., Nitzbon, J., Langer, M., Boike, J., Lee, H., Berntsen, T. K. and Westermann, S.: Thaw processes in ice-rich permafrost landscapes represented with laterally coupled tiles in a land surface model, Cryosphere, 13, 561–609, 2019.

Abdalla, M., Hastings, A., Truu, J., Espenberg, M., Mander, Ü. and Smith, P.: Emissions of methane from northern peatlands: a review of management impacts and implications for future management options, Ecol. Evol., 6, 7080–7102, 2016.

Ahrens, B. and Reichstein, M.: Depth of understanding, Nat. Clim. Chang., 7, 762–763, 2017.

Ali, M. H. and Abustan, I.: A new novel index for evaluating model performance, J. Nat. Resour. Dev., 4, 1–9, 2014.

Andresen, C. G., Lawrence, D. M., Wilson, C. J., McGuire, A. D., Koven, C., Schaefer, K., Jafarov, E., Peng, S., Chen, X., Gouttevin, I., Burke, E., Chadburn, S., Ji, D., Chen, G., Hayes, D. and Zhang, W.: Soil moisture and hydrology projections of the permafrost region - a model intercomparison, Cyrosph., 14, 445–459, 2020.

Anenberg, S. C., Schwartz, J., Shindell, D., Amann, M., Faluvegi, G., Klimont, Z., Janssens-Maenhout, G., Pozzoli, L., Van Dingenen, R., Vignati, E., Emberson, L., Muller, N. Z., Jason West, J., Williams, M., Demkine, V., Kevin Hicks, W., Kuylenstierna, J., Raes, F. and Ramanathan, V.: Global air quality and health co-benefits of mitigating near-term climate change through methane and black carbon emission controls, Environ. Health Perspect., 120, 831–839, 2012.

Anisimov, O. and Zimov, S.: Thawing permafrost and methane emission in Siberia: Synthesis of observations, reanalysis, and predictive modeling, Ambio, doi:doi.org/10.1007/s13280-020-01392-y, 2020.

Anisimov, O. A.: Potential feedback of thawing permafrost to the global climate system through methane emission, Environ. Res. Lett., 2, 045016, 2007.

Archer, D.: A data-driven model of the global calcite lysocline, Global Biogeochem. Cycles, 10, 511–526, 1996.

Arora, V. K., Boer, G. J., Friedlingstein, P., Eby, M., Jones, C. D., Christian, J. R., Bonan, G., Bopp, L., Brovkin, V., Cadule, P., Hajima, T., Ilyina, T., Lindsay, K., Tjiputra, J. F. and Wu, T.: Carbon-concentration and carbon-climate feedbacks in CMIP5 earth system models, J. Clim., 26, 5289–5314, 2013.

Arora, V. K., Melton, J. R. and Plummer, D.: An assessment of natural methane fluxes simulated by the CLASS-CTEM model, Biogeosciences, 15, 4683–4709, 2018.

Arora, V. K., Katavouta, A., Williams, R. G., Jones, C. D., Brovkin, V., Friedlingstein, P., Schwinger, J., Bopp, L., Boucher, O., Cadule, P., Chamberlain, M. A., Christian, J. R., Delire, C., Fisher, A. R. A., Hajima, T., Ilyina, T., Joetzjer, E., Kawamiya, M., Koven, C. D., Krasting, J. P., Law, R. M., Lawrence, D. M., Lenton, A., Lindsay, K., Pongratz, J., Raddatz, T., Séférian, R., Tachiiri, K., Tjiputra, J. F., Wiltshire, A., Wu, T. and Ziehn, T.: Carbon-concentration and carbon-climate feedbacks in CMIP6 models and their comparison to CMIP5 models, Biogeosciences, 17, 4173–4222, 2020.

Aselmann, I. and Crutzen, P. J.: Global distribution of natural freshwater wetlands and rice paddies, their net primary productivity, seasonality and possible methane emissions, J. Atmos. Chem., 8, 307–358, 1989.

Avis, C. A., Weaver, A. J. and Meissner, K. J.: Reduction in areal extent of high-latitude wetlands in response to permafrost thaw, Nat. Geosci., 4, 444–448, 2011.

Barba, J., Bradford, M., Brewer, P., Bruhn, D., Covey, K., von Haren, J., Megonigal, J., Mikkelsen, T., Pangala, S., Pihlatie, M., Poulter, B., Rivas-Ubach, A., Schadt, C., Terazawa, K., Warner, D., Zhang, Z. and Vargas, R.: Methane emissions from tree stems: a new frontier in the global carbon cycle, New Phytol., 222, 18–28, 2019.

Bastviken, D., Tranvik, L. J., Downing, J. A., Crill, P. M. and Enrich-Prast, A.: Freshwater methane emissions offset the continental carbon sink, Sci. , 331, 50–50, 2011.

Biskaborn, B. K., Smith, S. L., Noetzli, J., Matthes, H., Vieira, G., Streletskiy, D. A., Schoeneich, P., Romanovsky, V. E., Lewkowicz, A. G., Abramov, A., Allard, M., Boike, J., Cable, W. L., Christiansen, H. H., Delaloye, R., Diekmann, B., Drozdov, D., Etzelmüller, B., Grosse, G., Guglielmin, M., Ingeman-Nielsen, T., Isaksen, K., Ishikawa, M., Johansson, M., Johannsson, H., Joo, A., Kaverin, D., Kholodov, A., Konstantinov, P., Kröger, T., Lambiel, C., Lanckman, J. P., Luo, D., Malkova, G., Meiklejohn, I., Moskalenko, N., Oliva, M., Phillips, M., Ramos, M., Sannel, A. B. K., Sergeev, D., Seybold, C., Skryabin, P., Vasiliev, A., Wu, Q., Yoshikawa, K., Zheleznyak, M. and Lantuit, H.: Permafrost is warming at a global scale, Nat. Commun., 10, 1–11, 2019.

Blake, L. I., Tveit, A., Øvreås, L., Head, I. M. and Gray, N. D.: Response of methanogens in arctic sediments to temperature and methanogenic substrate availability, PLoS One, 10, 1–18, 2015.

Blazewicz, S. J., Petersen, D. G., Waldrop, M. P. and Firestone, M. K.: Anaerobic oxidation of methane in tropical and boreal soils: Ecological significance in terrestrial methane cycling, J. Geophys. Res. Biogeosciences, 117, 1–9, 2012.

Blodau, C.: Carbon cycling in peatlands - A review of processes and controls, Environ. Rev., 10, 111–134, 2002.

Blodau, C., Basiliko, N. and Moore, T. R.: Carbon turnover in peatland mesocosms exposed to different water table levels, Biogeochemistry, 67, 331–351, 2004.

Bloom, A. A., Bowman, K. W., Lee, M., Turner, A. J., Schroeder, R., Worden, J. R., Weidner, R., McDonald, K. C. and Jacob, D. J.: A global wetland methane emissions and uncertainty dataset for atmospheric chemical transport models (WetCHARTs version 1.0), Geosci. Model Dev., 10, 2141–2156, 2017.

Bogard, M., Kuhn, C., Johnston, S., Striegl, R., Holtgrieve, G., Dornblaser, M., Spencer, R., Wickland, K. and Butman, D.: Negligible cycling of terrestrial carbon in many lakes of the arid circumpolar landscape, Nat. Geosci., 12, 180–185, 2019.

Bohn, T. J., Melton, J. R., Ito, A., Kleinen, T., Spahni, R., Stocker, B. D., Zhang, B., Zhu, X., Schroeder, R., Glagolev, M. V., Maksyutov, S., Brovkin, V., Chen, G., Denisov, S. N., Eliseev, A. V., Gallego-Sala, A., McDonald, K. C., Rawlins, M. A., Riley, W. J., Subin, Z. M., Tian, H., Zhuang, Q. and Kaplan, J. O.: WETCHIMP-WSL: Intercomparison of wetland methane emissions models over West Siberia, Biogeosciences, 12, 3321–3349, 2015.

Bridgham, S. D., Cadillo-Quiroz, H., Keller, J. K. and Zhuang, Q.: Methane emissions from wetlands: biogeochemical, microbial, and modeling perspectives from local to global scales, Glob. Chang. Biol., 19, 1325–1346, 2013.

Bruhwiler, L., Bousquet, P., Houweling, S. and Melton, J.: Modeling of atmospheric methane using inverse (and forward) approaches, in AMAP Assessment 2015: Methane as an Arctic climate forcer, pp. 77–90, Arctic Monitoring and Assessment Programme (AMAP), Oslo, Norway., 2015.

Brune, A., Frenzel, P. and Cypionka, H.: Life at the oxic-anoxic interface: microbial activities and adaptations, FEMS Microbiol. Rev., 24, 691–710, 2000.

Burke, E. J., Hartley, I. P. and Jones, C. D.: Uncertainties in the global temperature change caused by carbon release from permafrost thawing, Cryosphere, 6, 1063–1076, 2012.

Cadillo-Quiroz, H., Bräuer, S., Yashiro, E., Sun, C., Yavitt, J. and Zinder, S.: Vertical profiles of methanogenesis and methanogens in two contrasting acidic peatlands in central New York State, USA, Environ. Microbiol., 8, 1428–1440, 2006.

Cao, M., Marshall, S. and Gregson, K.: Global carbon exchange and methane emissions from natural wetlands: Application of a process-based model, J. Geophys. Res., 101, 14399–14414, 1996.

Chadburn, S. E., Krinner, G., Porada, P., Bartsch, A., Beer, C., Belelli Marchesini, L., Boike, J., Ekici, A., Elberling, B., Friborg, T., Hugelius, G., Johansson, M., Kuhry, P., Kutzbach, L., Langer, M., Lund, M., Parmentier, F. J. W., Peng, S., Van Huissteden, K., Wang, T., Westermann, S., Zhu, D. and Burke, E. J.: Carbon stocks and fluxes in the high latitudes: Using site-level data to evaluate Earth system models, Biogeosciences, 14, 5143–5169, 2017.

Chen, Y. and Murrell, J. C.: Methanotrophs in moss, Nature, 3, 595–596, 2010.

Christensen, T., Prentice, I., Kaplan, J., Haxeltine, A. and Sitch, S.: Methane flux from northern wetlands and tundra: An ecosystem source modelling approach, Tellus, 48, 652–661, 1996.

Christensen, T. R., Van Huissteden, K. and Sachs, T.: Natural terrestrial methane sources in the Arctic, in AMAP Assessment 2015: Methane as an Arctic climate forcer, pp. 15–26, Arctic Monitoring and Assessment Programme (AMAP), Oslo, Norway., 2015.

Christensen, T. R., Arora, V. K., Gauss, M., Höglund-Isaksson, L. and Parmentier, F. J. W.: Tracing the climate signal: mitigation of anthropogenic methane emissions can outweigh a large Arctic natural emission increase, Sci. Rep., 9, 1–8, 2019.

Ciais, P., Sabine, C., Bala, G., Bopp, L., Brovkin, V., Canadell, J., Chhabra, A., DeFries, R., Galloway, J., Heimann, M., Jones, C., Le Quéré, C., Myneni, R. B., Piao, S. and Thornton, P.: Carbon and other biogeochemical cycles, in Climate Change 2013: The Physical Science Basis. Contribution of Working Group I to the Fifth Assessment Report of the Intergovernmental Panel on Climate Change, pp. 465–570, Cambridge University Press, Cambridge, UK and New York, NY, USA., 2013.

Comyn-Platt, E., Hayman, G., Huntingford, C., Chadburn, S. E., Burke, E. J., Harper, A. B., Collins, W. J., Webber, C. P., Powell, T., Cox, P. M., Gedney, N. and Sitch, S.: Carbon budgets for 1.5 and 2°C targets lowered by natural wetland and permafrost feedbacks, Nat. Geosci., 11, 568–573, 2018.

Conrad, R.: The global methane cycle: Recent advances in understanding the microbial processes involved, Environ. Microbiol. Rep., 1, 285–292, 2009.

Cooper, M. D. A., Estop-Aragonés, C., Fisher, J. P., Thierry, A., Garnett, M. H., Charman, D. J., Murton, J. B., Phoenix, G. K., Treharne, R., Kokelj, S. V., Wolfe, S. A., Lewkowicz, A. G., Williams, M. and Hartley, I. P.: Limited contribution of permafrost carbon to methane release from thawing peatlands, Nat. Clim. Chang., 7, 507–511, 2017.

Corbett, J. E., Tfaily, M. M., Burdige, D. J., Glaser, P. H. and Chanton, J. P.: The relative importance of methanogenesis in the decomposition of organic matter in northern peatlands, J. Geophys. Res. Biogeosciences, 120, 280–293, 2015.

Couwenberg, J., Dommain, R. and Joosten, H.: Greenhouse gas fluxes from tropical peatlands in south-east Asia, Glob. Chang. Biol., 16, 1715–1732, 2010.

Cox, P. M.: Description of the TRIFFID Dynamic Global Vegetation Model, Exeter, UK., 2001.

Cox, P. M., Betts, R. A., Jones, C. D., Spall, S. A. and Totterdell, I. J.: Acceleration of global warming due to carbon-cycle feedbacks in a coupled climate model, Nature, 408, 184–187, 2000.

Crichton, K. A., Bouttes, N., Roche, D. M., Chappellaz, J. and Krinner, G.: Permafrost carbon as a missing link to explain CO2 changes during the last deglaciation, Nat. Geosci., 9, 683–686, 2016.

Crill, P. M. and Thornton, B. F.: Whither methane in the IPCC process?, Nat. Clim. Chang., 7, 678–680, 2017.

Dargie, G. C., Lewis, S. L., Lawson, I. T., Mitchard, E. T. A., Page, S. E., Bocko, Y. E. and Ifo, S. A.: Age, extent and carbon storage of the central Congo Basin peatland complex, Nature, 542, 86–90, 2017.

Dean, J. F., Middelburg, J. J., Röckmann, T., Aerts, R., Blauw, L. G., Egger, M., Jetten, M. S. M., de Jong, A. E. E., Meisel, O. H., Rasigraf, O., Slomp, C. P., in't Zandt, M. and Dolman, A. J.: Methane feedbacks to the global climate system in a warmer world, Rev. Geophys., 56, 207–250, 2018.

Dlugokencky, E.: Global methane monthly means, [online] Available from: https://www.esrl.noaa.gov/gmd/ccgg/trends_ch4/ (Accessed 1 July 2020), 2020.

Dlugokencky, E. J., Nisbet, E. G., Fisher, R. and Lowry, D.: Global atmospheric methane: Budget, changes and dangers, Philos. Trans. R. Soc. A Math. Phys. Eng. Sci., 369, 2058–2072, 2011.

Dmitrenko, I. A., Kirillov, S. A., Tremblay, L. B., Kassens, H., Anisimov, O. A., Lavrov, S. A., Razumov, S. O. and Grigoriev, M. N.: Recent changes in shelf hydrography in the Siberian Arctic: Potential for subsea permafrost instability, J. Geophys. Res. Ocean., 116, C10027, 2011.

Dunfield, P., Knowles, R., Dumont, R. and Moore, T. R.: Methane production and consumption in temperate and subarctic peat soils: Response to temperature and pH, Soil Biol. Biogeochem., 25, 321–326, 1993.

Duval, T. and Radu, D.: Effect of temperature and soil organic matter quality on greenhouse gas production from temperate poor and rich fen soils, Ecol. Eng., 114, 167–172, 2018.

Eby, M., Zickfeld, K., Montenegro, A., Archer, D., Meissner, K. J. and Weaver, A. J.: Lifetime of anthropogenic climate change: Millennial time scales of potential CO2 and surface temperature perturbations, J. Clim., 22, 2501–2511, 2009.

Eby, M., Weaver, A. J., Alexander, K., Zickfeld, K., Abe-Ouchi, A., Cimatoribus, A. A., Crespin, E., Drijfhout, S. S., Edwards, N. R., Eliseev, A. V., Feulner, G., Fichefet, T., Forest, C. E., Goosse, H., Holden, P. B., Joos, F., Kawamiya, M., Kicklighter, D., Kienert, H., Matsumoto, K., Mokhov, I. I., Monier, E., Olsen, S. M., Pedersen, J. O. P., Perrette, M., Philippon-Berthier, G., Ridgwell, A., Schlosser, A., Von Deimling, T. S., Shaffer, G., Smith, R. S., Spahni, R., Sokolov, A. P., Steinacher, M., Tachiiri, K., Tokos, K., Yoshimori, M., Zeng, N. and Zhao, F.: Historical and idealized climate model experiments: An intercomparison of Earth system models of intermediate complexity, Clim. Past, 9, 1111–1140, 2013.

Ekici, A., Lee, H., Lawrence, D. M., Swenson, S. C. and Prigent, C.: Ground subsidence effects on simulating dynamic high-latitude surface inundation under permafrost thaw using CLM5, Geosci. Model Dev., 12, 5291–5300, 2019.

Elder, C. D., Xu, X., Walker, J., Schnell, J. L., Hinkel, K. M., Townsend-Small, A., Arp, C. D., Pohlman, J. W., Gaglioti, B. V. and Czimczik, C. I.: Greenhouse gas emissions from diverse Arctic Alaskan lakes are dominated by young carbon, Nat. Clim. Chang., 8, 166–171, 2018.

Eliseev, A. V., Mokhov, I. I., Arzhanov, M. M., Demchenko, P. F. and Denisov, S. N.: Interaction of the methane cycle and processes in wetland ecosystems in a climate model of intermediate complexity, Atmos. Ocean. Phys., 44, 147–162, 2008.

Estop-Aragonés, C., Knorr, K.-H. and Blodau, C.: Controls on in situ oxygen and dissolved inorganic carbon dynamics in peats of a temperate fen, J. Geophys. Res., 117, G02002, 2012.

Etheridge, D. M., Steele, L. P., Francey, R. J. and Langenfelds, R. L.: Atmospheric methane between 1000 A.D. and present: Evidence of anthropogenic emissions and climatic variability, J. Geophys. Res. Atmos., 103, 15979–15993, 1998.

Etminan, M., Myhre, G., Highwood, E. J. and Shine, K. P.: Radiative forcing of carbon dioxide, methane, and nitrous oxide: A significant revision of the methane radiative forcing, Geophys. Res. Lett., 43, 12614–12623, 2016.

Eyring, V., Bony, S., Meehl, G. A., Senior, C. A., Stevens, B., Stouffer, R. J. and Taylor, K. E.: Overview of the Coupled Model Intercomparison Project Phase 6 (CMIP6) experimental design and organization, Geosci. Model Dev., 9, 1937–1958, 2016.

Fiedler, S., Stevens, B., Gidden, M., Smith, S. J., Riahi, K. and Van Vuuren, D.: First forcing estimates from the future CMIP6 scenarios of anthropogenic aerosol optical properties and an associated Twomey effect, Geosci. Model Dev., 12, 989–1007, 2019.

Frolking, S., Roulet, N. T., Moore, T. R., Lafleur, P. M., Bubier, J. L. and Crill, P. M.: Modeling seasonal to annual carbon balance of Mer Bleue Bog, Ontario, Canada, Global Biogeochem. Cycles, 16, 1–21, 2002.

Ganesan, A. L., Schwietzke, S., Poulter, B., Arnold, T., Lan, X., Rigby, M., Vogel, F. R., Van der Werf, G. R., Janssens-Maenhout, G., Boesch, H., Pandey, S., Manning, A. J., Jackson, R. B., Nisbet, E. G. and Manning, M. R.: Advancing scientific understanding of the global methane budget in support of the Paris Agreement, Global Biogeochem. Cycles, 33, 1475–1512, 2019.

Gao, X., Adam Schlosser, C., Sokolov, A., Anthony, K. W., Zhuang, Q. and Kicklighter, D.: Permafrost degradation and methane: Low risk of biogeochemical climate-warming feedback, Environ. Res. Lett., 8, 035014, 2013.

Gauthier, M., Bradley, R. and Šimek, M.: More evidence that anaerobic oxidation of methane is prevalent in soils: Is it time to upgrade our biogeochemical models?, Soil Biol. Biochem., 80, 167–174, 2015.

Gedney, N. and Cox, P. M.: The sensitivity of global climate model simulations to the representation of soil moisture heterogeneity, J. Hydrometeorol., 4, 1265–1275, 2003.

Gedney, N., Cox, P. M. and Huntingford, C.: Climate feedback from wetland methane emissions, Geophys. Res. Lett., 31, L20503, 2004.

Gedney, N., Huntingford, C., Comyn-Platt, E. and Wiltshire, A.: Significant feedbacks of wetland methane release on climate change and the causes of their uncertainty, Environ. Res. Lett., 14, 084027, 2019.

Gernaat, D. E. H. J., Calvin, K., Lucas, P. L., Luderer, G., Otto, S. A. C., Rao, S., Strefler, J. and Van Vuuren, D. P.: Understanding the contribution of non-carbon dioxide gases in deep mitigation scenarios, Glob. Environ. Chang., 33, 142–153, 2015.

Gidden, M. J., Riahi, K., Smith, S. J., Fujimori, S., Luderer, G., Kriegler, E., Van Vuuren, D. P., Van Den Berg, M., Feng, L., Klein, D., Calvin, K., Doelman, J. C., Frank, S., Fricko, O., Harmsen, M., Hasegawa, T., Havlik, P., Hilaire, J., Hoesly, R., Horing, J., Popp, A., Stehfest, E. and Takahashi, K.: Global emissions pathways under different socioeconomic scenarios for use in CMIP6: A dataset of harmonized emissions trajectories through the end of the century, Geosci. Model Dev., 12, 1443–1475, 2019.

Girkin, N. T., Turner, B. L., Ostle, N., Craigon, J. and Sjögersten, S.: Root exudate analogues accelerate CO2 and CH4 production in tropical peat, Soil Biol. Biochem., 117, 48–55, 2018.

Glagolev, M., Kleptsova, I., Filippov, I., Maksyutov, S. and Machida, T.: Regional methane emission from West Siberia mire landscapes, Environ. Res. Lett., 6, 045214, 2011.

de Grandpré, I., Fortier, D. and Stephani, E.: Degradation of permafrost beneath a road embankment enhanced by heat advected in groundwater, Can. J. Earth Sci., 49, 953–962, 2012.

Grant, R. F.: Simulation of methanogenesis in the mathematical model ecosys, Soil Biol. Biochem., 30, 883–896, 1998.

Gruber, S.: Derivation and analysis of a high-resolution estimate of global permafrost zonation, Cryosphere, 6, 221–233, 2012.

Gumbricht, T., Roman-Cuesta, R., Verchot, L., Herold, M., Wittmann, F., Householder, E., Herold, N. and Murdiyarso, D.: An expert system model for mapping tropical wetlands and peatlands reveals South America as the largest contributor, Glob. Chang. Biol., 23, 3581–3599, 2016.

Hansen, J., Lacis, A., Rind, D., Russell, G., Stone, P., Fung, I., Ruedy, R. and Lerner, J.: Climate sensitivity: Analysis of feedback mechanisms, Geophys. Monogr. Ser., 29, 130–163, 1984.

Harmsen, M., Fricko, O., Hilaire, J., Van Vuuren, D. P., Drouet, L., Durand-Lasserve, O., Fujimori, S., Keramidas, K., Klimont, Z., Luderer, G., Aleluia Reis, L., Riahi, K., Sano, F. and Smith, S. J.: Taking some heat off the NDCs? The limited potential of additional short-lived climate forcers' mitigation, Clim. Change, doi:https://doi.org/10.1007/s10584-019-02436-3, 2019a.

Harmsen, M., Van Vuuren, D. P., Bodirsky, B. L., Chateau, J., Durand-Lasserve, O., Drouet, L., Fricko, O., Fujimori, S., Gernaat, D. E. H. J., Hanaoka, T., Hilaire, J., Keramidas, K., Luderer, G., Moura, M. C. P., Sano, F., Smith, S. J. and Wada, K.: The role of methane in future climate strategies: mitigation potentials and climate impacts, Clim. Change, doi:10.1007/s10584-019-02437-2, 2019b.

Hegarty, T.: Temperature coefficient (Q10), seed germination and other biological processes, Nature, 243, 305–306, 1973.

Helbig, M., Quinton, W. L. and Sonnentag, O.: Warmer spring conditions increase annual methane emissions from a boreal peat landscape with sporadic permafrost, Environ. Res. Lett., 12, 115009, 2017.

Hmiel, B., Petrenko, V. V., Dyonisius, M. N., Buizert, C., Smith, A. M., Place, P. F., Harth, C., Beaudette, R., Hua, Q., Yang, B., Vimont, I., Michel, S. E., Severinghaus, J. P., Etheridge, D., Bromley, T., Schmitt, J., Faïn, X., Weiss, R. F. and Dlugokencky, E.: Preindustrial 14CH4 indicates greater anthropogenic fossil CH4 emissions, Nature, 578, 409–412, 2020.

Hodson, E. L., Poulter, B., Zimmermann, N. E., Prigent, C. and Kaplan, J. O.: The El Nino-Southern Oscillation and wetland methane interannual variability, Geophys. Res. Lett., 38, L08810, 2011.

Hoehler, T. and Alperin, M.: Methane minimalism, Nature, 507, 436–437, 2014.

Hoehler, T. M., Alperin, M. J., Albert, D. B. and Martens, C. S.: Field and laboratory studies of methane oxidation in an anoxic marine sediment: Evidence for a methanogen-sulfate reducer consortium, Global Biogeochem. Cycles, 8, 451–463, 1994.

Höglund-Isaksson, L.: Global anthropogenic methane emissions 2005–2030: Technical mitigation potentials and costs, Atmos. Chem. Phys., 12, 9079–9096, 2012.

Hopcroft, P. O., Valdes, P. J. and Beerling, D. J.: Simulating idealized Dansgaard-Oeschger events and their potential impacts on the global methane cycle, Quat. Sci. Rev., 30, 3258–3268, 2011.

Houweling, S., Dentener, F. and Lelieveld, J.: Simulation of preindustrial atmospheric methane to constrain the global source strength of natural wetlands, J. Geophys. Res. Atmos., 105, 17243–17255, 2000.

Hu, H., Landgraf, J., Detmers, R., Borsdorff, T., Aan de Brugh, J., Aben, I., Butz, A. and Hasekamp, O.: Toward global mapping of methane with TROPOMI: First results and intersatellite comparison to GOSAT, Geophys. Res. Lett., 45, 3682–3689, 2018.

Hugelius, G., Strauss, J., Zubrzycki, S., Harden, J. W., Schuur, E. A. G., Ping, C. L., Schirrmeister, L., Grosse, G., Michaelson, G. J., Koven, C. D., O'Donnell, J. A., Elberling, B., Mishra, U., Camill, P., Yu, Z., Palmtag, J. and Kuhry, P.: Estimated stocks of circumpolar permafrost carbon with quantified uncertainty ranges and identified data gaps, Biogeosciences, 11, 6573–6593, 2014.

In't Zandt, M. H., Liebner, S. and Welte, C. U.: Roles of thermokarst lakes in a warming world, Trends Microbiol., 28, 769–779, 2020.

IPCC: Climate change 2014: Synthesis report. Contribution of Working Groups I, II, and III to the fifth assessment report of the Intergovernmental Panel on Climate Change, edited by R. K. Pachauri, M. R. Allen, V. R. Barros, J. Broome, W. Cramer, R. Christ, J. A. Church, L. Clarke, Q. Dahe, P. Dasgupta, N. K. Dubash, O. Edenhofer, I. Elgizouli, C. B. Field, P. Forster, P. Friedlingstein, J. Fuglestvedt, L. Gomez-Echeverri, S. Hallegatte, G. Hegerl, M. Howden, K. Jiang, B. J. Cisneros, V. Kattsov, H. Lee, K. J. Mach, J. Marotzke, M. D. Mastrandrea, L. Meyer, J. Minx, Y. Mulugetta, K. O'Brien, M. Oppenheimer, J. J. Pereira, R. Pichs-Madruga, G.-K. Plattner, H.-O. Pörtner, S. B. Power, B. Benjamin Preston, N. H. Ravindranath, A. Reisinger, K. Riahi, M. Rusticucci, R. Scholes, K. Seyboth, Y. Sokona, R. Stavins, T. F. Stocker, P. Tschakert, D. van Vuuren, J.-P. van Ypersele, L. Meyer, S. Brinkman, L. van Kesteren, N. Leprince-Ringuet, and F. van Boxmeer, Geneva., 2014.

IPCC: Global warming of 1.5°C. An IPCC special report on the impacts of global warming of 1.5°C above pre-industrial levels and related global greenhouse gas emission pathways, edited by V. Masson-Delmotte, P. Zhai, H.-O. Pörtner, D. Roberts, J. Skea, P. R. Shukla, A. Pirani, W. Moufouma-Okia, C. Péan, R. Pidcock, S. Connors, J. B. R. Matthews, Y. Chen, X. Zhou, M. I. Gomis, E. Lonnoy, T. Maycock, M. Tignor, and T. Waterfield., 2018.

Isaksen, I. S. A., Gauss, M., Myhre, G., Walter Anthony, K. and Ruppel, C.: Strong atmospheric chemistry feedback to climate warming from Arctic methane emissions, Global Biogeochem. Cycles, 25, GB2002, 2011.

Jackson, R. B., Saunois, M., Bousquet, P., Canadell, J. G., Poulter, B., Stavert, A. R., Bergamaschi, P., Niwa, Y., Segers, A. and Tsuruta, A.: Increasing anthropogenic methane emissions arise equally from agricultural and fossil fuel sources, Environ. Res. Lett., 15, 071002, 2020.

Jauhiainen, J., Takahashi, H., Heikkinen, J. E. P., Martikainen, P. J. and Vasander, H.: Carbon fluxes from a tropical peat swamp forest floor, Glob. Chang. Biol., 11, 1788–1797, 2005.

Jones, A., Haywood, J. M. and Jones, C. D.: Can reducing black carbon and methane below RCP2.6 levels keep global warming below 1.5 °C?, Atmos. Sci. Lett., 19(6), 1–5, 2018.

Keller, D. P., Oschlies, A. and Eby, M.: A new marine ecosystem model for the University of Victoria Earth System Climate Model, Geosci. Model Dev., 5, 1195–1220, 2012.

Kettunen, A., Kaitala, V., Lehtinen, A., Lohila, A., Alm, J., Silvola, J. and Martikainen, P. J.: Methane production and oxidation potentials in relation to water table fluctuations in two boreal mires, Soil Biol. Biochem., 31, 1741–1749 [online] Available from: www.elsevier.com/locate/soilbio, 1999.

Kim, Y.: Effect of thaw depth on fluxes of CO2 and CH4 in manipulated Arctic coastal tundra of Barrow, Alaska, Sci. Total Environ., 505, 385–389, 2015.

Kirschke, S., Bousquet, P., Ciais, P., Saunois, M., Canadell, J. G., Dlugokencky, E. J., Bergamaschi, P., Bergmann, D., Blake, D. R., Bruhwiler, L., Cameron-Smith, P., Castaldi, S., Chevallier, F., Feng, L., Fraser, A., Heimann, M., Hodson, E. L., Houweling, S., Josse, B., Fraser, P. J., Krummel, P. B., Lamarque, J.-F., Langenfelds, R. L., Le Quéré, C., Naik, V., Palmer, P. I., Pison, I., Plummer, D., Poulter, B., Prinn, R. G., Rigby, M., Ringeval, B., Santini, M., Schmidt, M., Shindell, D. T., Simpson, I. J., Spahni, R., Paul Steele, L., Strode, S. A., Sudo, K., Szopa, S., Van der Werf, G. R., Voulgarakis, A., Van Weele, M., Weiss, R. F., Williams, J. E. and Zeng, G.: Three decades of global methane sources and sinks, Nat. Geosci., 6, 813–823, 2013.

Kirtman, B., Power, S. B., Adedoyin, J. A., Boer, G. J., Bojariu, R., Camilloni, I., Doblas-Reyes, F. J., Fiore, A. M., Kimoto, M., Meehl, G. A., Prather, M., Sarr, A., Schär, C., Sutton, R., Van Oldenborgh, G. J., Vecchi, G. and Wang, H. J.: Near-term climate change: Projections and predictability, in Climate Change 2013: The Physical Science Basis. Contribution of Working Group I to the Fifth Assessment Report of the Intergovernmental Panel on Climate Change, pp. 953–1028, Cambridge University Press, Cambridge, UK and New York, NY, USA., 2013.

Kleinen, T. and Brovkin, V.: Pathway-dependent fate of permafrost region carbon, Environ. Res. Lett., 13, 094001, 2018.

Knoblauch, C., Beer, C., Liebner, S., Grigoriev, M. N. and Pfeiffer, E.-M.: Methane production as key to the greenhouse gas budget of thawing permafrost, Nat. Clim. Chang., 8, 309–312, 2018.

Kokelj, S. V. and Jorgenson, M. T.: Advances in thermokarst research, Permafr. Periglac. Process., 24, 108–119, 2013.

Koven, C. D., Ringeval, B., Friedlingstein, P., Ciais, P., Cadule, P., Khvorostyanov, D., Krinner, G. and Tarnocai, C.: Permafrost carbon-climate feedbacks accelerate global warming, Proc. Natl. Acad. Sci. U. S. A., 108, 14769–14774, 2011.

Koven, C. D., Riley, W. J., Subin, Z. M., Tang, J. Y., Torn, M. S., Collins, W. D., Bonan, G. B., Lawrence, D. M. and Swenson, S. C.: The effect of vertically resolved soil biogeochemistry and alternate soil C and N models on C dynamics of CLM4, Biogeosciences, 10, 7109–7131, 2013.

Koven, C. D., Schuur, E. A. G., Schädel, C., Bohn, T. J., Burke, E. J., Chen, G., Chen, X., Ciais, P., Grosse, G., Harden, J. W., Hayes, D. J., Hugelius, G., Jafarov, E. E., Krinner, G., Kuhry, P., Marchenko, S. S., McGuire, A. D. and Natali, S. M.: A simplified, data-constrained approach to estimate the permafrost carbon–climate feedback, Philos. Trans. R. Soc. A, 373, doi:doi.org/10.1098/rsta.2014.0423, 2015a.

Koven, C. D., Lawrence, D. M. and Riley, W. J.: Permafrost carbon−climate feedback is sensitive to deep soil carbon decomposability but not deep soil nitrogen dynamics, Proc. Natl. Acad. Sci. U. S. A., 112, 3752–3757, 2015b.

Koven, C. D., Hugelius, G., Lawrence, D. M. and Wieder, W. R.: Higher climatological temperature sensitivity of soil carbon in cold than warm climates, Nat. Clim. Chang., 7, 817–822, 2017.

Kwon, M., Jung, J., Tripathi, B., Göckede, M., Lee, Y. and Kim, M.: Dynamics of microbial communities and CO2 and CH4 fluxes in the tundra ecosystems of the changing Arctic, J. Microbiol., 57, 325–336, 2019.

Lawrence, D. M., Koven, C. D., Swenson, S. C., Riley, W. J. and Slater, A. G.: Permafrost thaw and resulting soil moisture changes regulate projected high-latitude CO2 and CH4 emissions, Environ. Res. Lett., 10, 2015.

Lawrence, D. M., Hurtt, G. C., Arneth, A., Brovkin, V., Calvin, K. V, Jones, A. D., Jones, C. D., Lawrence, P. J., de Noblet-Ducoudré, N., Pongratz, J., Seneviratne, S. I. and Shevliakova, E.: The Land Use Model Intercomparison Project (LUMIP) contribution to CMIP6: Rationale and experimental design, Geosci. Model Dev., (9), 2973–2998, 2016.

Legates, D. R. and McCabe, J. R.: Evaluating the use of “goodness-of-fit” measures in hydrologic and hydroclimatic model validation, Water Resour. Res., 35, 233–241, 1999.

Levy, P. E., Burden, A., Cooper, M. D. A., Dinsmore, K. J., Drewer, J., Evans, C., Fowler, D., Gaiawyn, J., Gray, A., Jones, S. K., Jones, T., Mcnamara, N. P., Mills, R., Ostle, N., Sheppard, L. J., Skiba, U., Sowerby, A., Ward, S. E. and Zieliński, P.: Methane emissions from soils: Synthesis and analysis of a large UK data set, Glob. Chang. Biol., 18, 1657–1669, 2012.

Lofton, D. D., Whalen, S. C. and Hershey, A. E.: Effect of temperature on methane dynamics and evaluation of methane oxidation kinetics in shallow Arctic Alaskan lakes, Hydrobiologia, 72, 209–222, 2014.

Loulergue, L., Schilt, A., Spahni, R., Masson-Delmotte, V., Blunier, T., Lemieux, B., Barnola, J., Raynaud, D., Stocker, T. and Chappellaz, J.: Orbital and millennial-scale features of atmospheric CH4 over the past 800,000 years, Nature, 453, 383–386, 2008.

Lovley, D. R. and Klug, M. J.: Model for the distribution of sulfate reduction and methanogenesis in freshwater sediments, Geochim. Cosmochim. Acta, 50, 11–18, 1986.

Lupascu, M., Wadham, E. R. C. and Pancost, R. D.: Temperature sensitivity of methane production in the permafrost active layer at Stordalen, Sweden: A comparison with non-permafrost northern wetlands, Arctic, Antarct. Alp. Res., 44, 469–482, 2012.

MacDougall, A. H. and Knutti, R.: Projecting the release of carbon from permafrost soils using a perturbed parameter ensemble modelling approach, Biogeosciences, 13, 2123–2136, 2016.

MacDougall, A. H., Avis, C. A. and Weaver, A. J.: Significant contribution to climate warming from the permafrost carbon feedback, Nat. Geosci., 5, 719–721, 2012.

MacDougall, A. H., Zickfeld, K., Knutti, R. and Matthews, H. D.: Sensitivity of carbon budgets to permafrost carbon feedbacks and non-CO2 forcings, Environ. Res. Lett., 10, 125003, 2015.

Marthews, T. R., Dadson, S. J., Lehner, B., Abele, S. and Gedney, N.: High-resolution global topographic index values for use in large-scale hydrological modelling, Hydrol. Earth Syst. Sci., 19, 91–104, 2015.

Mastepanov, M., Sigsgaard, C., Tagesson, T., Ström, L., Tamstorf, M. P., Lund, M. and Christensen, T. R.: Revisiting factors controlling methane emissions from high-Arctic tundra, Biogeosciences, 10, 5139–5158, 2013.

Matthes, K., Funke, B., Andersson, M. E., Barnard, L., Beer, J., Charbonneau, P., Clilverd, M. A., Dudok De Wit, T., Haberreiter, M., Hendry, A., Jackman, C. H., Kretzschmar, M., Kruschke, T., Kunze, M., Langematz, U., Marsh, D. R., Maycock, A. C., Misios, S., Rodger, C. J., Scaife, A. A., Seppälä, A., Shangguan, M., Sinnhuber, M., Tourpali, K., Usoskin, I., Van De Kamp, M., Verronen, P. T. and Versick, S.: Solar forcing for CMIP6 (v3.2), Geosci. Model Dev., 10, 2247–2302, 2017.

Matthews, E. and Fung, I.: Methane emission from natural wetlands: Global distribution, area and environmental characteristics of sources, Global Biogeochem. Cycles, 1, 61–86, 1987.

Matthews, H. D., Weaver, A. J., Meissner, K. J., Gillett, N. P. and Eby, M.: Natural and anthropogenic climate change: Incorporating historical land cover change, vegetation dynamics and the global carbon cycle, Clim. Dyn., 22, 461–479, 2004.

McCalley, C. K., Woodcroft, B. J., Hodgkins, S. B., Wehr, R. A., Kim, E.-H., Mondav, R., Crill, P. M., Chanton, J. P., Rich, V. I., Tyson, G. W. and Saleska, S. R.: Methane dynamics regulated by microbial community response to permafrost thaw, Nature, 514, 478–481, 2014.

McGuire, A. D., Anderson, L. G., Christensen, T. R., Dallimore, S., Guo, L., Hayes, D. J., Heimann, M., Lorenson, T. D., Macdonald, R. W. and Roulet, N.: Sensitivity of the carbon cycle in the Arctic to climate change, Ecol. Monogr., 79, 523–555, 2009.

McGuire, A. D., Koven, C. D., Lawrence, D. M., Clein, J. S., Xia, J., Beer, C., Burke, E., Chen, G., Chen, X., Delire, C., Jafarov, E., MacDougall, A. H., Marchenko, S., Nicolsky, D., Peng, S., Rinke, A., Saito, K., Zhang, W., Alkama, R., Bohn, T. J., Ciais, P., Decharme, B., Ekici, A., Gouttevin, I., Hajima, T., Hayes, D. J., Ji, D., Krinner, G., Lettenmaier, D. P., Luo, Y., Miller, P. A., Moore, J. C., Romanovsky, V., Schädel, C., Schaefer, K., Schuur, E. A. G., Smith, B., Sueyoshi, T. and Zhuang, Q.: Variability in the sensitivity among model simulations of permafrost and carbon dynamics in the permafrost region between 1960 and 2009, Global Biogeochem. Cycles, 30, 1015–1037, 2016.

McGuire, A. D., Lawrence, D. M., Koven, C., Clein, J. S., Burke, E., Chen, G., Jafarov, E., MacDougall, A. H., Marchenko, S., Nicolsky, D., Peng, S., Rinke, A., Ciais, P., Gouttevin, I., Hayes, D. J., Ji, D., Krinner, G., Moore, J. C., Romanovsky, V., Schädel, C., Schaefer, K., Schuur, E. A. G. and Zhuang, Q.: Dependence of the evolution of carbon dynamics in the northern permafrost region on the trajectory of climate change, Proc. Natl. Acad. Sci. U. S. A., 115, 3882–3887, 2017.

Meinshausen, M., Vogel, E., Nauels, A., Lorbacher, K., Meinshausen, N., Etheridge, D. M., Fraser, P. J., Montzka, S. A., Rayner, P. J., Trudinger, C. M., Krummel, P. B., Beyerle, U., Canadell, J. G., Daniel, J. S., Enting, I. G., Law, R. M., Lunder, C. R., O'Doherty, S., Prinn, R. G., Reimann, S., Rubino, M., Velders, G. J. M., Vollmer, M. K., Wang, R. H. J. and Weiss, R.: Historical greenhouse gas concentrations for climate modelling (CMIP6), Geosci. Model Dev., 10, 2057–2116, 2017.

Meinshausen, M., Nicholls, Z., Lewis, J., Gidden, M., Vogel, E., Freund, M., Beyerle, U., Gessner, C., Nauels, A., Bauer, N., Canadell, J., Daniel, J., John, A., Krummel, P., Luderer, G., Meinshausen, N., Montzka, S., Rayner, P., Reimann, S., Smith, S., Berg, M. V. D., Velders, G. J., Vollmer, M. and Wang, H. J.: The SSP greenhouse gas concentrations and their extensions to 2500, Geosci. Model Dev., 13, 3571–3605, 2019.

Meissner, K. J., Weaver, A. J., Matthews, H. D. and Cox, P. M.: The role of land surface dynamics in glacial inception: A study with the UVic Earth System Model, Clim. Dyn., 21, 515–537, 2003.

Melton, J. R., Wania, R., Hodson, E. L., Poulter, B., Ringeval, B., Spahni, R., Bohn, T., Avis, C. A., Beerling, D. J., Chen, G., Eliseev, A. V., Denisov, S. N., Hopcroft, P. O., Lettenmaier, D. P., Riley, W. J., Singarayer, J. S., Subin, Z. M., Tian, H., Zürcher, S., Brovkin, V., Van Bodegom, P. M., Kleinen, T., Yu, Z. C. and Kaplan, J. O.: Present state of global wetland extent and wetland methane modelling: Conclusions from a model inter-comparison project (WETCHIMP), Biogeosciences, 10, 753–788, 2013.

Mengis, N., Keller, D. P., MacDougall, A. H., Eby, M., Wright, N., Meissner, K. J., Oschlies, A., Schmittner, A., MacIsaac, A. J., Matthews, H. D. and Zickfeld, K.: Evaluation of the University of Victoria Earth System Climate Model version 2.10 (UVic ESCM 2.10), Geosci. Model Dev., 13, 4183–4204, 2020.

Le Mer, J. and Roger, P.: Production, oxidation, emission and consumption of methane by soils: A review, Eur. J. Soil Biol., 37, 25–50, 2001.

Metje, M. and Frenzel, P.: Methanogenesis and methanogenic pathways in a peat from subarctic permafrost, Environ. Microbiol., 9, 954–964, 2007.

Miller, S. M., Worthy, D. E. J., Michalak, A. M., Wofsy, S. C., Kort, E. A., Havice, T. C., Andrews, A. E., Dlugokencky, E. J., Kaplan, J. O., Levi, P. J., Tian, H. and Zhang, B.: Observational constraints on the distribution, seasonality, and environmental predictors of North American boreal methane emissions, Global Biogeochem. Cycles, 28, 146–160, 2014.

Mitsch, W. and Mander, Ü.: Wetlands and carbon revisited, Ecol. Eng., 114, 1–6, 2018.

Moore, T. and Roulet, N.: Methane flux: Water table relations in northern wetlands, Geophys. Res. Lett., 20, 587–590, 1993.

Moosavi, S. and Crill, P.: CH4 oxidation by tundra wetlands as measured by a selective inhibitor technique, J. Geophys. Res. Atmos., 103, 29093–29106, 1998.

Myhre, G., Shindell, D., Bréon, F.-M., Collins, W., Fuglestvedt, J., Huang, J., Koch, D., Lamarque, J.-F., Lee, D., Mendoza, B., Nakajima, T., Robock, A., Stephens, G., Takemura, T. and Zhang, H.: Anthropogenic and natural radiative forcing, in Climate Change 2013: The Physical Science Basis. Contribution of Working Group I to the Fifth Assessment Report of the Intergovernmental Panel on Climate Change, pp. 659–740, Cambridge University Press, Cambridge, UK and New York, NY, USA., 2013.

Naik, V., Voulgarakis, A., Fiore, A. M., Horowitz, L. W., Lamarque, J. F., Lin, M., Prather, M. J., Young, P. J., Bergmann, D., Cameron-Smith, P. J., Cionni, I., Collins, W. J., Dalsøren, S. B., Doherty, R., Eyring, V., Faluvegi, G., Folberth, G. A., Josse, B., Lee, Y. H., MacKenzie, I. A., Nagashima, T., Van Noije, T. P. C., Plummer, D. A., Righi, M., Rumbold, S. T., Skeie, R., Shindell, D. T., Stevenson, D. S., Strode, S., Sudo, K., Szopa, S. and Zeng, G.: Preindustrial to present-day changes in tropospheric hydroxyl radical and methane lifetime from the Atmospheric Chemistry and Climate Model Intercomparison Project (ACCMIP), Atmos. Chem. Phys., 13, 5277–5298, 2013.

Nauta, A. L., Heijmans, M. M. P. D., Blok, D., Limpens, J., Elberling, B., Gallagher, A., Li, B., Petrov, R. E., Maximov, T. C., Van Huissteden, J. and Berendse, F.: Permafrost collapse after shrub removal shifts tundra ecosystem to a methane source, Nat. Clim. Chang., 5, 67–70, 2015.

Neumann, R. B., Moorberg, C. J., Lundquist, J. D., Turner, J. C., Waldrop, M. P., McFarland, J. W., Euskirchen, E. S., Edgar, C. W. and Turetsky, M. R.: Warming effects of spring rainfall increase methane emissions from thawing permafrost, Geophys. Res. Lett., 46, 1393–1401, 2019.

Nicholls, Z. R. J., Meinshausen, M., Lewis, J., Gieseke, R., Dommenget, D., Dorheim, K., Fan, C., Fuglestvedt, J., Gasser, T., Golüke, U., Goodwin, P., Kriegler, E., Leach, N. J., Marchegiani, D., Quilcaille, Y., Samset, B. H., Sandstad, M., Shiklomanov, A. N., Skeie. R. B., Smith, C. J., Tanaka, K., Tsutsui, J. and Xie, Z.: Reduced complexity model intercomparison project phase 1: Protocol, results and initial observations, Geosci. Model Dev., 13, 5175–5190, 2020.

Nisbet, E. G., Manning, M. R., Dlugokencky, E. J., Fisher, R. E., Lowry, D., Michel, S. E., Myhre, C. L., Platt, S. M., Allen, G., Bousquet, P., Brownlow, R., Cain, M., France, J. L., Hermansen, O., Hossaini, R., Jones, A. E., Levin, I., Manning, A. C., Myhre, G., Pyle, J. A., Vaughn, B. H., Warwick, N. J. and White, J. W. C.: Very strong atmospheric methane growth in the 4 years 2014–2017: Implications for the Paris Agreement, Global Biogeochem. Cycles, 33, 318–342, 2019.

Nzotungicimpaye, C.-M. and Zickfeld, K.: The contribution from methane to the permafrost carbon feedback, Curr. Clim. Chang. Reports, 3, 58–68, 2017.

Nzotungicimpaye, C.-M., MacDougall, A. H., Melton, J. R., Treat, C. C., Eby, M., Lesack, L. F. W. and Zickfeld, K.: WETMETH 1.0: A new wetland methane model for implementation in Earth system models, Geosci. Model Dev., In review, doi:https://doi.org/10.5194/gmd-2020-176, 2020.

O'Connor, F. M., Boucher, O., Gedney, N., Jones, C. D., Folberth, G. A., Coppell, R., Friedlingstein, P., Collins, W. J., Chappellaz, J., Ridley, J. and Johnson, C. E.: Possible role of wetlands, permafrost, and methane hydrates in the methane cycle under future climate change: A review, Rev. Geophys., 48, RG4005, 2010.

O'Neill, B. C., Tebaldi, C., Van Vuuren, D. P., Eyring, V., Friedlingstein, P., Hurtt, G., Knutti, R., Kriegler, E., Lamarque, J. F., Lowe, J., Meehl, G. A., Moss, R., Riahi, K. and Sanderson, B. M.: The scenario model intercomparison project (ScenarioMIP) for CMIP6, Geosci. Model Dev., 9, 3461–3482, 2016.

O'Neill, B. C., Kriegler, E., Ebi, K. L., Kemp-Benedict, E., Riahi, K., Rothman, D. S., Van Ruijven, B. J., Van Vuuren, D. P., Birkmann, J., Kok, K., Levy, M. and Solecki, W.: The roads ahead: Narratives for shared socioeconomic pathways describing world futures in the 21st century, Glob. Environ. Chang., 42, 169–180, 2017.

Oh, Y., Zhuang, Q., Liu, L., Welp, L. R., Lau, M. C. Y., Onstott, T. C., Medvigy, D., Bruhwiler, L., Dlugokencky, E. J., Hugelius, G., D'Imperio, L. and Elberling, B.: Reduced net methane emissions due to microbial methane oxidation in a warmer Arctic, Nat. Clim. Chang., 10, 317–321, 2020.

Olefeldt, D., Turetsky, M. R., Crill, P. M. and McGuire, A. D.: Environmental and physical controls on northern terrestrial methane emissions across permafrost zones, Glob. Chang. Biol., 19, 589–603, 2013.

Olefeldt, D., Goswami, S., Grosse, G., Hayes, D., Hugelius, G., Kuhry, P., McGuire, A. D., Romanovsky, V. E., Sannel, A. B. K., Schuur, E. A. G. and Turetsky, M. R.: Circumpolar distribution and carbon storage of thermokarst landscapes, Nat. Commun., 7, 13043, 2016.

Olefeldt, D., Euskirchen, E. S., Harden, J., Kane, E., McGuire, A. D., Waldrop, M. P. and Turetsky, M. R.: A decade of boreal rich fen greenhouse gas fluxes in response to natural and experimental water table variability, Glob. Chang. Biol., 23, 2428–2440, 2017.

Orr, J. C.: On ocean carbon-cycle model comparison, Tellus B, 51, 509–510, 1999.

Overduin, P. P., Liebner, S., Knoblauch, C., Günther, F., Wetterich, S., Schirrmeister, L., Hubberten, H. W. and Grigoriev, M. N.: Methane oxidation following submarine permafrost degradation: Measurements from a central Laptev Sea shelf borehole, J. Geophys. Res. Biogeosciences, 120, 965–978, 2015.

Pandey, S., Houweling, S., Krol, M., Aben, I., Monteil, G., Nechita-Banda, N., Dlugokencky, E. J., Detmers, R., Hasekamp, O., Xu, X., Riley, W. J., Poulter, B., Zhang, Z., McDonald, K. C., White, J. W. C., Bousquet, P. and Röckmann, T.: Enhanced methane emissions from tropical wetlands during the 2011 La Niña, Sci. Rep., 7, 45759, 2017.

Pangala, S. R., Enrich-Prast, A., Basso, L. S., Peixoto, R. B., Bastviken, D., Hornibrook, E. R. C., Gatti, L. V., Ribeiro, H., Calazans, L. S. B., Sakuragui, C. M., Bastos, W. R., Malm, O., Gloor, E., Miller, J. B. and Gauci, V.: Large emissions from floodplains trees close the Amazon methane budget, Nature, 522, 230–234, 2017.

Panikov, N. S. and Dedysh, S. N.: Cold season CH4 and CO2 emission from boreal peat bogs (West Siberia): Winter fluxes and thaw activation dynamics, Global Biogeochem. Cycles, 14, 1071–1080, 2000.

Papa, F., Prigent, C., Aires, F., Jimenez, C., Rossow, W. B. and Matthews, E.: Interannual variability of surface water extent at the global scale, 1993-2004, J. Geophys. Res. Atmos., 115, D12111, 2010.

Parmentier, F.-J. W., Silyakova, A., Biastoch, A. and Kretschmer, K.: Natural marine methane sources in the Arctic, in AMAP Assessment 2015: Methane as an Arctic climate forcer, pp. 27–38, Arctic Monitoring and Assessment Programme (AMAP), Oslo, Norway., 2015.

Paudel, R., Mahowald, N. M., Hess, P. G. M., Meng, L. and Riley, W. J.: Attribution of changes in global wetland methane emissions from pre-industrial to present using CLM4.5-BGC, Environ. Res. Lett., 11, 034020, 2016.

Peltola, O., Vesala, T., Gao, Y., Räty, O., Alekseychik, P., Aurela, M., Chojnicki, B., Desai, A. R., Dolman, A. J., Euskirchen, E. S., Friborg, T., Göckede, M., Helbig, M., Humphreys, E., Jackson, R. B., Jocher, G., Joos, F., Klatt, J., Knox, S. H., Kowalska, N., Kutzbach, L., Lienert, S., Lohila, A., Mammarella, I., Nadeau, D. F., Nilsson, M. B., Oechel, W. C., Peichl, M., Pypker, T., Quinton, W., Rinne, J., Sachs, T., Samson, M., Schmid, H. P., Sonnentag, O., Wille, C., Zona, D. and Aalto, T.: Monthly gridded data product of northern wetland methane emissions based on upscaling eddy covariance observations, Earth Syst. Sci. Data, 11, 1263–1289, 2019.

Pickett-Heaps, C. A., Jacob, D. J., Wecht, K. J., Kort, E. A., Wofsy, S. C., Diskin, G. S., Worthy, D. E. ., Kaplan, J. O., Bey, I. and Drevet, J.: Magnitude and seasonality of wetland methane emissions from the Hudson Bay Lowlands (Canada), Atmos. Chem. Phys., 11, 3773–3779, 2011.

Poindexter, C. M., Baldocchi, D. D., Matthes, J. H., Knox, S. H. and Variano, E. A.: The contribution of an overlooked transport process to a wetland's methane emissions, Geophys. Res. Lett., 43, 6276–6284, 2016.

Popp, T. J., Chanton, J. P., Whiting, G. J. and Grant, N.: Evaluation of methane oxidation in the rhizosphere of a Carex dominated fen in north central Alberta, Canada, Biogeochemistry, 51, 259–281, 2000.

Poulter, B., Bousquet, P., Canadell, J. G., Ciais, P., Peregon, A., Saunois, M., Arora, V. K., Beerling, D. J., Brovkin, V., Jones, C. D., Joos, F., Gedney, N., Ito, A., Kleinen, T., Koven, C. D., McDonald, K., Melton, J. R., Peng, C., Peng, S., Prigent, C., Schroeder, R., Riley, W. J., Saito, M., Spahni, R., Tian, H., Taylor, L., Viovy, N., Wilton, D., Wiltshire, A., Xu, X., Zhang, B., Zhang, Z. and Zhu, Q.: Global wetland contribution to 2000-2012 atmospheric methane growth rate dynamics, Environ. Res. Lett., 12, 094013, 2017.

Prather, M. J. and Holmes, C. D.: Overexplaining or underexplaining methane's role in climate change, Proc. Natl. Acad. Sci. U. S. A., 114, 5324–5326, 2017.

Prather, M. J., Holmes, C. D. and Hsu, J.: Reactive greenhouse gas scenarios: Systematic exploration of uncertainties and the role of atmospheric chemistry, Geophys. Res. Lett., 39, L09803, 2012.

Prigent, C., Matthews, E., Aires, F. and Rossow, W. B.: Remote sensing of global wetland dynamics with multiple satellite data sets, Geophys. Res. Lett., 28, 4631–4634, 2001.

Prigent, C., Papa, F., Aires, F., Rossow, W. B. and Matthews, E.: Global inundation dynamics inferred from multiple satellite observations, 1993-2000, J. Geophys. Res. Atmos., 112, D12107, 2007a.

Prigent, C., Papa, F., Aires, F., Rossow, W. B. and Matthews, E.: Global inundation dynamics inferred from multiple satellite observations, 1993-2000, J. Geophys. Res. Atmos., 112, D12107, 2007b.

Prigent, C., Papa, F., Aires, F., Jiménez, C., Rossow, W. B. and Matthews, E.: Changes in land surface water dynamics since the 1990s and relation to population pressure, Geophys. Res. Lett., 39, L08403, 2012.

Ramanathan, V. and Xu, Y.: The Copenhagen Accord for limiting global warming: Criteria, constraints, and available avenues, Proc. Natl. Acad. Sci. U. S. A., 107, 8055–8062, 2010.

Rao, S., Klimont, Z., Leitao, J., Riahi, K., Van Dingenen, R., Reis, L. A., Calvin, K., Dentener, F., Drouet, L., Fujimori, S., Harmsen, M., Luderer, G., Heyes, C., Strefler, J., Tavoni, M. and Van Vuuren, D. P.: A multi-model assessment of the co-benefits of climate mitigation for global air quality, Environ. Res. Lett., 11, 124013, 2016.

Reeburgh, W.: Methane consumption in Cariaco Trench waters and sediments, Earth Planet. Sci. Lett., 28, 337–344, 1976.

Rhodes, R. H., Faïn, X., Stowasser, C., Blunier, T., Chappellaz, J., McConnell, J. R., Romanini, D., Mitchell, L. E. and Brook, E. J.: Continuous methane measurements from a late Holocene Greenland ice core: Atmospheric and in-situ signals, Earth Planet. Sci. Lett., 368, 9–19, 2013.

Rhodes, R. H., Brook, E. J., McConnell, J. R., Blunier, T., Sime, L. C., Faïn, X. and Mulvaney, R.: Atmospheric methane variability: Centennial-scale signals in the Last Glacial Period, Global Biogeochem. Cycles, 31, 575–590, 2017.

Riahi, K., Van Vuuren, D. P., Kriegler, E., Edmonds, J., O'neill, B. C., Fujimori, S., Bauer, N., Calvin, K., Dellink, R., Fricko, O., Lutz, W., Popp, A., Cuaresma, J. C., KC, S., Leimbach, M., Jiang, L., Kram, T., Rao, S., Emmerling, J., Ebi, K., Hasegawa, T., Havlik, P., Humpenöder, F., Aleluia, L., Silva, D., Smith, S., Stehfest, E., Bosetti, V., Eom, J., Gernaat, D., Masui, T., Rogelj, J., Strefler, J., Drouet, L., Krey, V., Luderer, G., Harmsen, M., Takahashi, K., Baumstark, L., Doelman, J. C., Kainuma, M., Klimont, Z., Marangoni, G., Lotze-Campen, H., Obersteiner, M., Tabeau, A. and Tavoni, M.: The shared socioeconomic pathways and their energy, land use, and greenhouse gas emissions implications: An overview, Glob. Environ. Chang., 42, 153–168, 2017.

Ribeiro-Kumara, C., Köster, E., Aaltonen, H. and Köster, K.: How do forest fires affect soil greenhouse gas emissions in upland boreal forests? A review, Environ. Res., 184, doi:10.1016/j.envres.2020.109328, 2020.

Riley, W. J., Subin, Z. M., Lawrence, D. M., Swenson, S. C., Torn, M. S., Meng, L., Mahowald, N. M. and Hess, P.: Barriers to predicting changes in global terrestrial methane fluxes: Analyses using CLM4Me, a methane biogeochemistry model integrated in CESM, Biogeosciences, 8, 1925–1953, 2011.

Ringeval, B., Friedlingstein, P., Koven, C., Ciais, P., De Noblet-Ducoudré, N., Decharme, B. and Cadule, P.: Climate-CH4 feedback from wetlands and its interaction with the climate-CO2 feedback, Biogeosciences, 8, 2137–2157, 2011.

Rivkina, E., Laurinavichius, K., McGrath, J., Tiedje, J., Shcherbakova, V. and Gilichinsky, D.: Microbial life in permafrost, Adv. Sp. Res., 33, 1215–1221, 2004.

Rogelj, J., Shindell, D., Jiang, K., Fifita, S., Forster, P., Ginzburg, V., Handa, C., Kheshgi, H., Kobayashi, S., Kriegler, E., Mundaca, L., Séférian, R. and Vilariño, M. V.: Mitigation pathways compatible with 1.5°C in the context of sustainable development, in Global warming of 1.5°C. An IPCC special report on the impacts of global warming of 1.5°C above pre-industrial levels and related global greenhouse gas emission pathways, pp. 93–174., 2018.

Rogelj, J., Forster, P. M., Kriegler, E., Smith, C. J. and Séférian, R.: Estimating and tracking the remaining carbon budget for stringent climate targets, Nature, 571, 335–342, 2019.

Roslev, P. and King, G.: Regulation of methane oxidation in a freshwater wetland by water table changes and anoxia, FEMS Microbiol. Ecol., 19, 105–115, 1996.

Roulet, N., Moore, T., Bubier, J. and Lafleur, P.: Northern fens: methane flux and climatic change, Tellus, 44B, 100–105, 1992.

Ruppel, C.: Permafrost-associated gas hydrate: Is it really approximately 1 % of the global system?, J. Chem. Eng. Data, 60, 429–436, 2015.

Ruppel, C. D. and Kessler, J. D.: The interaction of climate change and methane hydrates, Rev. Geophys., 55, 126–168, 2017.

Saunois, M., Bousquet, P., Poulter, B., Peregon, A., Ciais, P., Canadell, J. G., Dlugokencky, E. J., Etiope, G., Bastviken, D., Houweling, S., Mcdonald, K. C., Marshall, J., Melton, J. R., Morino, I., Naik, V., O'Doherty, S., Parmentier, F.-J. W., Patra, P. K., Peng, C., Peng, S., Peters, G. P., Pison, I., Prigent, C., Prinn, R., Ramonet, M., Riley, W. J., Saito, M., Santini, M., Schroeder, R., Simpson, I. J., Spahni, R., Steele, P., Takizawa, A., Thornton, B. F., Tian, H., Tohjima, Y., Viovy, N., Voulgarakis, A., Van Weele, M., Van Der Werf, G. R., Weiss, R., Wiedinmyer, C., Wilton, D. J., Wiltshire, A., Worthy, D., Wunch, D., Xu, X., Yoshida, Y., Zhang, B., Zhang, Z. and Zhu, Q.: The global methane budget 2000–2012, Earth Syst. Sci. Data, 8, 697–751, 2016a.

Saunois, M., Jackson, R. B., Bousquet, P. and Canadell, J. G.: The growing role of methane in anthropogenic climate change, Environ. Res. Lett., 11, 120207, 2016b.

Saunois, M., Stavert, A. R., Poulter, B., Bousquet, P., Canadell, J. G., Jackson, R. B., Raymond, P. A., Dlugokencky, E. J., Houweling, S., Patra, P. K., Ciais, P., Arora, V. K., Bastviken, D., Bergamaschi, P., Blake, D. R., Brailsford, G., Bruhwiler, L., Carlson, K. M., Carrol, M., Castaldi, S., Chandra, N., Crevoisier, C., Crill, P. M., Covey, K., Curry, C. L., Etiope, G., Frankenberg, C., Gedney, N., Hegglin, M. I., Höglund-Isaksson, L., Hugelius, G., Ishizawa, M., Ito, A., Janssens-Maenhout, G., Jensen, K. M., Joos, F., Kleinen, T., Krummel, P. B., Langenfelds, R. L., Laruelle, G. G., Liu, L., Machida, T., Maksyutov, S., McDonald, K. C., McNorton, J., Miller, P. A., Melton, J. R., Morino, I., Müller, J., Murguia-Flores, F., Naik, V., Niwa, Y., Noce, S., O'Doherty, S., Parker, R. J., Peng, C., Peng, S., Peters, G. P., Prigent, C., Prinn, R., Ramonet, M., Regnier, P., Riley, W. J., Rosentreter, J. A., Segers, A., Simpson, I. J., Shi, H., Smith, S. J., Steele, L. P., Thornton, B. F., Tian, H., Tohjima, Y., Tubiello, F. N., Tsuruta, A., Viovy, N., Voulgarakis, A., Weber, T. S., Van Weele, M., Van der Werf, G. R., Weiss, R. F., Worthy, D., Wunch, D., Yin, Y., Yoshida, Y., Zhang, W., Zhang, Z., Zhao, Y., Zheng, B., Zhu, Q., Zhu, Q. and Zhuang, Q.: The global methane budget 2000–2017, Earth Syst. Sci. Data, 12, 1561–1623, 2020.

Schädel, C., Bader, M. K.-F., Schuur, E. A. G., Biasi, C., Bracho, R., Čapek, P., De Baets, S., Diáková, K., Ernakovich, J., Estop-Aragones, C., Graham, D. E., Hartley, I. P., Iversen, C. M., Kane, E., Knoblauch, C., Lupascu, M., Martikainen, P. J., Natali, S. M., Norby, R. J., O'Donnell, J. A., Roy C., T., Šantrůčková, H., Shaver, G., Sloan, V. L., Treat, C. C., Turetsky, M. R., Waldrop, M. P. and Wickland, K. P.: Potential carbon emissions dominated by carbon dioxide from thawed permafrost soils, Nat. Clim. Chang., 6, 950–953, 2016.

Schaefer, H.: On the causes and consequences of recent trends in atmospheric methane, Curr. Clim. Chang. Reports, 5, 259–274, 2019.

Schaefer, K., Zhang, T., Bruhwiler, L. and Barrett, A. P.: Amount and timing of permafrost carbon release in response to climate warming, Tellus B, 63, 165–180, 2011.

Schaefer, K., Lantuit, H., Romanovsky, V. E., Schuur, E. A. G. and Witt, R.: The impact of the permafrost carbon feedback on global climate, Environ. Res. Lett., 9, 085003, 2014.

Schlesinger, W. H. and Bernhardt, E. S.: Wetland ecosystems, in Biogeochemistry: An analysis of global change, pp. 233–273, Academic Press, Cambridge, MA, USA., 2013.

Schmidt, A., Mills, M. J., Ghan, S., Gregory, J. M., Allan, R. P., Andrews, T., Bardeen, C. G., Conley, A., Forster, P. M., Gettelman, A., Portmann, R. W., Solomon, S. and Toon, O. B.: Volcanic radiative forcing from 1979 to 2015, J. Geophys. Res. Atmos., 123, 12491–12508, 2018.

Schmittner, A., Oschlies, A., Matthews, H. D. and Galbraith, E. D.: Future changes in climate, ocean circulation, ecosystems, and biogeochemical cycling simulated for a business-as-usual CO2 emission scenario until year 4000 AD, Global Biogeochem. Cycles, 22, GB1013, 2008.

Schneider von Deimling, T., Meinshausen, M., Levermann, A., Huber, V., Frieler, K., Lawrence, D. M. and Brovkin, V.: Estimating the near-surface permafrost-carbon feedback on global warming, Biogeosciences, 9, 649–665, 2012.

Schneider von Deimling, T., Grosse, G., Strauss, J., Schirrmeister, L., Morgenstern, A., Schaphoff, S., Meinshausen, M. and Boike, J.: Observation-based modelling of permafrost carbon fluxes with accounting for deep carbon deposits and thermokarst activity, Biogeosciences, 12, 3469–3488, 2015.

Schuur, E. A. G. and Mack, M. C.: Ecological response to permafrost thaw and consequences for local and global ecosystem services, Annu. Rev. Ecol. Evol. Syst., 49, 279–301, 2018.

Schuur, E. A. G., Bockheim, J., Canadell, J. G., Euskirchen, E., Field, C. B., Goryachkin, S. V., Hagemann, S., Kuhry, P., Lafleur, P. M., Lee, H., Mazhitova, G., Nelson, F. E., Rinke, A., Romanovsky, V. E., Shiklomanov, N., Tarnocai, C., Venevsky, S., Vogel, J. G. and Zimov, S. A.: Vulnerability of permafrost carbon to climate change: Implications for the global carbon cycle, Bioscience, 58, 701–714, 2008.

Schuur, E. A. G., Abbott, B. W., Bowden, W. B., Brovkin, V., Camill, P., Canadell, J. G., Chanton, J. P., Chapin, F. S., Christensen, T. R., Ciais, P., Crosby, B. T., Czimczik, C. I., Grosse, G., Harden, J., Hayes, D. J., Hugelius, G., Jastrow, J. D., Jones, J. B., Kleinen, T., Koven, C. D., Krinner, G., Kuhry, P., Lawrence, D. M., McGuire, A. D., Natali, S. M., O'Donnell, J. A., Ping, C. L., Riley, W. J., Rinke, A., Romanovsky, V. E., Sannel, A. B. K., Schädel, C., Schaefer, K., Sky, J., Subin, Z. M., Tarnocai, C., Turetsky, M. R., Waldrop, M. P., Walter Anthony, K. M., Wickland, K. P., Wilson, C. J. and Zimov, S. A.: Expert assessment of vulnerability of permafrost carbon to climate change, Clim. Change, 119, 359–374, 2013.

Schuur, E. A. G., McGuire, A. D., Schädel, C., Grosse, G., Harden, J. W., Hayes, D. J., Hugelius, G., Koven, C. D., Kuhry, P., Lawrence. D. M., Natali, S. M., Olefeldt, D., Romanovsky, V. E., Schaefer, K., Turetsky, M. R., Treat, C. C. and Vonk, J. E.: Climate change and the permafrost carbon feedback, Nature, 520, 171–179, 2015.

Schwietzke, S., Sherwood, O. A., Bruhwiler, L. M. P., Miller, J. B., Etiope, G., Dlugokencky, E. J., Michel, S. E., Arling, V. A., Vaughn, B. H., White, J. W. C. and Tans, P. P.: Upward revision of global fossil fuel methane emissions based on isotope database, Nature, 538, 88–91, 2016.

Segers, R.: Methane production and methane consumption: A review of processes underlying wetland methane fluxes, Biogeochemistry, 41, 23–51, 1998.

Serreze, M. C. and Barry, R. G.: Processes and impacts of Arctic amplification: A research synthesis, Glob. Planet. Change, 77, 85–96, 2011.

Shakhova, N., Semiletov, I., Leifer, I., Salyuk, A., Rekant, P. and Kosmach, D.: Geochemical and geophysical evidence of methane release over the East Siberian Arctic Shelf, J. Geophys. Res. Ocean., 115, C08007, 2010.

Shakhova, N., Semiletov, I. and Chuvilin, E.: Understanding the permafrost–hydrate system and associated methane releases in the east siberian arctic shelf, Geosciences, 9, 1–23, 2019.

Shindell, D., Kuylenstierna, J. C. I., Vignati, E., Van Dingenen, R., Amann, M., Klimont, Z., Anenberg, S. C., Muller, N., Janssens-Maenhout, G., Raes, F., Schwartz, J., Faluvegi, G., Pozzoli, L., Kupiainen, K., Höglund-Isaksson, L., Emberson, L., Streets, D., Ramanathan, V., Hicks, K., Oanh, N. T. K., Milly, G., Williams, M., Demkine, V. and Fowler, D.: Simultaneously mitigating near-term climate change and improving human health and food security, Sci. , 335, 183–188, 2012.

Shindell, D. T., Walter, B. P. and Faluvegi, G.: Impacts of climate change on methane emissions from wetlands, Geophys. Res. Lett., 31, L21202, 2004.

Shoemaker, J. K., Schrag, J. P., Molina, M. J. and Ramanathan, V.: What role for short-lived climate pollutants in mitigation policy?, Sci. , 342, 1323–1324, 2013.

Singleton, C. M., McCalley, C. K., Woodcroft, B. J., Boyd, J. A., Evans, P. N., Hodgkins, S. B., Chanton, J. P., Frolking, S., Crill, P. M., Saleska, S. R., Rich, V. I. and Tyson, G. W.: Methanotrophy across a natural permafrost thaw environment, ISME J., 12, 2544–2558, 2018.

Sjögersten, S., Black, C., Evers, S., Hoyos-Santillan, J., Wright, E. and Turner, B.: Tropical wetlands: A missing link in the global carbon cycle?, Global Biogeochem. Cycles, 28, 1371–1386, 2014.

Sjögersten, S., Aplin, P., Gauci, V., Peacock, M., Siegenthaler, A. and Turner, B. L.: Temperature response of ex-situ greenhouse gas emissions from tropical peatlands: Interactions between forest type and peat moisture conditions, Geoderma, 324, 47–55, 2018.

Smemo, K. A. and Yavitt, J. B.: Anaerobic oxidation of methane: An underappreciated aspect of methane cycling in peatland ecosystems?, Biogeosciences, 8, 779–793, 2011.

Song, C., Xu, X., Sun, X., Tian, H., Sun, L., Miao, Y., Wang, X. and Guo, Y.: Large methane emission upon spring thaw from natural wetlands in the northern permafrost region, Environ. Res. Lett., 7, 034009, 2012.

Stevens, B., Fiedler, S., Kinne, S., Peters, K., Rast, S., Müsse, J., Smith, S. J. and Mauritsen, T.: MACv2-SP: A parameterization of anthropogenic aerosol optical properties and an associated Twomey effect for use in CMIP6, Geosci. Model Dev., 10, 433–452, 2017.

Strauss, J., Schirrmeister, L., Grosse, G., Wetterich, S., Ulrich, M., Herzschuh, U. and Hubberten, H. W.: The deep permafrost carbon pool of the Yedoma region in Siberia and Alaska, Geophys. Res. Lett., 40, 6165–6170, 2013.

Strauss, J., Schirrmeister, L., Grosse, G., Fortier, D., Hugelius, G., Knoblauch, C., Romanovsky, V., Schädel, C., Schneider von Deimling, T., Schuur, E. A. G., Shmelev, D., Ulrich, M. and Veremeeva, A.: Deep Yedoma permafrost: A synthesis of depositional characteristics and carbon vulnerability, Earth-Science Rev., 172, 75–86, 2017.

Tagesson, T., Mastepanov, M., Mölder, M., Tamstorf, M. P., Eklundh, L., Smith, B., Sigsgaard, C., Lund, M., Ekberg, A., Falk, J. M., Friborg, T., Christensen, T. R. and Ström, L.: Modelling of growing season methane fluxes in a high-Arctic wet tundra ecosystem 1997-2010 using in situ and high-resolution satellite data, Tellus, Ser. B Chem. Phys. Meteorol., 65, 1–25, 2013.

Tarnocai, C., Canadell, J. G., Schuur, E. A. G., Kuhry, P., Mazhitova, G. and Zimov, S.: Soil organic carbon pools in the northern circumpolar permafrost region, Global Biogeochem. Cycles, 23, GB2023, 2009.

Taylor, K. E., Stouffer, R. J. and Meehl, G. A.: An overview of CMIP5 and the experiment design, Bull. Am. Meteorol. Soc., 93, 485–498, 2012.

Thompson, R. L., Sasakawa, M., Machida, T., Aalto, T., Worthy, D., Lavric, J. V., Myhre, C. L. and Stohl, A.: Methane fluxes in the high northern latitudes for 2005-2013 estimated using a Bayesian atmospheric inversion, Atmos. Chem. Phys., 17, 3553–3572, 2017.

Thornton, B., Wik, M. and Crill, P. M.: Double-counting challenges the accuracy of high-latitude methane inventories, Geophys. Res. Lett., 43, 12569–12577, 2016.

Thornton, B. F. and Crill, P.: Arctic permafrost: Microbial lid on subsea methane, Nat. Clim. Chang., 5, 723–724, 2015.

Tokarska, K. and Gillett, N.: Cumulative carbon emissions budgets consistent with 1.5°C global warming, Nat. Clim. Chang., 8, 296–299, 2018.

Tokarska, K. B., Schleussner, C. F., Rogelj, J., Stolpe, M. B., Matthews, H. D., Pfleiderer, P. and Gillett, N. P.: Recommended temperature metrics for carbon budget estimates, model evaluation and climate policy, Nat. Geosci., 12, 964–971, 2019.

Tootchi, A., Jost, A. and Ducharne, A.: Multi-source global wetland maps combining surface water imagery and groundwater constraints, Earth Syst. Sci. Data, 11, 189–220, 2019.

Treat, C. C., Natali, S. M., Ernakovich, J., Iversen, C. M., Lupascu, M., McGuire, A. D., Norby, R. J., Roy Chowdhury, T., Richter, A., Santruckova, H., Schädel, C., Schuur, E. A. G., Sloan, V. L., Turetsky, M. . R. and Waldrop, M. P.: A pan-Arctic synthesis of CH4 and CO2 production from anoxic soil incubations, Glob. Chang. Biol., 21, 2787–2803, 2015.

Treat, C. C., Bloom, A. A. and Marushchak, M. E.: Nongrowing season methane emissions–a significant component of annual emissions across northern ecosystems, Glob. Chang. Biol., 24, 3331–3343, 2018.

Turetsky, M. R., Kane, E. S., Harden, J. W., Ottmar, R. D., Manies, K. L., Hoy, E. and Kasischke, E. S.: Recent acceleration of biomass burning and carbon losses in Alaskan forests and peatlands, Nat. Geosci., 4, 27–31, 2011.

Turetsky, M. R., Kotowska, A., Bubier, J., Dise, N. B., Crill, P., Hornibrook, E. R. C., Minkkinen, K., Moore, T. R., Myers-Smith, I. H., Nykänen, H., Olefeldt, D., Rinne, J., Saarnio, S., Shurpali, N., Tuittila, E. S., Waddington, J. M., White, J. R., Wickland, K. P. and Wilmking, M.: A synthesis of methane emissions from 71 northern, temperate, and subtropical wetlands, Glob. Chang. Biol., 20, 2183–2197, 2014.

Turetsky, M. R., Abbott, B. W., Jones, M. C., Walter Anthony, K., Olefeldt, D., Schuur, E. A. G., Grosse, G., Kuhry, P., Hugelius, G., Koven, C., Lawrence, D. M., Gibson, C., Sannel, A. B. K. and McGuire, A. D.: Carbon release through abrupt permafrost thaw, Nat. Geosci., 13, 138–143, 2020.

UNFCCC: The United Nations Framework Convention on Climate Change (UNFCCC) Paris Agreement. [online] Available from: https://unfccc.int/files/essential_background/convention/application/pdf/english_paris_agreement.pdf, 2015.

Vonk, J. E. and Gustafsson, Ö.: Permafrost-carbon complexities, Nat. Geosci., 6, 675–676, 2013.

Walter Anthony, K., Anthony, P., Grosse, G. and Chanton, J.: Geologic methane seeps along boundaries of Arctic permafrost thaw and melting glaciers, Nat. Geosci., 5, 419–426, 2012.

Walter Anthony, K., Daanen, R., Anthony, P., Schneider von Deimling, T., Ping, C.-L., Chanton, J. P. and Grosse, G.: Methane emissions proportional to permafrost carbon thawed in Arctic lakes since the 1950s, Nat. Geosci., 9, 679–682, 2016.

Walter Anthony, K., Von Deimling, S., Nitze, I., Frolking, S., Emond, A., Daanen, R., Anthony, P., Lindgren, P., Jones, B. and Grosse, G.: 21st-century modeled permafrost carbon emissions accelerated by abrupt thaw beneath lakes, Nat. Commun., 9, 1–11, 2018.

Walter, K. M., Zimov, S. A., Chanton, J. P., Verbyla, D. and Chapin III, F. S.: Methane bubbling from Siberian thaw lakes as a positive feedback to climate warming, Nature, 443, 71–75, 2006.

Walvoord, M. A. and Kurylyk, B. L.: Hydrologic impacts of thawing permafrost - A review, Vadose Zo. J., 15, 1–20, 2016.

Walz, J., Knoblauch, C., Böhme, L. and Pfeiffer, E. M.: Regulation of soil organic matter decomposition in permafrost-affected Siberian tundra soils - Impact of oxygen availability, freezing and thawing, temperature, and labile organic matter, Soil Biol. Biochem., 110, 34–43, 2017.

Wania, R., Ross, I. and Prentice, I. C.: Integrating peatlands and permafrost into a dynamic global vegetation model: 1. Evaluation and sensitivity of physical land surface processes, Global Biogeochem. Cycles, 23, GB3014, 2009.

Wania, R., Ross, I. and Prentice, I. .: Implementation and evaluation of a new methane model within a dynamic global vegetation model: LPJ-WHyMe v1.3.1, Geosci. Model Dev., 3, 565–584, 2010.

Wania, R., Melton, J. R., Hodson, E. L., Poulter, B., Ringeval, B., Spahni, R., Bohn, T., Avis, C. A., Chen, G., Eliseev, A. V., Hopcroft, P. O., Riley, W. J., Subin, Z. M., Tian, H., Van Bodegom, P. M., Kleinen, T., Yu, Z. C., Singarayer, J. S., Zürcher, S., Lettenmaier, D. P., Beerling, D. J., Denisov, S. N., Prigent, C., Papa, F. and Kaplan, J. O.: Present state of global wetland extent and wetland methane modelling: methodology of a model inter-comparison project (WETCHIMP), Geosci. Model Dev., 6, 617–641, 2013.

Wanninkhof, R.: Relationship between wind speed and gas exchange over the ocean revisited, Limnol. Oceanogr. Methods, 12, 351–362, 2014.

Weaver, A. J.: Toward the second commitment period of the Kyoto Protocol, Sci. , 332, 795–796, 2011.

Weaver, A. J., Eby, M., Wiebe, E. C., Bitz, C. M., Duffy, P. B., Ewen, T. L., Fanning, A. F., Holland, M. M., MacFayden, A., Matthews, H. D., Meissner, K. J., Saenko, O., Schmittner, A., Wang, H. and Yoshimori, M.: The UVic Earth System Climate Model: Model description, climatology, and applications to past, present and future climates, Atmosphere-Ocean, 39, 361–428, 2001.

West, J. J., Fiore, A. M., Horowitz, L. W. and Mauzerall, D. L.: Global health benefits of mitigating ozone pollution with methane emission controls, Proc. Natl. Acad. Sci. U. S. A., 103, 3988–3993, 2006.

Whalen, S. C.: Biogeochemistry of methane exchange between natural wetlands and the atmosphere, Environ. Eng. Sci., 22, 73–94, 2005.

Wheeler, B. D.: Water and plants in freshwater wetlands, in Eco-Hydrology, edited by A. J. Baird and R. L. Wilby, pp. 127–180, Routledge, London., 1999.

Whiticar, M. J. and Faber, E.: Methane oxidation in sediment and water column environments-Isotope evidence, Adv. Org. Geochemistry, 10, 759–768, 1985.

Wik, M., Varner, R. K., Walter Anthony, K., MacIntyre, S. and Bastviken, D.: Climate-sensitive northern lakes and ponds are critical components of methane release, Nat. Geosci., 9, 99–105, 2016.

Wild, B., Gentsch, N., Čapek, P., Diáková, K., Alves, R. J. E., Bárta, J., Gittel, A., Hugelius, G., Knoltsch, A., Kuhry, P., Lashchinskiy, N., Mikutta, R., Palmtag, J., Schleper, C., Schnecker, J., Shibistova, O., Takriti, M., Torsvik, V. L., Urich, T., Watzka, M., Šantrůčková, H., Guggenberger, G. and Richter, A.: Plant-derived compounds stimulate the decomposition of organic matter in arctic permafrost soils, Sci. Rep., 6, 25607, 2016.

Willmott, C. J.: Some comments on the evaluation of model performance, Bull. Am. Meteorol. Soc. , 63, 1309–1313, 1982.

WMO: The global climate in 2015-2019, Geneva. [online] Available from: https://library.wmo.int/doc_num.php?explnum_id=9936, 2019.

Woo, M.: Permafrost hydrology, Springer, Heidelberg., 2012.

Wu, Y., Verseghy, D. and Melton, J.: Integrating peatlands into the coupled Canadian Land Surface Scheme (CLASS) v3.6 and the Canadian Terrestrial Ecosystem Model (CTEM) v2.0, Geosci. Model Dev., 9, 2639–2663, 2016.

Wuebbles, D. J. and Hayhoe, K.: Atmospheric methane and global change, Earth-Science Rev., 57, 177–210, 2002.

Xu, X., Elias, D. A., Graham, D. E., Phelps, T. J., Carroll, S. L., Wullschleger, S. D. and Thornton, P. E.: A microbial functional group-based module for simulating methane production and consumption: Application to an incubated permafrost soil, J. Geophys. Res. G Biogeosciences, 120, 1315–1333, 2015.

Xu, X., Yuan, F., Hanson, P. J., Wullschleger, S. D., Thornton, P. E., Riley, W. J., Song, X., Graham, D. E., Song, C. and Tian, H.: Reviews and syntheses: Four decades of modeling methane cycling in terrestrial ecosystems, Biogeosciences, 13, 3735–3755, 2016.

Yvon-Durocher, G., Allen, A. P., Bastviken, D., Conrad, R., Gudasz, C., St-Pierre, A., Thanh-Duc, N. and Del Giorgio, P. A.: Methane fluxes show consistent temperature dependence across microbial to ecosystem scales, Nature, 507, 488–491, 2014.

Zalman, C. A., Meade, N., Chanton, J., Kostka, J. E., Bridgham, S. D. and Keller, J. K.: Methylotrophic methanogenesis in sphagnum-dominated peatland soils, Soil Biol. Biochem., 118, 156–160, 2018.

Zhang, B., Tian, H., Lu, C., Chen, G., Pan, S., Anderson, C. and Poulter, B.: Methane emissions from global wetlands: An assessment of the uncertainty associated with various wetland extent data sets, Atmos. Environ., 165, 310–321, 2017a.

Zhang, T., Barry, R. G., Knowles, K., Heginbottom, J. A. and Brown, J.: Statistics and characteristics of permafrost and ground-ice distribution in the Northern Hemisphere, Polar Geogr., 31, 47–68, 2008.

Zhang, Z., Zimmermann, N. E., Stenke, A., Li, X., Hodson, E. L., Zhu, G., Huang, C. and Poulter, B.: Emerging role of wetland methane emissions in driving 21st century climate change, Proc. Natl. Acad. Sci. U. S. A., 114, 9647–9652, 2017b.

Zhang, Z., Zimmermann, N. E., Calle, L., Hurtt, G., Chatterjee, A. and Poulter, B.: Enhanced response of global wetland methane emissions to the 2015-2016 El Niño-Southern Oscillation event, Environ. Res. Lett., 13, 074009, 2018.

Zhu, Q., Peng, C., Chen, H., Fang, X., Liu, J., Jiang, H., Yang, Y. and Yang, G.: Estimating global natural wetland methane emissions using process modelling: spatio-temporal patterns and contributions to atmospheric methane fluctuations, Glob. Ecol. Biogeogr., 24, 959–972, 2015.

Zickfeld, K., Eby, M., Matthews, H. D. and Weaver, A. J.: Setting cumulative emissions targets to reduce the risk of dangerous climate change, Proc. Natl. Acad. Sci. U. S. A., 106, 16129–16134, 2009.

Zickfeld, K., Eby, M., Weaver, A. J., Alexander, K., Crespin, E., Edwards, N. R., Eliseev, A. V., Feulner, G., Fichefet, T., Forest, C. E., Friedlingstein, P., Goosse, H., Holden, P. B., Joos, F., Kawamiya, M., Kicklighter, D., Kienert, H., Matsumoto, K., Mokhov, I. I., Monier, E., Olsen, S. M., Pedersen, J. O. P., Perrette, M., Philippon-Berthier, G., Ridgwell, A., Schlosser, A., Von Deimling, T. S., Shaffer, G., Sokolov, A., Spahni, R., Steinacher, M., Tachiiri, K., Tokos, K. S., Yoshimori, M., Zeng, N. and Zhao, F.: Long-term climate change commitment and reversibility: An EMIC intercomparison, J. Clim., 26, 5782–5809, 2013.

Zimov, S. A., Schuur, E. A. G. and Stuart Chapin III, F.: Permafrost and the global carbon budget, , 1612–1613, 2006.

Zona, D., Gioli, B., Commane, R., Lindaas, J., Wofsy, S. C., Miller, C. E., Dinardo, S. J., Dengel, S., Sweeney, C., Karion, A., Chang, R. Y.-W., Henderson, J. M., Murphy, P. C., Goodrich, J. P., Moreaux, V., Liljedahl, A., Watts, J. D., Kimball, J. S., Lipson, D. A. and Oechel, W. C.: Cold season emissions dominate the Arctic tundra methane budget, Proc. Natl. Acad. Sci. U. S. A., 113, 40–45, 2016.

Appendix A. Temperature-dependent Q_{10} coefficient for CH_4 production

Figure A1 illustrates the different shapes of the temperature-dependency function for CH_4 production ($Q_{10}^{\frac{T_i - T_0}{10}}$; $T_0 = 273.15$ K) across a range of temperatures when considering: (i) a constant Q_{10} of 4.2; and (ii) a temperature-dependent Q_{10} coefficient given by $Q_{10}(T_i) = 1.7 + 2.5 \tanh [0.1 (T_{ref} - T_i)]$, where $T_{ref} = 308.15$ K. The temperature-dependent $Q_{10}(T_i)$ implies an optimal temperature for CH_4 production in WETMETH around 300.15 K (dashed vertical line). When $Q_{10}(T_i)$ decreases to reach negative values, its value in WETMETH is set to 10^{-3} to represent a very small methanogenic response to temperature changes (Figure A1).

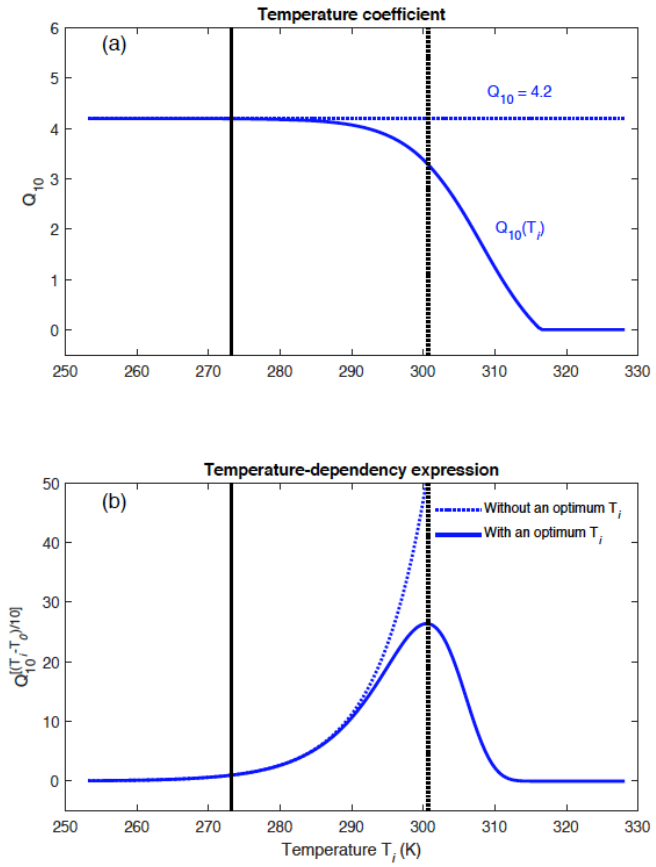

Figure A1. (a) Differences between a constant Q_{10} coefficient and a temperature-dependent $Q_{10}(T_i)$ coefficients and (b) implications for the temperature-dependency expression for CH_4 production ($Q_{10}[(T_i - T_0)/10]$).

Appendix B. Applied minor modification to the TOPMODEL approach

The TOPMODEL approach implemented in the UVic ESCM is based on the formulation by Gedney and Cox for global land surface models (Gedney and Cox, 2003). This approach combines the simulated hydrology with a prescribed topographic index to determine the occurrence of wetlands (surface inundation) and soil moisture heterogeneity at the sub-grid scale. The occurrence of wetlands is simulated in an area whose local topographic index (Λ) satisfies the following condition:

$$\Lambda_{\min} \leq \Lambda \leq \Lambda_{\max} , \tag{B.1}$$

where $\Lambda_{\min}$ is a lower threshold that can be related to under-saturation conditions and $\Lambda_{\max}$ is an upper threshold that can be related to over-saturation conditions.

In the initial work by Gedney and Cox, $\Lambda_{\min}$ depends on the transmissivity of the entire soil column ($\mathrm{T}(0)$), the transmissivity of the soil column below the mean water table depth (z_w) of the grid box ($\mathrm{T}(z_w)$) as well as the mean topographic index (Λ_{mean}). It is calculated as $\Lambda_{\min} = \ln\frac{\mathrm{T}(0)}{\mathrm{T}(z_w)} + \Lambda_{\mathrm{mean}}$. While Λ_{mean} is static and prescribed with a topographic index map, both transmissivities ($\mathrm{T}(0)$ and $\mathrm{T}(z_w)$) are simulated and non-static for a specific grid cell. Hence, $\Lambda_{\min}$ is a non-static and grid-dependent threshold. Unlike $\Lambda_{\min}$, $\Lambda_{\max}$ is a static and global threshold. This threshold is applied to constrain the occurrence of wetlands in areas of stagnant water based on the assumption that locations where the water table rises well above the surface would be characterized by streamflow.

For the current study, a minor modification is applied to the above TOPMODEL approach. The revision consists of using a non-static and grid-dependent $\Lambda_{\max}$ instead of a static and global threshold. Following the formulation by Comyn-Platt and colleagues (Comyn-Platt et al., 2018), an expression for $\Lambda_{\max}$ that depends on $\Lambda_{\min}$ is currently used in the UVic ESCM. This threshold is defined as:

$$\Lambda_{\max} = \Lambda_{\min} + \Lambda_{\mathrm{range}} , \tag{B.2}$$

where Λ_{range} is a global tuning parameter (Λ_{range}= 0.93 in the version of the UVic ESCM used in this study).

In summary, unlike the initial work by Gedney and Cox (Gedney and Cox, 2003), the modified TOPMODEL approach considers two non-static and grid-dependent thresholds (Λ_{min} and Λ_{max}) for the identification of wetlands across the globe.

Appendix C. Unit conversion for potential CH_4 production rates

Here, we describe steps followed for converting units of maximum CH_4 production rates measured in laboratory incubations from a soil weight basis (µg C g DW^{-1} hr^{-1}) to a soil volume basis (kg C m^{-3} s^{-1}). This unit conversion relies on the soil bulk density (BD in g cm^{-3}) from the site of origin. The following two steps illustrate the applied unit conversion. In the first step, the potential CH_4 production rates ($P_{d,0}$) are converted from µg C g DW^{-1} hr^{-1} to µg C cm^{-3} hr^{-1} as follows:

$$P_{d,1} = (BD)\, P_{d,0} \quad \text{(C.1)}$$

Then, the conversion of $P_{d,1}$ from µg C cm^{-3} hr^{-1} to kg C m^{-3} s^{-1} is done as follows:

$$P_{d,2} = \frac{\delta}{\gamma} P_{d,1}, \quad \text{(C.2)}$$

where δ encompasses the conversion factors from µg to kg and from cm^{-3} to m^{-3} ($\delta = 10^{-3}$ kg m^{-3}); and γ is the number of seconds per hour (γ = 3600 s).

Appendix D. Supplementary figures for Chapter 3

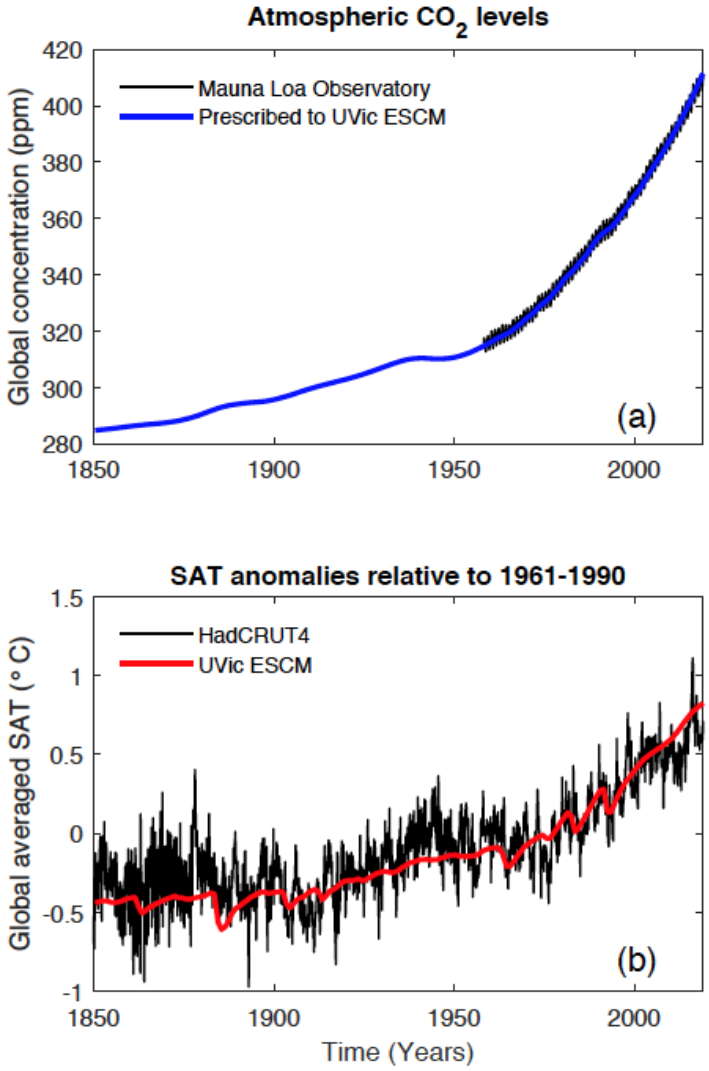

Figure D1. **Illustration of the global climate conditions from 1850 through 2019 as simulated by the fully coupled UVic ESCM: (a) Atmospheric CO_2 concentration prescribed to the model in comparison to measurements from the Mauna Loa Observatory. (b) Global surface air temperature (SAT) anomalies relative to 1961-1990 in comparison to the HadCRUT4 dataset.**

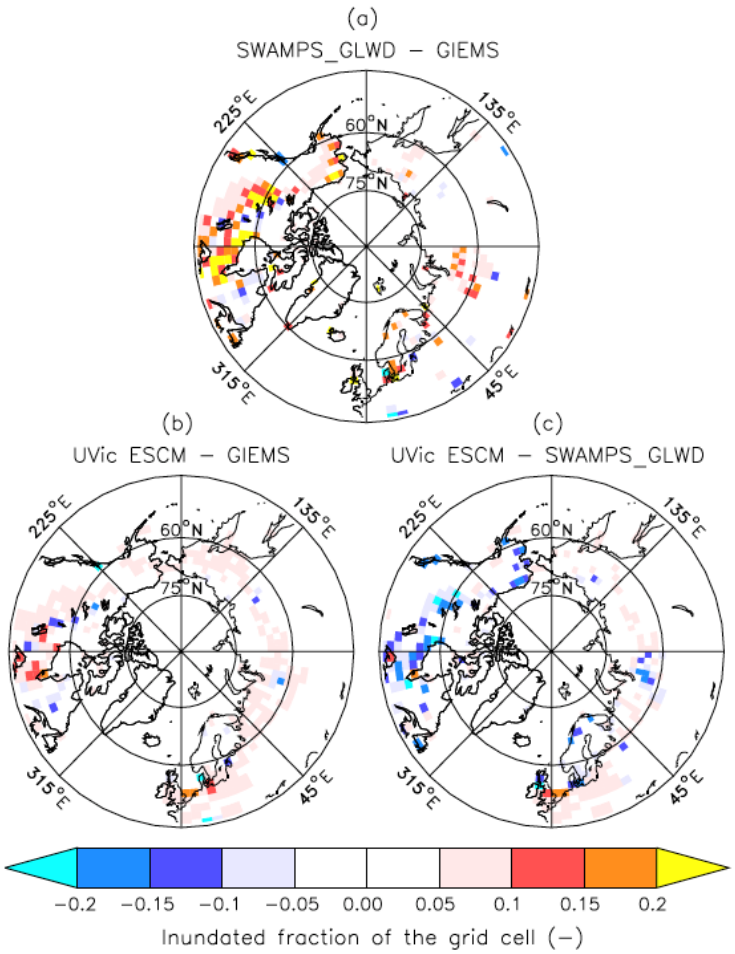

Figure D2. **Differences in northern wetland extents (inundated fractions of grid cells) between two datasets (GIEMS and SWAMPS-GLWD) and the UVic ESCM over the 2000-2007 period: (a) SWAMPS-GLWD – GIEMS, (b) UVic ESCM – GIEMS, and (c) UVic ESCM – SWAMPS-GLWD. The comparison period corresponds to the overlap period for the two datasets.**

Appendix E. Statistical evaluation for Chapter 3

Methods

We consider four metrics to evaluate the model performance with respect to wetland extents and CH_4 emissions: the mean bias error (MBE), the mean absolute error (MAE), the root mean square error (RMSE), and the coefficient of determination (R^2). These metrics allow to compare a set of observations (Y) and their predictions (X) (Ali and Abustan, 2014; Willmott, 1982).

MBE, MAE and RMSE are difference metrics and their respective formulas for a sample size n are given below:

$$\mathrm{MBE} = \frac{1}{n}\sum_{i=1}^{n}(X_i - Y_i) \quad \text{(E.1)}$$

$$\mathrm{MAE} = \frac{1}{n}\sum_{i=1}^{n}|X_i - Y_i| \quad \text{(E.2)}$$

$$\mathrm{RMSE} = \sqrt{\frac{1}{n}\sum_{i=1}^{n}(X_i - Y_i)^2} \quad \text{(E.3)}$$

R^2 is a correlation metric from the linear regression theory. It is a measure of the extent to which X predicts the total variability in Y and is given by:

$$\mathrm{R}^2 = \frac{\sum_{i=1}^{n}(\hat{Y}_i - \bar{Y})^2}{\sum_{i=1}^{n}(Y_i - \bar{Y})^2} \ , \quad \text{(E.4)}$$

where $\hat{Y}_i$ is the predicted value of X_i and $\bar{Y}$ is the mean of Y. R^2 varies between 0 and 1, with $\mathrm{R}^2 \sim 1$ ($\mathrm{R}^2 \sim 0$) indicating a strong (weak) linear correlation between X and Y.

For wetland extents, we use two observation-based datasets: GIEMS (Papa et al., 2010; Prigent et al., 2001, 2007b, 2012) and SWAMPS-GLWD (Poulter et al., 2017). In each case, we calculate the metrics over grid cells containing wetlands for both the UVic ESCM and the dataset. For wetland CH4 emissions, we use three upscaled flux measurements (UFMs) from across northern regions (>45°N): RF-DYPTOP, RF-GLWD, and RF-PEATMAT (Peltola et al., 2019). At the global scale, we use three process-based model ensembles: GCP-CH4 (Poulter et al., 2017), WetCHARTs (Bloom et al., 2017), and WETCHIMP (Melton et al., 2013). We calculate the metrics over grid cells in

which the UVic ESCM and the UFM or model ensemble both predict CH4 emissions (positive CH4 fluxes). We use MATLAB version R2018b for all calculations.

Results for wetland extents

Results listed in Table E1 show that: (i) wetlands in the UVic ESCM are better simulated across northern regions (>45°N) than at the global scale (e.g. RMSE and R^2), and (ii) the model agrees better with SWAMPS-GLWD than with GIEMS at the regional and global scale (all performance metrics). R^2 values suggest a weak linear correlation between our simulated and the estimated wetland extents globally. However, a previous study argues that R^2 and other correlation-based metrics are not best measures for evaluating the goodness-of-fit of hydrologic and hydroclimatic models as these metrics were found to be over-sensitive to extreme values (outliers) and insensitive to additive and proportional differences between observations and model predictions (Legates and McCabe, 1999). As a reference, our comparison of GIEMS to SWAMPS-GLWD yields R^2 = 0.12 for northern high-latitudes (>45°N) and R^2 = 0.22 for the globe.

Results for wetland CH_4 emissions

Table E2 lists the evaluation statistics for wetland CH_4 emissions. For wetlands north of 45°N, results show that the UVic ESCM has no preferential agreement with one of the three UFMs (all performance metrics). Based on the compared grid cells, however, the UVic ESCM simulates more CH_4 emissions than RF-DYPTOP (MBE > 0) and less CH_4 emissions than RF-GLWD and RF-PEATMAP (MBE < 0). At the global scale, the UVic ESCM compares similarly to the three model ensembles (all performance metrics); although simulated CH_4 emissions are higher than those predicted by the WetCHARTs ensemble (MBE > 0) and lower than those predicted by GCP-CH4 and WETCHIMP ensembles (MBE < 0).

At both the regional and global scale, R^2 values suggest a weak linear correlation between the UVic ESCM and the different UFMs or model ensembles (Table E2). As a reference, the inter-comparison of the UFMs yields R^2 values between 0.1 and 0.4 (0.14 for RF-DYPTOP and RF-GLWD; 0.32 for RF-DYPTOP and RF-PEATMAP; 0.33 for RF-GLWD and RF-PEATMAP). The inter-comparison of the model ensembles yields R^2 values ranging from 0.25 to 0.55 (0.25 for WetCHARTs and WETCHIMP; 0.28 for GCP-CH4 and WETCHIMP; 0.55 for WetCHARTs and GCP-CH4). The highest R^2 value for

WetCHARTs and GCP-CH4 may be justified by the fact that the two model ensembles are based on the same wetland dataset (SWAMPS-GLWD) (Bloom et al., 2017; Poulter et al., 2017). However, the comparison of these two model ensembles with respect to wetland CH_4 emission intensities (CH_4 emissions per unit of wetland area) yields a small R^2 value (R2 < 0.1). In fact, the comparison between the UVic ESCM and the three model ensembles as well as the inter-comparison of the model ensembles all yield small R^2 values (R^2 < 0.1) for both northern and global wetlands. This result suggests that large-scale wetland CH_4 intensities are generally not consistent across process-based models.

Table E1. Statistics for the model performance evaluation with respect to northern (>45°N) and global wetland extents. The UVic ESCM is compared to two global wetland datasets over the 2000-2007 period: GIEMS and SWAMPS-GLWD. Mean annual maximum extents over the same period are shown for reference. *n* represents the number of grid cells used in each comparison.

	Mean annual max. extent (x 10^6 km^2)	Statistical comparison with the UVic ESCM				
		n (—)	MBE (km^2)	MAE (km^2)	RMSE (km^2)	R^2 (—)
Northern (>45°N)						
UVic ESCM	4.76	—	—	—	—	—
GIEMS	3.05	429	787.5	1788.3	2374.7	0.09
SWAMPS-GLWD	4.71	690	-108.9	1712.7	2504.5	0.36
Global						
UVic ESCM	12.57	—	—	—	—	—
GIEMS	9.33	869	1024.9	3681.2	6175.5	0.05
SWAMPS-GLWD	10.59	1395	1124.2	2887.0	4234.1	0.11

The comparison of GIEMS to SWAMPS-GLWD yields MBE = -966.7 km^2; MAE = 1898.9 km^2; RMSE = 3313.3 km^2; and R^2 = 0.12 for wetlands north of 45°N (*n* = 506). The comparison yields MBE = -65.1 km^2; MAE = 2852.5 km^2; RMSE = 5668.7 km^2; and R^2 = 0.22 for global wetlands (*n* = 1222).

Table E2. **Statistics for the model performance evaluation with respect to CH_4 emissions from northern (>45°N) and global wetlands. For northern wetland CH_4 emissions, the model is compared to three upscaled flux measurements over the 2013-2014 period: RF-DYPTOP, RF-GLWD and RF-PEATMAP. For global wetland CH_4 emissions, the model is compared to three process-based model ensembles over the 2001-2004 period: GCP-CH4, WetCHARTs and WETCHIMP. Annual mean wetland CH_4 emissions over the same period are shown for reference. *n* represents the number of grid cells used in each comparison.**

	Annual mean emissions (Tg CH_4 yr^{-1})	Statistical comparison with the UVic ESCM				
		n (—)	MBE (Tg CH_4 yr^{-1})	MAE (Tg CH_4 yr^{-1})	RMSE (Tg CH_4 yr^{-1})	R^2 (—)
Northern (>45°N)						
UVic ESCM	33.2	—	—	—	—	—
RF-DYPTOP	30.6 ± 9.2	562	0.0041	0.0433	0.0675	0.14
RF-GLWD	37.6 ± 11.8	370	-0.0379	0.0723	0.1044	0.24
RF-PEATMAP	31.7 ± 9.4	351	-0.0256	0.0531	0.0862	0.20
Global						
UVic ESCM	154.4	—	—	—	—	—
GCP-CH4	160.4 ± 28.1	1219	-0.0007	0.1167	0.2501	0.11
WetCHARTs	147.3 ± 31.6	1388	0.0153	0.1037	0.2342	0.16
WETCHIMP	182.9 ± 43.1	1539	-0.0092	0.1061	0.2220	0.19

The comparison of RF-DYPTOP to RF-GLWD yields MBE = -0.0304 Tg CH_4 yr^{-1}; MAE = 0.0661 Tg CH_4 yr^{-1}; RMSE = 0.1073 Tg CH_4 yr^{-1}; and R^2 = 0.14 (*n* = 468). The comparison of RF-DYPTOP to RF-PEATMAP yields MBE = -0.0219 Tg CH_4 yr^{-1}; MAE = 0.0575 Tg CH_4 yr^{-1}; RMSE = 0.0846 Tg CH_4 yr^{-1}; and R^2 = 0.32 (*n* = 365). The comparison of RF-GLWD to RF-PEATMAP yields MBE = 0.0085 Tg CH_4 yr^{-1}; MAE = 0.0677 Tg CH_4 yr^{-1}; RMSE = 0.1023 Tg CH_4 yr^{-1}; and R^2 = 0.33 (*n* = 266).

The comparison of GCP-CH4 to WetCHARTs yields MBE = 0.0213 Tg CH_4 yr^{-1}; MAE = 0.0641 Tg CH_4 yr^{-1}; RMSE = 0.1735 Tg CH_4 yr^{-1}; and R^2 = 0.55 (*n* = 1727). The comparison of GCP-CH4 to WETCHIMP yields MBE = -0.0192 Tg CH_4 yr^{-1}; MAE = 0.0991 Tg CH_4 yr^{-1}; RMSE = 0.2433 Tg CH_4 yr^{-1}; and R^2 = 0.28 (*n* = 1780). The comparison of WetCHARTs to WETCHIMP yields MBE = -0.0304 Tg CH_4 yr^{-1}; MAE = 0.0641 Tg CH_4 yr^{-1}; RMSE = 0.1735 Tg CH_4 yr^{-1}; and R^2 = 0.25 (*n* = 2103).

References for the statistical evaluation

Ali, M. H. and Abustan, I.: A new novel index for evaluating model performance, J. Nat. Resour. Dev., 4, 1–9, 2014.

Bloom, A. A., Bowman, K. W., Lee, M., Turner, A. J., Schroeder, R., Worden, J. R., Weidner, R., McDonald, K. C. and Jacob, D. J.: A global wetland methane emissions and uncertainty dataset for atmospheric chemical transport models (WetCHARTs version 1.0), Geosci. Model Dev., 10, 2141–2156, 2017.

Comyn-Platt, E., Hayman, G., Huntingford, C., Chadburn, S. E., Burke, E. J., Harper, A. B., Collins, W. J., Webber, C. P., Powell, T., Cox, P. M., Gedney, N. and Sitch, S.: Carbon budgets for 1.5 and 2°C targets lowered by natural wetland and permafrost feedbacks, Nat. Geosci., 11, 568–573, 2018.

Gedney, N. and Cox, P. M.: The sensitivity of global climate model simulations to the representation of soil moisture heterogeneity, J. Hydrometeorol., 4, 1265–1275, 2003.

Legates, D. R. and McCabe, J. R.: Evaluating the use of “goodness-of-fit” measures in hydrologic and hydroclimatic model validation, Water Resour. Res., 35, 233–241, 1999.

Melton, J. R., Wania, R., Hodson, E. L., Poulter, B., Ringeval, B., Spahni, R., Bohn, T., Avis, C. A., Beerling, D. J., Chen, G., Eliseev, A. V., Denisov, S. N., Hopcroft, P. O., Lettenmaier, D. P., Riley, W. J., Singarayer, J. S., Subin, Z. M., Tian, H., Zürcher, S., Brovkin, V., Van Bodegom, P. M., Kleinen, T., Yu, Z. C. and Kaplan, J. O.: Present state of global wetland extent and wetland methane modelling: Conclusions from a model inter-comparison project (WETCHIMP), Biogeosciences, 10, 753–788, 2013.

Papa, F., Prigent, C., Aires, F., Jimenez, C., Rossow, W. B. and Matthews, E.: Interannual variability of surface water extent at the global scale, 1993-2004, J. Geophys. Res. Atmos., 115, D12111, 2010.

Peltola, O., Vesala, T., Gao, Y., Räty, O., Alekseychik, P., Aurela, M., Chojnicki, B., Desai, A. R., Dolman, A. J., Euskirchen, E. S., Friborg, T., Göckede, M., Helbig, M., Humphreys, E., Jackson, R. B., Jocher, G., Joos, F., Klatt, J., Knox, S. H., Kowalska, N., Kutzbach, L., Lienert, S., Lohila, A., Mammarella, I., Nadeau, D. F., Nilsson, M. B., Oechel, W. C., Peichl, M., Pypker, T., Quinton, W., Rinne, J., Sachs, T., Samson, M., Schmid, H. P., Sonnentag, O., Wille, C., Zona, D. and Aalto, T.: Monthly gridded data product of northern wetland methane emissions based on upscaling eddy covariance observations, Earth Syst. Sci. Data, 11, 1263–1289, 2019.

Poulter, B., Bousquet, P., Canadell, J. G., Ciais, P., Peregon, A., Saunois, M., Arora, V. K., Beerling, D. J., Brovkin, V., Jones, C. D., Joos, F., Gedney, N., Ito, A., Kleinen, T., Koven, C. D., McDonald, K., Melton, J. R., Peng, C., Peng, S., Prigent, C., Schroeder, R., Riley, W. J., Saito, M., Spahni, R., Tian, H., Taylor, L., Viovy, N., Wilton, D., Wiltshire, A., Xu, X., Zhang, B., Zhang, Z. and Zhu, Q.: Global wetland contribution to 2000-2012 atmospheric methane growth rate dynamics, Environ. Res. Lett., 12, 094013, 2017.

Prigent, C., Matthews, E., Aires, F. and Rossow, W. B.: Remote sensing of global wetland dynamics with multiple satellite data sets, Geophys. Res. Lett., 28, 4631–4634, 2001.

Prigent, C., Papa, F., Aires, F., Rossow, W. B. and Matthews, E.: Global inundation dynamics inferred from multiple satellite observations, 1993-2000, J. Geophys. Res. Atmos., 112, D12107, 2007.

Prigent, C., Papa, F., Aires, F., Jiménez, C., Rossow, W. B. and Matthews, E.: Changes in land surface water dynamics since the 1990s and relation to population pressure, Geophys. Res. Lett., 39, L08403, 2012.

Willmott, C. J.: Some comments on the evaluation of model performance, Bull. Am. Meteorol. Soc. , 63, 1309–1313, 1982.